ΕΛΛΗΝΙΚΗ ΔΗΜΟΚΡΑΤΙΑ
ΠΑΝΕΠΙΣΤΗΜΙΟ ΜΑΚΕΔΟΝΙΑΣ

Algorithms for Cognitive Radio Network and Cognitive Radio Network Cloud

Ioanna C. Kakalou

Thessaloniki May 2020

Abstract

COGNITIVE RADIO NETWORK AND COGNITIVE RADIO NETWORK CLOUD

This dissertation's innovation is concentrated on the introduction and description of a reference network framework for Cognitive Medium Access Control and SDR Services and Abstract Cognitive Medium Access Control and SDR Services integration and deployment on all the OSI layers in a heterogeneous wireless network. The necessity of lower layers services and applications conceptualization within the Cognitive Radio Cycle is the main issue that this dissertation manifests whilst providing algorithms for responding to diverse issues within the Cognitive Radio Network and Cognitive Radio Network Cloud.

The current challenges in Cognitive Radio Network (CRN) are storing of large amount of data, processing them in real time and the exchanging of nodes' current status on-the-fly. These challenges are in contrast to the limited storage and processing ability (plus battery lifetime) of Cognitive Devices thus the need for additional capabilities arise. Cognitive Radio Network Cloud (CRNC) is an infra-structure consisting of mobile nodes and the cloud whose primary goal is to keep an up-to-date status of the spectrum availability in the network. Demanding tasks, e.g. signal intelligence, could be off-loaded to powerful nodes locally allowing the local network to be self-organized. By allowing self-organizing networks to be deployed locally, huge heterogeneous wireless networks such as 5G and 6G evolve, which can mitigate their dynamic spectrum access and control to meet the end users and wireless network performance requirements.

Self-organizing Cognitive Radio Networks in an immense heterogeneous wireless network along with Dynamic Spectrum Access, Management and Control Mitigation on demand or not on demand to respond to network needs in real time and on the fly can be realized with high level abstraction and conceptualization of Cognitive Medium Access Control and SDR Services and Abstract Cognitive Medium Access Control and SDR Services integration and deployment on all the Open Systems

Interconnection (OSI) layers, cross-platform and cross-network, cross-operator. Central coordination would be applicable for triggering local nomad network to be self-organized, as well for hand-off or for meeting QoE, radio network performance, institutional metrics.

Network clustering on Cognitive Medium Access Control and SDR Services/Applications and Abstract Cognitive Medium Access Control and SDR Services/Applications Level may be feasible. Artificial Intelligence and other technologies will enable efficient distributed control. Radio Environment Maps are powerful technology to this direction. Off-loading to local powerful nodes increase network performance and QoE which are essential for 5G, 6G network for urban and rural radio environments.

A new mathematic method of mathematic game unfolding is introduced i.e. a new mathematic method for generating games without coordination and a corresponding mathematic game model as an application of the proposed mathematic method to for the Cognitive Radio Network and Cognitive Radio Cloud Security was introduced. Other mathematic game reaching Nash Equilibriums also were introduced. Deterministic automata and Machine Learning were also introduced as well as other mathematic formulas applicable to the corresponding network protocols, mathematic models for steady-state-Lyapunov filtering algorithm for enhanced CRN-SDR signal processing and mathematic formulas for Non-Reciprocal Channels in Massive MIMO CRN were also introduced in this dissertation.

Keywords: Cognitive Radio Network, Cognitive Radio Network Cloud, Software Defined Network, SDR, Cognitive Radio Medium Access Control, Cognitive Radio MAC, 5G, 6G, Cognitive Radio Medium Access Control on the Cloud, Systems of Systems Benefits for Cognitive Radio Network Cloud, Network Service Chaining, NVF, Cognitive Radio Software Define Network, Sustainability, Cognitive Radio Sensor Network, Machine Learning, Broadcasting in Cognitive Radio Network Cloud, Primary User Emulation Attack Detection, Method in Imperfect Games Theory for Formulating Imperfect Game Models of coordination without collaboration, Multiscale Decision Making for Control in Sensing and Cognitive Radio Cloud, Cognitive Radio Network Massive MIMO, Cognitive Radio Environment Maps, Heterogeneous Cognitive Radio Network and Cognitive Radio Network Cloud.

ΠΑΝΕΠΙΣΤΗΜΙΟ ΜΑΚΕΔΟΝΙΑΣ

Algorithms for Cognitive Radio Network and Cognitive Radio Cloud

Ioanna Kakalou

Dissertation submitted by Ioanna Kakalou

In partial fulfillment of requirements for the Doctorate degree at University of Macedonia

Examination Committee:

1. Psannis Konstantinos, Associate Professor (supervisor), Applied Informatics Dept., University of Macedonia
2. Petridou Sofia, Assistant Professor, Applied Informatics Dept., University of Macedonia
3. Mamatas Eleftherios, Assistant Professor, Applied Informatics Dept., University of Macedonia
4. Karagiannidis Georgios, Professor, Electrical Engineering And Computer Engineering Dept., Aristotle University
5. Sarigiannidis Panagiotis, Assistant Professor, Electrical Engineering and Computer Engineering Dept., University of Western Macedonia
6. Goudos Sotirios, Associate Professor, Physics Dept., Aristotle University
7. Kokkonis Georgios, Assistant Professor, Business Administration, University of Western Macedonia

Thessaloniki 2020

Acknowledgements

I would like to thank my supervisor Prof. K.E.Psannis for giving me the opportunity to continue research and accepted me for the Doctoral Course at December (Christmas) 2015.

Dedication

my father

PHD DISSERTATION CONTENTS

Introduction

COGNITIVE RADIO NETWORK AND COGNITIVE RADIO NETWORK CLOUD

Cognitive radio is a promising technology that answers the spectrum scarcity problem arising with the growth of usage of wireless networks and mobile services. Cognitive Radio Network and Cognitive Radio Network Cloud will a key technologies for 5G and 6G Heterogeneous Network deployment for next generation Space-Air-Ground-Sea integrated communication and wireless tactile network.

.

1.1. INTRODUCTION

Radio Spectrum is a public good and the recent years due to the vast increase of mobile users and mobile applications as well as the need for Quality of Experience (QoE) of the end user, a spectrum scarcity was a main issue in wireless networks leading to the introduction of a new key technology namely the Cognitive Radio for the underutilized licensed spectrum bands broadening the radio spectrum usage and management. So far the unlicensed band i.e. the Industrial Scientific Medical Band was overcrowded. So, the necessity for utilizing the licensed spectrum band when the unlicensed users do not interfere with the licensed users and Cognitive management of the Spectrum i.e. intelligent access and management also called Dynamic Spectrum Access arise. The Cognitive Radio research has been started in the USA by utilizing the TV white spaces and now Cognitive Radio technology follows a cognition cycle for effectively utilizing all frequencies [5G Deployment, State of Play in Europe, USA and Asia, Directorate General for Internal Policies, European Union, April 2019].

1.2. PROBLEM STATEMENT

Cognitive radio based on the Software Defined Radio (SDR) that can reconfigures its parameters - modulation, frequency etc., it adds a cognitive cycle in order to observe the environment, orient, plan, design, act and learn from past experiences.

There are three important quality metrics that define efficiency of spectrum sensing which are a) the detection probability (Pd) i.e. the probability that the PU is present and the sensing outcome is PU present, b) false alarm probability (Pf) the probability that PU is not present and the sensing outcome is PU present c) misdetection probability i.e. the probability that PU is present and the sensing outcome id not present. Both false alarm and misdetection probabilities degrade sensing efficiency. If the secondary user detects a signal *y(n)*, the decision on spectrum sensing may be given by double hypothesis test:

$$H1: y(n) = x(n) + w(n) \quad (1)$$

$$H0: y(n) = w(n) \quad (2)$$

The $H1$ shows that the primary user's signal $x(n)$ and noise $w(n)$ are present whilst in $H0$ only noise $w(n)$ is present. Then in cooperative mode the SUs sensing outcome may be forwarded to the fusion center as simple bit "1" for PU presence or "0" for PU absence and then a hard decision will be reached which may not be accurate or the sample bits may be forwarded to the fusion center and a soft decision will be reached based on applied rule.

Interference is a main issue in the Cognitive Radio Network (CRN) and as long as the interference threshold is not reached the unlicensed or secondary users of the Cognitive Radio Network may transmit.

The Cognitive Radio Network perceives the radio environment. The CRN learn the radio environment and adjusts the internal states to the statistical changes of RF mainly and the configuration parameters such as frequency band, modulation, transmission power in real-time. It is a network that establishes the communication between the nodes/users of the Cognitive Radio Network. Parameter reconfiguration is made according to the wireless environment, topology, the operating conditions and the user requirements. The quality of communication for the licensed i.e. primary users and unlicensed users i.e. secondary users which should not interfere to the former primary users' communications and the optimal spectrum usage as well as the network performance are main goals.

1.3. METHODOLOGY

This dissertation's innovation is concentrated on the introduction and description of a reference network framework for Cognitive Medium Access Control and SDR Services and Abstract Cognitive Medium Access Control and SDR Services integration and deployment on all the OSI layers in a heterogeneous wireless network providing reference protocol communication and platform definition, reference heterogeneous network architecture and system architecture, related technologies to be encompassed. The necessity of lower layers services and applications conceptualization within the Cognitive Radio Cycle is the main issue that this dissertation manifests whilst providing algorithms for responding to diverse issues within the Cognitive Radio Network and Cognitive Radio Network Cloud and evaluating them with experiments where appropriate. References are provided where necessary and within the evaluation sections.

As the proposed algorithms, architecture, systems as part of the immense heterogeneous network respond to a specific issue and network problem each time e.g. Machine Learning, Software Defined Networking, Optimal Signal Processing, Broadcasting, Sustainability, Security, Channel Non-Reciprocity for Massive MIMO, Radio Environments Maps, the metrics which are defined each time correspond to the particular cases whilst new formulas, mathematic models as well as a new mathematic method of mathematic game unfolding in game theory, mathematic game models reaching Nash Equilibriums, deterministic automata are introduced.

1.4. THESIS STATEMENT

The current challenges in Cognitive Radio Network are storing of large amount of data, processing them in real time and the exchanging of nodes' current status on-the-fly. These challenges are in contrast to the limited storage and processing ability (plus battery lifetime) of Cognitive Devices thus the need for additional capabilities arise. Cognitive Radio Network Cloud (CRNC) is an infra-structure consisting of mobile nodes and the cloud whose primary goal is to keep an up-to-date status of the spectrum availability in the network. The large amount of sensing data and processing of MIMO antennae as well as the signal intelligence as a whole can be mitigated to the cloud.

Demanding tasks, e.g. signal intelligence, could be off-loaded to powerful nodes locally allowing the local network to be self-organized. By allowing self-organizing networks to be deployed locally, huge heterogeneous wireless networks such as 5G and 6G evolve, which can mitigate their dynamic spectrum access and control to meet the end users and wireless network performance requirements. A critical issue in CR Infrastructure-less network deployment on the cloud would be the Standard Interface Operability (SIO) for CR users to connect to the cloud or local powerful nodes. SIO would allow easy access and utilization of powerful wireless and mobile local nodes and infrastructure network front-end.

This dissertation and research work presented in the following chapters participated in this effort or the international research community on wireless network by introducing Cognitive Medium Access Control and SDR Services and Abstract Cognitive Medium Access Control and SDR Services integration to achieve higher degree of conceptualization of Cognitive Medium Access Control and SDR Services utilized in the upper stack layers of OSI and meet a common goal such as smart radio environment utilization locally or globally, QoE, higher wireless network performance. The technologies that may be employed are current technologies such as Virtual Machines and Network Function Virtualization, Network Chaining. The concept of Cognitive Medium Access Control and SDR Services and their conceptualization to an abstract level covering the seven layers of the OSI stack and respond to edge requirements of the huge 5G, 6G heterogeneous networks.

Cognitive Medium Access Control and SDR Services integration and deployment on all the OSI layers and 5G and 6G huge and heterogeneous network would require high level of scheduling and interaction. High level of scheduling and interaction will trigger eventually adaptation “knobs” within the local and global system would necessiate high level of interaction on all OSI stack layers of Cognitive Medium Access Control and SDR Services and Abstract Cognitive Medium Access Control and SDR Services in this reference network framework for cross-operator, cross-network operability context generation, QoE, radio network demands, cross-operator, cross-border.

This dissertation and the subsequent research work introduced a framework of this Cognitive Medium Access Control and SDR Services and application and Abstract Cognitive Medium Access Control and SDR Services integration and deployment framework. In particular in this framework optimal algorithms have been introduced to implement protocols for solving diverse issues such as native Cognitive Medium Access Control, Software Defined Networking coordination, Sustainability, Broadcasting, Security, massive MIMO technology and imperfect CSI for reciprocal channels, Multiscale Decision Making with Machine Learning and Game Theory for Efficient Sensing Scheduling and Spectrum Sensing Control, Enhanced Signal Processing and Radio Environment Maps for the Cognitive Radio Network and Cognitive Radio Cloud. As huge heterogeneous next generation wireless networks is a necessity, proposing such high level design of low layer services and applications cross-layer, cross-network, cross-operator would make feasible 5G and 6G - Space-Air-Ground-Sea integrated communication and wireless tactile network- and allow them to evolve.

1.5. OUTLINE

This document is structured in fifteen chapters. In the second, third, fourth and fifth chapters include the introduction and description of a reference network framework for Cognitive Medium Access Control and SDR Services and Abstract Cognitive Medium Access Control and SDR Services integration and deployment on all the OSI layers in a heterogeneous wireless network providing reference protocol communication and platform definition, reference heterogeneous network architecture and system architecture, related technologies to be encompassed. Chapter six includes sensing algorithms comparison for CRN, chapter seven a Reinforcement Learning Scheme for Dynamic Spectrum Access, chapter eight a proposal for Software Define Networking solution in Cognitive Radio Sensor Networks. Chapter nine provides a solution for supporting CRN Sustainability.

Chapter ten introduce network solutions for CRN Broadcasting, and chapter eleven introduces a new mathematic model in game theory and a new game form and applies it to security problem in CRN. Chapter twelve introduces Multi-Scale Decision Making machine learning to Control Spectrum Sensing and Scheduling. In chapter thirteen enhanced signal processing is proposed and chapter fourteen provides the formulas for Massive MIMO in CRN with imperfect CSI and Non-reciprocal channels. Finally Radio Environment Maps technology Architecture is proposed for CRN and CRNC enhancement.

Chapter 2

COGNITIVE RADIO NETWORK

Cognitive radio is a promising technology that answers the spectrum scarcity problem arising with the growth of usage of wireless networks and mobile services. Cognitive Radio Network Edge Computing will enhance the Cognitive Radio Network (CRN) capabilities and along with some adjustments in its operation will be a key technology for 5G Heterogeneous Network deployment.

Cognitive radio based on the Software Defined Radio (SDR) that can reconfigures its parameters - modulation, frequency etc., it adds a cognitive cycle [1] in order to observe the environment, orient, plan, design, act and learn from past experiences. Cognitive radio senses the spectrum for vacancies, so called “spectrum holes”, for the Cognitive Radio Network (CRN) Users to transmit. In case of the licensed spectrum when the licensed users, i.e. Primary Users (PUs), vacate the spectrum the CRN users, also called Secondary Users (SUs), can access it. There are limitations to the interference the Secondary Users can cause to the Primary Users. On the other hand, the underutilized spectrum resulted in an immense need for Dynamic Spectrum Access that exploits spectrum opportunistically.

Dynamic Spectrum Access includes amongst others sensing, spectrum management, spectrum sharing and spectrum mobility. For spectrum sensing - Primary Users detection - Cognitive Radio uses filter detection, energy detection and feature detection. The spectrum management includes characterization, selection and reconfiguration of the spectrum (channel, modulation, bandwidth, power and transmission time). On appearance of the Primary User, the Secondary User has to vacate the channel immediately and continue transmission in another vacant channel. Spectrum sharing is essential for avoiding overlapping of multiple cognitive radios as well as handoff (loss of connection for mobile Secondary User or poor Quality of Service).

CRN uses machine learning, genetic algorithms, game theory techniques, knowledge representation and optimization techniques for efficient resources allocation. Further, the CRN learns the network conditions [2] and encompasses past experiences to its cognitive cycle.

The Cognitive Radio uses the first OSI layer (Software Defined Radio - SDR) and second OSI layer (Cognitive Medium Access Control - MAC) basically but actually relies on the whole OSI stack and the decisions made in the CRN have to meet the whole network's needs.

1.1. SOFTWARE DEFINED RADIO

The Software Defined Radio where the parameters of transmission such as frequency, modulation, protocol are reconfigured, is the precursor of Cognitive Radio Network. Reconfiguration is achieved with algorithms for signal processing which are controlled by software.

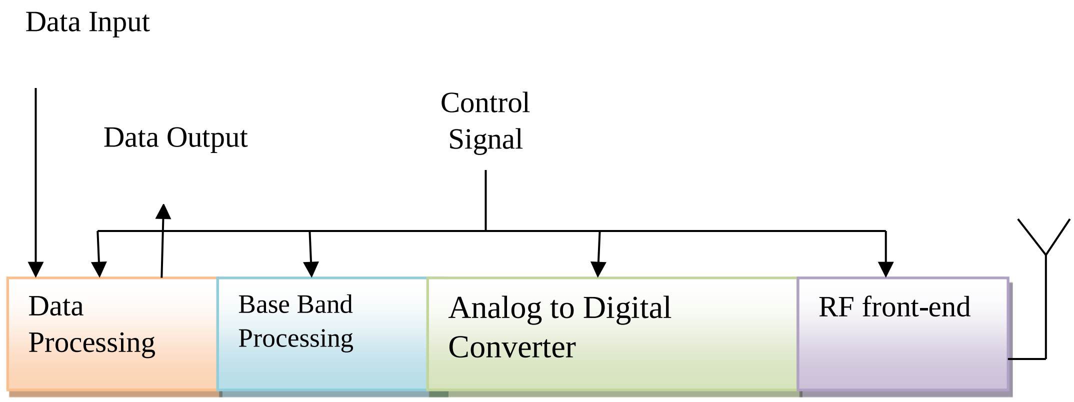

Figure 1.1: The SDR tranceiver

The SDR main functions are following:

1. Operating in various frequencies for various users.
2. Supporting various patterns and interfaces for the same pattern.
3. Supporting various services such as telephony and broadband wireless access to internet.
4. Transmitting and receiving in various frequencies simulteneusly.

Those parameters can be configured for each user, can be configured for some times in the system' lifetime, can be configured for each connection or dynamically for each slot.

1.2. Cognitive Radio Network

The Cognitive Radio Networks (CRN) employ SDR but provide intelligent functionality for spectrum management and access by unlicensed users.

The CRN term was introduced by Haykin [1] describing an intelligent wireless communication system which perceives the radio environment. The CRN learn the radio environment and adjusts the internal states to the statistical changes of RF mainly and the configuration parameters such as frequency band, modulation, transmission power in real-time. It is a network that establishes the communication between the nodes/users of the Cognitive Radio Network. Parameter reconfiguration is made according to the wireless environment, topology, the operating conditions and the user requirements. The quality of communication for the licensed i.e. primary users and unlicensed users i.e. secondary users which should not interfere to the former primary users' communications and the optimal spectrum usage are main goals.

The physical layer architecture of SDR and the higher levels which adjust such as the Medium Access Control or higher which cooperate to compose applications and services for the Cognitive Radio Network.

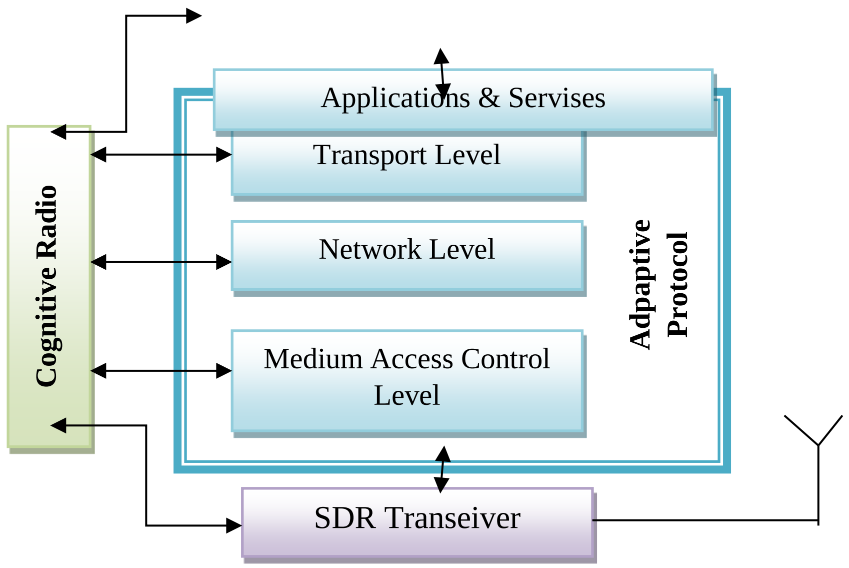

Figure 1.2: The Cognitive Radio Network Protocol Stack

1.3. FUNCTIONALITY

Spectrum sensing is a main function which ascertains the spectrum status and the primary users' presence. The Cognitive Transceiver utilizes each transmission opportunity so called spectrum hole i.e. spectrum frequencies which are not in use and to proceed in optimal spectrum management for the CRN user in terms of transmission power and transmission duration.

Spectrum management may be central and in that case there is cooperative control i.e. a controller updates the radio environment information of the rest of the nodes. Spectrum management may be not-cooperative and in that case each terminal is responsible to update the radio environment information so the complexity is increased.

Spectrum analysis utilizes the former information to detect the next transmission opportunity for the secondary users i.e. the spectrum hole which is defined by the interference, spectrum vacancy duration, collission probability with the primary users, as well as the acceptable level of interference to the primary users' transmissions so to meet the quality metrics for transmission.

Spectrum Access is determined by the Cognitive Radio Medium Access Control Protocol (CR-MAC) which is responsible to further avoid collisions with the primary users and to follow fixed allocation such as FDMA, TDMA, CDMA or random access schemes such as ALOHA,CSMA/CA [3].

Spectrum mobility is when a primary user begins transmission at a spectrum hole then the secondary users should vacate the frequency and continue transmission in another spectrum hole without performance degradation. This spectrum hand-off triggers the parameters' update of the protocols of all levels.

1.4. DYNAMIC SPECTRUM ACCESS

Dynamic Spectrum Access is defines as the mechanism [2] which adapts the spectrum resources usage in the near future to the dynamic radio environment.

According to [4] there is the common use model which allows the users to access the spectrum in the ISM band, the networks may be homogeneous or heterogeneous with cognitive capabilities which then will be defined as symmetric or non-symmetric respectively [3][5].

In the shared-use model both the primary and secondary users access the spectrum opportunistically and in the exclusive-use model the primary/licensed users provide the use to the secondary user.

Opportunistic spectrum use may restrict the secondary users' transmissions as the transmission power cannot exceed a certain limit of temperature interference to the primary users' transmissions. In that case, a solution may be the transmission to a broader spectrum band with lower transmission power which assumes that the primary users transmit continually.

Opportunistic spectrum use allows the secondary users to detect spectrum holes in space, time and frequency and transmit. The opportunistic spectrum access phases are the exploration so to sense the spectrum and analyze the results and the exploitation which involves the decision making and hand-off.

1.5. COGNITIVE RADIO NETWORK COMPONENTS

Cognitive Radio Network Components function follows a cognitive cycle of environment observation, priority setting, design, decision making, action, update of all stages of learning and the final update of the state of Cognitive Radio [6].

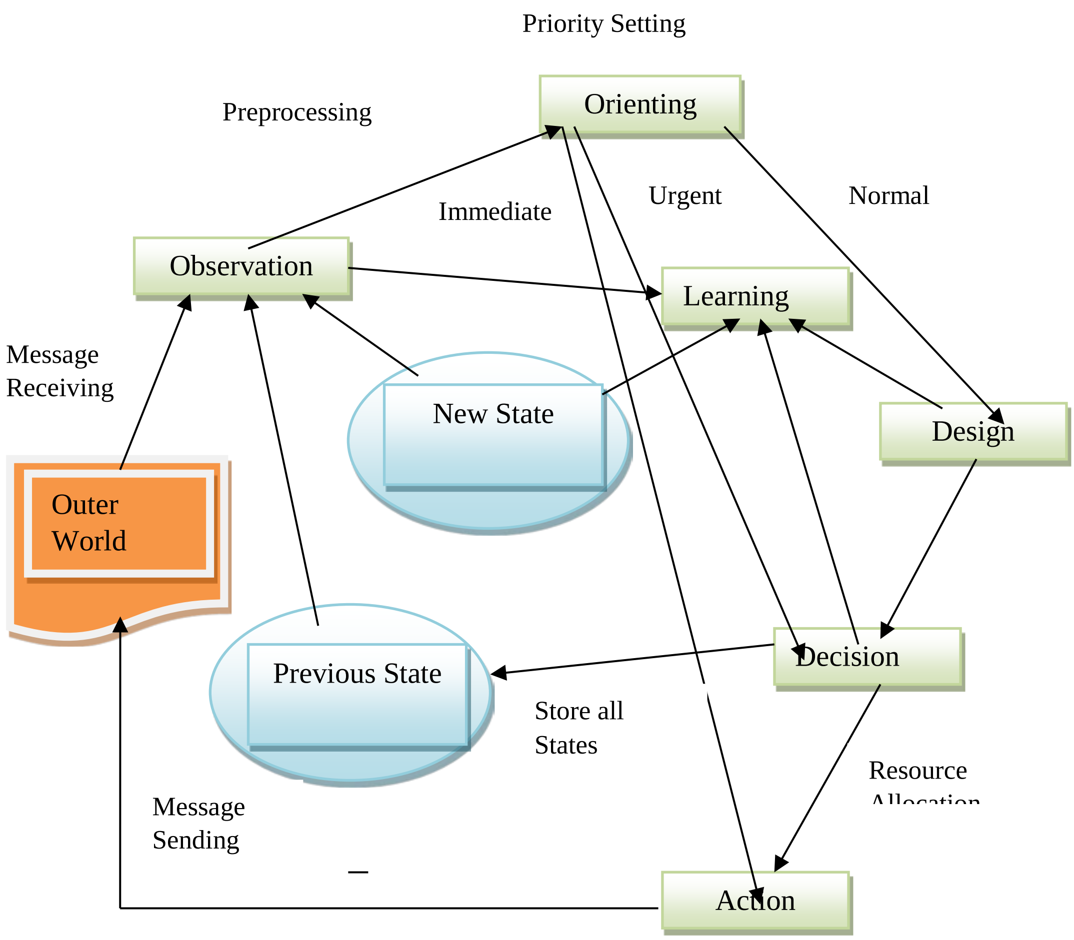

Figure 1.3: The Cognitive Cycle

The Cognitive Cycle is implemented by:

- **The transceiver** and basically the SDR which performs the spectrum sensing i.e. the radio environment observation.
- **The spectrum analyser** which uses known signals to detect the presence or non-presence of licensed users, to separate spectrum holes and apply signal processing to avoid interference.

- **Knowledge extraction and Learning:** this process is implemented for observing and learning the primary users' behavior so a knowledge database is maintained.
- **Decision Making:** The optimal decision for spectrum access may be a cooperative or competitive process for secondary users.

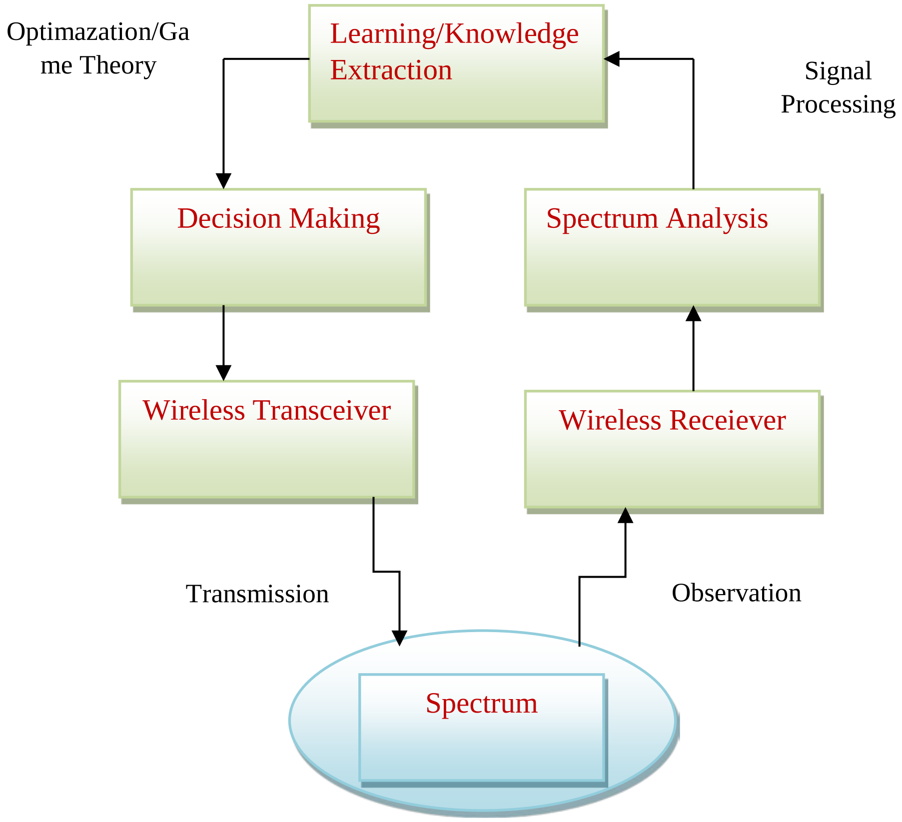

Figure 1.4: The Cognitive Radio Components

1.6. Interference Temperature

The FCC Spectrum Policy Task Force of USA introduced a metric for unlicensed users' interference to the licensed users which is the interference temperature I_T. Interference temperature is similar to the noise temperature but covers random noise and deterministic interference from other sources. The CR-receiver estimates for each frequency the interference temperature based on the quality of the signal.

Interference temperature in degrees Kelvin is given by the equation below:

$I_T\,(f_c\,,W)=P_1\,(f_c\,,W)/KW$

Where P_1 is the average interference power in Watts for spectrum W Hz and central frequency f_c and K the Boltzman constant ($K=1.38x10^{-23}$ Joules/degrees Kelvin).

There are two models for interference temperature the ideal and the generalized. In the former, the estimation is performed during primary user's transmission or it will not be accurate. The signal has to be known and the temperature will be measured with known signals at the right moment. The equation describing the interference limits is given below:

$I_T\,(f_i\,, W_i\,) + M_i\,P/KW_i \leq I_L\,(f_i\,)$ [7][8]

If there are n signals of licensed users in the band with i user of spectrum W_i with central frequency of f_i .

Where I Є [1..n] , and $0 \leq M_i \leq 1$ a multiplicative factor of attenuation due to path loss and fading.

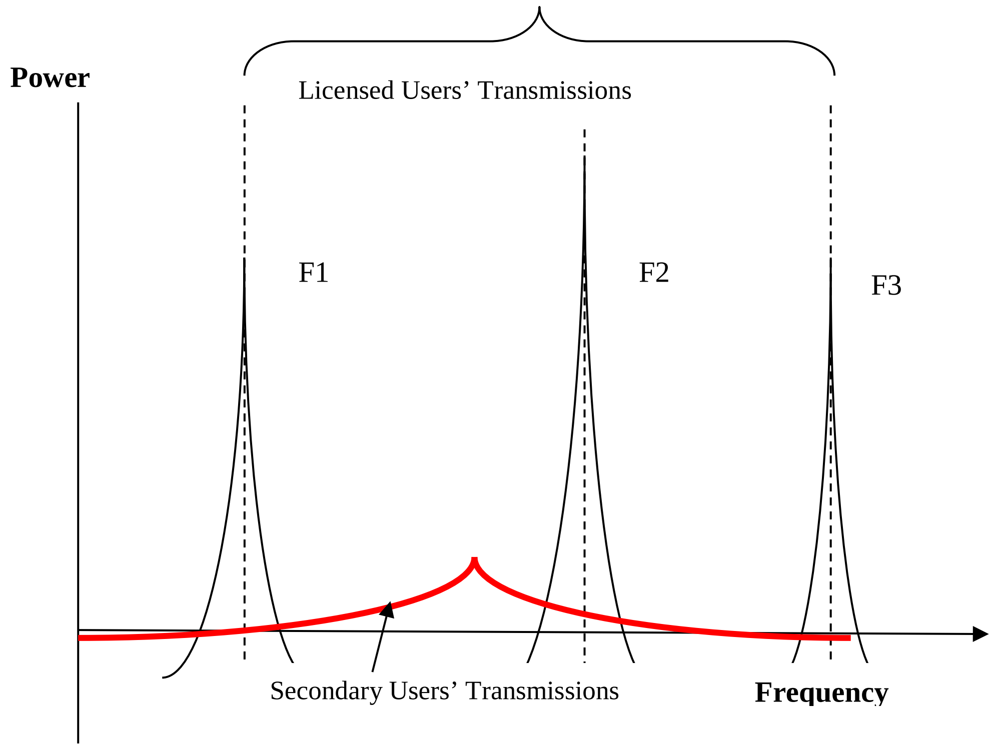

Figure 1.5 : Interference Temperature for Licensed Users

In the generalized model there is no information about the primary user's signal and the former equation is generalized and includes both licensed and unlicensed users and the interference temperature is estimated for the spectrum W of the unlicensed user. So, the upper limit of the transmission power is estimated to determine the permitted rate r:

$R=W \log(1 + S/(\sigma^2 + P_I)$,

S: the transmission powerς, σ^2 : noise power, P_I :interference power.

1.7. SPECTRUM ANALYSIS

Spectrum Analysis detects the licensed users' signals with or without the cooperation of unlicensed users relying on the interference control. If the unlicensed users do not cooperate and consequently exchange measurements and observations the model is described by the equation below:

$$x(t) = \begin{cases} n(t), & H_0 \\ h \times s(t) + n(t), & H_1 \end{cases}$$

x(t) is the received signal of the unlicensed user, s(t) is the licensed user signal, n(t) is the white Gaussian noise and h is the channel gain. The H_0 , H_1 describe the non-presence and presence of the licensed user.

The probability P_d =probability (H_1 , H_1) : describes the successive detection, the probability P_f =probability(H_1 ,H_0): describes the non-successive detection and the probability P_m = probability (H_0 ,H_1): describes misdetection.

There are three methods a) that of matched filter detection or coherent detection, b) transmitter power detection c) cyclostationary feature detection [8].

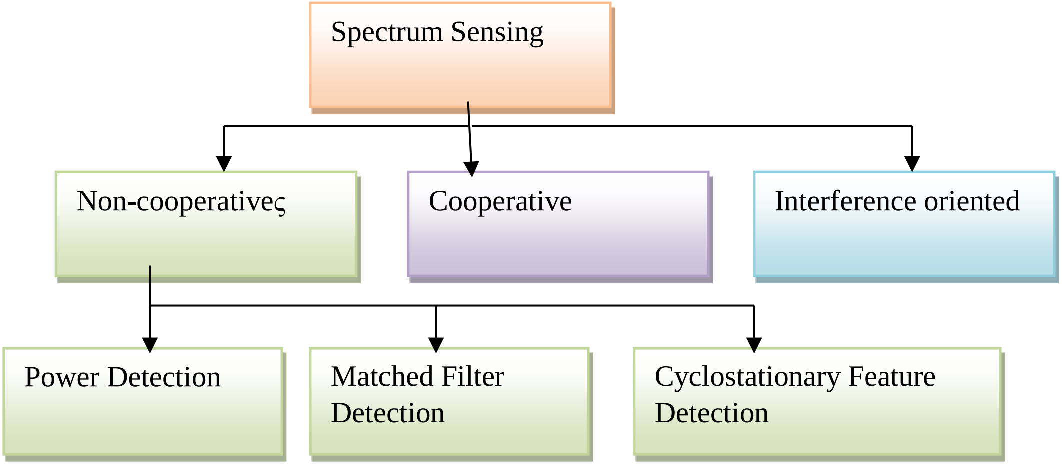

Figure 1.6: Spectrum Sensing

In the former case the filter will optimize the SNR of the received signal and will compare it to a known template. Known signal can be created if the licensed user's signal includes prefixes, timestamps, codes that can create the signal. For the Gaussian noise such a filter is optimal [8] [9]. That is to say this method is applicable only if the licensed user's signal is known.

If the signal is not known then the second method is preferred as it applies a band pass filter as long as the observation takes place and checks whether a certain limit has been exceeded which denotes the primary user's presence in the spectrum band. If there is no fading the probabilities are given by the equations below:

$$P_d = Q(\sqrt{2\gamma}, \sqrt{\lambda})$$

$$P\_f = \Gamma(m, \lambda/2)/\Gamma(m)$$

Where γ is the SNR of the received signl and λ the energy detection limit, Q is the generalized Marcum Q-function.

If there is shadowing and multipath fading the probabilities are given below:

$$P_d = \int_x Q(\sqrt{2\gamma}, \sqrt{\lambda}) f_\gamma(x) dx$$

Where $f_\gamma(x)$ is the probability distribution function for SNR.

If the detection error probability is high then there must be other secondary users beside the primary user.

The cyclostationary feature detection method depends on the autocorrelation of primary user's signal i.e. if it is periodical. This method is more accurate but requires longer processing time and pattern recognition may be applied.

Both methods can be combined for better results. The power detection method nay be applied to a more crowded spectrum band and then in band zone with low energy cyclostationary feature detection may be applied.

The spectrum sensing with information exchange between the secondary nodes which increases the complexity may respond to the hidden terminal node problem where the hidden node due to geographical position cannot detect the othe r secondary node and communication establishment with a third node is required to overcome this misdetection.

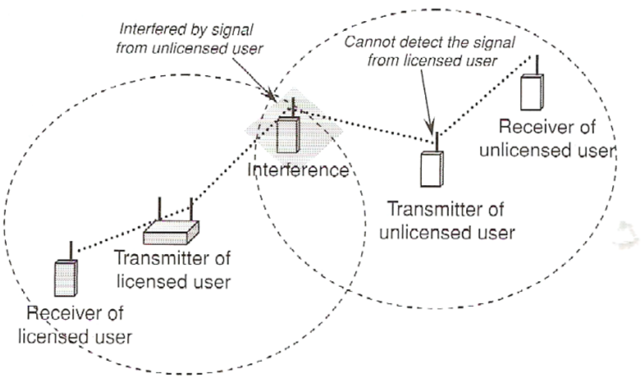

Figure 1.7 : The hidden terminal problem

In spectrum sensing based on interference algorithms measure the noise/interference level by all signal sources to the primary receiver. This information will be utilized by the secondary users to decide their spectrum access without exceeding the temperature interference level.

1.8. SPECTRUM ANALYSIS AND DECISION MAKING

Spectrum analysis will characterize spectrum band according to frequency, bandwidth, interference, channel capacity and primary users' activity.

The analysis may be local or cooperative by exchanging information and has to consider that the spectrum sensing may be inaccurate, and how the spectrum holes will be utilized e.g. modulation, power and how they will be assigned to the secondary users.

Decision making may be locally-competitively as local optimum or globally cooperatively for global optimum to be achieved with central or distributed process. If the decision making is centralized then spectrum management is easier whilst the distributed method suffers by the hidden terminal problem and the increased control information exchange.

1.9. CHALLENGES FOR COGNITIVE RADIO RESEARCH

The interference limit estimation may be inaccurate e.g. if the secondary user does not know the primary user's position which is essential for interference estimation or if the primary user is a passive device.

In multiple users networks the spectrum sensing information may be cooperatively managed and coordinated. The longer the observation period the more accurate the result and the shorter the transmission duration i.e. higher throughput. If the observation is not accurate the collisions and interference in licensed users' transmissions will occur.

In multichannel transmission like OFDM, the channel which are sensed are more that the available interfaces at the transceiver so that some of them will be selected each time for sensing affecting the system' performance. Some of the channels which are most occupied by licensed users should not be preferred. Channel selection is an optimization problem.

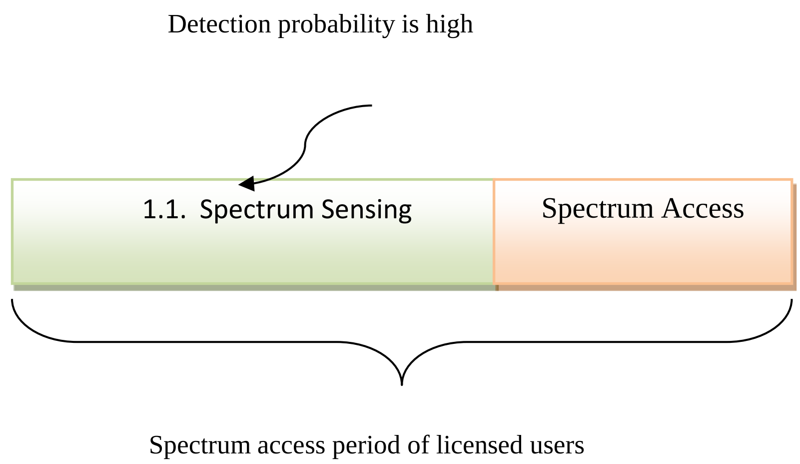

Figure 1.8 : Long Observation Period

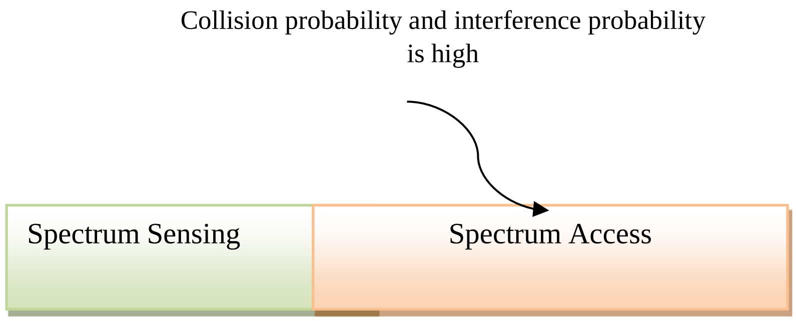

Figure 1.9: Short Observation Period

1.10. SPECTRUM SENSING

Each spectrum access opportunity quality for the unlicensed user depends on duration, SNR, correlation with the other spectrum access opportunities. This information may in accurate and noisy. Artificial Intelligent is applied for better results. In a decision model the transmission duration and SNR of the spectrum as well as the optimization of the throughput and the minimization of interference to the licensed users has to be considered.

In a radio environment where licensed and unlicensed users coexist it is vital the policy which each user follows to be known. In case that all users cooperate for common goal then provided that there are certain limitations information exchange in a distributed manner, negotiation and coordination must be achieved.

In the competitive policy each user aims to optimize the throughput while minimizing the total interference to the licensed users. The optimal decision making is a matter of rest users' activity observation i.e. the need for a distributed algorithm arise.

1.1.1. SPECTRUM TRANSFER

When a licensed user starts transmitting then the unlicensed users have to vacate those frequencies and transfer their transmissions to another spectrum band. For this reason spectrum holes i.e. spectrum vacancies for transmission should be known and this information should available and updated periodically or on demand.

This transfer requires certain time which should be considered by the upper protocol stack levels so to adjust their timers. An adaptive cross-layer framework should be developed.

When this transmission transfer to another spectrum band occurs the target band should be vacant from other unlicensed users too, which is known with the term self-coexistence- synchronization is a matter which should be considered by the Cognitive Radio Medium Access Control Protocol.

1.12. CROSS-LAYER DESIGN

The Cognitive Radio Networks due to their ability to adapt to the radio environment, they need to update information and send messages in a hierarchical layers communication model. The information exchange affects the operation of each layer separately should be dedicated to each one without the intervention of other layers. This may be possible with cross-layer design which would undertake information update.

According to [8] :

The physical layer would adapt power of transmission, modulation, frequency, spectrum band, gain, channel coding, wavelength and rate.

The medium access control level would adapt the packet type, the packet length, the rate, the slot, channel assignment, retransmission probability and protocol.

The network and transport levels would assign routing metrics, algorithms, parameters for congestion control and throughput control.

The application level would assign source coding e.g. for video when the data rate is decreased due to coding.

As the layers' goal may collide, an optimal solution should be achieved each time. This increases complexity and provided that information may be inaccurate, methods which decrease computation complexity of an optimization problem should be explored.

1.13. TOPOLOGY EXPLOITATION

Local transmission information may be updated periodically and exploited by the unlicensed users. GPS is utilized in the form of geolocation databases and local beacons [8] [10].

In the geolocation databases information model the licensed users broadcast the information related to their transmission and geolocation e.g. for TV band there is a base station for unlicensed users which performs channel and slot assignment and forwards this information to the base station of the licensed users for approval.

When local beacon are utilized the base station receives the information periodically from the unlicensed users and this information is broadcasted to them and then they proceed to spectrum access and report to the base station so that a common spectrum management view is maintained.

The geolocation information accuracy will define the level of interference.

Chapter 3

COGNITIVE RADIO NETWORK AND COGNITIVE RADIO NETWORK CLOUD

Cognitive radio is a promising technology that answers the spectrum scarcity problem arising with the growth of usage of wireless networks and mobile services. Cognitive Radio Network Edge Computing will enhance the Cognitive Radio Network (CRN) capabilities and along with some adjustments in its operation and expansion of its operation on all seven layer OSI stack, Cognitive Radio Network Cloud [11] [12] would be feasible and designated as a key technology for 5G and 6G Heterogeneous Network deployment.

1.1. MOBILE CLOUD

Mobile Cloud Computing Forum introduced Cloud Computing leveraging to the Mobile Network. "Mobile Cloud Computing at its simplest refers to an infrastructure where both the data storage and the Data Processing happen outside of the mobile device. Mobile cloud applications move the computing power and data storage away from mobile phones and into the cloud, bringing applications and mobile computing to not just smart phone users but a much broader range of mobile subscribers" - Mobile Cloud Computing Forum (MCC-Forum, 2011).

There are several existing definitions of "Mobile Cloud Computing", and different concepts of the "Mobile Cloud": applications run as thin clients to powerful remote servers on the one hand and on the other hand mobile devices may establish peer-to-peer connections locally with other powerful devices providing resources without the cost of latency and bandwidth issues. These systems are self-organized [13] and they could offload jobs on local mobile resources. A cloudlet may be a cluster of multi-core computers connected to the cloud and if it is not available, the mobile device will have to be served by the cloud. A virtual machine is built in the cloudlet to which the mobile devices connect as thin clients. Open issues are the distribution of processing, storage and networking capacity, the trade-off between QoS and cost for cloudlet providers and security. The CloudClone is another implementation of local service infrastructure that creates a clone of an application. CloudClones do not virtualize native resources.

Mobile Cloud has to address, besides the basic requirements of the cloud, i.e. scalability, availability and self-awareness, the loss of connectivity, mobility and power issues.

Cloud Computing can serve Mobile Cloud in many aspects [13]:

- Extend battery life. Actually remote application execution can save energy up to 45% for numerical computations
- Improve Data storage and processing power
- Improve reliability.

1.2. COGNITIVE RADIO NETWORK CLOUD

Multiple Virtual Machines (VMs) can be deployed in a single platform to share the hardware resources. Traffic can be routed to a VM from a physical interface and from VM back to the physical interface. Cloud and virtualization technologies are key enablers.

The current challenges in Cognitive Radio Network are storing of large amount of data, processing them in real time and the exchanging of nodes' current status on-the-fly. These challenges are in contrast to the limited storage and processing ability (plus battery lifetime) of Cognitive Devices thus the need for additional capabilities arise. Cognitive Radio Network Cloud (CRNC) is an infra-structure consisting of mobile nodes and the cloud whose primary goal is to keep an up-to-date status of the spectrum availability in the network for all (Primary and Secondary Users) to access. The network status will be maintained in the cloud and updated by the networks nodes. The need for intense and accurate sensing made Multiple-Input/Multiple-Output (MIMO) technology appropriate for Cognitive Radio. The large amount of sensing data and processing of MIMO antennae as well as the signal intelligence as a whole can be mitigated to the cloud. Current research on Cognitive Radio Mobile Cloud is limited. In the following paragraphs, a review on the existing research work on this field is presented along with the arising Cognitive Radio Network Cloud challenges and requirements.

A CRNC prototype, as proposed in [13], collects sensing data, processes them in real time, and provides the results to all nodes. So, CRNC should also be able of running the cognition cycle for the network. The nodes will continually report to the cloud their status, store and process their data and plan. Thus the control messages exchange between the mobile nodes will be eliminated and only data transfer will occur.

In [14] the data transfer between a mobile node *A* and *B* will occur after the cloud has reserved the resources in the multi-hop cognitive network path: $A\text{->}C_i\text{->}B$ (where C_i denotes all the rest cognitive nodes in the path) or the data transfer will take place directly between node A and node B as soon as the necessary resources reservation has been made by the cloud. Another issue that will be answered by the cloud architecture is that there will be no data loss upon Primary User arrival.

Actually, there are two options of implementing data transmission:

- the cloud will reserve the resources along the transmission path and then transmission will occur between the wireless nodes without the cloud's interception
- the data will be send to the cloud and then will be copied to the destination node.

In the latter case, there will be no data loss upon Primary User arrival as they will be stored in the cloud instead. The Secondary Users' requests for spectrum access will arrive to the cloud in First Come First Served (FCFS) order but policies can be applied on the queue for implementing QoS classes.

Overlapping, hidden terminal node problem or exposed terminal problem will be avoided [15] as the cloud keeps the geolocation position of each node – the overlapping nodes will be well-known for a given data transmission - whilst the handoff will be seamless. Common Control Channel (CCC) was the solution in ad-hoc networks to handle the coordination and resources management between the nodes as well as the hidden terminal problem. When all the control messages of the network are transmitted via one channel, this make the network vulnerable to congestion and attacks (there are protocols [16] that deal with this problem though); the cloud overcomes the CCC problem.

CRNC should cover both Cognitive Radio (CR) Infrastructure Networks and Cognitive Radio Infrastructure-less Networks (Figure 3.1). Cognitive Radio

Infrastructure-less networks, although they are self-organized and implement distributed resources allocation, still suffer the limited storage, processing ability and power supply. Demanding tasks, e.g. signal intelligence, could be off-loaded to powerful nodes locally allowing the local network to be self-organized. A critical issue in CR Infrastructure-less network deployment on the cloud would be the Standard Interface Operability for CR users to connect to the cloud or local powerful nodes.

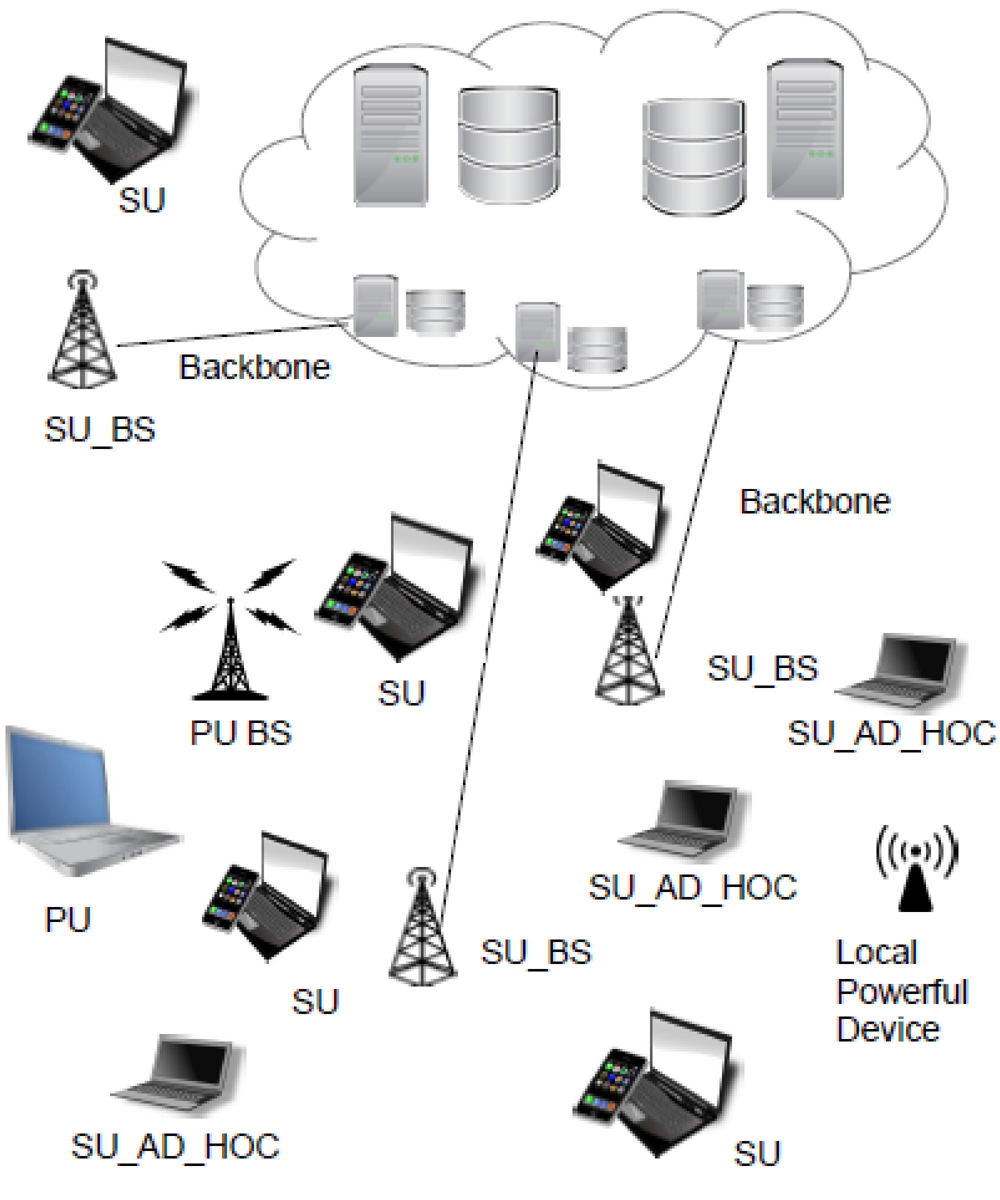

Figure 3.1: The Cognitive Radio Network Cloud

The CRNC should accommodate databases for past experience information and databases for the sensing data. Cognitive Radio use the past experience to learn its environment and plan. The cognitive nodes will connect to cloud front devices playing the broker's role to provide their sensing reports as proposed in [14] or data for processing. Those devices will split data and the processing load to the intermediate cloud computers. There is a tradeoff between the degree of parallelism and the data exchange. In [14] they use a scalable method to partition the geographical area according to the SUs' density in order to eliminate the processing time and then call the Map/Reduce; the time and location are the keys for Map and location the key for Reduce. The Sparse Bayesian Learning Algorithm is used in [14] to estimate the cooperative sensing outcome. The CRNC architecture in [15] includes the Interface, the Controller, the Query Processor, Database and the Knowledge Database. A Game Theoretic Resources Allocation in the CRNC is presented in [17], where the Secondary Users adapt their power in a distributed manner and the greedy behavior is controlled by the cloud manager.

In [18] the geolocation of idle bands and the SUs' transmission requirements such as data rate and the timestamp, are reported to the cloud server. The decision for a channel availability is taken upon the energy detection threshold and the bandwidth threshold. The cloud server reports the available channels to the nodes which then select the channel that satisfies their transmission requirements best. The authors consider both device-to-device and device-to-infrastructure communication. The authors in [19] propose a cloud architecture for Cognitive Radio Networks where the SUs are equipped with a GPS - sensing by the SUs is avoided at all.

The authors in [20] introduce powerful mobile devices which act as resources providers serving the Cognitive Radio Network when the application data size and complexity is below a threshold, otherwise they are served by the cloud. They have also developed a technology called MapReduce on Opportunistic Environments or Opportunistic Cloud to ensure job completion and good performance of MapReduce [21] by building a private cloud where dedicated nodes in the cloud supplement are volatile wireless nodes e.g. in terms of jamming. Cooperative sensing and localization for Power Map reconstruction are proposed in [22] [23].

Multiple-input/multiple-output (MIMO) systems are capable of achieving a capacity gain and/or increasing link robustness in CRN but they increase processing time, energy consumption and processing data amount [24]. In [25] they propose a sub-optimal solution with parallel QR-factorization algorithms to establish an adaptive transmitter system by dynamically selecting the antennae - making use of the parallel computing of the cloud.

Chapter 4

SOFTWARE DEFINED RADIO AND COGNITIVE MEDIUM ACCESS CONTROL ON THE CLOUD

A necessity for a Cognitive Medium Access Control on the Cloud arises: as the Primary Users can utilize the spectrum anytime, continuous sensing and storage of the huge amount of sensing data as well as real-time processing are required. A Mobile Edge Computing architecture and Cognitive Radio Network Virtualization would make feasible Lower layers' Services and Applications that could decrease latency, increase the QoE and security. Lower layer Cognitive Radio Services and applications would increase capabilities not only within the RAN but within local mobile network on a peer-to-peer basis for access and backhauling.

The current challenges in Cognitive Radio Network are storing of large amount of data, processing them in real time and the exchanging of nodes' current status on-the-fly. These challenges are in contrast to the limited storage and processing ability (plus battery lifetime) of Cognitive Devices thus the need for additional capabilities arise. Cognitive Radio Network Cloud (CRNC) is an infra-structure consisting of mobile nodes and the cloud whose primary goal is to keep an up-to-date status of the spectrum availability in the network for all (Primary and Secondary Users) to access. The network status will be maintained in the cloud and updated by the networks nodes.

The need for intense and accurate sensing made Multiple-Input/Multiple-Output (MIMO) technology appropriate for Cognitive Radio. The large amount of sensing data and processing of MIMO antennae as well as the signal intelligence as a whole can be mitigated to the cloud.

A CRNC prototype, as proposed in [11], collects sensing data, processes them in real time, and provides the results to all nodes. So, CRNC should also be able of running the cognition cycle for the network. The nodes will continually report to the cloud their status, store and process their data and plan. Thus the control messages exchange between the mobile nodes will be eliminated and only data transfer will occur.

Actually, there are two options of implementing data transmission:

- the cloud will reserve the resources along the transmission path and then transmission will occur between the wireless nodes without the cloud's interception

- the data will be send to the cloud and then will be copied to the destination node.

In the latter case, there will be no data loss upon Primary User arrival as they will be stored in the cloud instead. The Secondary Users' requests for spectrum access will arrive to the cloud in First Come First Served (FCFS) order but policies can be applied on the queue for implementing QoS classes.

Cognitive Radio Infrastructure-less networks, although they are self-organized and implement distributed resources allocation, still suffer the limited storage, processing ability and power supply. Demanding tasks, e.g. signal intelligence, could be off-loaded to powerful nodes locally allowing the local network to be self-organized. A critical issue in CR Infrastructure-less network deployment on the cloud would be the Standard Interface Operability for CR users to connect to the cloud or local powerful nodes.

The CRNC should accommodate databases for past experience information and databases for the sensing data. Cognitive Radio use the past experience to learn its environment and plan.

The cognitive nodes will connect to cloud front devices playing the broker's role to provide their sensing reports as proposed in [11] or data for processing. Those devices will split data and the processing load to the intermediate cloud computers. There is a tradeoff between the degree of parallelism and the data exchange.

A necessity for a Cognitive Medium Access Control on the Cloud arises: as the Primary Users can utilize the spectrum anytime, continuous sensing and storage of the huge amount of sensing data as well as real-time processing are required. A Mobile Edge Computing architecture and Cognitive Radio Network Virtualization would make feasible Lower layers' Services and Applications that could decrease latency, increase the QoE and security. Lower layer Cognitive Radio Services and applications on the Edge Computing would increase capabilities not only within the RAN but within local mobile network on a peer-to-peer basis for access and backhauling. In the latter case, ad-hoc networks or vehicles would leverage powerful local nodes allowing them to be self-organized.

A proposal for such an architecture is presented in Figure 4.1 with the Cognitive Radio Edge Computing (CREC) Server to offload storage and processing at the Radio

Access Network (RAN) or at the local powerful nodes in the form of access services provision for the Cognitive Radio Network by virtualizing the Cognitive Medium Access Control and SDR functionality and resources and leveraging the connection to the core network and the Cloud connection.

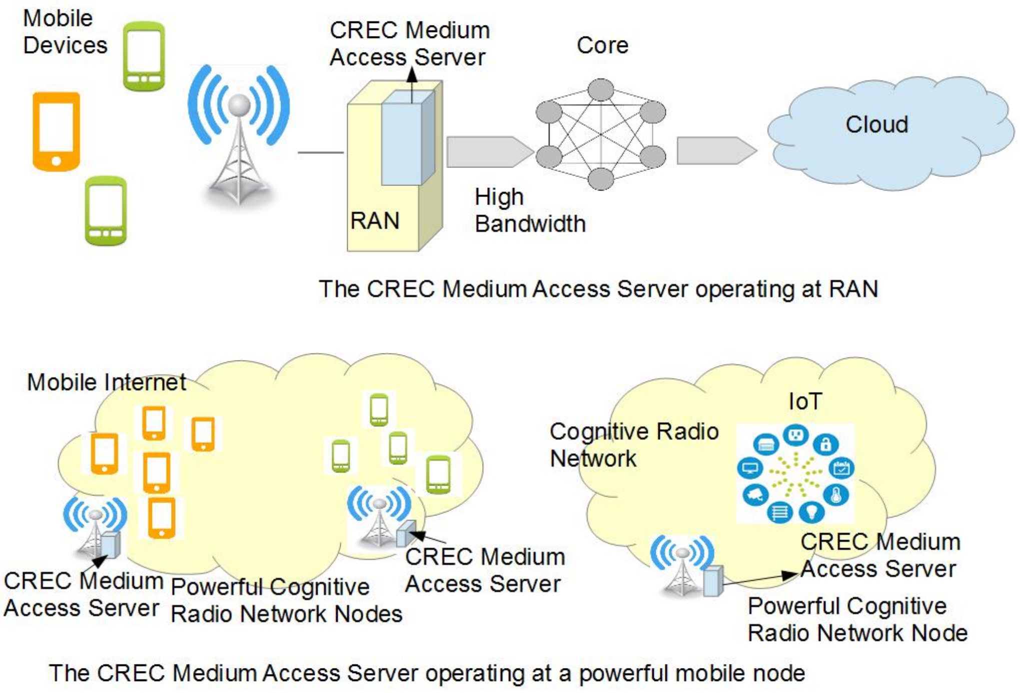

Figure 5.3: The CREC Medium Access Server deployed on the RAN and locally

The Cognitive Medium Access Control is available as a service and adapts to the wireless nodes' requirements. The SU node will run the corresponding Virtual Machine for each Cognitive Medium Access Control service and its application. Virtual Machines communicate via the application platform which run on the server. The server would connect to the cloud for further support. The Cognitive Radio uses the first OSI layer (Software Defined Radio - SDR) and second OSI layer (Cognitive Medium Access Control - CMAC) basically but actually relies on the whole OSI stack and the decisions made in the CRN have to meet the whole network needs. A high degree of interaction takes place within the CRN to achieve optimal network performance.

Cognitive Medium Access Control and SDR Services would utilize upper stack functionality for amongst others QoE which is essential in next generation wireless networks. As next generation wireless networks should respond to an increasing demand of mobile users and mobile applications along with QoE demand for urban and rural radio environments with satellite communications to participate in the communication coverage.

The Cognitive Medium Access Control and SDR Services creation, quality and management would depend on the local network, core network themselves as well as the local radio environment and its interconnection with the surround networks so to speak of an heterogeneous radio environment and network cooperating amongst others to centralize or distribute control over the huge network on demand or not, on-the-fly as well, satisfying the needs of upper stack layers i.e. responding to real life needs of users, providers, organizations etc.

According to the Document WINNF-TS-0008 Version V2.0.0 of Wireless Innovation Forum [26] “an active instance of a service is defined as a running implementation of the service that is connected to the radio application in conformance with the service interface”. However as the definitions of Services as specified by the Wireless Innovation Forum cover up to the network OSI layer demands, the need for more complicated Services as described in the previous paragraph arise in the demanding radio network as oriented by the next generation wireless networks 5G, 6G and satellite communications. Cognitive Medium Access Control and SDR Services integration to achieve a common goal such as higher wireless network performance or higher degree of conceptualization of Cognitive Medium Access Control and SDR Services utilized in the upper stack layers to satisfy the real life needs of users, providers, organizations etc. in the 5G and 6G framework which embody terahertz technologies, visible light communication, sparse theory, new channel coding technology, large scale antenna, Cognitive Radio, special technical issues for Space-Air-Ground-Sea integrated communication and wireless tactile network.

For example Document WINNF-TS-3001 of Wireless Innovation Forum defines the implementation of an “Energy Management Application Programming Interface (EM-API) Figure 4.2 with the objective of making it straight forward to manage energy consumption in Software Defined Systems (SDS), in particular in Software Defined Radios (SDRs) and the platforms with which SDRs may be integrated.

According to WINNF-TS-3001 “the EM-API assumes that an SDS may consist of various components. Such components may include any of the following:

a. an energy source (battery, vehicular power, prime power etc.),

b. a platform (people or vehicles of many different kinds),

c. one or more applications (reasons to exchange voice, video, data) to accomplish some task, and applications may operate embedded inside some device or may reside in a separate unit (like a smart phone),

d. remote controllers (for example a vehicular adapter for a radio, a remote controller for a drone or robot, or a smart display running an application to accomplish something for its user), and/or

e. a software Defined Radio (SDR) or Cognitive Radio (CR)

Furthermore, many such SDSs may interact with each other as a network to accomplish one or more overall objectives, and at the systems of systems level may find adjustment of energy consumption at one location in the network could be desirable to many other system performance metrics.

Often, the adaption mechanisms are also referred to as “knobs” even though these adaption mechanisms are changes internal to the software, not explicitly external knobs to be manipulated by a human.”

Cognitive Radio Medium Access Control and SDR Services integration and deployment on all the OSI layers and 5G and 6G huge and heterogeneous network would require high level of scheduling and interaction which new key technologies [27] e.g. which shorten Transmission Time Interval (TTI) may enable. High level of scheduling and interaction will trigger eventually adaptation “knobs” within the local and global system in the framework of Cognitive Medium Access Control and SDR Services and application and of new abstract Cognitive Medium Access Control and SDR Services and applications for cross-operator, cross-network operability context generation, QoE, radio network demands, cross-operator, cross-border.

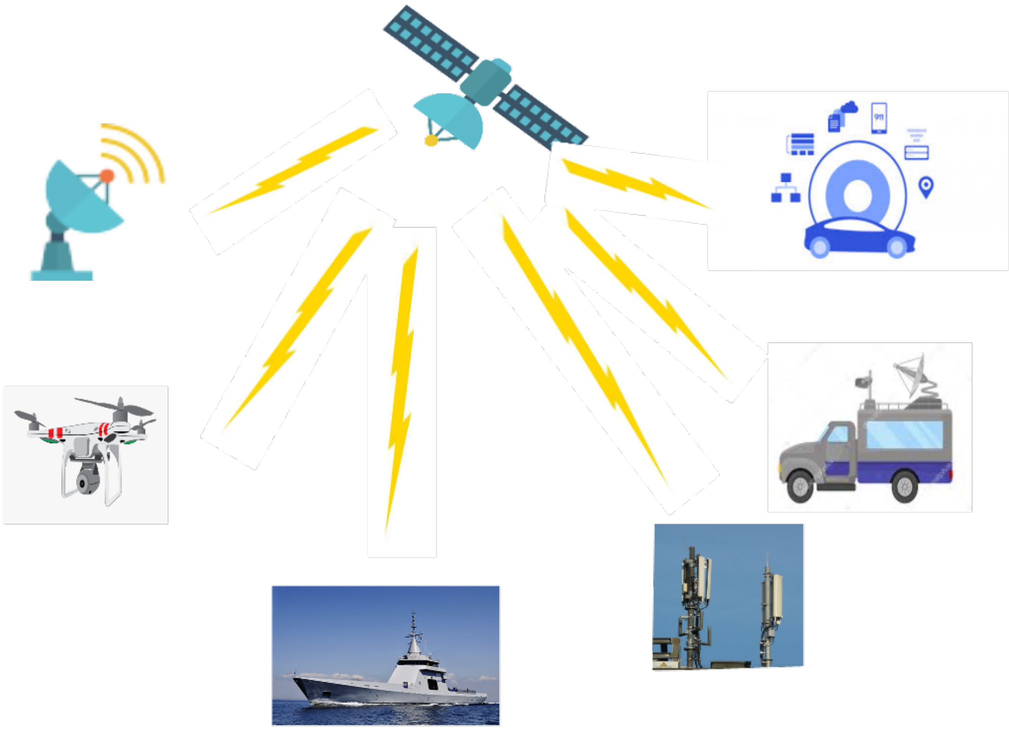

Figure 4.2: Systems of Systems benefits- System Deployment

Chapter 5

COGNITIVE RADIO NETWORK AND NETWORK SERVICE CHAINING TOWARDS 5G: CHALLENGES AND REQUIREMENTS

Cognitive radio is a promising technology that answers the spectrum scarcity problem arising with the growth of usage of wireless networks and mobile services. Cognitive Radio Network Edge Computing will enhance the Cognitive Radio Network (CRN) capabilities and along with some adjustments in its operation will be a key technology for 5G Heterogeneous Network deployment.

Cognitive radio based on the Software Defined Radio (SDR) that can reconfigures its parameters - modulation, frequency etc., it adds a cognitive cycle [11] [12] in order to observe the environment, orient, plan, design, act and learn from past experiences. Cognitive radio senses the spectrum for vacancies, so called “spectrum holes”, for the Cognitive Radio Network (CRN) Users to transmit. In case of the licensed spectrum when the licensed users, i.e. Primary Users (PUs), vacate the spectrum the CRN users, also called Secondary Users (SUs), can access it. There are limitations to the interference the Secondary Users can cause to the Primary Users. On the other hand, the underutilized spectrum resulted in an immense need for Dynamic Spectrum Access that exploits spectrum opportunistically.

Dynamic Spectrum Access includes amongst others sensing, spectrum management, spectrum sharing and spectrum mobility. For spectrum sensing - Primary Users detection - Cognitive Radio uses filter detection, energy detection and feature detection. The spectrum management includes characterization, selection and reconfiguration of the spectrum (channel, modulation, bandwidth, power and transmission time). On appearance of the Primary User, the Secondary User has to vacate the channel immediately and continue transmission in another vacant channel. Spectrum sharing is essential for avoiding overlapping of multiple cognitive radios as well as handoff (loss of connection for mobile Secondary User or poor Quality of Service).

CRN uses machine learning, genetic algorithms, game theory techniques, knowledge representation and optimization techniques for efficient resources allocation. Further, the CRN learns the network conditions [16] and encompasses past experiences to its cognitive cycle [13].

The Cognitive Radio uses the first OSI layer (Software Defined Radio - SDR) and second OSI layer (Cognitive Radio Medium Access Control - CRMAC) basically but actually relies on the whole OSI stack and the decisions made in the CRN have to meet the whole networks needs. A high degree of interaction takes place within the CRN to achieve optimal network performance. Thus, the research work considers Cognitive Radio Cloud and proposes a Cognitive Radio Edge Computing architecture to expand the CRN's capabilities and performance whilst by placing Network Service Chaining for the Access level as a key technology for an increasing Cognitive Radio Access diversity. The proposed solution would support the 5G Heterogeneous Networks as well – an analysis of challenges and requirements of 5G Network is provided to justify the former considerations and proposals within 5G. Although current research work on Cognitive Radio Network Cloud (CRNC) has started to unveil, this research work goes beyond and bypass the existing limitations in Cognitive Radio Network with enhancements on Radio Access capabilities to respond to the vast needs of future Wireless/Mobile Networks - the 5G example was presented.

This chapter is organized as follows: section (II) is an introduction to Mobile Cloud and Mobile Edge Computing, section (III) presents the CRN requirements and challenges, the CRNC, current research work on this field and proposes a server-based architecture for Cognitive Radio Access for Network Service Chaining on the Access Layer Level. Section (IV) is a brief discussion on the 5G requirements and challenges whilst section (V) combines the Cognitive Radio Access Network Service Chaining solution to the 5G Heterogeneous Network deployment.

5.1 MOBILE-EDGE COMPUTING AND NETWORK SERVICE CHAINING

Mobile-edge Computing provides a highly distributed computing environment that can be used to deploy services and delay-sensitive and context-aware applications to be executed in close proximity to mobile users. This creates an ecosystem where new services are developed in and around the base station.

The work of ETSI MEC –RAN aims to provide IT and cloud-computing capabilities within the Radio Access Network (RAN). The key element of Mobile-edge Computing (MEC) is the MEC application server which is integrated at the RAN element. The MEC-RAN provides computing resources, storage capacity, connectivity, and access to user traffic, radio and network information.

Mobile-edge Computing allows cloud application services to be hosted alongside mobile network elements and also facilitates leveraging of the available real-time network and radio information. The MEC-RAN delivers information from the radio network relating to users and cells, and is based on network-layer signaling messages. MEC-RAN also provides measurement and statistics information related to the user plane.

Multiple Virtual Machines (VMs) can be deployed in a single platform to share the hardware resources. Traffic can be routed to a VM from a physical interface and from VM back to the physical interface. Cloud and virtualization technologies (Network Functions Virtualization-NFV) are key enablers for Mobile-edge Computing.

The ETSI MEC-RAN covers network layer signaling only and does not infiltrate to the lower layers. As a consequence, the traffic shaping service is a basic service.

Network service chaining is a key technology enabling automated provisioning of network applications with different characteristics. The “chain” in service chaining represents the services that can be connected across the network using software provisioning. New services can be instantiated as software-only, running on commodity hardware.

Network service chaining capabilities mean that a large number of virtual network functions can be connected together in an NFV environment. Because it’s done in software using virtual circuits, these connections can be set up and torn down as needed with service chain provisioning through the “NFV orchestration layer”.

5.2 COGNITIVE RADIO NETWORK CLOUD

A necessity for a Cognitive Medium Access Control on the Cloud arises: as the Primary Users can utilize the spectrum anytime, continuous sensing and storage of the huge amount of sensing data as well as real-time processing are required. A Mobile Edge Computing architecture and Cognitive Radio Network Virtualization would make feasible Lower layers’ Services and Applications that could decrease latency, increase the QoE and security. Lower layer Cognitive Radio Services and applications on the Edge Computing would increase capabilities not only within the RAN but within local mobile network on a peer-to-peer basis for access and backhauling. In the latter case, ad-hoc networks or vehicles would leverage powerful local nodes allowing them to be self-organized. A proposal for such an architecture is presented in Figure 5.2 with the Cognitive Radio Edge Computing (CREC) Server to offload storage and processing at the Radio Access Network (RAN) or at the local powerful nodes in the form of access services provision for the Cognitive Radio Network by virtualizing the lower layer's functionality and resources and leveraging the connection to the core network and the Cloud connection.

We can distinguish three parts of the CREC Access Server:

- the basic one covers the lower layers' functionality's and resources' virtualization i.e. Software Defined Radio (SDR) and resources, which are infrastructure-oriented
- the application platform that supports the services such as Local Network Access Control, Handover etc. for the applications that would respond to e.g. QoS
- the virtual machines with the applications. Each virtual machine with the application will run at the SU node.

Network Service Chaining allows the creation of new access capabilities and is performed at the application platform. The server may run at a RAN or at a powerful local/wireless node to which other nodes can connect on a peer-to-peer basis (device-to-device communication) reducing latency. The Cognitive Medium Access Control is available as a service and adapts to the wireless nodes' requirements. The SU node will run the corresponding Virtual Machine for each Cognitive Medium Access Control service and its application. Virtual Machines communicate via the application platform which run on the server. The server would connect to the cloud for further support. The proposed architecture is flexible, reduces latency and easily adaptable as more services and applications are adjusted in a simple way.

Services can connect through the network composing a powerful Network Service Chaining for Cognitive Radio Networks controlling access and providing high level QoE to the network users.

The Cognitive Medium Access Control and SDR Services creation, quality and management would depend on the local network, core network themselves as well as the local radio environment and its interconnection with the surround networks so to speak of an heterogeneous radio environment and network cooperating amongst others to centralize or distribute control over the huge network on demand or not, on-the-fly as well, satisfying the needs of upper stack layers i.e. responding to real life needs of users, providers, organizations etc. Cognitive Medium Access Control and SDR Services integration and deployment on all the OSI layers and 5G and 6G huge and heterogeneous network would require high level of scheduling and interaction which new key technologies may enable.

High level of scheduling and interaction will trigger eventually adaptation “knobs” within the local and global system in the framework of Cognitive Medium Access Control and SDR Services and application and of new abstract Cognitive Medium Access Control and SDR Services and applications for cross-operator, cross-network operability context generation, QoE, radio network demands, cross-operator, cross-border.

In Figure 5.4 we can see an CREC Server being part of the RAN and connected to the core network and the Cloud and in the second case being part of powerful nodes operating locally e.g. for an IoT network. In Figure 5.3 (a) we can see the Service, Application Registration and Data sending for computations and processing to the CREC Server operating at a powerful node of a local Network A. Later the CREC Server decides to initiate the handover process for the SU and sends a handover request to the local Network B. The SU is notified and registers to Network B. In Figure 5.4 (b) the Server operates at the RAN and the SU registers its Service and Application and sends Data to the Server for processing. The Server processes the amount of data that are not computationally intensive and the rest are passed to the Cloud for processing. Later a handover process is initiated and the request is passed to the Cloud e.g. to update the network topology database of the Cognitive Radio Network.

5.3 5G - Challenges And Requirements

Mobile networks will become the primary means of network access for person-to-person and person-to-machine connectivity where access to information and data sharing are possible anywhere, anytime. An increasingly diverse set of services, applications and users with diverse requirements and flexible spectrum use of all non-contiguous spectrum would also characterize 5G, 6G technologies. A vastly diverse range of things (IoT) would be connected that imply new functions to be developed. Millions of low cost connected devices and sensors that need to operate on battery would require low energy consumption reduced by a factor of 1000 to improve connected device battery lifetime. 1,000 times the today's traffic volume would be supported in an affordable, sustainable way, cost and energy efficiently.

Next generation wireless-access networks would need to support fiber-like data rates at 10 Gbps to make possible ultra-high definition visual communications and immersive multimedia interactions and support mobile cloud service; 100 Mbps should be generally available whilst 1 Mbps should be the baseline everywhere (Figure 5.1).

Ultra large data rates, latency of one millisecond, always-on users per cell reaching several millions and signaling loads to almost 100% would be included in performance requirements. Another challenges for 5G network are: less than one millisecond latency for real-time mobile applications and communications, maximum ten milliseconds switching time between different radio access technologies for seamless delivery of services would be included, too. On the quest for efficient usage of radio link, modulation techniques like non-linear-multiple-user-pre-coding, joint modulation and coding, physical network coding and advanced physical layer adaptation are tested. For example, Non-Orthogonal-Multiple Access (NOMA) for multiple access which is an intra-cell multi-user multiplexing scheme using the power domain and Faster-Than-Nyquist (FTN) are included in research efforts. Air interface and Radio Access Network (RAN) would accommodate massive capacity, extremely large amount of connections, high speeds for new network deployments. Latency reduction will improve User Experience so techniques such as pre-scheduling, local gateway, local breakout, local server, local cache, shortened Transmission Time Interval (TTI), faster decoding and Quality of Service (QoS) will control network delay, backhaul delay, radio access delay and terminal delay. The new RAT with new numerology - wider subcarrier spacing - will achieve shortened Transmission Time Interval (TTI) and thus reduced latency to 1ms.

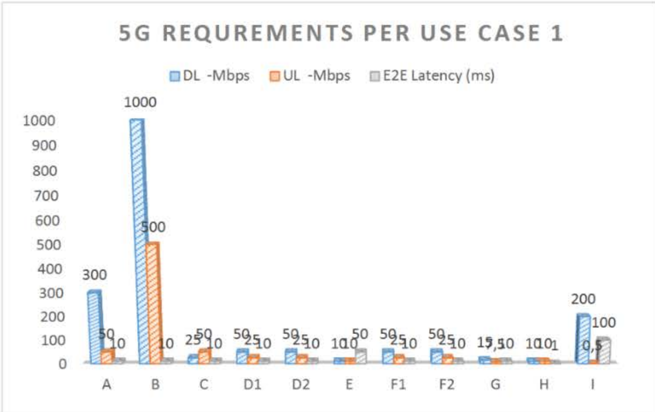

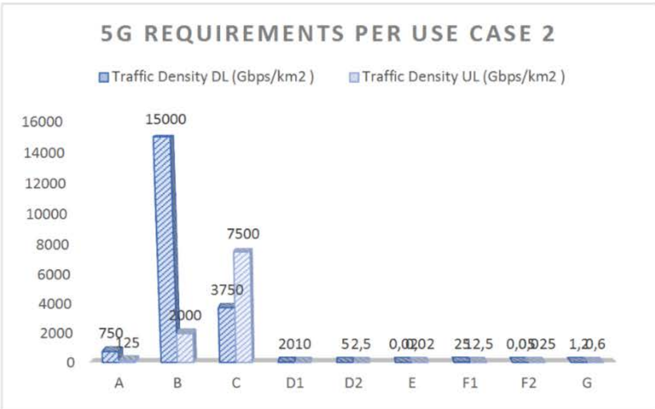

A: Broadband access in dense areas
B: Indoor ulrta high broadband access
C: Broadband access in crowd
D1: 50+Mbps everywhere/suburban
D2: 50+ Mbps everywhre/rural
E: Ultra low cost broadband for ARPU areas
F1: Mobile broadband per train
F2: Mobile broadband per car
G: Airplane connectivity
H: Ultra high reliability -ultra low latency
I: Broadband like services

Figure 5.1: 5G requirements per Use Case

Advanced antenna solutions with multiple elements (massive MIMO) including beam-forming and spatial multiplexing will achieve high data rates and capacity. Massive MIMO technologies experience small interference and consequently higher throughput.

5G unlike previous mobile networks technologies will have to proceed not only to flexible and efficient use of available non—contiguous spectrum but extend the operation range for wireless access into higher frequencies above 10GHz (the spectrum from 10GHz to 100GHz i.e. the mmW range is considered so that the multi-Gbps data rates to be feasible). Advances in waveform technologies, multiple access, coding and modulation would improve spectral efficiency so as to support scalability of massive IoT connectivity and decrease latency. Computationally intensive and adaptive new air interfaces are necessary. Single-frequency full-duplex radios will increase spectrum efficiency, reduce network cost and increase energy efficiency. Plug-and-play will be essential in deployment allowing nodes to self-organize spectrum blocks for access and backhauling.

The extension of mobile devices' capabilities would be necessary for device-based on demand mobile networking for services like device-to-device communications. Advanced device-to-device communication would enhance spectrum efficiency and reduce latency as the offloading of network data locally will minimize processing cost and signaling. A single radio resources could be reused by different groups of users of the cellular network, if the interference occurred within those groups is tolerable. Advanced Small Cell technology will utilize higher frequencies bands taking advantage of the vast bandwidth makes it suitable for dense small cell deployment where massive MIMO will be essential. Furthermore, user-centric Virtual Cells that consist of a group of BSs are introduced for 5G. In-band wireless backhaul can be used between the BSs for cooperative communication reducing cost and complexity for the network backhaul.

Service requirements need to be mapped to the best combinations of frequency and radio resources by spectrum access and programmable air interface technologies. Software Defined Networking and Cloud architectures will enable customization of mobile technologies and QoS guarantees. Cloud computing would allow leveraging of new services and applications and provide on demand processing, storage and network capacity. The cloud will enable seamless connections between people and human-machine and will coordinate network resources for inter-RAT, inter-frequency, inter-site radio access for efficient network management. Virtualization and Software Defined Networking are technologies that can simplify and optimize the 5G network. Multi-Radio Access Technologies (RAT) convergence and intelligent management would lie on the cloud. Not only that but in the 5G, network capabilities such as bandwidth, latency, QoS would be configurable allowing the access to a wider range of services. 5G Network would integrate also existing and heterogeneous networks with diverse requirements.

5.4 CRNC FOR 5G HETEROGENEOUS NETWORK

In general, massive MIMO is an evolving technology of Next generation networks, which is energy efficient, robust, secure and spectrum efficient [25]. According to [25] Massive MIMO technology would:

- improve energy efficiency by 100 times and the capacity of the order of 10 and more
- can be put together with the help of low power and less costly components
- decrease latency on the air interface
- encompass simple multiple access layer
- increase the signal strength against interference. The proposed Cognitive Radio Access Server (Figure 5.3) which is supported by the cloud would be an appropriate architecture for fast processing of the computational load of the Massive MIMO technology.

There are mainly two spectrum sharing techniques that enable mobile broadband systems to share spectrum i.e. distributed solutions and centralized solutions in 5G. Distributed spectrum sharing techniques is more efficient as it can take place in a local framework. Besides the centralized and distributed spectrum sharing considerations, Cognitive Radio with Dynamic Spectrum Management will enhance the network and application performance in 5G. The proposed Cognitive Radio Access Server would accommodate centralized solutions and distributed solutions at local powerful nodes (Figure 5.4, Figure 5.5). Access and Backhauling convergence would be easily deployed. Furthermore, Full-Duplex Cognitive Radios will be empowered to support 5G.

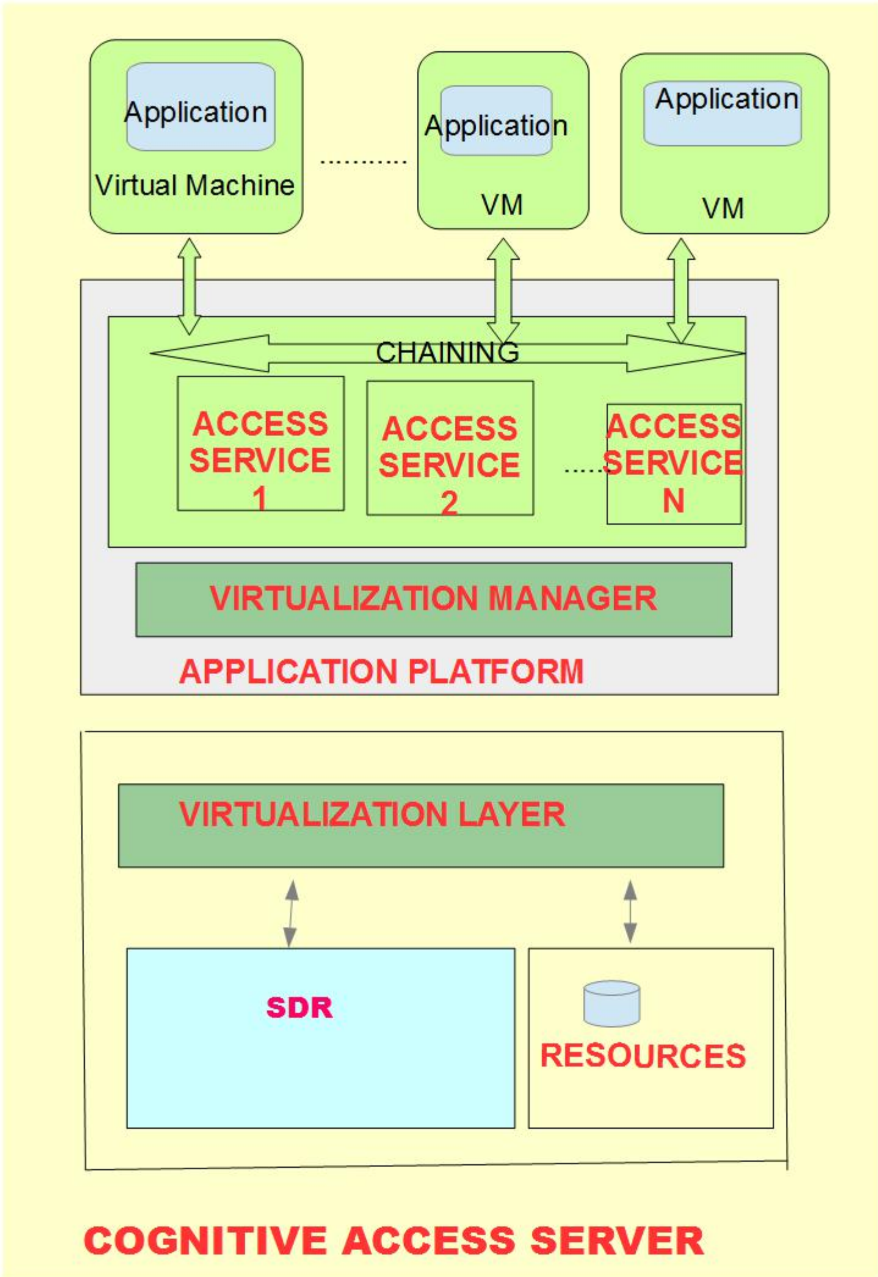

Figure 5.2: The Cognitive Radio Access Server

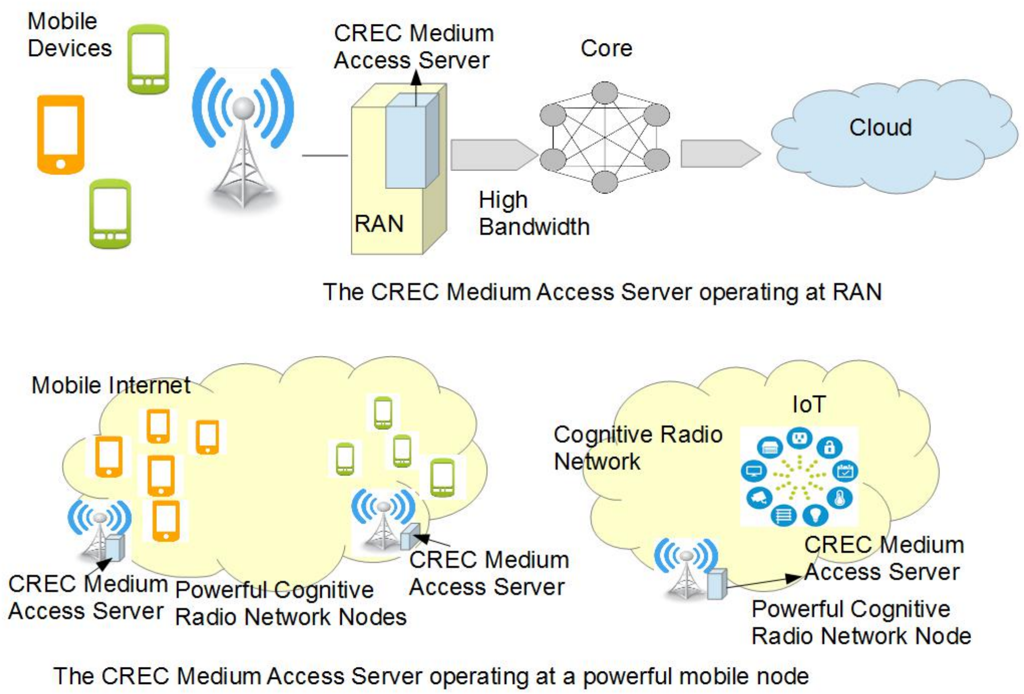

Figure 5.3: The CREC Medium Access Server deployed on the RAN and locally

If a device links directly to another device or apprehends its transmission through the support of other devices, then it will be on the device level (device-to-device communication). So the combined resources of the numerous mobile devices and other available stationary devices in the local area will be exploited. This method supports user mobility and identifies the potential of mobile clouds to perform collective sensing. Cognitive Radio Access as a platform service will enable 5G network to accommodate heterogeneous networks with diverse requirements e.g. for small cell dense environments when the Cognitive Radio Access Server runs the adaptive access services on the local vicinity and wireless backhaul between BSs for

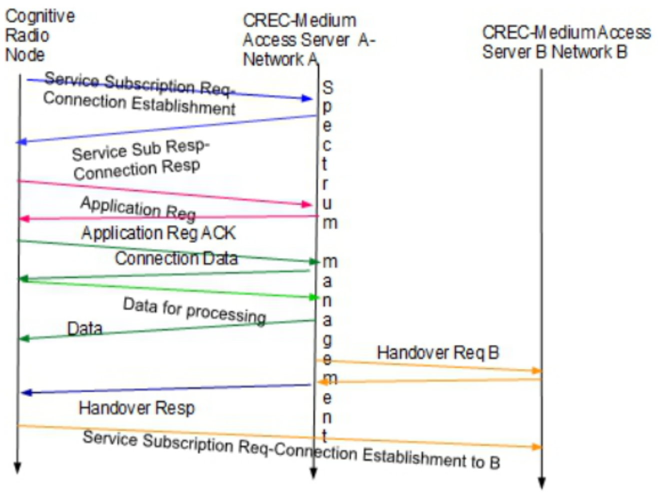

(a) CREC Server operating locally

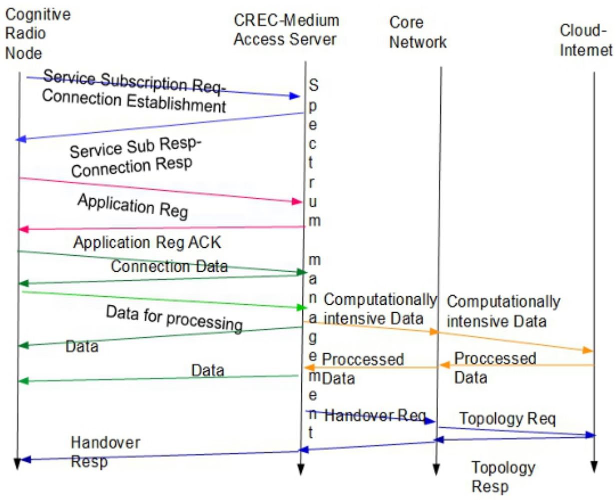

(b) CREC Server operating at the RAN

Figure 5.4: CREC- Medium Access Server operating: a) at a powerful local node; b) on the RAN

cooperative communication. Network Service Chaining would be realized enabling end-user to make best choices, introducing high level QoE based on the enhanced air interfaces and capabilities of 5G signifying a new era in network infrastructures.

5.5 CONCLUSION

This research work [11] makes a revision of Cognitive Radio Network requirements and challenges - including Cognitive Radio Network Cloud, Mobile Edge Computing, Network Service Chaining - and provides a review of current research work on CRNC that would support all the rest. Distributed resources/spectrum management (devices as resources providers), centralized resources/spectrum management (cloud) and processing offloading would be easily feasible with the proposed Cognitive Radio Edge Computing Access Server paradigm. Furthermore, it introduces an Cognitive Radio Access Server which will support the 5G Heterogeneous Network operating as a platform service providing Radio Access accelerating NFV and the dispersion of SDR and CRN MAC functioning to al OSI layers in case of a highly capacity backhaul when the cloud support is needed. Otherwise the resources/spectrum management will be performed locally, effectively enabling Network Service Chaining in end-user-oriented mode in the diverse wireless environment of 5G Network. Thus bypassing its limitations Cognitive Radio Network will respond to the vast needs of future Wireless/Mobile networks - the 5G example was presented.

Chapter 6

SPECTRUM SENSING ALGORITHMS FOR COGNITIVE RADIO NETWORK

A Survey on Spectrum Sensing Algorithms for Cognitive Radio Networks

Cognitive radio (CR) has emerged as one of the most promising candidate solutions to answer the spectrum scarcity problem. Spectrum sensing is an essential task in improving spectrum utilization efficiency. This research work [28] constitutes a brief survey of CR sensing algorithms along with the corresponding CR system characteristics as well as the techniques that enhance sensing parameters. Special attention is paid to the use of sub-Nyquist techniques, including compressive sensing (CS). Conclusions and future challenges in spectrum sensing in CR are further provided.

6.1. INTRODUCTION

CR technology has been proposed as a potential solution to increase the efficiency of underutilized spectrum band allowing opportunistic access to unlicensed users as soon as the licensed users do not transmit or co-exist, thus, when interference imposed to licensed users is below a certain threshold. Spectrum access may rely on a priori knowledge of PU's activities or real time measurement of PU's activity known as spectrum sensing. Reliable spectrum sensing is a key issue in efficient spectrum utilization.

The next motivation for a continued research on spectrum sensing is the creation of the so-called Radio Environment Maps (REM), or other databases designed for storing and processing of the available context information. In the context of 5G or next generation systems historical knowledge, past experience and database information as well as real time spectrum sensing data will define the framework of an efficient spectrum management scheme.

6.2. COOPERATIVE, NON-COOPERATIVE SPECTRUM SENSING

The hidden node problem, shadowing and fading problems degrade the performance of non-cooperative i.e. single node sensing thus making cooperation between the SUs on the spectrum sensing essential for mitigating those effects. In cooperative sensing the SUs perform local sensing and then forward the result to a fusion center where a global decision about PU presence will be made according to a rule and on a decision threshold that will be applied at the fusion center. The selection of fusion center may be centralized, cluster-based, distributed and relay- assisted. The underlay paradigm allows SUs to operate simultaneously with the PUs provided that interference is maintained below a threshold. In overlay systems the secondary users overhear the transmissions of the primary users, then use this information along with sophisticated signal processing and coding techniques to maintain or improve the performance of primary users, while also obtaining some additional bandwidth for their own communication. In interweave systems the secondary users detect the absence of primary user signals in space, time, or frequency, and opportunistically access the spectrum.

There are three important quality metrics that define efficiency of spectrum sensing which are a) the detection probability (Pd) i.e. the probability that the PU is present and the sensing outcome is PU present, b) false alarm probability (Pf) the probability that PU is not present and the sensing outcome is PU present c) misdetection probability i.e. the probability that PU is present and the sensing outcome id not present. Both false alarm and misdetection probabilities degrade sensing efficiency. If the secondary user detects a signal *y(n)*, the decision on spectrum sensing may be given by double hypothesis test:

$$H1: y(n) = x(n) + w(n) \quad (1)$$

$$H0: y(n) = w(n) \quad (2)$$

The $H1$ shows that the primary user's signal $x(n)$ and noise $w(n)$ are present whilst in $H0$ only noise $w(n)$ is present.Then in cooperative mode the SUs sensing outcome may be forwarded to the fusion center as simple bit "1" for PU presence or "0" for PU absence and then a hard decision will be reached which may not be accurate or the sample bits may be forwarded to the fusion center and a soft decision will be reached based on applied rule. The reported message from different SU node is combined by embracing the fusion rule and then building the final decision. Various combining rules (Fusion rules) are used: AND rule, OR rule, Majority rule and K outof N rule. Detection and False alarm probability is calculated globally to get the quality of detection and can be expressed as:

$$Q_D = \sum_{i=K}^{N} (1 - P_D)^{N-i} {P_D}^{i} \qquad (3)$$

$$Q_F = \sum_{i=K}^{N} (1 - P_F)^{N-i} {P_F}^{i} \qquad (4)$$

where, *QD* is the global detection probability, *Qf* is the global false alarm probability. Finally the reporting of global information and global decision on the channel availability to different SU nodes is done. This step may differ depending upon the type of network topology used.

6.3. ALGORITHMS AND PARAMETRS

In Table 6.1 an overview of recent sensing algorithms proposed in literature and their differentiation on the system and algorithm characteristics are presented. Namely, topology and cooperative or non-cooperative sensing, the sensing technique, the hard/soft decision, the rule applied at the fusion node, the optimization of the threshold for the decision to be made at the fusion node, the evolutionarily algorithms or other efficient algorithms that contribute to the final decision, past experience sensing information that may be used, the hardware enhancements such as multiple receiver that increase SNR, the number the SUs, the multiple levels at the PU transmissions and Imperfect of Perfect Channel State Information (CSI) considered by the algorithm are presented.

In many sensing schemes efficient optimization tools such as evolutionary algorithms [29] or immunological computation based on biological immune system have been applied. The differential evolution algorithm arised to a powerful optimization tool applied to many applications as with only few control parameters they solve numerous type problems including multi-objective, multi- constrained optimization problems.

6.4. SPECTRUM SENSING TECHNIQUES

There are various spectrum sensing methods proposed to identify the presence of spectrum hole and optimize the detection probability. The SUs perform spectrum sensing with one of the following methods: on energy detection, cyclostationarity, matched filter, waveform, covariance, Eigen value, wavelet, and spectral estimation.

The energy-detection scheme compares signal with a predefined threshold λ_E to make a decision about PU presence and avoids the need for prior knowledge of the PUs. Both the implementation and computational complexity are relatively

low. A major drawback is that it has poor detection performance under low SNR scenarios, and cannot differentiate between the signals from PUs and the interference from other cognitive radio.

The matched filtering method is an optimal approach for spectrum sensing since it maximizes the signal-to-noise ratio (SNR) in the presence of additive noise. This advantage is achieved by correlating the received signal with a template.

Cyclostationary feature detection detects and distinguishes between different types of primary signals by exploiting their cyclostationary features. This technique is used at very low SNR detection. Wavelet Packet Transform (WPT) technique is based on the decomposition of frequency bands into lower and higher bands at different levels. The signal of interest is primarily of low frequency and noise is of high frequency. After filtration, half of the samples can be neglected according to Nyquist criterion.

Covariance Based Method is based on the fact that the covariance of the wireless signal and the additive noise component is generally different. Filter Bank Method involves a set of bandpass filters for signal analysis. Multitaper Method uses orthonormal Slepian sequences as tapers where tapers indicate the window function. The Slepian sequences have most of the energy of its Fourier Transform is within a given frequency band for a finite sample size. This allows one to trade the spectral resolution for reduced variance of the spectral estimate without leaking signal energy into adjacent bands. Therefore, it is considered one of the suitable techniques for spectrum sensing. In Multiple Antenna Technique, CR receiver is outfitted with multiple antennas to improve the SNR of the received signal. The method is based by Maximal Ratio Combining (MRC) technique. MIMO enhances the performance of the signal detection by sensing at low SNRs.

Topology	Detection Scheme	Cooperative/ Non-Cooperative	Hard/ Soft Decision	Spectrum Access	Rule	Threshold Optimi-zation	#SUs	Evolutio-nary Scheme	Past Exp.	Multiple receiver	Multiple PU transmitting levels	CSI	Refe-rence
Decentralized	-	Non - Cooperative	-	Overlay	-	-	All	Yes	No	No	No	Imperfect	[30]
Centralized	Energy	Cooperative	Soft	Inteweave	-	Yes	All	Yes	No	No	No	Perfect	[31]
Decentralized	Filter Band	Non-Cooperative	-	Interweave	Neyman-Pearson	Yes	All	No	No	Yes	No	Imperfect	[32]
Centralized	Energy	Cooperative/ Non-Cooperative	Hard	Interweave	-	No	On demand	Yes	Yes	No	No	Imperfect	[33]
Centralized	Energy	Cooperative	Hard	Interweave	-	No	All	Yes	No	No	No	Perfect	[34]
Cluster-based	Energy	Cooperative	Soft	Interweave	Non-parametric Bayesian	No	All	No	No	No	No	Imperfect	[35]
Centralized	Energy	Cooperative	Soft	Interweave	Bayesian	No	All	No	No	No	No	Imperfect	[36]
Centralized	Energy	Cooperative	Hard	Interweave	Modified Majority	Yes	All	No	No	No	Yes	Perfect	[37]
Relay	Energy	Cooperative	Soft	Interweave	parametric	No	-	Yes	No	Yes	No	Perfect	[38]
Centralized	Energy	Cooperative	Hard	Interweave	Neyman-Pearson	Soft-valued	All	Yes	No	No	Yes	Imperfect	[39]
Centralized	Energy	Cooperative	Soft	Underlay	Bayesian	Yes	All	Yes	No	No	No	Perfect	[13]
Centralized	Energy	Cooperative	Soft	Interweave	-	Yes	Optimal	No	No	No	No	Perfect	[40]

Table 6.1

6.5. NARROWBAND- WIDEBAND SENSING

The wideband spectrum sensing techniques aim to sense a frequency bandwidth that exceeds the coherence bandwidth of the channel. The wideband signal is sampled by a high sampling rate at ADC, after which a serial-to-parallel conversion circuit is acquired to divide sampled data into parallel data streams. Fast Fourier transform (FFT) converts the wideband signals to the frequency domain. The wideband spectrum is divided into a series of narrowband spectra. Then binary hypotheses tests, where H0 denotes the absence of PUs and H1 denotes the presence of PUs define the spectrum opportunities.

Compressive Sensing (CS) [41] is a novel sampling paradigm which states that it is feasible, with overwhelming probability that a signal is reconstructed based on samples taken but with far fewer samples than those dictated by the traditional well-established Nyquist criterion stating that for accurate signal reconstruction one must adjust sampling rate to be at least twice the highest frequency present in the mathematical expression of the signal. Hence, the sub Nyquist rate that CS theory claims to be adequate for signal reconstruction is directly proportional to the actual signal bandwidth. The signal vector may have all but few elements set to zero (s-sparse signal) or few elements with large magnitude while neglecting the rest of the entries.

CS theory deals with recovering an s-sparse signal vector x of dimensions N×1, s<<N by means of a transformation matrix A of dimensions m×N, thus producing the measurement vector y of dimensions m×1 with m<N. The domain of signal x is called the sparsity domain. The mathematical expression of the above problem is given in (1):

$$\arg\min\|x\|_0 \qquad \text{s.t. } y=Ax \qquad (5)$$

Further notion on finding the appropriate sparsity basis or the use of another l_p norm than the l_0 quasi-norm due to initial problem intractability is beyond the scope of this survey. The rest of this section is dedicated to CS theory applied to CR systems.

The application of CS theory to CR systems is beneficial as in cognitive radio, because of the spectrum underutilization, sparsity condition is valid and transmitted signals are compressible. In cognitive radio the signal sampling should be as fast as possible, even with high dimensional signals to reduce the processing time and accelerate the scanning process. The main benefit introduced by leveraging CS in cognitive radio systems is the ability to sense the same frequency band with fewer samples than those dictated by the traditional methods or a wider frequency band with the same number of samples.

However in practice, there are limitations and challenges imposed on the design of a compressed sensing system related namely with the sensing matrix, sparsity, hardware implementation, uncertainty due to the noisy and interference, recovery uncertainty, and RIP proof [42]. The unstructured nature and randomness of the sensing matrix makes its construction complex, costly, and requires high memory storage. A straightforward problematic issue is that sparsity may not hold in the frequency domain hence finding a proper sparsification matrix is a major issue. Regarding the reconstruction process, the choice of the appropriate method depends on whether accuracy or computational speed is required i.e. when selecting iterative methods for CS recovery. Another scientific issue is considering an approximately sparse signal in the frequency domain, where CS provides an approximation of the sparse solution [42]. Regarding limitations in hardware, the application of CS allows tackling the issue of impractical or costly Analog-to-Digital-Converters for the purpose of wideband spectrum sensing.

Most of the proposed compressive sensing techniques consider the Gaussian noise with known or unknown variance. Besides, interference, high level of noise uncertainty, channel uncertainty, and imperfections degrade the performance of CS in real scenarios [43] [44]. All these are open research issues [45] that have to be answered in order to leverage the potential benefits of CS.

CS application to CR systems can be realized by means of both centralized and distributed techniques. In particular, in the distributed schemes and specifically sensor networks, the capability of simultaneous sensing and compression was investigated in [46].

6.6 CONCLUSION AND FUTURE CHALLENGES

Spectrum sensing is a cornerstone for efficient spectrum utilization in CR and the parameters that define its functionality were discussed in this brief survey. CS theory has been applied in this direction to alleviate computational burden and relieve hardware of impractical requirements in wideband sensing. Some challenges regarding CR systems with CS theory applied are sparsity order estimation given its time varying nature in realistic scenarios. The claim that adaptive learning of this sparsity order can be beneficial could be combined by the fact that in CS theory samples are non-adaptive. There may be a solution to the above contrast. The specification of the desired sparsity basis is another important future challenge. A generic sensing matrix construction is missing from this field as the above matrices have a case dependent characteristic.

The utilization of the huge amount of sensing data and efficient processing as well as historical or past experience data derived by the aforementioned sensing methods along with REMs, the realization of promising techniques such as CS and technologies e.g. MIMO along with improved hardware solutions that meet all requirements and constraints will define the framework of spectrum exploitation in the future CR networks and moreover the 5G and next generation networks.

Chapter 7

MACHINE LEARNING IN COGNITIVE MEDIUM ACCESS CONTROL

A Reinforcement Learning-based Cognitive MAC Protocol

A Multi-Channel Cognitive MAC Protocol for ad-hoc cognitive networks that uses a distributed learning reinforcement scheme is proposed in this research work [16]. The proposed protocol learns the Primary User (PU) traffic characteristics and then selects the best channel to transmit. The scheme, which addresses overlay cognitive networks, avoids collision with the PU nodes and manages to exceed the performance of the less adaptive statistical channel selection schemes in normal and especially bursty traffic environments. The simulation analysis results have shown that the performance of our proposed scheme outperforms that of the CREAM-MAC scheme.

7.1. Introduction

Cognitive Radio was introduced to answer the spectrum scarcity problem. The MAC protocol of a Cognitive Radio network is supposed to enable the so called Secondary Users (SU) network nodes to dynamically access unused or under-utilized licensed spectrum. The licensed users also called Primary Users (PUs) can share the spectrum with the SUs whom can access the spectrum in underlay and overlay mode. In underlay spectrum access the secondary user limits its transmission power below the interference temperature limit so as not to disturb licensed users' transmission. The interference temperature is a metric of the quality of the received signal and includes noise and interference of other sources signals. In the overlay spectrum access, the SUs can only access the spectrum opportunistically at the absence of the PUs. The SUs have to sense the spectrum for vacancies namely "spectrum holes" and decide whether to access the spectrum or not usually based on the PU collision probability.

In the Cognitive Radio Network (CRN), the SUs interfere with each other and this factor, i.e. aggregated interference, has to be considered and estimated. When the number of the SUs and their traffic characteristics are not known, then arises the problem that the common control channel answers. In ad-hoc networks that lack of a central entity, synchronization is difficult and thus has to be addressed by the protocol. Cluster-based architectures were introduced in CRNs to reduce congestion in channel access. These architectures do not share a common control channel.

This research work introduces a MAC Protocol for CR wireless ad-hoc networks for opportunistically spectrum access with a distributed learning reinforcement scheme for channel selection based on SUs observations of PU traffic and with minor computational demands and avoids collisions with the PUs and keeps SUs synchronised.

7.2. RELATED WORK

A scheduling algorithm for multi-hop CR network was proposed in [47] which determines the time slot and channel for transmission by SUs presuming that each SU has a different set of available channels. A heuristic-based distributed algorithm was proposed. It consists of two phases for allocating slots in all channels. In the first one each node chooses the time slot and the channel for each link and in the second this information is propagated in the network and each node makes the necessary adjustments.

The statistical channel allocation MAC (SCA-MAC) [48] employs a control channel and aggregated data channels whilst the selection of the range of channels for transmission is an optimization problem. The protocol outperforms the random scheme. In [49] a cluster-based cognitive radio network was introduced where local traffic can be exchanged through cluster-heads and inter-cluster communication is achieved via the gateway node. There is no common control channel and the role of coordinator for nodes communication is assigned to the cluster head at the communication channel of the cluster-head. Transmission is based on superframes that include a beacon period for synchronization of the cluster heads resource allocation information.

The CREAM-MAC [50] is a protocol based on IEEE 802.11 DCF that limits each channel access time to a value of Tdmax so as to limit the interference to PUs. Protocols that reserve channels for data transmissions similar with the well-known IEEE 802.11 DCF standard are DSA-MAC [51], DCRMAC[8], HC-MAC [52], DDMAC [53], SMA[54].

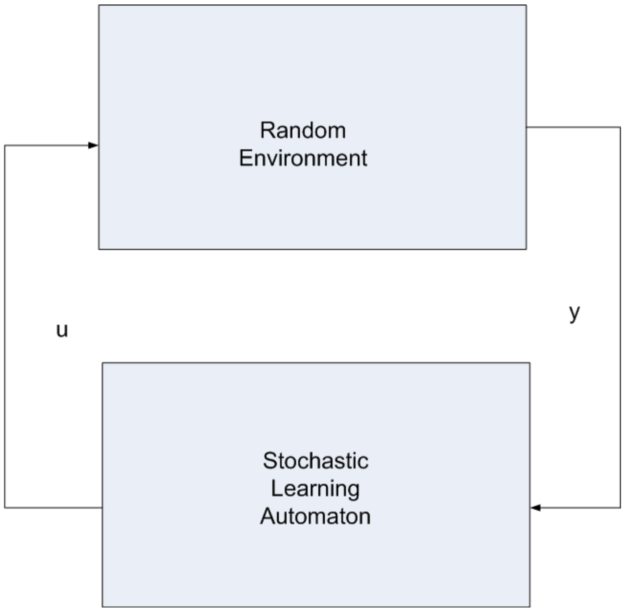

Figure 7.1. A stochastic learning automaton

7.3. PRIMARY AND SUs MODEL AND PROTOCOL DESCRIPTION

7.3.1. STOCHASTIC AUTOMATA AND REINFORCEMENT LEARNING

A Learning Automaton is a control mechanism that follows a predetermined sequence of operations or adapts to changes in the environment. The adaptation is the result of the learning process i.e. the permanent change in the learning automaton behavior toward a final goal as a result of the past experience. The term stochastic refers to the adaptive nature of the learning automaton. A stochastic automaton has no information of the optimal action, but selects an action randomly then the environment is observed and the action probability is updated based on the response from the environment. This procedure is repeated and the algorithm that guarantees the desired learning process is called a reinforcement scheme.

Let $w1, w2, .. w_m$ be the mutually exclusive responses of the environment, Pi the probability of the occurrence of the i^{th} response, then the reinforcement scheme of the Learning automaton can be described as:

$Pi(n+1) = \lambda Pi(n) + (1-\lambda)a_i(n)$ *n=0,1,2 (1)*

Where $Pi(n)$ is the probability of the occurrence of the i^{th} response on time n for the x_i input.

$$0 < \lambda < 1, 0 < \alpha_i(n) \leq 1$$
$$\sum_{i=1}^{m} a_i(n) = 1 \qquad (2)$$

Equation (1) describes a linear reinforcement scheme and it can be easily shown that if $\alpha_i(n)=\alpha_i$ then:

$$P_i(n+1) = \lambda^n P_n(0) + (1-\lambda^n)a_i \qquad (3)$$

And $\lim_{n\to\infty} P_i(n) = a_i \qquad (4)$

The reinforcement learning can be formulated by learning automata. A stochastic learning automaton operating in a random environment is shown in Figure 7.1. At each step, the random environment provides a feedback of satisfactory or unsatisfactory performance to the stochastic learning automaton known as a penalty $y = 0$ with probability $1\text{-}\pi_i$ and $y = 1$ with probability π_i respectively.

A stochastic learning automaton is a quintuple {Y,Q,U,F,G} where Y is the environment response set and it consists of only two elements i.e. If it takes 0 then is said P-Model, if it takes finite number values in the range [0,1] then is said Q-Model and if it takes arbitrary numbers in the range
[0,1] then is said S-Model. Q is the finite set of states Q={$q1,q2,\ldots qs$}, U is the finite set of the stochastic learning automaton outputs U={$u_1,u_2,\ldots,u_m$}, F is the state transition function q(n+1)=F[y(n), q(n)] and G is the u(n)=G[q(n)]. The function G can be either stochastic or deterministic whilst function F is stochastic and this stochastic nature of learning automata makes them suitable for learning systems.

If $Imin$=min{π_1, $\pi_2,\ldots,\pi_m$} then the optimal output of the stochastic learning automaton is u_β and the reinforcement scheme is said optimal if

$$\lim_{n\to\infty} \mathbb{E}\{P_\beta(n)\} = 1 \qquad (5)$$

The reinforcement scheme is said $\in -optimal$ if

$$\lim_{\lambda \to 0} \lim_{n \to \infty} \mathbb{E}\{P_\beta(n)\} = 1 \quad (6)$$

And $\in -optimality$ ensures that the operation of the stochastic learning automaton is very close to optimality, where λ is the learning rate.

7.3.2. TRANSMISSION OPPORTUNITY DETECTION

We assume a wireless network of CR-enabled nodes equipped with a radio dedicated to the common control channel, a radio for data transmission and sensors for channel sensing. The spectrum licensed to PUs consists of *M* channels. The nodes' transceivers can operate to any of the *M* channels. According to the sensing outcome of each sensing period, a state is assigned to each channel. The ON state represents that the PU transmit state and the OFF state means the SUs can opportunistically access the channel. A vector *state[i]* maps the state of each channel.

Presuming that the traffic of PUs comes in bursts, the SUs have to detect those opportunities in spectrum that are "good" i.e. they are mostly likely for successful transmission as they will not be interrupted. Due to the burstyness of its traffic, a PU which transmits during a sensing slot, most likely will transmit during the next sensing slot in order to complete its transmission.

To learn the burstyness of PUs' traffic, each SU employs a learning automata mechanism for each channel *i*. The mechanism in [12] estimates the probability *P[i,t] that* channel *i* will be occupied via PU transmission at time *t* (where *t* is measured in sensing slots).

After each sensing period, this probability is updated according to the following scheme:

- If channel *i* is occupied by a PU, then P *[i,t*] is increased: *P[i,t+1] =P[i,t] +L*(1-P[i,t])* (7)
- If channel *i* is occupied by PU, then *P[i,t]* is decreased: *P[i,t+1] =P[i,t] - L*(P[i,t] -α)* (8)

It holds that *L,α* ∈ *(0,1)* and *P[i,t]* ∈ *(α,1)* ∀ *i,t. L* is a parameter that governs the speed of the automaton(7)(8) convergence.

The lower the value of L, the more accurate the estimation made by the automaton; a fact that comes at the expense of convergence speed. Parameter "α" prevents the probabilities *P[i,t]* from taking values in the neighborhood of zero and thus increases the adaptivity of the automaton.

After estimating the channel usage made by the PUs, the protocol has to identify transmission opportunities for the secondary ones. Thus, the probability that a SU at channel I can transmit is then equal to *S[i,t] =1-P[i,t]*. We update (7) and (8) with S[i, t+1]=1-P[i, t+1] and S[i]=1-P[i]. We have the following linear reinforcement scheme for the stochastic learning automaton of P-Model:

- If channel *i* is not occupied by a PU, then S *[i,t]* is increased: *S[i,t+1] =S[i,t] (1-L)+L*(1- a) (9)*

- If channel *i* is occupied by PU, then *S[i,t]* is decreased: *S[i,t+1] =S[i,t] (1-L) (10)*

The probabilities *S[i,t+1]* are updated at the end of each sensing slot. As (1-α) is constant according to (1), (3), (4) and due to the use of very small value (i.e. 10^{-4}) for parameter α mentioned above(7)(8)(9), during the burst of the licensed user at channel i, the S*[i,t]* will approach zero whilst during a spectrum hole on the channel, it will approach *(1-α).* For very small values of α and according to (5):

$$\lim_{t\to\infty} \mathbb{E}\{S[i,t]\} = \mathbb{E}\{\lim_{t\to\infty} S[i,t]\} = 1 \qquad (11)$$

Thus the channel selection learning reinforcement scheme is optimal for very small values of α. An opportunity discover function provides the SU with the best selection metric i.e. the first channel in S*[i,t]* that is also idle according to *state[i]* . The algorithm decreases the selection probability of channel *i*, if it is occupied by a PU during the last sensing slot and increases the selection probability of channel *i*, if the channel is not occupied by a PU. As PU traffic comes in bursts the selection probability of channel *i* keeps decreasing. On the other hand, as the spectrum holes are contiguous, the selection probability will increase when the PU is not transmitting on channel *i*.

This paper introduces an architecture where the SUs form clusters of nodes which experience the same PUs presence and local traffic can be exchanged within the cluster whilst remote traffic is achieved by the inter-cluster communication. A common control channel answers the problem of aggregated interference uncertainty. The protocol introduced in this paper employs a common control channel for resource reservation per cluster in order to limit the aggregated interference of SUs and to handle the hidden terminal and multi-channel hidden terminal problems. The common control channel is dynamically selected as the most reliable and with the best selection metric.

The proposed protocol relies on the synchronization achieved within the cluster by the use of the distributed scheme as the sender and receiver experience the presence of the same PUs and they share the same channel selection probabilities. As there are no collisions between SUs and PUs, transmissions are identified and SUs are synchronized. For spectrum sensing, energy detection and cyclostationary feature detection can be employed.

7.3.3. SPECTRUM SENSING INACCURACY

If spectrum sensing is not accurate then the selection metric S[i,t+1] is modified by the term:

$$S'[i,t+1] = S[i,t+1] + L(1-\alpha)(1-L)^{N+1} \quad (12)$$
$$S'[i,t+1] = S[i,t+1] - L(1-a)(1-L)^{N+1} \quad (13)$$

The equations above stand for PU misdetection and false alarm cases. In PU misdetection the selection metric is updated wrongly according to equation (9) for N slots in the sequence –as long as faulty sensing occurs- and then as the system seems to overcome misdetection, the selection update is done according to equation (10). Thus, we have an increase

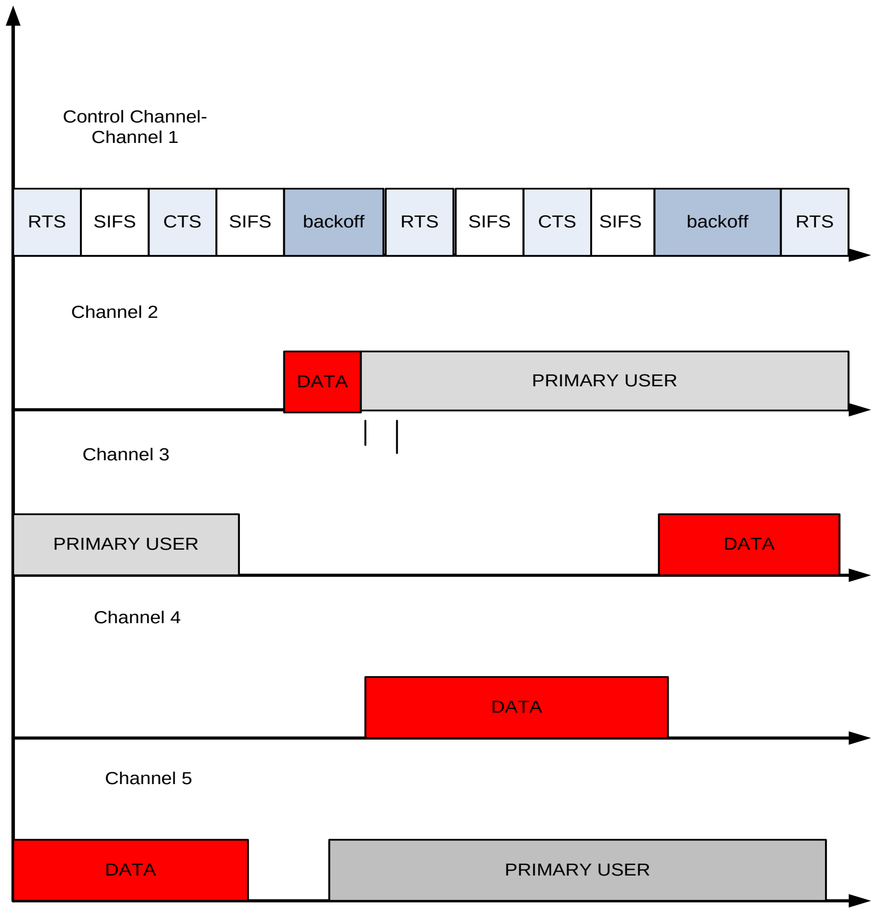

Figure 7.

2. Example of the proposed protocol operation

in the term as appearing in equation (12). On the other hand, false alarm causes a selection metric update for N sensing slots in a sequence according to equation (10) and then the system overcomes false alarm by persistent updating the selection metric according to equation (9). Hence, we have again a decrease in the value of the selection metric by the term appearing at equation (13).

The limit of the error term is zero:

$$\lim_{N\to\infty} L(1-\alpha)(1-L)^{N+1} = 0 \qquad (14)$$

Thus for higher values of L the error term reaches very small values around 10^{-4} in a few slots. The proposed reinforcement learning scheme can operate in inaccurate sensing conditions as the system overcomes inaccurate sensing easily when the value of *L* is high.

7.3.4. SUS CHANNEL ACCESS

The control packets are namely ReadyToSend / ClearToSend/ACKnowledgement. The ACKnowlegdement is returned to the sender at the successful completion of data transfer on the data channel. In case of unsuccessful handshake binary exponential back-off is invoked. The SU that wants to transmit and finds the control channel busy backs off for a period of 2^{CW} **Min_Waiting_Period* where *CW* is the contention window and *Min_Waiting_Period* is the minimal backoff period.

The whole handshake procedure for data channel reservation is shown in Fig. 2 for each user that wins the contention. If data transmission is interrupted by the PU presence then data transmission continues in the first available channel provided by the opportunity discover function. On successful data reception an ACK message is returned to the sender via the data channel.

The RTS/CTS messages between the nodes of the same cluster do not include the available channels on each node as they experience the presence of the same PUs. The nodes remain synchronized with the learning automata and so the RTS/CTS messages hold other information useful for cluster operations e.g. for cluster orientation.

Cluster operations are the necessary functions taking places in the control channel and they are responsible for the cluster orientation, neighborhood orientation, the voting process for the selection of the control channel. When the quality of the control channel drops or PU presence occurs and remains so for at least period Tc, a voting process based on both the quality of the signal and the learning reinforcement scheme metric will determine the next control channel of the cluster. Upon collapse of CC the cluster e.g. due to jamming, nodes will mitigate to the next channel with the better metric of all channels.

The cluster synchronization is necessary when a node entering the cluster or experiencing synchronization problems e.g. at the limits of the cluster, thus wants to synchronize itself with the rest of the cluster, they will be supported by the cluster via the control messages. The nodes will demonstrate their cluster orientation information within their RTS/CTS messages. Each cluster operation is related to a certain field update with the appropriate information in the control messages.

Neighboring clusters neither can share the same control channel nor allow data transmission on the control channels of their neighboring clusters. They cannot share the same control channel in order to allow nodes belonging to different clusters to communicate avoiding overlapping. Furthermore, data transmission with no collisions on the non-control channels is guaranteed by the control messages whilst the communication on the control channel can be guaranteed if the nodes of the neighboring clusters do not interfere with the control channel operation i.e. no data transmission can take place at a channel that operates as control channel of a neighboring cluster.

SUs on different clusters communicate asynchronously-i.e. they have to agree upon data transmission channel- at the receiver's Control Channel.

7.4. PERFORMANCE EVALUATION

We used simulation analysis in order to evaluate the performance of the proposed protocol. The OMNET package was used. As our main goal is to show the superiority of learning PUs' traffic characteristics for identifying transmission opportunities, we compared the performance of the proposed scheme with that of CREAM-MAC [6], which identifies transmission opportunities via gathering statistics on licensed channels usage by PUs. The simulation parameters of CREAM-MAC were identical with those of the paper [51] experiment. The parameters used in our simulations are: transmission rate of 2Mbps per channel, 30 SUs, 30 channels and PUs activity which follows the exponential distribution. The proposed protocol is compared to CREAM-MAC for a maximum interference period Tdmax = 10msec in terms of aggregate throughput (Figure. 7.3,7.4,7.5), access delay (Figure. 7.7) and collision with the PU ratio (Figure 7.8). The data packet length is assumed to be 20,000 bits and *Min_Waiting_Period* is assumed to be 10ms. A one cluster architecture was simulated for the proposed protocol.

In all the experiments the Learning Automata-based Multi-Channel Cognitive MAC outperforms the CREAM-MAC.

In the former two experiments (see Figure 7.2, and Figure 7.3) the aggregated throughput is studied for different PU burst lengths when the bursts are generated every 2s and 0.1s

However the proposed protocol seems to be less affected by the changes in PU burst length as it utilizes the most of the spectrum holes for every PU burst generation rate that learns, something that does not hold for CREAM-MAC as its performance drops significantly by the PU burst length.

In the third experiment(Figure 7.5) the aggregated throughput is studied for different PU burst arrival rates when the PU burst length is 100,000 bits.. The fourth experiment (Figure 7.6) follows the results of the third experiment and studies the SU channel utilization for different PU burst arrival rates and PU burst length equal to 100,000 bits. As the PU burst generation rate increases, the difference in performance of the two protocols also increases. This is due to the increase of the collisions with the licensed users that CREAM-MAC cannot predict; whereas these are avoided by our proposed protocol.

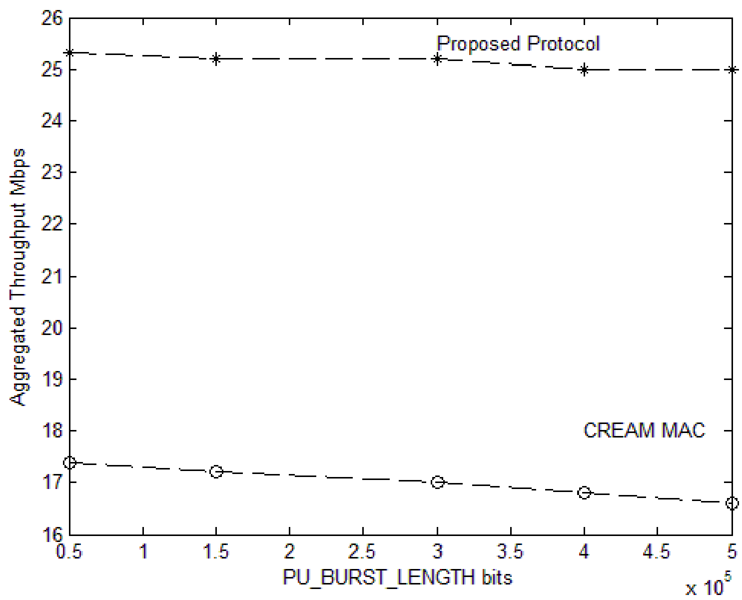

Figure 7.3. The aggregated throughput versus the PU burst length for burst generation every 2s.

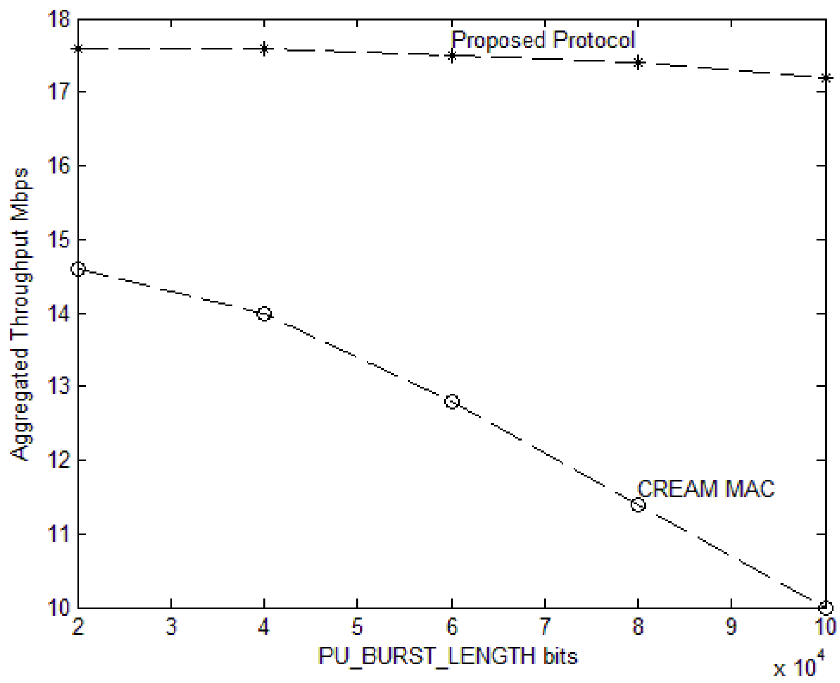

Figure 7.4. The aggregated throughput versus PU burst length for burst generation every 0.1s.

The access delay was studied for different PU burst arrival rates (Figure 7.7) with PU burst length of 100,000 bits. As the PU burst mean arrival rate increases, the variance of the PU traffic distribution decreases. Then the mean arrival rate of the statistics becomes better metric for the PU traffic and thus the performance of CREAM-MAC increases in terms of access delay.

In the last experiment the burst length equals 100,000 bits (Figure 7.8). According to the results, the proposed protocol predicts and avoids completely collisions with the PUs.

The main reason behind the superiority of the proposed protocol compared to CREAM-MAC, is that the former learns the PUs’ traffic-PU traffic distribution characteristics and burst As the Learning Reinforcement Scheme is optimal there is no collision with the PU packets. The statistics metrics seem inefficient as they do not avoid collision with the PU and they do not utilize sufficiently the spectrum holes; the CREAM-MAC does not differentiate its response to long and short spectrum holes, i.e. in the former

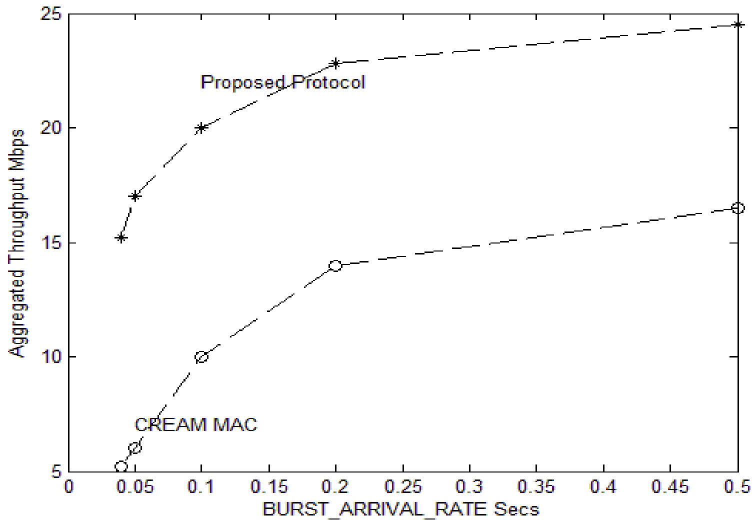

Figure 5: The aggregated throughput versus the burst arrival rate.

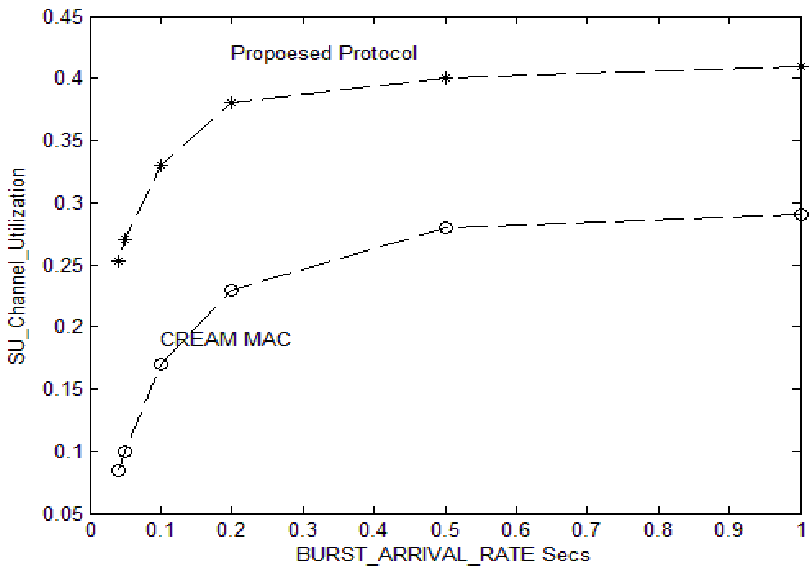

Figure 7.6. The SU channel utilization versus burst arrival rate.

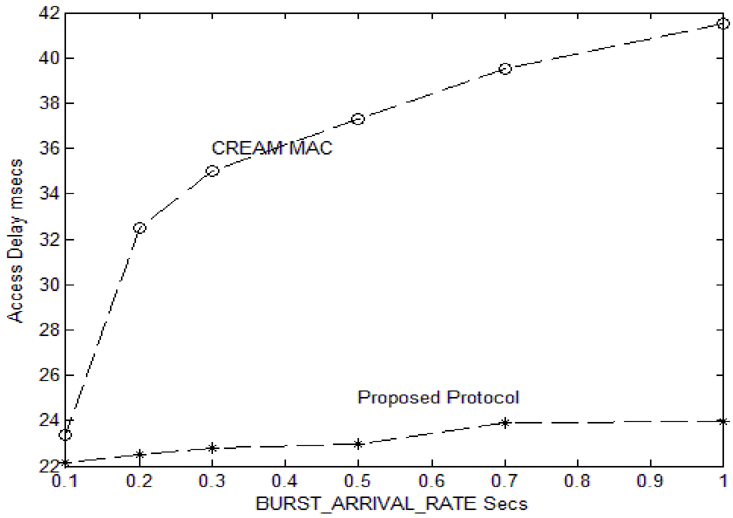

Figure 7.7: The access delay versus the burst arrival rate.

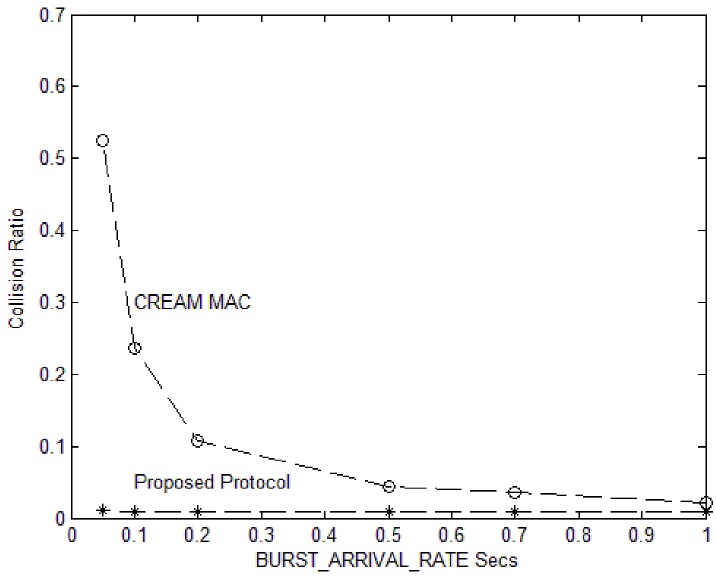

Figure 7.8. The collision ratio versus the burst arrival rate

case it bypasses opportunities and in the latter it does not avoid collision. The statistics do not overtake opportunities on the channels with the worse statistics when they experience longer spectrum vacancies due to PU-traffic distribution variance. The statistics do not respond promptly to the network conditions.

7.5. CONCLUSION

Most of the proposed MAC protocols reported in the literature utilize statistics on spectrum usage in licensed channels so as to identify transmission opportunities over these channels for SUs. However, using these statistics does not capture the fact that, nowadays, most traffic is of bursty nature; something that is not exploited in the identification of transmission opportunities. This research work proposes a Multi-Channel Cognitive MAC Protocol for ad-hoc cognitive networks that uses a reinforcement learning scheme for channel selection and access based on observations of PUs traffic. The protocol learns the bursty nature of PUs' traffic to exceed the performance of the less adaptive statistical channel selection scheme as statistics change only when the PUs traffic pattern scheme changes and avoid collision with the PUs. The proposed scheme is shown to have better performance compared to the transmission opportunities via a statistics mechanism and avoids collision with the PUs. In the future work QoS will be considered in accordance with the proposed scheme.

Chapter 8

THE HETEROGENEOUS COGNITIVE RADIO NETWORK IS SUPPORTED BY SOFTWARE DEFINED NETWORK

SDN-based QoS Provisioning and Interference Management in Heterogeneous CRN

Cognitive Radio is a promising technology to maximize spectrum efficiency that can be applied to dense residential infrastructure and heterogeneous networks. This research work [59] proposes a Software Defined Networking (SDN) system model for coordinated adaptive spectrum sharing and interference management; the SDN system model leverages the fact that Primary User (PU) network traffic is bursty with an optimal reinforcement learning scheme and takes into account network topology information and data rate requirements of active flows. The scheme learns PU traffic, and as a result, it optimizes spectrum brokerage to the active flows for QoS provisioning and performs interference mitigation.

8.1. INTRODUCTION

Cognitive Radio (CR) is a promising technology used to maximize spectrum efficiency through opportunistic spectrum access; i.e., Cognitive Radio Users-Secondary Users (SUs) access the underutilized licensed spectrum when it is vacated by the Licensed Users (Primary Users). Due to rapid increase in the number of smart mobile devices, heterogeneous small cell networks for residential areas come to answer this need allowing high quality voice, data and multimedia services to mobile devices indoors. Heterogeneous Cognitive Networks (HCN) with multiple base station tiers are necessary to meet the high data rates. Critical issues in HCN are interference between overlapping Cognitive Base Stations and interference between Cognitive Cells and Primary Users (PU).

There are major challenges to this scheme such as i) autonomous cross-tier and intra-tier interference mitigation and ii) full radio resource exploitation. Any uncoordinated spectrum access will result in interference between SUs and hence result in a low spectral efficiency [60].

A Software Defined Network (SDN) controller may solve the spectrum allocation problem and find an optimal interference free spectrum assignment such that the throughput of all active flows, active virtual circuits, is maximized. This paper focuses on SU co-existence schemes in infrastructure and infrastructure-less environments as soon as the latter facilitate a connection, i.e., a node connected to SDN that would play the role of coordinator and would operate as a self-organized network for information distribution.

In this research work, an SDN-based Cognitive Radio architecture for residential networks is introduced that leverages the fact that the network traffic comes in bursts currently. The proposed scheme which enhances the MAC layer capabilities which role is crucial in the SDN network. The system employs an optimal reinforcement learning scheme and satisfies data rate requirements of active flows maximizes the minimum data rate per active flow, performs interference mitigation and has high performance according to the comparative study. To the best of the authors knowledge there is only another one research work for spectrum brokerage and interference management in residential SDN CR networks which the proposed research work outperforms.

The rest of the chapter is organized as follows. Section II references related work. Section III presents the system model. Section IV presents the reinforcement learning scheme, while Section V the proposed system. In Section VI the simulation results are presented. The cloud-based SDN controller manages interference, while the Reinforcement Learning Scheme learns PU traffic and good transmission opportunities; as a result, the Reinforcement Learning Scheme outperforms spectrum brokerage in [61].

8.2. RELATED WORK

In [61], a spectrum allocation based on the active flows as defined by OpenFlow for secure channels and interference for dense residential areas is presented. To the best of our knowledge, this paper is the only research work that performs spectrum brokerage based on active-flows, so a comparative study with [61] was straightforward. In [62], a strategic game is developed for the intra-tier interference mitigation only, and this proposed scheme achieves required statistical delay guarantees.

The user association problem in the heterogeneous cognitive networks is studied in [63], but it does not consider active flows, too. In [64], the authors proposed a control algorithm for cooperation under both the relay model and the interference model. In [65] an SDN architecture is introduced where there is no a spectrum brokerage scheme, but the CR-User Equipments (UEs) might ask for an extension of the requested time.

The work presented in [66] is an integration of an IP based cognitive network and an OpenFlow enabled fully functional WLAN into an SDN core.

8.3. SYSTEM MODEL

This paper introduces an SDN-Medium Access Control (MAC) operating in Infrastructure and Infrastructure-less, i.e., two-tier Heterogeneous Network. In the former case, a Cognitive Radio Base Station (CR-BS) serves a number of End-User Equipment (CR-UEs), and in the latter case, a multi-tier node serves the ad hoc network nodes. In the rest of the paper, the terms BS/coordinator, CR-UE/ad hoc network nodes will be used within the system model as soon as OpenFlow interfaces exist. The CR-BSs are connected to the Internet via a wired technology and the SDN controller for secure connections. The CR-BSs are deployed in dense residential areas, and this is the reason that CR-BSs may be stand-alone or collocated with other CR-BSs. In the former case, the CR-BS must handle interference with the Primary User only, while in the latter case, it must handle both interference with the PUs and interference with other CR-BSs. The communication between neighboring CR-BSs is limited to beacon exchange for neighbor discovery.

The CR-BSs are connected to the cloud, where an SDN controller manages interference, coordinates the spectrum sharing in the Cognitive Radio Network of CR-BSs and ensures that all CR-BSs in interference range are separated in frequency. According to network topology, the same controller controls collocated cells. Each Cognitive Device i.e., CR-UE, listens to these beacons, measures the signals and then connects to the CR-BS with the best receiving signal. Each CR-UE is associated with a CR-BS, and this information is sent to the SDN. In collocated CR-BSs, each CR-UE belongs to one CR-BS, and the SDN controller in the cloud manages interference.

Spectrum sensing and interference measurement are performed in each Cognitive Radio Cell. As a CR-BS and its CR-UEs are in short distance, spectrum sensing is performed by the CR-BS offloading the end devices. Each CR-BS runs a Reinforcement Learning Scheme to learn and adapt to the PU traffic that prioritizes channel use, based on their provision of “good” transmission opportunities; i.e., the transmission would not be interrupted by PU arrival. The PU traffic comes in bursts, and this traffic is leveraged by the Reinforcement Learning Scheme to avoid interference with the PU.

The controller receives updates of the changing network traffic and interference conditions and coordinates channel sharing in time between the active flows of the cells. As PU traffic is bursty, a priority of the channel list changes in sufficient time intervals that do not degrade the performance of the system.

8.4. PU COLLISION AVOIDANCE

A Reinforcement Learning Scheme for spectrum management is introduced to avoid interference with PU and find a good transmission opportunity, i.e., one in which the SU transmission will not collide with the PU. The stochastic learning automaton of the P-Model of the scheme runs on each CR-BS as described below:

• If channel i is not occupied by a PU, the sensing outcome is 0 at sensing slot t; then the metric of probability of good transmission opportunity for channel i, $S\ [i,t]$ is increased:

$$S[i,t+1] = S[i,t] * (1-L) + L * (1-\alpha) \tag{2}$$

If channel i is occupied by PU, the sensing outcome is 1, at sensing slot t, and $S[i,t]$ is decreased:

$$S[i,t+1] = S[i,t] * (1-L) \tag{3}$$

The probabilities $S[i,t+1]$ are updated at the end of each sensing slot. The constants $L, \alpha \in (0,1)$ guide the speed of learning automaton convergence. For very small values of α and according to (1), the reinforcement learning scheme is optimal and avoids collision with PU totally:

$$\lim_{t\to\infty} \mathbb{E}\{S[i,t]\} = \mathbb{E}\{\lim_{t\to\infty} S[i,t]\} = 1 \tag{4}$$

Where $\mathbb{E}\{.\}$ stands for expectation. If spectrum sensing is not accurate, then the selection metric of prediction of $t+1$ slot $S[i,t+1]$ is modified by the term below, i.e. for N continuous slots the sensing outcome was not PU present and the scheme increases (5) or PU present and the scheme decreases (6) for false alarm:

$$S'[i,t+1] = \{S[i,t+1-N] * \big((1-L) + L * (1-\alpha)\big\} +$$
$$+\{S[i,t-N] * (1-L) + L * (1-\alpha)\} + \cdots +$$
$$+\{S[i,t+1-m] * (1-L) + L * (1-\alpha)\} + \cdots +$$
$$+\{S[i,t+1] * (1-L) + L * (1-\alpha)\} =$$
$$= S[i,t+1] + L * (1-\alpha) * (1-L)^{N+1} \qquad (5)$$

$$S'[i,t+1] = S[i,t+1-N] * (1-L) +$$
$$+S[i,t-N] * (1-L) + \cdots +$$
$$+S[i,t+1-m] * (1-L) + \cdots + S[i,t+1] * (1-L) =$$
$$= S[i,t+1] - L * (1-\alpha)(1-L)^{N+1} \qquad (6)$$

$$1 < m < N-1$$

In equations (5) and (6) the computations used the $S[i,t+1-N]$ outcome of the scheme i.e. when the non accurate sensing had started and the scheme was sequentially updated for the next N slot. Finally, all the terms were expressed in terms of $S[i,t+1]$ recursively. As shown by (5) and (6), the error for misdetection and false alarm is the term $L * (1-\alpha)(1-L)^{N+1}$, which increases or decreases the correct term $S[i,t+1]$. The limit of the error for the PU misdetection and false alarm is zero.

$$lim_{\{N\to\infty\}}(1-\alpha) * (1-L)^{N+1} = 0 \qquad (7)$$

Thus, for higher values of L, the error term reaches very small values approximately 10^{-4} in a few slots. The proposed reinforcement learning scheme can operate under inaccurate sensing conditions as the system overcomes inaccurate sensing, i.e., PU misdetection/false alarm, which occurs easily when the value of L is high. The authors in [2] did not make such considerations.

8.5. Proposed System

The CR-BS collects the data of each CR-UE. The spectrum problem to be solved is to find the best spectrum vacancy each time for the Cognitive Radio Cell so that the transmission of the Cognitive User will not collide with the PU. We also want to maximize throughput of all active flows by prioritizing channel assignment for the max-min fairness and avoiding interference. A collision with the PU may occur as soon as the SU starts transmission and PU arrives, so the Medium Access Control Protocol must handle this case as well. For that reason, the CR-BS runs the reinforcement learning scheme for each channel, and based on the sensing outcome, a channel list *List[i]* is computed as follows:

$$If\ S[i,t] > S[j,t]\ then\ List[k] = i\ \ and\ List[n] = j, where\ k < n \qquad (8)$$

The sub-channel with the highest metric i.e., the channel that currently provides the best transmission opportunity, is put in the table with highest priority, i.e., as a first entry in the table *List[]*. The CR-BS measures the link quality and creates the *SNR[]* table with the SNR values of each sub-channel for all CR-UEs, which are under its coordination. If the channel suffers low quality that is below a certain threshold, this channel will not be selected for transmission:

$$If\ SNR[i] < threshold\ then\ List[k] = -1 \qquad (9)$$

The CR-BS sends the table *List[]* to the SDN-controller whenever the table *List[]*is updated. In case of collocated CR-BSs, they must avoid collision among themselves, in addition to collision with the PUs. The collocated CR-BSs send their tables *List[]* to the SDN-controller that keeps network topology information and a max cliques graph of the collocated BSs to avoid overlapping collocated BSs and interference. Even if the CR-BSs are collocated, they may have different table *List[]* lists because they experience different levels of interference. The CR-BS should select the first entry in its table *List[]*. If the entries of the tables of the CR-BS coincide, the SDN-controller will proceed to channel sharing in time that is based on the active flows demand report of each CR-BS. Indeed, the SDN-controller will proceed in proportional channel sharing in time based on the number of active flows, their spectrum demands and tables *List[]*. Assignments will start from the first entry for each CR-BS by solving the max-min fairness problem, which appears next.

There is the set V of CR-BS nodes, and for each CR-BS $v \in V$, there is a set of associated CR-UEs Wv. For each $v \in V$, there is a set of sub-channels Sv, which are for secondary usage at node v.

If channel *i* has a higher metric than j and it is assigned to an active flow, this implies that for N more slots channel i's PU was not present, and as a result, the metric of the channel is higher than j's. So, at time *t-N*, channel i's metric is equal to the metric of channel *j* at time *t*. It holds that

$$S[i,t] - S[j,t] = S[i,t-N](1-L)^N +$$
$$+(1-\alpha)[1-(1-L)^N) - S[j,t]$$

$$\xRightarrow{S[i,t-N)=S(j,t)=So}$$

$$\Rightarrow D = S[i,t] - S[j,t]$$
$$= (1-\alpha)[1-(1-L)^N] + [(1-L)^N - 1]S_o =$$
$$= [1-(1-L)^N](1-\alpha-So) \qquad (10)$$

$$\lim_{N\to\infty} D = 1-\alpha-So \qquad (11)$$

$$If \ \ D < \varepsilon \Rightarrow So > 1-\alpha-\varepsilon, \quad 0<\varepsilon<1 \qquad (12)$$

We can assume that channel *i* is assigned to an active flow only if the current metric value of *i* satisfies (12) to ensure that the assignment leads to a channel with good opportunities for transmission; i.e., the transmission will not be interrupted by PU arrivals.

An optimal assignment matrix $A_{v,s}$ based on table *List[]* has to be computed such that

$$A_{v,s} = \left\{ \begin{matrix} 1, if\ subchannel\ s\ is\ assigned\ to\ v\ and\ \ So>1-\alpha-\varepsilon \\ 0,\ \ otherwise \end{matrix} \right\} \qquad (13)$$

Where $\tau_{v,w}$ is the time share given to CR-UE and $f_{v,w}$ is the number of active flows in a link, BW is the subchannel's bandwidth, $\gamma'^{s}_{v,w}$ is the average per subchannel SNR > threshold. The minimum data rate per flow must be maximized.

$$argmax_A min_{\substack{v\in V \\ w\in Wv}} \left(\frac{\tau_{v,w}}{f_{v,w}} x \sum_{s\in S} A_{v,s} \ x R'^{s}_{v,w}\right) \qquad (14)$$

where the average bit rate per sub-channel is given by

$$R'^{s}_{v,w} = BWxlog_2\left(1 + \gamma'^{s}_{v,w}\right) \qquad (15)$$

$$Subject\ to{:}\ \ R_{v,w} > R_{v,w}{}^{0} \qquad (16)$$

$$\gamma'^{s}_{v,w} \geq \gamma o \qquad (17)$$

$$\gamma_m(n) \geq \gamma_0(n) \qquad (18)$$

Where $\gamma_m(n)$ represents the interference caused to the Primary User n. The transmission power P_j of a base station j and X_{vw} the fast fading for CR-UE w, the power received by CR-UE w can be written: $P_v K r_{v,w}^{-\eta} X_{v,w} Y_{v,w}$ which takes into account fading and shadowing, K represents the mean value of the received power at distance $r_{v,w}^{-\eta}$ where $X_{v,w}$ is a RV representing the Rayleigh fading effects, whose pdf is $p(x) = e^{-x}$, the distance $r_{v,w}^{-\eta}$ from the transmitter ($CR - BS_v$), and where $Y_{v,w} = 10^{\frac{\xi_{v,w}}{10}}$ [66] represents the shadowing effect and is given by the form:

$$\gamma'^{s}_{v,w} \triangleq \frac{P_v r_{v,v}^{-\eta} X_o Y_0}{\sum_{w\in W \cup V' \cup W'} P_w r_{w,v}^{-\eta} X_{w,v} Y_{w,v}} \qquad (19)$$

W, V' and W' are the sets of CR-UEs belonging to the same CR-BS, the neighboring CR-BSs and the CR-UEs that belong to neighboring CR-BSs. For $\gamma_m(n)$ we consider that multi-path fading and shadowing are negligible comparing to path loss and is given by :

$$\gamma_m(n)\frac{p_m(n)xL_{m,m}(n)}{No+\sum_{\cup j}p_j(n)L_{j,m}(n)} \qquad (20)$$

Where $L_{j,m}$ the path losses between the PU and SUs given by $L_{i,j}(n) = \frac{G_{t,i}G_{r,j}}{{d_{i.j}}^{a}}\left(\frac{c}{4\pi f}\right)$ (21) $G_{t,i}$ and $G_{r,j}$ are the antenna gains of the transmitter and the receiver respectively, $d_{ij}$is the distance between the transmitter *i* and receiver *j*, *c* the speed of light and *f* the frequency.

The spectrum brokerage to active flows is based on the output *List[]* of the Reinforcing Learning Scheme. For example, when the SDN-controller assigns a sub-channel to an active flow, it starts from the sub-channel that appears first in the *List[]*, and if the data rate requirement is not satisfied, it will proceed to the next entry in the table *List[]* to avoid an assignment to a sub-channel at which a transmission is most likely to be interrupted by a PU arrival. The minimum data rate assignment has to be maximized always beginning from the first entry of table *List[]*. In [61], the sub-channel selection is based on the sub-channel statistics, and then the authors maximize the minimum data rate per flow; but this way, some good sub-channels for transmission are bypassed.

8.6. EVALUATION

Simulation is the evaluation method applied to the proposed system, and it is performed at the Medium Access Control (MAC) level; i.e., the requirements of active flows were passed to the MAC layer as parameters. The OMNET environment was used. The PU bursts were generated following an exponential distribution—one PU per channel, and the size of bursts varied between 50,000 to 200,000 bits. Thirty sub-channels were considered for the experiments, and the polling slot was set to 10 ms. The transmission rate was set to 2 Mbps the channel that was selected for uplink or downlink. The PU distributions were every 0.001s, 0.005s, 0.02s, 0.033s, and 0.04s. The active flows have different data rate requirements. The experiments are a comparative study with [61]. The reinforcement learning scheme learns PU traffic avoiding collisions and predicting the best spectrum opportunities. So, active flows transmission is not interrupted whilst the controller assures interference mitigation. The total throughput in uplink is evaluated in experiments which are described below.

1st Experiment: The experiment considers two collocated CR-BSs that communicate with the SDN-controller. In the first CR-BS, there is only one active flow, and in the second CR-BS, the number of active flows is varying (Figure 8.1).

2nd Experiment: In the second experiment, the conditions are the same as in first experiment, except for the low link quality that exists in some sub-channels in the cells, and those sub-channels are excluded from selection. (Figure 8.2).

3rd Experiment: In the third experiment, the number of cells increases to three with one active flow in the first cell and two active flows in the second cell, while the number of active flows in the third cell varies (Figure 8.3).

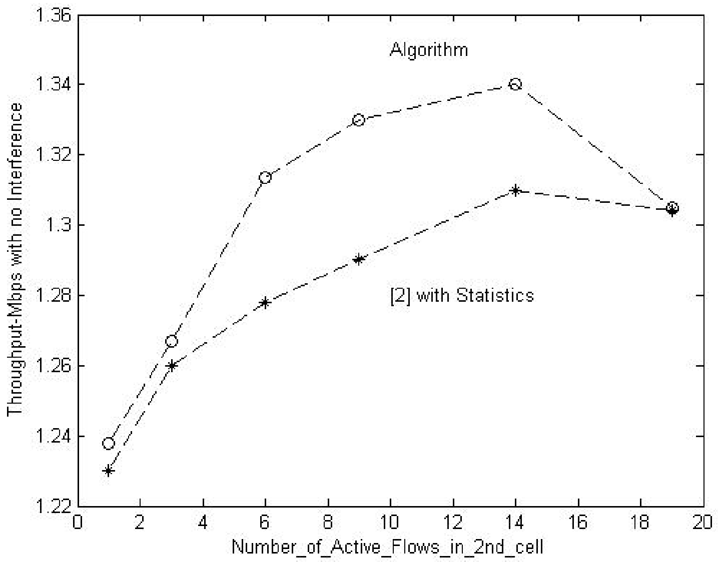

Figure 8.1: The first experiment for two cells

Sub-channel selection in [61] does not differentiate short and long spectrum holes so that a collision with PU or a transmission opportunity loss may occur. It does not overtake opportunities on the channels with worse statistics when they experience longer spectrum vacancies due to PU-traffic distribution variance. Sub-channel selection also overlooks shorter spectrum holes in channels with good statistics; this action results in collisions with the PU and degrades the performance of the protocol [61].

8.7. CONCLUSION

This research work proposes an SDN system for coordinated spectrum brokerage and interference mitigation in infrastructure and heterogeneous dense residential networks; the SDN system predicts PU network traffic to avoid collisions at all and maximize the throughput of active flows. The proposed system outperformed the only related research work dedicated to the same network.

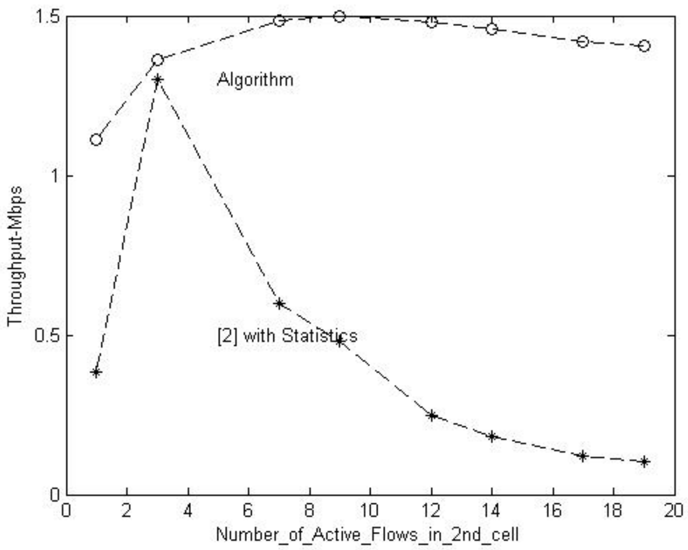

Figure 8.2: The second experiment for two cells

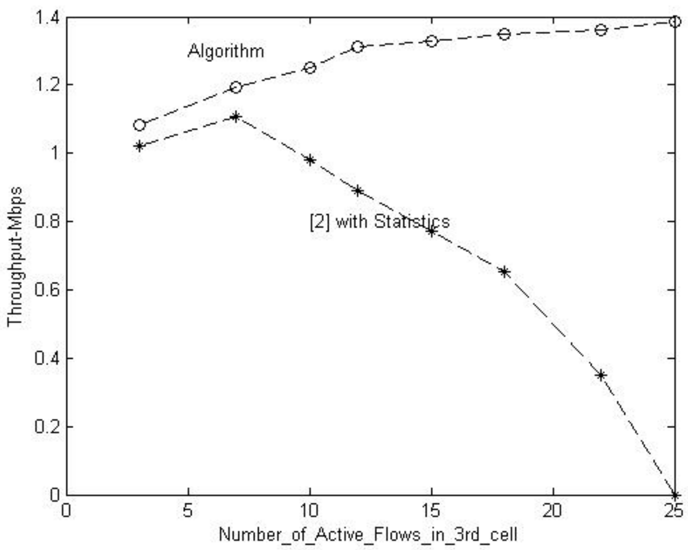

Figure 8.3: The third experiment for three cells

Chapter 9

SUSTAINABILITY IN COGNITIVE RADIO NETWORK AND CLOUD

Sustainable and Efficient Data collection in Cognitive Radio Sensor Networks

Cognitive Radio is a promising technology that maximize spectrum efficiency and can apply to Wireless Sensor Networks. This research work [68] proposes a system architecture which introduces enhancements at lower layers of a Software Defined Network of Wireless Sensors Network with Cognitive Radio capabilities for efficient sensors' power management, energy consuming channel handoffs elimination, efficient spectrum brokerage, and QoS provision in terms of data rate to the sensors' applications via the SDN flows. The large Wireless Sensors Network is divided into clusters for power efficiency- as sensors operate in lower power - which connect to a cloud-assisted Central Controller. The protocol encompasses an optimal reinforcement learning scheme for efficient spectrum utilization that enables efficient sensors' data collection, while sustainability issues are satisfied. Software Defined Wireless Sensor Network dynamically adapts to the spectrum and interference conditions on per flow basis and predicts Primary Users' traffic to totally avoid collision with the licensed users. The paper is concentrated on sustainable solutions for sensors' data collection by the cluster heads leveraging the Cognitive Radio Network facilities and taking into account the demands of the applications running on the sensors. The Cognitive Radio Sensor Network is considered as large organized on a local basis to extend networks lifetime and allow resource reuse.

9.1. INTRODUCTION

Wireless Sensor Networks (WSNs) have various applications in many areas. However, the limitations in power and storage ability of the sensors make the cloud a strong backbone solution for the WSN [69] [70] as energy consumption, latency, quality of service etc. can be improved [71]. Cognitive Radio is a promising technology to maximize spectrum efficiency through opportunistic spectrum access, i.e. Cognitive Radio Users access the underutilized licensed spectrum, when it is vacated by the Licensed Users-Primary Users (PUs). Cognitive Radio technology applied to WSN for better spectrum utilization.

Software-defined Wireless Sensor Networks (SDSNs) consist of software-defined sensor nodes that can dynamically load different programs on-demand according to the real-time sensing requests. On an SDN Wireless Sensor Network communications are performed via secure channels. Cloud computing helps SDWSN to fulfil its sensing requirements by reprogramming sensors on demand thus cloud-assisted SDWSN is gaining much of attention. The sensor nodes' dense deployment make SDWSN a spectrum demanding network where opportunistic spectrum access increases spectrum efficiency. Cognitive Radio Sensor Networks (CRSNs) can be also regarded as SDSNs as the radio access can be dynamically adjusted on-demand according to the real-time requirements [72].

The Cognitive Radio Base Station or Cognitive Radio Cluster Head in cluster-based architectures utilize thenetwork intelligence whilst the sensors assume data forwarding [72].

In CRSNs one main issue to be solved is minimization of the energy consuming spectrum handoffs due to Primary User's (PU's) arrival, i.e. the sensors that operate as Secondary Users have to vacate the spectrum on a PU arrival. Maximization of energy efficiency to extend the sensors lifetime, fair spectrum allocation to the sensor nodes based on selected criteria, efficient spectrum utilization, interference management are some of the issues to be solved. Furthermore, QoS requirements may be satisfied by the network and priorities to sensor nodes or data can also be employed to increase the efficiency of the network.

There are three categories or radio resource allocation schemes: a) centralized b) cluster-based c) distributed. In the centralized scheme, all the sensors communicate directly with the Base Station (BS) or Sink Node (SN) making essential higher transmission power whilst allowing optimal global solutions to be feasible. Not only that but as the data collection time increases, it makes this solution inappropriate for delay sensitive applications. When the sensor network is extended, a cluster-based scheme is preferable as spectrum sensing and resource allocations are performed locally i.e. sensing reports do not have to be sent to the central BS and the spectrum resources do not have to be shared amongst all the sensors of the whole network. As the number of sensors belonging to the cluster is smaller reducing signaling, the sensors can transmit on lower power. The distributed solution does not provide optimal resource allocation solution.

Mobile Sensor Networks have been introduced where Mobile Sinks collect the data [73]. In Software Defined Networks (SDN) a cloud controller may solve the spectrum allocation problem and find an optimal interference free spectrum assignment for overlapping Cognitive Radio Base Stations or Clusters such that the throughput of all active flows is maximized. SDN technology has been applied to Mobile Sensor Networks [74], too.

In this paper, optimal sustainable solutions for power allocation, data rate assignment based on the data rate requirements of the applications which run on the sensors, are proposed. Efficient spectrum brokerage is introduced for large SDN sensor networks which are divided to clusters to localize data collection, decisions and support time sensitive data. The research work is concentrated on sustainable solutions for sensors' data collection by the cluster heads leveraging the Cognitive Radio Network facilities and taking into account the demands of the applications running on the sensors. As the data forwarding to the Base Station/Sink Node is performed via selected channels and can be optimized via routing protocols or other techniques [75] [76] and the communication overhead of the proposed system with the cloud-assisted controller is minimum, the paper does not focus on this part of communication.

Clusterization is essential for a large sensor network for to be functional.

The sensors communicate with the local Controller and the local controller with the Base Station/Sink Node via secure channels as defined by the SDN interfaces for wireless sensors networks. The network is organized in clusters so to extend its lifetime as the energy that the sensors need to operate for communicating with Base Station/Sink Node is high. Spectrum reuse is also feasible throughout the network. Efficient power allocation at the sensors can reduce the total energy consumption in the network and increase the network lifetime.

Furthermore efficient spectrum allocation is realized with a reinforcement learning scheme which reduces the energy consuming spectrum handoffs in the cognitive radio network which are critical for sensor network and in the same time avoids collision with the PUs at all and realizes dynamic control channel assignment so to avoid control channel attacks. Although the network achieves sustainable sensor's data collection in the same time allows QoS provision to the SDN flows in terms of data rate. The proposed protocol can be applied for Mobile Sensor Networks as soon as there exists SDN interfaces in the Mobile Sensor Network [77].

The rest of the paper is organized as follows. Section 2 is a reference to the related work. Section 3 presents the System Model, section 4.1 introduces the Reinforcement Learning Scheme of the Proposed Protocol, section 4.2 presents the Control Channel selection process and section 4.4 introduces the optimization problem solved for data rate assignment per flow and power and 4.4 describes the proposed algorithm. Finally the simulation results are presented in section 5.

9.2. RELATED WORK

Software Defined Wireless Sensor Network (SDWSN) has become a promising approach for ubiquitous sensing and energy-efficient management of wireless sensor network [78] [79] [80] [81] [82] [83]. In particular, in SDWSNs, the control logic is separated from the data plane devices such as sensors and implemented in a logically centralized controller that provides the sensor network management process. The limitations of WSNs are overcome with cloud-assisted software defined wireless sensor network (CSDWSN) and software-defined networking technologies for coordinating multiple resources.

Luo et al [78] synergized Software Defined Networking and Wireless Sensor Networks (WSN) and proposed a Software Defined WSN where the Sensor Open Flow was introduced in accordance to the Open Flow of Software Defined Wireless Networks. They propose a separation between data and control plane, and Sensor OpenFlow (SOF). The data plane consists of sensors performing flow-based packet forwarding, and the control plane consists of one or more controllers that perform network control. “The whole idea is to make the underlying network (i.e., data plane) programmable by manipulating a user-customizable flow table on each sensor via SOF”.

The authors in [79] introduce the concept of Software Defined Wireless Sensor Network and enabling technologies for its realization. The collaboration among Cloud-assisted Software Defined Wireless Sensor Network providers for resource and revenue sharing is modelled as a coalition game [81]. In [79] a Software-Defined Networking implementation is presented that comprises two main components: the SDN-enabled sensor node, which has an SDN switch and an SDN end-user device, and the SDN controller node, is introduced.

There have been also made efforts for distributing the control plane [84] [85] [86] [87] [88] [89] [90] [91].

In [87] the authors exhibit an approach of resource and revenue sharing with coalition development among Cloud-assisted Software Defined Wireless Sensor Network (CSDWSN) providers. The proposed method models the collaborations among the CSDWSN providers as a coalition game. A distributed solution for the control plane i.e. a clustering approach for an SDN ad-hoc IoT network has been introduced in [92] which testbed provides an environment for IoT and ad-hoc network deployment. It allows nodes to be connected with others via one SDN-compatible OVS switch and at the same time this switch is controlled by an SDN controller. Scalable solutions for SDN are presented in

[96] [97]. In [98] [99] cluster-based architecture are introduced.

Mobile Sensor Networks are proposed in [100], [101] where sensors can save energy by transmitting to mobile agents or mobile sinks and extend their lifetime. The mobile agent collects the data from the sensors and forwards them to the sink. The sink can be mobile, too, but it differs from the mobile agent as it can upload directly to the cloud. As data collection time is reduced, [102] proposed a routing protocol for time-sensitive applications. In [103] a routing protocol for hierarchical WSNs was proposed to extend network lifetime. A time adaptive schedule algorithm is designed to reduce data collection time and make system sustainable and in the same time mobile agents are used in [103]. There is some research on cognitive radio on spectrum handoffs but this is mainly achieved by using proactive sensing and use re-active sensing i.e. where a vacant channel is selected for handoff after the appearance of PU [105] [106] [107] [108] [109].

In this research work we introduce a Cluster-based Software Defined Sensor Network enhanced with Cognitive Radio capabilities. The sensors operate at lower energy as they communicate with the Cluster Head (CH) and not directly with the Base Station/Sink Node. Spectrum resources reuse and spectrum handoffs elimination is feasible throughout the whole Sensors Network. Collisions with the PUs are avoided. Cloud-assisted SDN controller allows optimization of data rate and power assignment based on the sensors' application requirements and the sensors' network lifetime constraints. To the best of authors' knowledge, there is no other research dedicated to such a network and furthermore which pairs sustainability issues with the provision of QoS to the sensors' applications'.

9.3. THE PROPOSED SYSTEM

This research work considers an SDN Cognitive Radio sensors network where sensors are organized in Clusters (Figure 9.1). The SDN implementation, makes it possible to support multiple applications running on the same infrastructure in a plug-and-play manner. This is achieved through the programmable data plane that supports different types of packet forwarding rules and the control plane that decouples upper applications form physical devices (sensor nodes) and provides a global view of the underlying network to the applications [75]. The corresponding application data flows through the SDN architecture are referred as flows.

This paper proposes enhancements to the SDN lower layers functionality i.e. medium access/physical, so that considerations like sustainability and QoS provisioning in terms of datarate/per flow and efficient spectrum brokerage with dynamic control channel assignment to avoid control channel attacks would be feasible.

In each Cluster there is a node that facilitates the control plane i.e. the Cluster Head, which serves the sensor nodes that are responsible only for data related functionality. The CH communicates with the other CHs and the Sink via an inter-domain link. The Clusters traffic is eventually forwarded to the Sink Node which connects to the main SDN Controller the one that is cloud-assisted.

In SDN Cognitive Radio Sensor Networks, the Cluster Head which realizes the Control Plane relies the traffic to the sink node via secure channels. The Cognitive Radio Sensor Network is considered as large so that its division to clusters is justified. The Clusters are organized on a local basis eliminating the transmission power required as transmitting to the CH consumes less energy than transmitting to the Sink Node directly i.e. extending Cluster’s lifetime and enabling spectrum reuse.

The intra-Cluster communication is performed at a Control Channel that is selected such that neighboring Clusters’ Control Channels do not overlap. There are sensor nodes namely gateway nodes or intermediate nodes which are responsible for neighboring clusters communication.

The Cluster Head (CH) performs SNR measurement of its available channels and if a channel’s SNR is below a certain threshold it excludes this channel from the list of Cognitive Radio Channels that aim to be Control Channels. In order the CH to choose the best available channel as Control Channel, it runs an optimal Reinforcement Learning Scheme to learn the Primary Users (PU) traffic and discovers the best transmission opportunities i.e. which they will not be disturbed by PU arrival. The sensors contribute to this process by reporting their SNR conditions. Although the cluster's size is small and the SNR conditions tend to be equal within in the cluster, there may be exceptions and for this reason the sensors can report their SNR status to the CH.

CH may be elected among other powerful sensor nodes and it is responsible for cluster monitoring and securing the cluster from attacks.

The CH also collects the data rate requirements of the sensors for their flows, and redirects this requirements to the sink to perform the optimization. The CHs cannot usually support highly computational tasks and for this reason those tasks are forwarded to the SN and the cloud. Upon receiving the optimization results the Cluster accepts the flow data rates and the sensors adjust their transmission power accordingly and data rate.

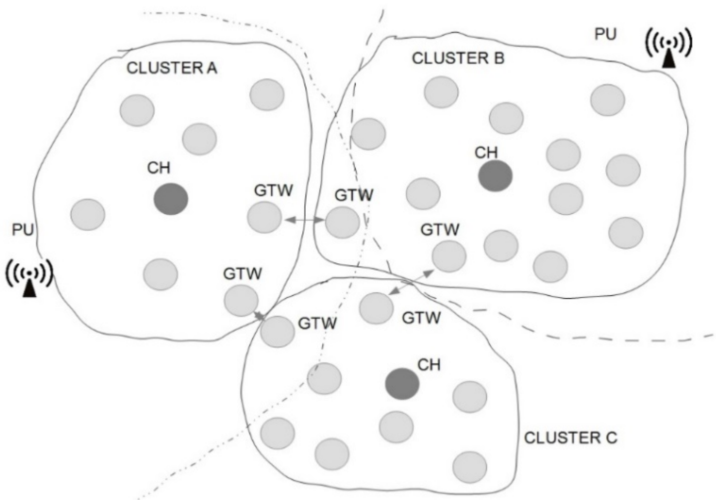

Figure 9.1: A Cluster-based SDN Cognitive Radio Sensors Network where we can distinguish the Cluster Heads (CH), Gateway nodes (GTW) and Primary Users (PU) Network.

9.4. THE PROPOSED SYSTEM MODEL

9.4.1. PU Colision Avoidance

The system encompasses a Reinforcement Learning Scheme to avoid interference to Primary Users and find a good transmission opportunity i.e. one that the SU's transmission will not collide with the PU. The stochastic learning automaton of P-Model runs on CH and sensors which have cognitive radio capabilities and appears below:

• If channel i is not occupied by a PU at sensing slot t, then the metric of probability of good transmission opportunity for channel $i, S\,[i,t]$ is increased:

$$S[i,t+1] = S[i,t]\,(1-L) + L * (1-\ a)\ (1)$$

• If channel i is occupied by PU at sensing slot t, then $S[i,t]$ is decreased:

$$S[i,t+1] = S[i,t]\,(1-L)\ (2)$$

The probabilities $S[i,t+1]$ are updated at the end of the sensing slot. $L, \alpha \in (0,1)$ are constants that guide the speed of learning automaton convergence. For very small values of α the limit of $S[i,t]$ is equal to unity so it is optimal, i.e. there would be no handoff during sensor data transmission:

$$\lim_{t\to\infty} \mathbb{E}\{S[i,t]\} = \mathbb{E}\{\lim_{t\to\infty} S[i,t]\} = 1 \qquad (3)$$

If spectrum sensing is not accurate then the selection metric $S[i,t+1]$ is modified by the term shown below for N continuous slots – i.e. at time $t-N$ misdetection or false alarm have started to occur and for the N consequent slots the sensing outcome was not accurate:

$$S'[i,t+1] = \{S[i,t+1-N] * \big((1-L) + L * (1-\alpha)\big\} +$$
$$+\{S[i,t+2-N] * (1-L) + L * (1-\alpha)\} + \cdots +$$
$$+\{S[i,t+1-m] * (1-L) + L * (1-\alpha)\} + \cdots +$$
$$+\{S[i,t+1] * (1-L) + L * (1-\alpha)\} =$$
$$= \{S[i,t-N] * (1-L) * (1-L) + L * (1-\alpha)\} +$$
$$+\{S[i,t+1-N] * (1-L) * (1-L) + L * (1-\alpha)\} + .. +$$
$$+\{S[i,t-m] * (1-L) * (1-L) + L * (1-\alpha)\} + \cdots +$$
$$+\{S[i,t] * (1-L) * (1-L) + L * (1-\alpha)\} = \cdots =$$
$$= S[i,t+1] + L * (1-\alpha) * (1-L)^{N+1} \qquad (4)$$

$$S'[i,t+1] = S[i,t+1-N] * (1-L) +$$
$$+S[i,t+2-N] * (1-L) + \cdots +$$
$$+S[i,t+1-m] * (1-L) + \cdots + S[i,t+1] * (1-L) =$$
$$= \{S[i,t-N] * (1-L) + L * (1-\alpha) * (1-L)\} +$$
$$+\{S[i,t+1-N] * (1-L) + L * (1-\alpha) * (1-L)\} + .. +$$
$$+\{S[i,t+1-m] * (1-L) + L * (1-L) * (1-L) + \cdots +$$
$$+S[i,t] * (1-L) + L * (1-L) * (1-L) = \cdots =$$
$$= S[i,t+1] - L * (1-\alpha)(1-L)^{N+1} \qquad (5)$$

As shown by (4) and (5) the error for misdetection and false alarm is the term $L * (1-\alpha)(1-L)^{N+1}$ increasing or decreasing the correct term $S[i,t+1]$. The limit of the error for PU misdetection and false alarm is zero:

$$lim_{\{N\to\infty\}}(1-\alpha) * (1-L)^{N+1} = 0 \qquad (6)$$

Thus for higher values of L the error term reaches very small values around 10^{-4} in a few slots. The proposed reinforcement learning scheme can operate in inaccurate sensing conditions as the system overcomes inaccurate sensing- i.e. PU misdetection/false alarm- easily when the value of L is high.

9.4.2. Control Channel Selection

The spectrum problem to be solved is to find the best spectrum vacancy each time for the cluster's control channel so that the Cognitive User's transmission will not collide with the PU and maximize throughput. The sensor traffic is bursty as it is generated on event detection.

For that reason, both the CH and sensors run the reinforcement learning scheme for each channel. As the cluster's size is considered small and PUs operate in high power, both CH and sensors will share the same outcome of the reinforcement learning scheme. So, they will be synchronized.

A channel table $List[i]$ is computed and updated by the reinforcement learning scheme outcome for each channel *i* at sensing slot *t* i.e. *S[i,t]* as follows:

$$If\ S[i,t]\ >\ S[j,t]\ for\ channels\ i\ and\ j\ respectively$$

$$then\ List[k] = i\ and\ List[n] = j\ with\ k > n\ (7)$$

The channel with the highest metric i.e. the channel that currently provides the best transmission opportunity is put in the table with highest priority i.e. as a first entry in the table $List[]$. We must notice that as PUs operate in high power there are more than one clusters that experience the presence of the same PU and as a results they coincide on the available channels but still they may suffer different levels of interference. So, the CH and sensors measure SNR too, and create a table with the current interference value for each channel i.e. $SNR[]$ and vector $SNRv[i]$. The entries of these tables will be set to either 1 or -1 if the SNR of the corresponding channel i is above or below the threshold respectively. If the channel suffers of interference that is below a certain threshold then this channel will be excluded from transmission in current cluster:

$$If\ SNR[i] < \ threshold\ then\ List[k] = -1,$$
$$SNRv[i] = -1$$

$$(where\ List[k]\ was\ prior\ List[k] = i)\ (8)$$

The CH receives the $SNRv$ of all sensors and excludes those channels which SNR is below the threshold from its $List[]$. Creates the vector $List_j[]$ for sensor j. Then sends the updated table $List[]$ to the main Controller so that the Controller would update the changing network traffic and interference conditions and coordinate channel brokerage in time between the clusters by avoiding Control Channel and back up control channel overlapping.

As PU traffic comes in bursts there is sufficient interval for the updated *List[]* by the central Controller to be effective within the cluster. Although the Clusters are nearby, they have different $List[]$ lists because they experience different levels of channel interference. The CH uses the updated by the Controller $List[]$ to send the $List[]XOR\ List_J[]$ to the sensor j. Upon PU presence at the control channel, as the whole cluster is synchronized, each sensor will transmit its sensing data to the next entry in the *List[]* table, i.e. backup control channel. Control Channel attacks are handled by the dynamic control channel allocation and no control channel information exchange among the sensors and the CH takes place.

The sensor node can choose to switch to “sleep mode” for further power saving. When the sensor node returns to the “ready state” scans the spectrum for beacons of the CH to learn the current control channel and as soon as its learning automaton converges, creates its own $List[]$ and estimates SNR. Then sends its $SNRv[]$ to the CH and waits to update its $List[]$. The scheme avoids PU collisions at all.

9.4.3. Per Flow Data Rate and Power Computation

We consider a large sensor network organized in clusters. If there are N sensors in a cluster, then as sensor traffic comes in bursts there would be K of them active each time and each would send its observation θ_k to the Cluster Head. Then the observation sent by sensor $k = 1,..,K$ under zero mean noise with covariance σ^k is:

$$x_k = \theta_k + \sigma^k : x_k \in [-W, W] \quad (9)$$

W is a known parameter depending on sensor's dynamic range.

For observations x_k based on a distribution having parameter value $\theta_k, d(x_k)$ an estimator of θk the bias is the mean of the difference $bd(\theta) = E[d(x_k) - \theta k]$. If $bd(\theta) = 0$ for all values of the parameter, then $d(xk)$ is called an unbiased estimator.

We can assess the quality of the estimator by computing the Mean Square Error (MSE) with bias-variance decomposition presentation:

$$MSE = E[(x_k - \theta_k)^2] =$$

$$= E(x_k - \left(E\left(x_k - b_d(\theta)\right)\right)^2\right] =$$

$$= E[(x_k - E[x_k])^2] + 2 * b_d(\theta) * E\left[x_k - E[x_k]\right] + b_d(\theta)^2$$

$$= Var(x_k) + b_d(\theta)^2 \quad (10)$$

Since the bias is zero the MSE depends on the variance of x_k. So, we do not have to know the pdf but only the variance of the received signal. The sensors operate at a range [-W, W] and if we quantize the signal received by one sensor in equal intervals of length $2W/2L-1$, and round the signal to the neighboring endpoints of these intervals as follows:

$$\text{Let } -W + i\Delta \leq x \leq -W + (i+1)\Delta \qquad (11)$$

$$0 \leq i \leq 2^L - 2 \qquad (12)$$

$$P\{x_L = -W + i\Delta\} = r \qquad (13)$$

$$P\{x_L = -W + (i+1)\Delta\} = 1 - r \qquad (14)$$

$$r = x + \frac{W - i\Delta}{\Delta} \in [1,1] \qquad (15)$$

the received signal, x_L, at the CH, according to [39], is an unbiased estimator of $\theta_L$with covariance σ^2 at an exponential rate as L increases.

$$E[|x_L - \theta_L|^2] \leq \sigma^2 + \frac{W^2}{(2^L-1)^2} \; for\ all\ L > 0 \qquad (16)$$

Where $\frac{W^2}{(2^L-1)^2}$ denotes the upper bound of quantization noise variance. For $L = B$ i.e. the available bandwidth, we have the quantization of one bit. The Best Linear Ubiased Estimator (BLUE) is applicable to amplitude estimation of known signals in noise.

We suppose that for each sensor there is a probabilistic bit rate assignment to it b_k [106] such that all sensor observations arrive at the Cluster Head (CH) at different bit rates according to the noise each sensor experience.

The Mean Square Error of the quantized Best Linear Unbiased Estimator (BLUE) [106] estimator of the total observation for K sensors that is received by the CH is:

$$E[|\hat{\theta} - \theta|^2] \leq \left(\sum_{k=1}^{K} \frac{1}{\sigma_\kappa{}^2 + \frac{W}{(2^{b_k - 1})^2}{}^2} \right)^{-1} \tag{17}$$

We want to optimize the network performance so we have to select the total bit rate for each sensor that is compliant to the noise which experiences and its total flows' data rate requirements. For example a sensor which experiences higher levels of noise should not be assigned high data rate unless it accepts to raise its transmission power something that would affect the sensors network lifetime in the long run, though. The transmission power is a function of the bit rate and in this paper work we will consider M-QAM models.

Each sensor based on its flows' data rate requirements computes the total data rate that would serve all of its flows and forwards its request to the CH. The CH collects the data rate requests of all sensors of the cluster. Then, the CH forwards the vector with the data rate request for each sensor to the Sink Node. Although the wireless sensors network is large, the three vectors communication overhead is not considerable as those vectors will be forwarded to the Sink Node only when they have been changed.

The Sink Node and the central SDN controller which is cloud-assisted should guarantee for the whole network that a) neighboring clusters that may share the same available channels do not have overlapping control channels by exploiting the available channels vectors b) each sensor receives the requested data rate if the corresponding power is acceptable for the network's lifetime by exploiting the data rate request vector. When the control or backup channels or data rate vectors change, the Sink Node has to be informed. The data rate allocation to each sensor can be formulated as a convex optimization problem solved at the cloud-assisted Sink Node.

We form the convex optimization problem as follows:

$$argmin\left(\sum_{k=1}^{K}\frac{1}{\sigma_k^2+\frac{W^2}{(2^{b_k-1})^2}}\right)^{-1} \tag{18}$$

$$subject\ to: \quad \sum_{k=1}^{K} b_k \le B_c \tag{19}$$

$$b_k \ge I_k \tag{20}$$

$$\sum_{k=1}^{K} P_k \le P_{cluster} \tag{21}$$

$$P_k = c_k * (2^{b_k}-1) \ge 0 \tag{22}$$

$$b_k = \sum_{i=1}^{F_k} b_k^i \tag{23}$$

We consider $P_k = f(b_k) = c_k * (2^{b_k}-1)$ the transmission power of the sensor which corresponds to its total flows' data rate b_k , $P_{Cluster}$ the total energy that the cluster sensors can consume, B_c the total bandwidth of channel c i.e. the connection between sensors and the CH and I_k the data rate requirement of all flows in sensor k and F_k the number of flows at sensor k, and b_k^i the data rate requirement of flow i at sensor k.

With the Lagrange method we transform the optimization problem (18) to its equivalent as follows:

$$argmax\left(\sum_{k=1}^{K}\sigma_k^2+\frac{W^2}{(2^{b_k-1})^2}\right)^{-1} \tag{24}$$

$$subject\ to: \quad \sum_{k=1}^{K} b_k \le B \tag{25}$$

$$b_k \ge I_k \tag{26}$$

$$\sum_{k=1}^{K} c_k(2^{b_k}-1) \leq P_{cluster} \qquad (27)$$

The Lagrange function L is then:

$$L(b_k,\lambda_1,\lambda_2,\mu_\kappa) = \left(\sum_{k=1}^{K}\left(\sigma_k^2+\frac{W^2}{(2^{b_k}-1)^2}\right)^{-1}\right) \; +$$

$$+\lambda_1\left(B-\sum_{k=1}^{K} b_k\right)+\sum_{k=1}^{K}\mu_k\,(b_k-I_k) \; +$$

$$+\lambda_2\left(P_{Cluster}-\left(\sum_{k=1}^{K}(c_k\,(2^{b_k}-1)\right)\right) \qquad (28)$$

We have to solve then the equations below:

$$\frac{\partial\left(\left(\sigma_k^2+\frac{W^2}{(2^{b_k}-1)^2}\right)^{-1}\right)}{\partial b_k}-\lambda_1 K+\sum_{k=1}^{K}\mu_k -$$

$$-\lambda_2\sum_{k=1}^{K} c_k b_k 2^{b_k-1} = 0 \qquad (29)$$

$$\lambda_1\left(\sum_{k=1}^{K} b_k - B_c\right) = 0 \qquad (30)$$

$$\mu_k(b_k-I_k)=0 \qquad (31)$$

$$\lambda_2\left(P_{Cluster}-\sum_{k=1}^{K} c_k(2^{b_k}-1)\right)=0 \qquad (32)$$

As soon as the total data rate per sensor is computed, the computation of the corresponding power per sensor is straightforward (22). The main controller returns to the CH two vectors with the data rates per flow: one for the control channel and one for the backup channel as they do not share the same bandwidth.

The Cluster also adjusts its control channel and backup control channel according to Controller's indication, so that it does not overlap with the neighboring clusters' control channels.

9.4.4. The proposed Algorithm

At sensor node:

- Scans for CH beacons
- Senses the spectrum - Runs the Reinforcement Learning Scheme
- Estimates SNR
- Sends the SNR vector to CH
- Waits for the updated XOR vector
- Senses spectrum
- Sends sensing data at the control channel or switches to backup channel is PU is present at the control channel and sends the data
- Switches to sleep mode

At the CH:

Initialization Phase

- Senses spectrum –Runs the Reinforcement Learning Scheme

- Estimates SNR
- Sends its $List[]$ to the Main Controller
- Receives the $List[]$ from the Main Controller
- Starts sending beacons to the control channel
- Waits for SNR vector from the sensors and the data rate requirements
- Sends the updated $List[]$ to the Main Controller
- Receives the updated by the Main Controller $List[]$
- Sends the XOR vector to the sensors

Main Phase

- Senses spectrum - Runs the Reinforcement Learning Scheme
- Sends beacons at the control channel
- Waits for SNR vector and data requirements from the sensors
- Waits for the sensors' data
- If the $List[]$ changes or the data rate requirements i.e. the control channel or the backup channel are not the best opportunities for transmission according to the Reinforcement Learning Scheme or the SNR vectors of its own and the sensor or the data rate requirements change, sends the new $List[]$ and data rate requirements to the Main Controller.
- Receives the new $List[]$ and the data rates vector from the Main Controller
- Sends the XOR vector and data rate to the sensors
- Switches to the new control channel
- Sends beacons to the new control channel
- Waits for sensors' data

- If the control channel is occupied by the PU switches to the backup control channel.
  - If the presence of PU at the control channel or the presence of PU at the backup control channel are followed by a change of the rank of those channels in the $List$[] table according to the Reinforcement Learning Scheme, then the sends the updated *List[]*to the Main Controller.
  - Waits for the response of Main Controller
  - Sends the XOR vector and data rates to the sensors
    - Starts sending beacons to the new control channel and keeps the updated information about the backup control channel
- Waits for sensors data

At the Main Controller

- Waits for the $List$[] and data rate requirements of the clusters
- If it receives a request examines the $List$[] and the graph it maintains with overlapping clusters.
  - Finds the $List$[] tables associated with the overlapping clusters in graph.
  - Proceeds in control channel and backup control channels brokerage to the overlapping clusters so that their control channels and backup control channels do not overlap. The best choice for each cluster is provided in terms of control channel assignment and only if there is a collision the channel with the higher bandwidth will be assigned to the cluster with the highest data rate demands.

- If the request includes data rate update, solves the optimization problem for the specific cluster with the cloud assistance and its record about the cluster power constraints.
- Sends the updated $List[]$ tables to all the associated clusters
- Sends the data rate vector to the cluster that initiated the request.

- Waits for the $List[]$ and data rate requirements
- If it receives only data rate request
  - Solves the optimization problem for the specific cluster with the cloud assistance and its record about the cluster power constraints for both the control channel and backup control channel.
  - Sends the data rate vector to the cluster that initiated the request.
- Waits for new requests to serve.

9.5. EVALUATION

The evaluation of the proposed architecture was concentrated on the evaluation of the cluster's performance. So, the evaluation method applied to the proposed cluster functionality. Channel handoffs, collision avoidance with the PU, best control channel selection, interference management, data rate allocation per flow among the clusters were tested. Power allocation and data rate assignment are used interchangeably.

The experiments consider the cases where clusters are overlapping as this scenario imposes more constraints to the cluster performance. Various scenarios of flows with different data rate requirements and various number of sensors were applied. The SNR conditions also vary in the experiments. Flow data rates were passed as parameters to the lower layer of the simulation as they have been pre-computed for each scenario [107]. The performance of the overlapping clusters depend on the available channels, the PUs traffic, the SNR they experience and the flows per sensor of each cluster. In experiments, we do not consider raise of sensor's power in case of very low SNR conditions.

The proposed control channel selection scheme is compared to a similar cluster architecture where the control channel selection is based on PU traffic statistics which are computed continually during the experiments so that we evaluate the control channel selection scheme for various flow data rate assignments scenarios. As the data rate assignment is optimal we consider optimal data rate assignement for both architectures in the comparative study.

The PU traffic was generated in bursts following exponential distribution and the size of bursts was varying between 50,000 to 200,000 bits. Thirty channels were considered for the experiments. The transmission rate was set to 2Mbps. The experiments conducted are described below:

The PUs' distributions were every (0.001)s but there was also a few channels with burst generation at (0.01)s, (0.005)s, (0.02)s, (0.033)s, (0.04)s.

1st Experiment: The experiment considers two overlapping clusters. In the first cluster there is only one active flow and in the second cluster the data rate requirements of the active flows are multiple of the data requirements of the first cluster's flow. The Throughput is evaluated as the flows' data rates in the second cluster increase. There are channels that suffer of very low SNR i.e. they are restricted for access. This experiment examines performance in the two clusters as it is likely that the cluster with the increasing traffic will have to deal with a control channel switch more often as it utilizes the control channel more often, provided that there are various SNR scenarios in the channels and PU traffic scenarios as well (Figure 9.2).

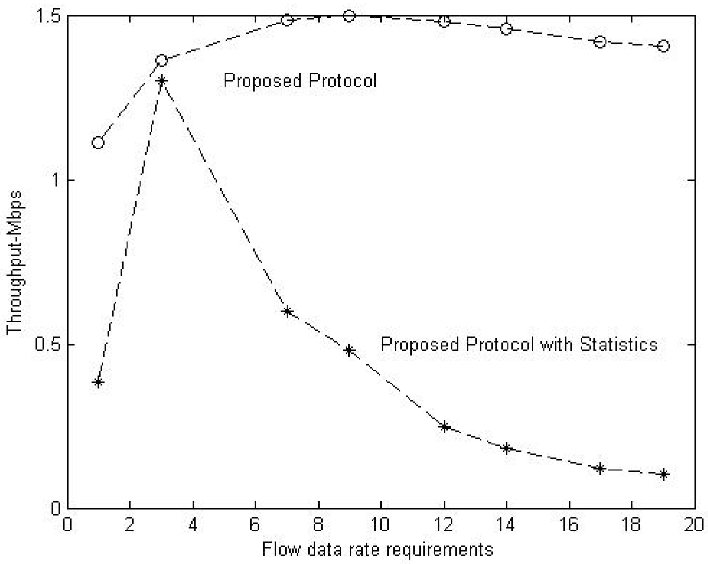

Figure 9. 2: The first experiment with two overlapping clusters

The proposed scheme outperforms the system with statistics as it leverages the spectrum holes more efficiently and as a result it is not affected by the active flows increasing number the way statistics are affected. The statistics does not differentiate its response to long and short spectrum holes, i.e. in the former case it bypasses opportunities and in the latter it does not avoid collision. The statistics do not also overtake opportunities on the channels with the worse statistics when they experience longer spectrum vacancies due to PU-traffic distribution variance. The control channel selection based on statistics cannot proceed to fine spectrum utilization and as the number of active flows increases the performance drops significantly. These hold for all experiments.

2nd Experiment: The second experiment's conditions are the same with the first experiment but the number of overlapping clusters increases to three with one active flow in the first cluster, one active flow with the same data rate requirements in the second cluster whilst the flows data rate requirements of the third cluster vary i.e. are multiple of data rate requirements of the first cluster. The increasing number of data rates do not have such a drastic effect for the proposed scheme comparing to the control channel selection based on statistics which is very sensitive to the number of overlapping clusters and flow data rates (Figure 9.3).

3rd Experiment: In the third experiment there are two overlapping clusters with the same flow data rates. Fifteen channels suffer of low SNR and are excluded by the CH (Figure 9.4).

4th Experiment: In the fourth experiment there are three overlapping clusters with the same flow data rates. There are eight channels suffering of very low SNR. The results for the proposed system are better in the fourth experiment than the third as there are fewer channels suffering of very low SNR. On the other, the results of the system which use statistics for control channel selection are worse than its results on the third experiment where there were more channels with very low SNR and two clusters. The increasing number of flows data rates do not have such a drastic impact on the proposed scheme comparing to the channel selection based on statistics which is very sensitive to the number of clusters and data rate requirements (Figure 9.5).

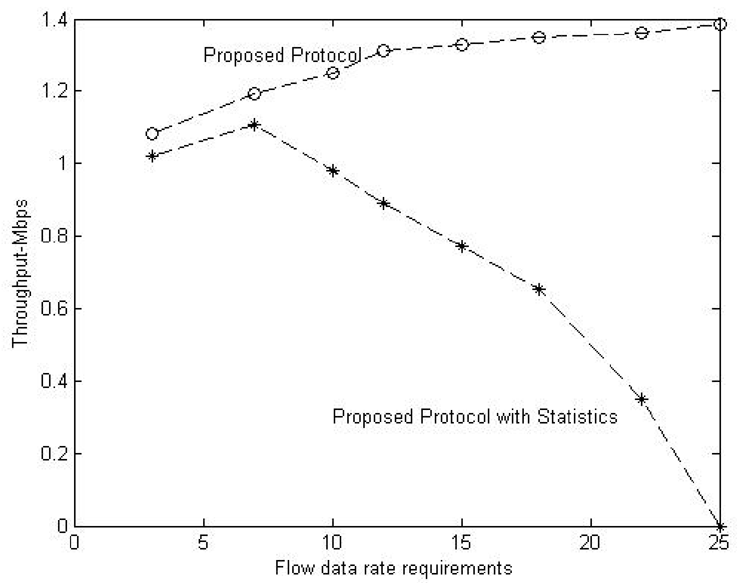

Figure 9. 3: The second experiment with three overlapping clusters

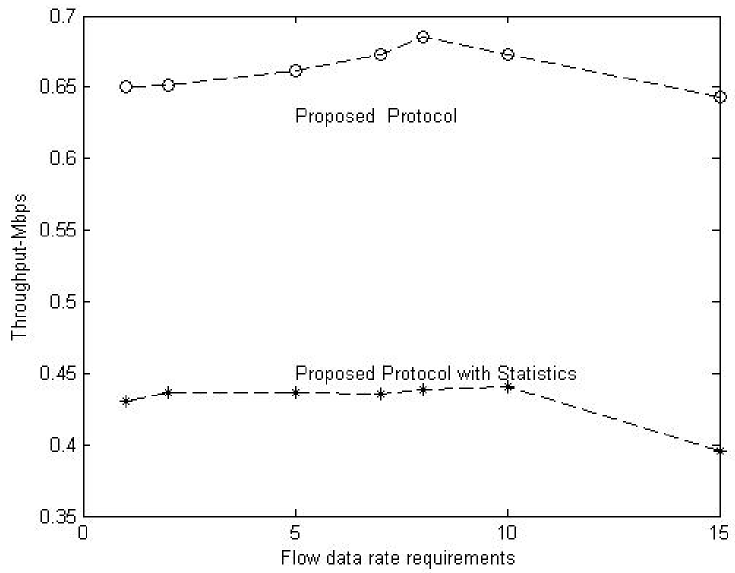

Figure 9.4: In the third experiment there are two overlapping clusters with the same flows' data rate requirements.

9.6. CONCLUSION

This paper proposes a sustainable Software Defined Wireless Sensor Networks architecture and it is concentrated on sustainable solutions for sensors' data collection by the cluster heads leveraging the Cognitive Radio Network facilities and taking into account the demands of the applications running on the sensors. The Cognitive Radio Network predicts PU network traffic and leverages bursty sensor traffic. The network is considered large and the Cluster architecture provides localization of decisions and support of time sensitive data collection as well as efficient spectrum reuse across network. Sustaianbility is applied in terms of sensors power operation, channel handoff elimination and collision avoidance with the PUs. Optimal solutions for power allocation, data rate assignment and spectrum utilization are introduced. The sensors operate at the minimum power allowing in the same time their applications to run at an acceptable QoS level. QoS provisioning in terms of data rate to the sensor applications is realized on per flow basis of the SDN network. The network's sustainability is improved by the clusters organization. An optimal Reinforcement Learning Scheme applied for control channel selection eliminates channel handoffs which consume a lot of energy as predicts PU traffic. The proposed solutions are optimal.

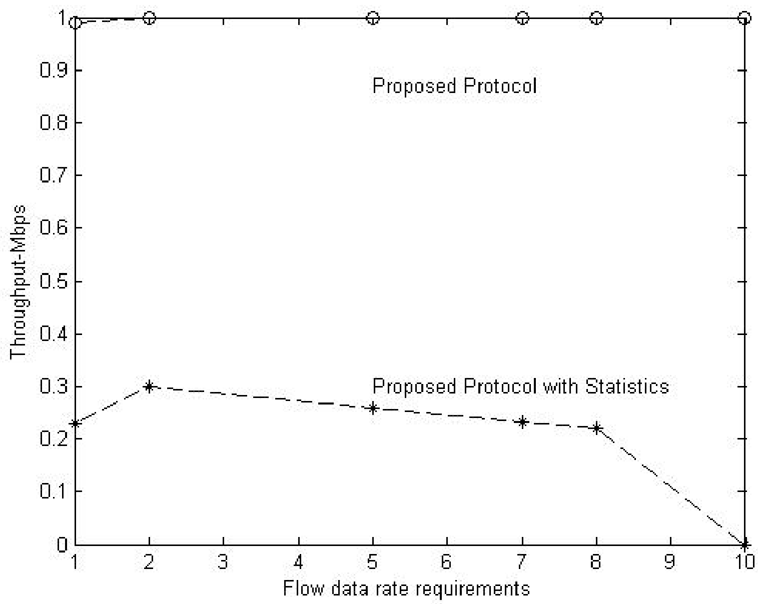

Figure 9. 5: In the fourth experiment there are three overlapping clusters with the same flows data rate requirements.

Chapter 10

BROADCASTING IN COGNITIVE RADIO AND CLOUD

Energy-Efficient Broadcasting with QoS and Collision Avoidance

This research work [119] introduces a Broadcast protocol for Cognitive Radio Cloud that organizes secondary users (SUs) into clusters in an optimal distributed manner based on the locally available channels with a dynamically selected Common Control Channel (CCC) by an optimal Reinforcement Learning Scheme. The Scheme predicts the best available channel i.e. the one that is going to be idle for longer period, avoiding collisions with the licensed users for the cluster's operation and providing reliable broadcast delivery i.e. a delivery that is not going to be disturbed and in the same time minimizing the CCC channel hopping which is energy consuming. The Local optimums are achieved without global network information. The protocol outperforms existing literature in Cognitive Radio Multi-Hop Ad-Hoc Networks Broadcast supporting Collision Avoidance at receiver's side whilst providing QoS without performance degradation filling a gap in literature. Collision Avoidance at receiver's side saves energy and resources for the network. The clusters are self-organized such that minimal radio equipment can be cloud-assisted on demand.

10.1. INTRODUCTION

In Cognitive Radio Networks, unlicensed users opportunistically access the spectrum [1] [11] [12]. Broadcasting may occur in the network to distribute packets of user-content or critical-content. Software Defined Radio (SDR) at physical layer and Cognitive Radio for Broadcasting have started to attract the attention of the scientific research community [120].

In Multi-Hop Ad-Hoc Networks broadcasting there is a large number of literature which is out-of-the scope of this paper, but for Cognitive Radio (CR) Multi-Hop Ad Hoc Networks the literature is limited and special issues have to be considered for the Broadcasting Protocol design. In CRN both the transmitter and receiver have to be synchronized to the same channel, and this holds for broadcasting, too. In literature, because CRN broadcasting may be disrupted by PUs, some protocols propose simultaneous transmissions in multiple channels to assure successful broadcasting.

However, simultaneous broadcasting in multiple channels implies additional radios for the network nodes otherwise they have to perform them in sequence with significant impact on latency [121]. Neighboring SUs should be synchronized to deliver control packets. Another issue is that as broadcasting is realized as a packet flooding in the network, multiplications of a packet may arrive to a SU. This is known as a Collision on the Receiver's Side and Collision Avoidance at the receiver's side is a problem that has to be handled by the broadcast protocol. Collision on the Receiver's side consumes energy and resources of the network because or unnecessary retransmissions.

The use of a Common Control Channel (CCC) which is applicable to Multi Hop Ad Hoc Networks , cannot ensure coordination in CRN as PUs' transmissions are of higher priority and interrupt the opportunistically access of SUs. Primary Users operate at a high level of power, so the PU's transmission radius is greater than the transmission radius of the SUs. Thus, SUs operate at lower power level i.e. locally. CCC establishment should consider the PU's traffic characteristics and the dynamically changing network environment so that the CCC and Broadcast Channel satisfy the basic requirements of CCC establishment, i.e., availability and reliability. The dynamic CCC selection should be efficient so to minimize CCC hoppping and consequently energy consumption. In [125] a distributed cluster-based architecture is proposed which does not refer to broadcasting and tits prerequisite such as collision avoidance at receiver's side which arise at broadcasting networks.

In [126], collision avoidance at receiver's side is supported but simultaneous retransmissions over multiple channels degrade the performance - recipients are unsynchronized. [126] does not provide QoS guarantees.

Lazos et al [127] proposed a cluster organization but reclustering requires global network information.

In CRBP [128], each node creates classes of the channels based on PU presence and combines them with bipartite connectivity graphs to form the local network topology. However, a bipartite graph search is needed when the broadcasting channel set is changed and requires global information. Collision avoidance on the receiver's side is not implemented in [129]. In [130], the authors achieve a rendezvous of the transmitter-receiver in the M^2 slots, where M is the number of available channels, which results in considerable delay and overhead. The authors in [131] engage global network information to reduce latency.

[132] considers the problem of multiple and single transceivers. [133] implements broadcasting with multi-antenna transmitters and single antenna receivers using orthogonal beamforming.

This research work introduces a broadcast protocol where no global network information is needed, where a dynamic common control channel is selected dynamically within a cluster. The common control channel is selected to ensure availability and reliability - with no collisions with PUs. Inter-cluster communication ensures collision avoidance on the receiver's side avoiding retransmission and extra energy consumption whilst fast reclustering makes it appropriate for vehicle's clouds [134]. So, no additional overhead and delay is achieved, and at the same time, the system provides QoS. To the best of our knowledge, there is no literature supporting both collision avoidance and QoS. Each SU is equipped with one radio and sensors.

CRs converge to local optimums. There is no packet overhead and delay efficiency is achieved, as the broadcast packet is transmitted only in the CCC which is common for all nodes in the cluster (one-hop distance) thus packet retransmissions between network nodes are avoided. PU collision is avoided by employing machine learning. Although collision avoidance at the receiver is guaranteed by slot assignment to neighboring clusters, the broadcast data packets occupy all slots of the CCC. Thus the proposed protocol sets up non-overlapping broadcasting paths throughout the network for the broadcast data packets with the minimum packet transmissions. The cluster is deployed locally so that its nodes overhear each other's beacons.

The chapter is organized as follows. In section II, the system's description is presented. Section III is a presentation of the bit rate maximization as achieved by the proposed protocol. In section IV, PU collision avoidance and channel hopping with the Reinforcement Learning Scheme is presented. The Broadcasting Protocol is presented in section V and the phases of the protocol in VI. Section VII is the evaluation section. Because the literature in Broadcast Protocols for Cognitive Radio Networks is limited the evaluation considered the most close to Broadcast Cognitive Radio Cloud network consept which is that of Broadcast Cognitive Radio Ad Hoc Networks.

10.2. SYSTEM DESCRIPTION

The SUs are organized in clusters locally; i.e., all the SUs that listen to the same channels belong to the same cluster eventually [134]. Each cluster selects a CCC to use for broadcasting too - and a second channel as a Backup CCC. For this reason, SUs employs machine learning so to learn the PUs' activity and select the best transmission opportunities for the unlicensed users. An SU transmission may be interrupted anytime by PU arrival so there is a need for efficient prediction and selection between spectrum vacancies. The CCC selection scheme is optimal and the channel with the best scheme's metric becomes the CCC. The most available and reliable channels are selected. The bandwidth requirements are satisfied, too.

As the SUs within a cluster share common PUs experience i.e. overhear the same PUs, the output of the reinforcement learning scheme is common for all. The scheme is optimal i.e. predicts PU traffic to avoid collision with the PUs. Despite that the SUs listen before transmit, collisions with the PU may occur if the PU arrives before the SU completes transmission. The Reinforcement Learning Scheme avoids such collisions as is optimal. The cluster head updates the channels selection list dynamically according to the sensing outcome in a descending order i.e. the best channel appears first at the list.

An SU who wants to join the network has to listen for beacons and join the cluster. If he does not hear beacons then he establishes a cluster himself. After cluster establishment, continuous inter-cluster communication is responsible for non-overlapping of the neighboring CCCs and B-CCCs. As the dynamic broadcast channel is selected such that collision with the PU is avoided, the broadcast packet is transmitted only once in the CCC within a cluster and is forwarded to the CCCs of the neighboring clusters i.e. two transmissions for a two-hop distance- no additional latency and delay. Inter-cluster communication is basically associated with broadcast idle period.

The clusters are self-organized and edge nodes are responsible for inter-cluster communication, i.e., nodes that reside at more than one clusters. Each SU tunes its radio to its cluster's CCC. The edge nodes tune their radios to the neighboring CCCs, too. In Figure 10.1 there are three PUs and their coverage areas and the secondary nodes are organized in two clusters with coordinating nodes Head 1 and Head 2. PU A and PU C affect cluster 1 and PU B and PU C cluster 2. The edge node in cluster 1 overhears PU B and communicates with cluster 2 in PU B's channel based on the PU B's non occupacy of the corresponding channel. There is another one SU in cluster 1 which overhears PU B but is not selected as edge node- the rest of the cluster does not overhear PU B. The cluster may be assisted by cloud location-based database for inter-cluster information retrieval. Grouping SUs with similar channel lists implicitly implements hard-decision cooperative sensing.

10.3. MAXIMIZATION OF BIT RATE FOR QOS PROVISION

In order to facilitate QoS provisioning, the system leverages the cloud connection if needed to locally solve the problem of maximization of achievable bit rate. For that reason, a bipartite graph is constructed and then the maximization of bit rate assigned to the bipartite graph's edges is solved locally i.e. for the neighboring clusters. The optimization problem is eliminated from the whole network to neighboring clusters. So, network performance is enhanced as PU activity is localized and by solving the optimization problem for local optimums instead of grouping SUs with similar channel lists for the whole network which is an NP-hard, is more efficient in terms of computational load and network responsiveness to radio network and network changes. In literature there are no cluster architectures for broadcast protocols with QoS provision and there are no broadcast protocols for cluster architectures supporting mobile users or vehicles in CRN. Mobile users and vehicles require frequent reclustering..

A cluster C, namely, the SU chosen as the cluster's head, creates a bipartite graph $G(Xi, Yi, Ai)$, where Xi vertices represent the intermediate nodes – i.e., the nodes belonging to the neighbor cluster and responsible for the communication with cluster C – and Yi represent the nodes belonging to the C cluster and playing the intermediate role for neighbor clusters, and Ai is the edge between Xi and Yi when broadcasting takes place, with broadcasting messages coming from cluster CXi and heading for the cluster for which nodes Yi are the intermediate nodes through cluster C.

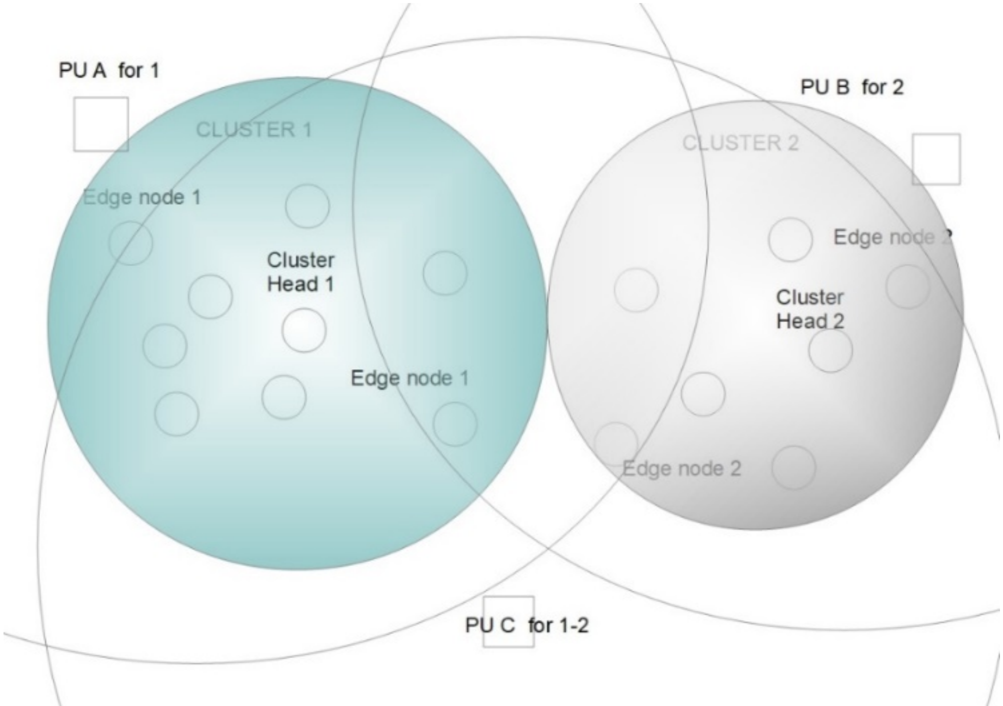

Figure 10.1: The cluster deployment

The achievable bit rate for channel n for a connection $Xi - Yj$ is:

$$Rn_{ij} = BWx\log_2\left[1 + \gamma_{ij}(n)\right] \qquad (1)$$

where BW is the bandwidth and $\gamma i, j\ (n)$ is the signal-to-interference-plus-noise-ratio (SINR) for the connection $Xi - Yj$. If we consider only path loss, $\gamma i, j\ (n)$ is given by the following form:

$$\gamma_{ij}(n) \triangleq \frac{p_i(n)xL_{i,i}(n)}{No + \sum_{j \in Yj \cup M} p_j(n)L_{j,i}(n)} \qquad (2)$$

where *No* stands for the additive white Gaussian noise with zero mean and variance *No*, whilst *Li,i* and *Lj,i* are the path losses for channel n given by the form below:

$$L_{i,j}(n) = \frac{G_{t,i}G_{r,j}}{{d_{i.j}}^{a}}\left(\frac{c}{4\pi f}\right) \tag{3}$$

$G_{t,i}$ and $G_{r,j}$ are the antenna gains of the transmitter and the receiver, respectively, di,j is the distance between them.

The formulas for the Signal to Interference Noise Ratio (SINR) estimation may be updated to cover multi-path fading and shadowing. So, the SINR formulas will be selected locally based on the cluster's radio environment e.g. for adapting to urban and rural areas.

We want to maximize the achievable bit rate and at the same time not to disturb the PU's activity; i.e., SU' transmitting power should be below a threshold. The SINR of PUs at each channel should be kept above a threshold too.

$$\gamma_m(n) = \frac{p_m(n)xL_{m,m}(n)}{No + \sum_{j\in Yj\cup Xj} p_j(n)L_{j,m}(n)} \tag{4}$$

The bipartite graph is updated and provides the connections of the broadcasting path.

We need to maximize the achievable bit rate in all available channels that may become the CCC and B-CCC of the cluster by adjusting the transmission power of nodes to meet the SINR constraints. This is a convex optimization problem formulated as shown below:

$$Maximize \sum_{n=1}^{N} R_n(i) = \sum_{n=1}^{N} BWx\log_2[1+\gamma_i(n)] \tag{5}$$

$Subject\ to$:

$$\gamma i(n) \geq \gamma o \tag{6}$$

$$p_i(n) \geq 0, i \in Xi \tag{7}$$

$$p_j(n) \geq 0, j \in Yj \tag{8}$$

$$\gamma m(n) \geq \gamma m_0 \tag{9}$$

$$pk(n) < Pm(n), k \in Xi \cup Yi \tag{10}$$

Inequality (6) satisfies the SINR constraint for the SUs, inequality (9) satisfies the SINR condition for the PU of channel n and inequality (10) is the power constraint for the SUs' transmissions. The intermediate nodes are informed with a beacon by Cluster C for the appropriate transmission power on all channels of cluster C that can be CCC or B-CCC and which offer the best transmission opportunities i.e. avoid collisions with the PUs. Thus the protocol supports mobile secondary users.

Each cluster runs a Reinforcement Learning Scheme in a distributed manner to avoid collision with the PUs and creates the list with the most favorable channels in descending order. The neighboring clusters have then to decide upon the final selection of their CCCs and B-CCCs such that they do not overlap and in the same time maximize the transmission rates for those channels so to meet the QoS constraints.

As the maximization of the bit rate concerns only the channels for which the signals do not suffer from low SINR and PU activity is below a threshold so that provide good transmission opportunities, the bipartite graph is updated only with the corresponding connections between the neighboring clusters.

As SINR changes for the moving vehicle the optimization problem has to be solved whenever a change occurs.

10.4. PU COLLISION AVOIDANCE AND CHANNEL HOPPING

A Learning Automaton is a control mechanism that adapts to changes in the environment. The conditions for a stochastic learning automaton of P-Model to be appears in [134] as well as the definition of the stochastic learning automaton which is introduced for the proposed protocol which is optimal too. $S[i,t]$ is the learning automaton metric for channel i at time t.

$$\lim_{t\to\infty} \mathbb{E}\{S[i,t]\} = \mathbb{E}\{\lim_{t\to\infty} S[i,t]\} =$$

$$\mathbb{E}\{\lim_{t\to\infty}\left(S[i,0](1-L)^t + L\sum_{i=0}^{t}(1-a)(1-L)^i + L(1-a)(1-L) \right)\} =$$

$$\xrightarrow{for\ n\ slots\ \ with\ no\ PU\ and\ k\ slots\ with\ PU=t}$$

$$\mathbb{E}\{\lim_{t\to\infty}\big(S[i,0](1-L)^t+(1-a)(1-L^2)\big)\}\Longrightarrow$$

$$\mathbb{E}\{\lim_{t\to\infty}S[i,t]\}=\mathbb{E}\big\{(1-\alpha)\big(1+L(1-L)\big)\big\}$$

$$=(1-\alpha)\big(1+L(1-L)\big)\xrightarrow{MAX(L(1-L))=0.25}$$

$$\xRightarrow{a=0,2}\lim_{t\to\infty}\mathbb{E}\{S[i,t]\}=1\qquad(11)$$

In the former paradigm it is optimal for $\alpha=0.2$. So, as soon as we decide about the speed of converge we can choose the value for α or L respectively such that the scheme is optimal. If spectrum sensing is inaccurate i.e. in cases of false alarm and misdetection, then for N times in sequence, the sensing is inaccurate. The scheme for a false alarm decreases when it should increase, and for misdetection, the scheme increases when it should decrease for N times in sequence:

$$S'[i,t+1]=\underbrace{\{S[i,t+1-N]((1-L)+L*(1-\alpha)\}}_{express\ misdetection\ \ at\ time\ t+1-N}+$$

$$+\cdots+$$

$$+\underbrace{\{\,S[i,t+1-m]*\ (1-L)\ +\ L*(1-\alpha)\,\}}_{express\ misdetection\ at\ time\ t+1-m}+\cdots+$$

$$+\underbrace{\{S[i,t+1]*(1-L)\ \ +\ L*(1-\alpha)\,\}}_{express\ misdetection\ at\ time\ t+1}=$$

$$=\quad\underbrace{\{S[i,t-N](1-L)(1-L)+L*(1-\alpha)\}}_{express\ misdetection\ at\ time\ t+1-N\ with\ respect\ to\ t-N}\quad+$$

$$+..+$$

$$+\quad\underbrace{\{S[i,t-m]*(1-L)(1-L)\ +L*(1-\alpha)\}}_{express\ misdetection\ at\ time\ t+1-mwith\ respect\ \ to\ t-m}\quad+\cdots+$$

$$+\underbrace{\{S[i,t]*(1-L)*(1-L)\ +\ L*(1-\alpha)\}}_{express\ misdetection\ at\ time\ t+1\ with\ respect\ to\ t}=\cdots=$$

$$=S[i,t+1]+L(1-\alpha)(1-L)^{N+1}\qquad(12)$$

The second part of the sum in (19) refers to the number of times in sequence the sensing outcome is a misdetection.

$$S'[i,t+1]=$$

$$= \underbrace{S[i,t+1-N](1-L)}_{express\ false\ alarm\ at\ time\ t+1-N} +$$

$$+\cdots+ \underbrace{S[i,t+1-m]*(1-L)}_{express\ false\ alarm\ at\ time\ t+1-m} +\cdots+$$

$$+ \underbrace{S[i,t+1]*(1-L)}_{express\ false\ alarm\ at\ time\ t+1} =$$

$$= [\ \underbrace{\{S[i,t-N](1-L)+L*(1-\alpha)]*(1-L)\}}_{express\ false\ alarm\ at\ time\ t+1-N\ with\ respect\ to\ t-N} +$$

$$+..+$$

$$+ \underbrace{\{[S[i,t-m]*(1-L)+L*(1-L)](1-L)\}}_{express\ false\ alarm\ at\ time\ t+1-m\ \ with\ respect\ to\ t-m} +..+$$

$$+ \underbrace{\{[S[i,t]*(1-L)+L*(1-L)](1-L)\}}_{express\ false\ alarm\ at\ time\ t+1\ with\ respect\ to\ t} = \cdots =$$

$$= S[i,t+1] - L(1-\alpha)(1-L)^{\ N+1} \qquad (13)$$

The second part of the sum in (20) refers to the number of times in sequence the sensing outcome is a false alarm. The error limit is zero [134] (11).

The SUs form clusters on available channels and run the Reinforcement Learning Scheme for estimating the two most favorable available channels to be selected as the CCC, B-CCC and maximize throughput.

If channel *i* has a higher metric than j and Control Channel Hopping has to take place, this implies that at time *t-N*, channel *i's* the scheme's outcome was equal to the outcome of channel *j* at time *t*:

$$S'[i,t] - S'[j,t] = S'[i,t-N](1-L)^N +$$

$$+(1-\alpha)[1-(1-L)^N) - S'[j,t]$$

$$\xRightarrow{S\prime[i,t-N)=S\prime(j,t)=So}$$

$$\Rightarrow Distance = S'[i,t] - S'[j,t]$$

$$= (1-\alpha)[1-(1-L)^N] + [(1-L)^N - 1]S'_o =$$

$$= [1-(1-L)^N](1-\alpha-S'o) \qquad (14)$$

$$\lim_{N\to\infty} Distance = 1-\alpha-S'o \qquad (15)$$

$$and$$

$$If\ \ Dinstance < \varepsilon_1 \Rightarrow S'o > 1-\alpha-\varepsilon_1 \qquad (16)$$

We accept a broadcast channel hopping to channel i, if $S[i,t] > 1 - \alpha - \varepsilon_1$ to ensure that the hopping leads to a channel with good opportunities for transmission.

As in Cognitive Radio Networks SUs transmissions are restricted by PU activity, not all the channel's bandwidth is available to SU. So, the better transmission opportunities are detected i.e. higher channel metric, a higher rate of the actual channel's bandwidth is available to Cognitive Radio Network. The reinforcement learning scheme does not depend on channel's statistics. A scheme based on statistics due to PU's traffic distribution variance would bypass longer vacancies in a channel with worse statistics and on the other hand would utilize shorter vacancies in a channel with better statistics. Thus, a scheme based on statistics does not utilize opportunities efficiently. As the scheme guarantees the best transmission opportunities and QoS is provided then the highest data rates (5) are leveraged.

10.5. BROADCASTING PROTOCOL DESCRIPTION

The CR-cluster head (CR-CH) collects the reinforcement learning scheme outcomes namely the channel table lists of central and edge cluster nodes and sets the channel table list of central nodes as the cluster's channel list. The reinforcement learning scheme learns the PU traffic as it is optimal so avoids collisions with the PUs at all. The channel with the best metric is the first entry in the table *List[]*.

Each SU measures interference and creates a table with the current interference value for each channel, the $SINR[]$. If SINR for a channel is below a certain threshold, it is restricted from transmission and updated as -1.

The transmitter broadcasts bandwidth requirement control packet to prioritize the transmissions in channels that meet the bandwidth constraints before the broadcasting starts. Each cluster adjusts the power of the related SUs to maximize the transmission rate and creates a second list *Bandwidth[]* with highest achievable bit rate appearing first in the list based on (5).

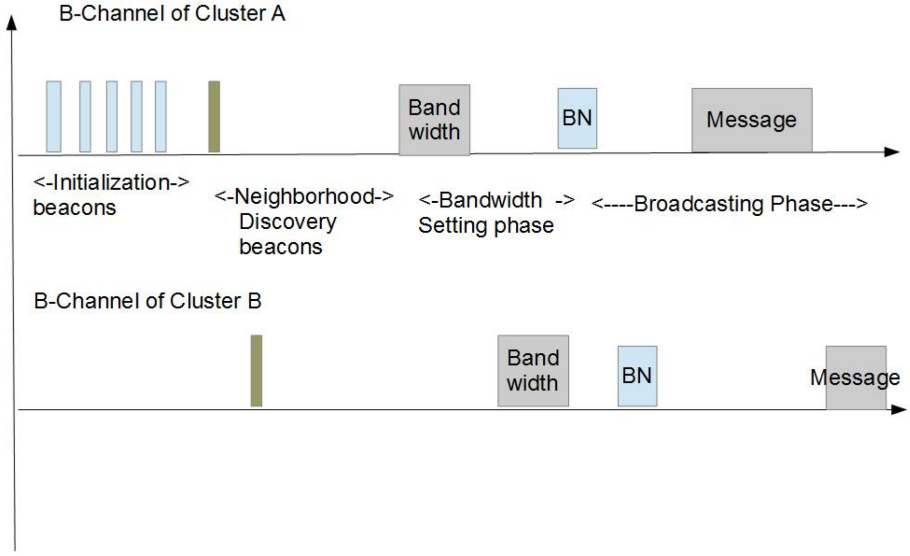

Figure 10.2: The three phases of the Broadcasting Protocol

The SU senses the spectrum and creates the *List[]*, *SINR[]* and *Bandwidth*[] tables, which will be used for the creation of the final channel list *List2[]* as follows:

Condition (16) must hold for a dedicated CCC or B-CCC to bypass the worst case scenario: PU collision.

Control beacons assist the cluster on defining its limits, discover neighbors, their corresponding CCCs/B-CCCs and intermediate nodes. The latter undertake the task of overhearing the neighboring broadcast channels for updates. Inter-cluster communication is responsible for non-overlapping of CCC and B-CCC channels of neighboring clusters.

In the meanwhile, the cluster nodes can receive assistance from the cloud. The clusters are self-organized locally (one-hop distance within the cluster as the communication is achieved via the CCC) with no global information is required but neighbor discovery. Dynamic broadcast channel avoids common control channel vulnerabilities, e.g., flooding attack sensitivity, and utilizes more efficiently time and space-varying spectrum opportunities.

Algorithm for CCC and B-CCC selection:

$FOR - Main\ loop$

$\{$

$FOR - i\ loop$

$\{$

$Scan \quad List[i]$

$if\ (List[i] = n\ \&\&\ SINR[n]! = -1 \quad \&\&$

$(S[i,t] - S[0,t] > 1 - \alpha - \varepsilon))$

$//check\ if\ the\ SINR\ is\ acceptable\ for\ channel\ n$

$\{$

$/Update\ List2\ table\ with\ the\ channels\ with$

$acceptable\ \ SINR\ in\ metrics'\ order$

$List2[] = n;$

$\}$

$Run\ maximatation\ of\ bit\ rate\ (5)$

$\left(\begin{array}{c} input: first\ entries\ of\ \ List2[\quad]of\ neighboring \\ clusters\ and\ cluster's\ own \end{array} \right)$

$\{output:$

$Update\ Bandwidth[\quad]\ list;$

$\}$

$//\ select\ the\ CCC\ and\ B - CCC\ from\ the\ current\ Bandwidth\ table$

$//set\ the\ first\ entry\ in\ the\ Bandwidth\ table\ as\ CCC$

$CCC = \ Bandwidth[0];$

$B - CCC = \ Bandwidth[1];$

$/Runthe\ Main - loop\ whenever\ List[\quad]OR\ SINR[\quad]$

$//OR\ \ new\ QoS\ requirements\ are\ updated$

$\}\ //END - Main\ loop$

Condition (16) must hold for a dedicated CCC or B-CCC to bypass the worst case scenario: PU collision.

Control beacons assist the cluster on defining its limits, discover neighbors, their corresponding CCCs/B-CCCs and intermediate nodes. The latter undertake the task of overhearing the neighboring broadcast channels for updates. Inter-cluster communication is responsible for non-overlapping of CCC and B-CCC channels of neighboring clusters.

In the meanwhile, the cluster nodes can receive assistance from the cloud. The clusters are self-organized locally (one-hop distance within the cluster as the communication is achieved via the CCC) with no global information is required but neighbor discovery. Dynamic broadcast channel avoids common control channel vulnerabilities, e.g., flooding attack sensitivity, and utilizes more efficiently time and space-varying spectrum opportunities.

10.6. BROADCAST PHASES DESCRIPTION

Initialization phase

- SU senses the spectrum and creates *List[]*, *SINR[]*, *List2[]* *Bandwidth[]* and identifies broadcasting channels CCC and B-CCC

- Sends a beacon (ID and channels list) at the CCC initiating the cluster and gets the first ID in the cluster. If there is no response in CCC, i.e., there are no other SUs proceeding with the next entry in the *List2[]* and performing the same steps to initiate a cluster establishment. In the latter case, the SUs that are present seem to be in a wider range of distance. SUs respond with beacons.

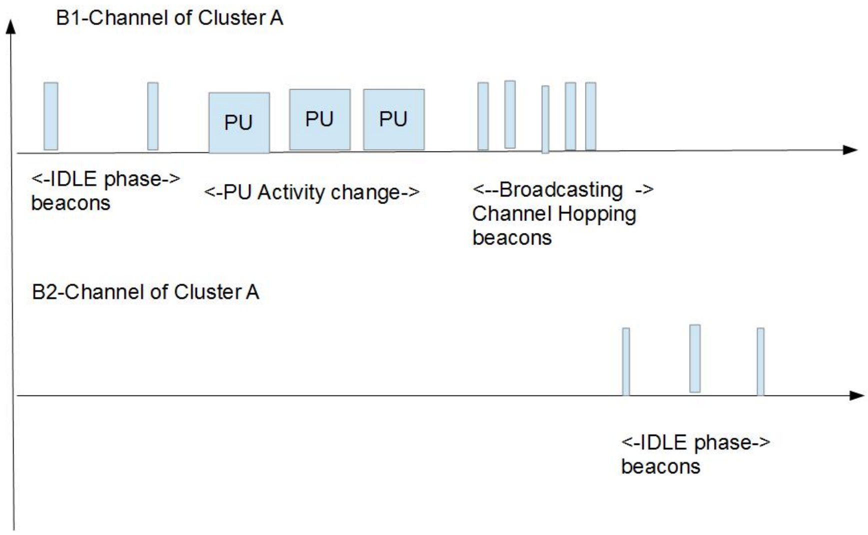

Figure 10.3: Broadcasting Channel Hopping phase

- Waits for the beacons of all other SUs sharing the same available channels. Beacons also synchronize the cluster.

Neighborhood Discovery

- The SU scans the List[] channels for beacons of neighboring clusters at their CCCs

- If he overhears a neighboring cluster's CCC, notifies the cluster nodes that will be the intermediate node for that cluster with a beacon (ID, Channel-ID) and sends a (ID, CCC, B-CCC) at the CCC' informing the neighbors of its cluster's own CCC, while the neighboring cluster replies with the slot number, which is given to its neighbors to transmit the BROADCAST_SETUP message in order to guarantee collision avoidance at the receiver's site. A broadcast packet is transmitted only once at the CCC of the cluster.

- If more than one nodes aim to be an intermediate node for a particular cluster, the one with the highest SINR is selected as an intermediate node. The intermediate node gives the identity to the neighbor cluster.

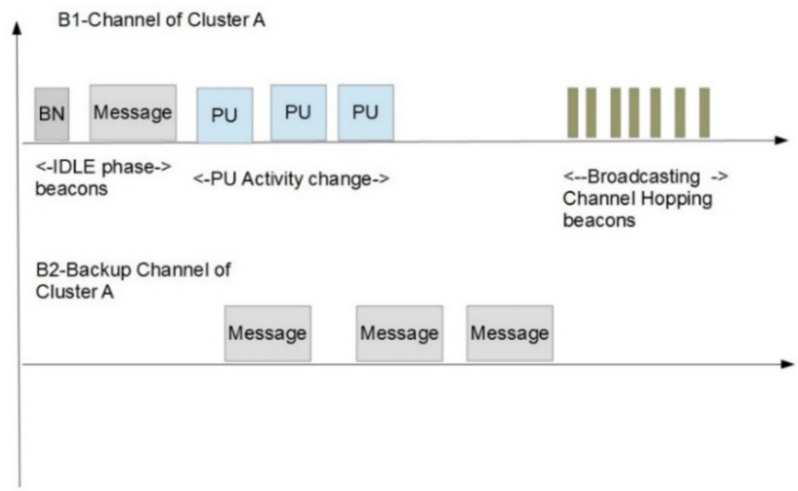

Figure 10.4: Backup Channel Hopping due to PU activity change during broadcasting

Idle phase

The intermediate nodes overhear the neighboring cluster’s broadcast channel for changes.

If the intermediate node is unavailable the cluster may obtain assistance from the cloud’s database.

The cluster's nodes send beacons periodically to reaffirm the broadcast channel, *List2[]* and for cluster synchronization. Each cluster informs its neighbors of the slot so that they can transmit a BROADCAST_SETUP.

Broadcast phase

- The cluster waits for BROADCAST_SETUP control message
- Updates table *Bandwidth[]*
- If a BROADCAST_SETUP control message arrives to the cluster from more than one neighboring clusters, then chooses the neighboring cluster whose intermediate node has the higher SINR to receive the broadcast messages from.
- Then informs the selected neighboring cluster with a beacon.
- Waits for broadcast BEGIN(BN) message.
- Broadcast data packets occupy all the slots of the CCC.
- Transmitter sends BROADCAST_END to end broadcast.

Broadcast Channel Hopping

- If the CCC has to change, the cluster and namely a node denoted as cluster head initiates the CCC hopping process and runs the Algorithm for CCC and B-CCC selection.
- Neighboring clusters cannot share the same CCC. The cluster that initiates first a channel as CCC, this cluster keeps this channel as CCC.
- Neighboring clusters exchange *List2[]* and CCC, B-CCC information with beacons
- If the algorithm for CCC and B-CCC selection has to be initiated during broadcasting then a node of the cluster i.e. the cluster head runs the algorithm while the

intermediate nodes of the cluster participate in the broadcasting. When the new CCC and B-CCC have been computed then the cluster informs its member and its neighbors with beacons whilst the slots assigned between the neighboring clusters remain the same. As soon as the broadcasting ends the cluster head initiates CCC and B-CCC selection process again but this time all of the cluster nodes will participate.

The proposed Broadcasting Protocol achieves fast reclustering, minimum control overhead, utilizes the spectrum efficiently by integrating an optimal machine learning scheme. Non-overlapping Broadcasting paths which restrict multiple copies of broadcast data packets are set during broadcast data delivery idle periods with beacons providing stability to the network and avoiding delay and bandwidth overhead. Each broadcast packet is transmitted at CCC with no additional delay, overhead and collision avoidance at receiver's side. Local optimums are reached.

10.7. SIMULATION RESULTS

The simulation results cover a comparative study with a multi-hop broadcast protocol for a CR Ad Hoc Network, namely, Bracer [126], which supports collision avoidance on the receiver's side, and with CRBP [128], which does not support collision avoidance on the receiver's side. [126] implements retransmissions of each data packet on multiple channels. Not all experiments involve [128] as it does not support collision avoidance, so [126] outperforms [128]. Simulation was performed with OMNET software.

For the experiments, a three-hop network was considered with five channels and ten channels, with PU traffic following an exponential distribution. One- hop delay was set to 1ms. There are two main groups of experiments, those with a five-channel cognitive network and those with a ten-channel cognitive network. For each main group of experiments, there were two sub-groups of experiments: one that included experiments that were conducted with various PU traffic scenarios and one that included experiments with various data packet lengths.

The average broadcast ratio, mean delay, broadcast overhead and collision rate were tested against a) six PU traffic scenarios for exponential distributed traffic: 1) 0.2s, 2) 0.4s and 0.5s, 3) 0.5s, 4) 0.5s and 0.7s, 5) 0.6s and 0.8s, 6) 0.7s and 0.9s; and b) five scenarios of different packet lengths for 0.5s exponential PU traffic. The BEGIN packet length was 200 bits, and the broadcast data packet length was 2000bits for the experiments where broadcast ratio, overhead, mean delay and collision rate were tested against different PU traffic scenarios.

For the proposed protocol, the broadcast burst following each BEGIN message was fourteen and twelve data packets. For [127], the parameter w=3 in the five-channel experiments; and w=4 in the ten-channel experiments.

The proposed protocol transmits only once each packet, whilst [127] retransmits the same packet to multiple channels as the receivers are unsynchronized which is a considerable overhead. This is the reason that the proposed protocol outperforms [8]. In fact, the unsynchronized receivers at [127] cannot avoid collision which increase the time that a packet requires to reach a receiver and the overhead as multiple copies have to be resent. Mean delay, collision ration and overhead were tested only for the proposed protocol and [127] as they are both support collision avoidance at receiver’s side, i.e. [127] outperforms [129]. Broadcast ration experiments included and [10] as [10] could provide good results on this experiment.

The experiments in Figure 10.8 and Figure 10.13 show that the proposed protocol is more tolerant to packet lengths increases than [127] as in [127] retransmissions occur blindly. The proposed protocol learns the PU traffic and utilizes longer spectrum vacancies more efficiently for the increasing broadcast data packet lengths.

Figure 10.5: Broadcast ration for six PU traffic scenarios and five channels

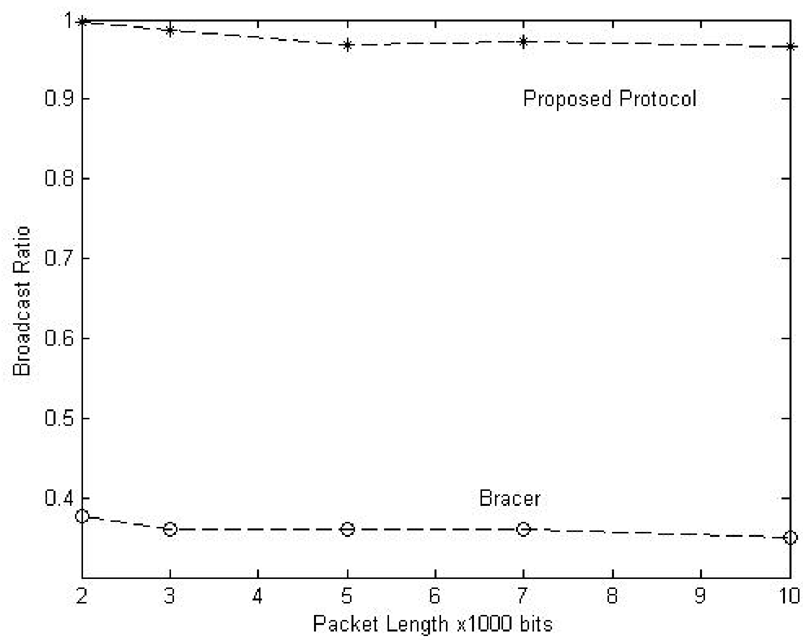

Figure 10.5: Broadcast ration for six PU traffic scenarios and five channels

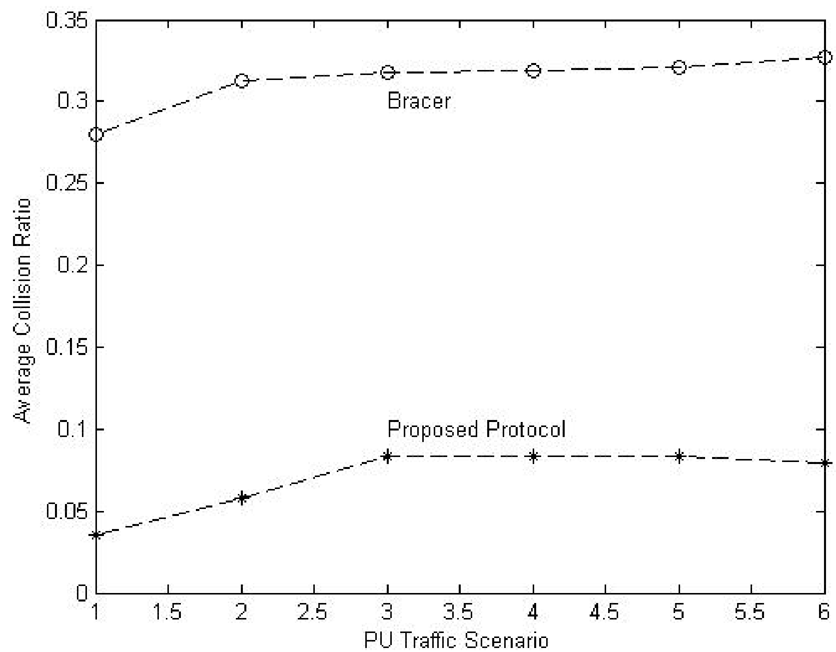

Figure 10.6: Collision Ratio for six PU traffic scenarios and five channels

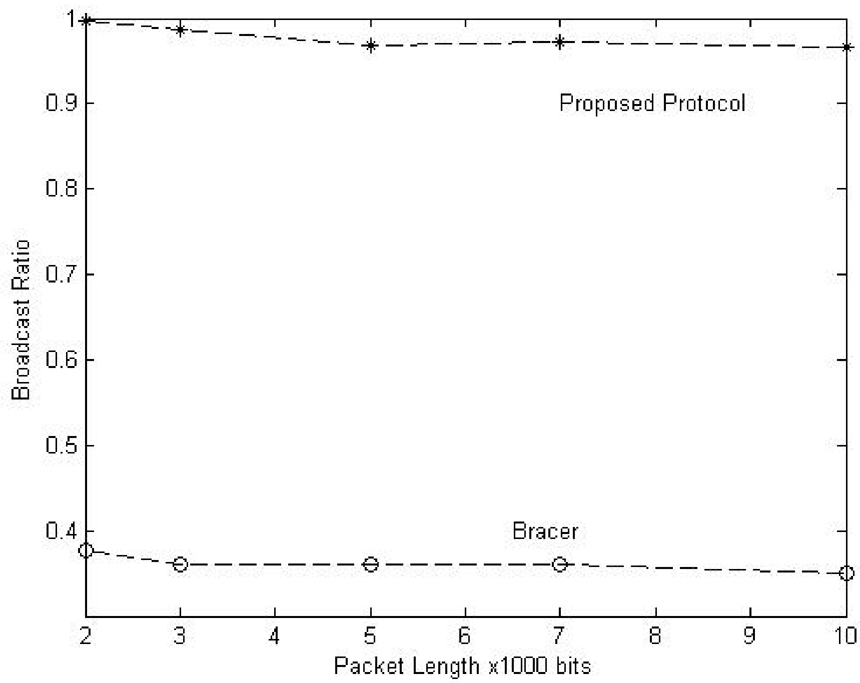

Figure 10.7: Broadcast Ration for various packet lengths and five channels

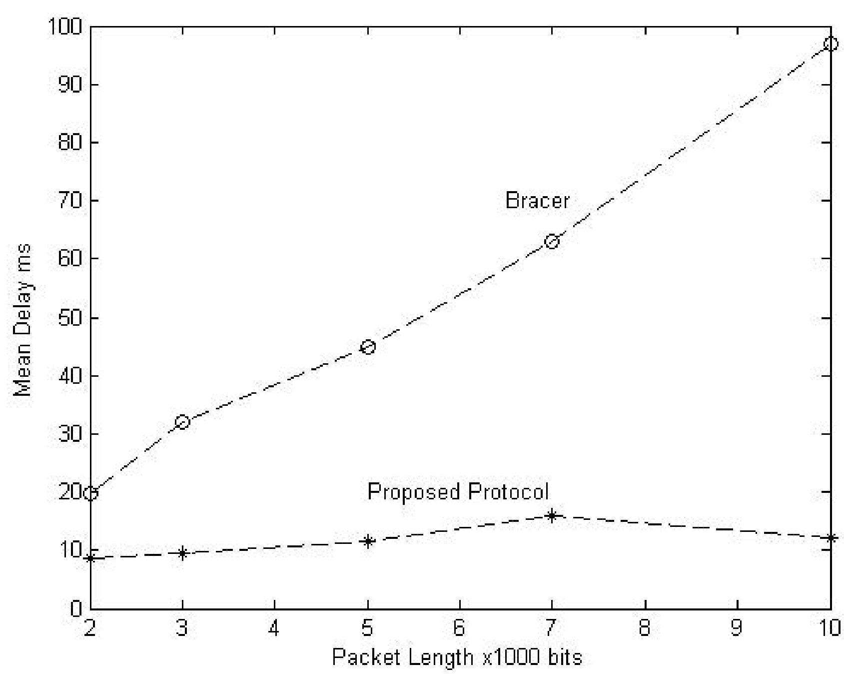

Figure 10.8: Mean Delay for five packet lengths and five channels

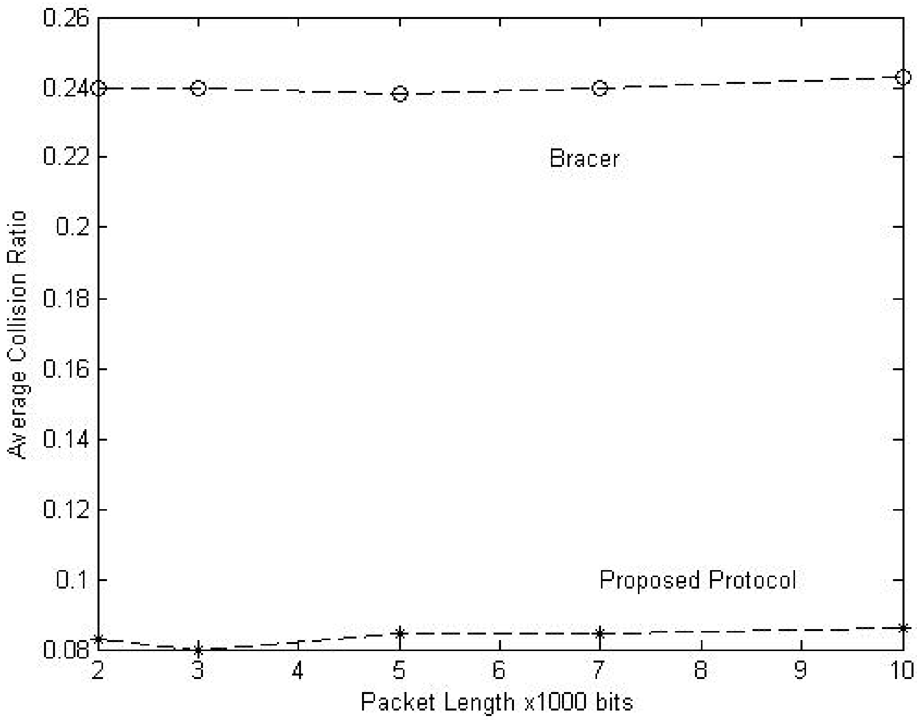

Figure 10.9: Collision Ratio for five packet lengths and five channels

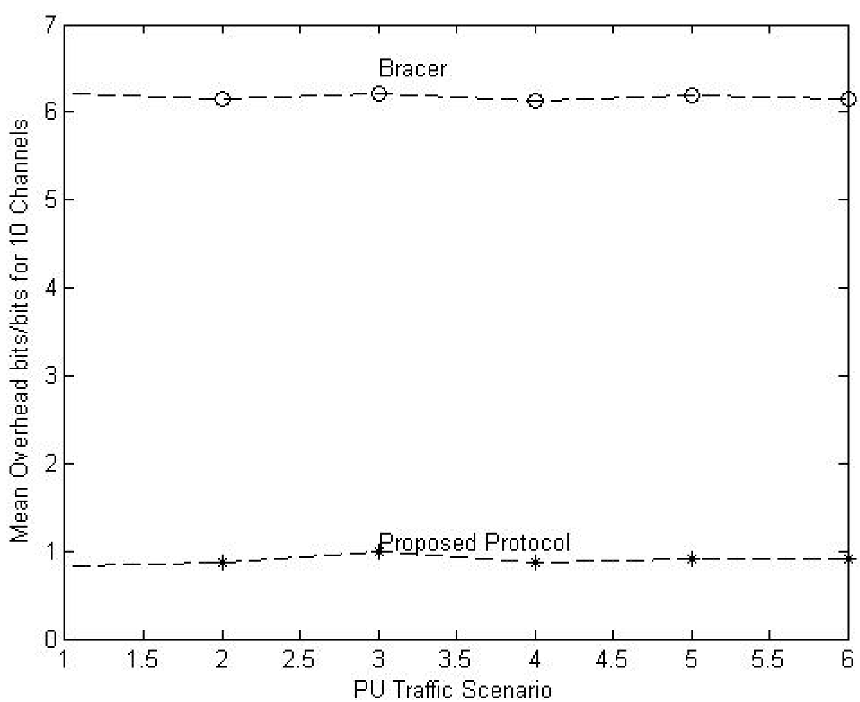

Figure 10.10: Overhead for six PU traffic scenarios and ten channels

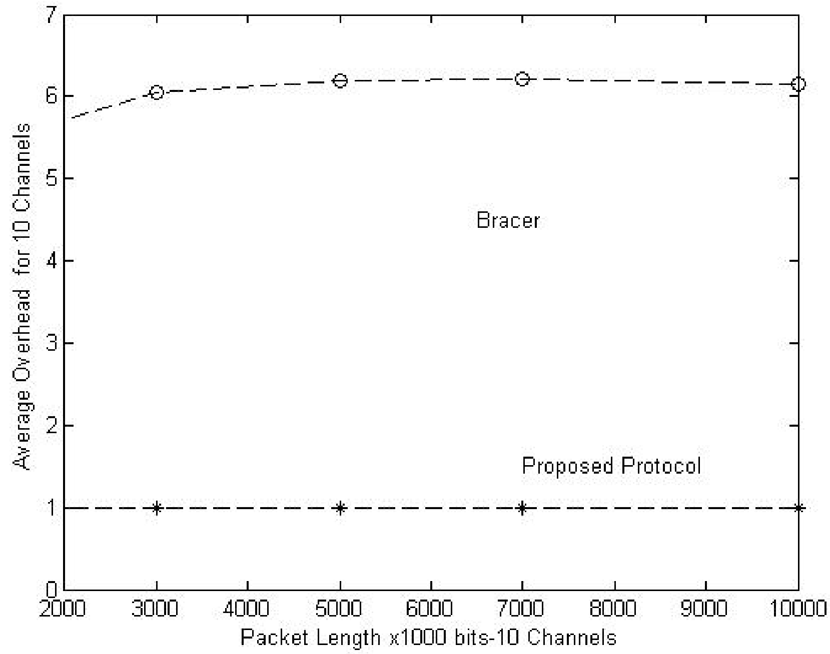

Figure 10.11: Overhead for five packet lengths and ten channels

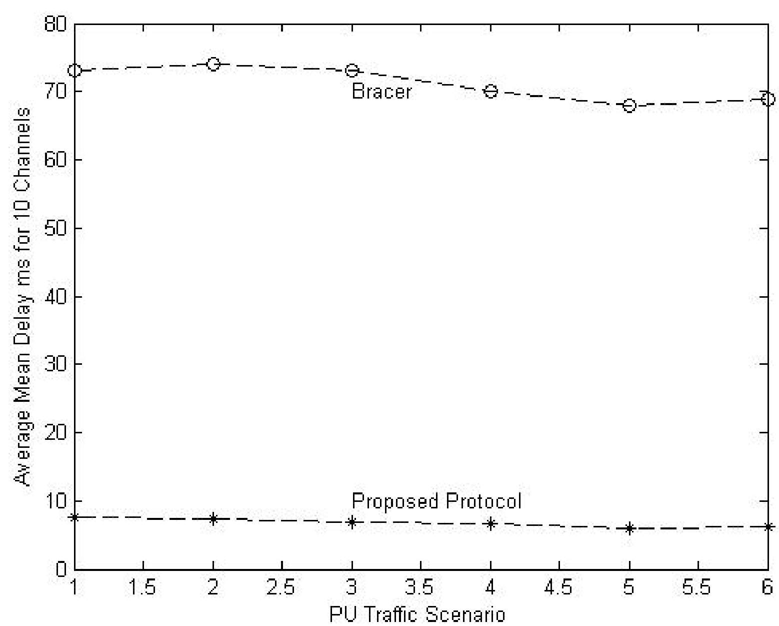

Figure 10.12: Mean Delay for six PU traffic scenarios and ten channels

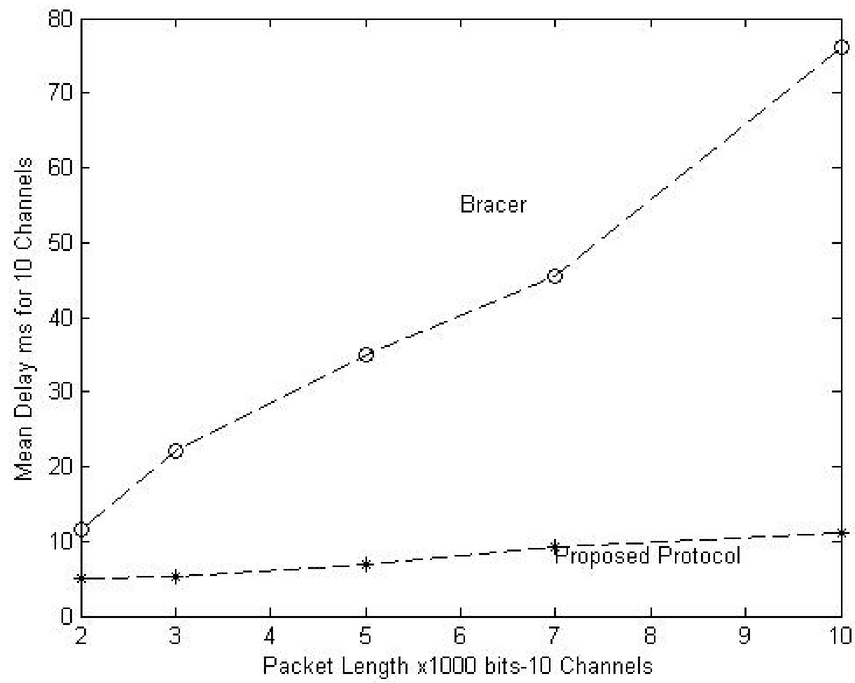

Figure 10.13: Mean Delay for five packet lengths and ten channels

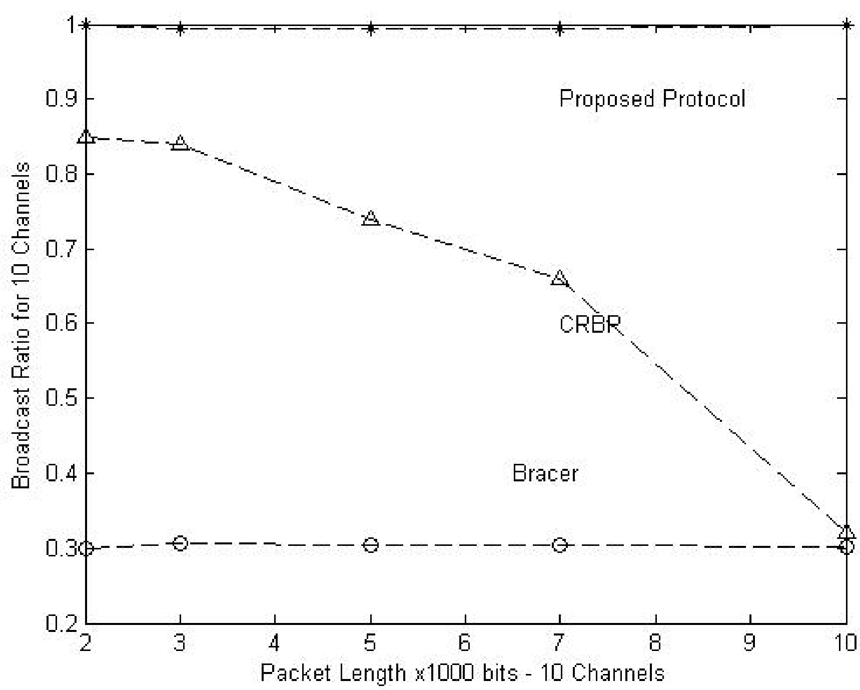

Figure 10.14: Broadcast Ration for five packet lengths and ten channels

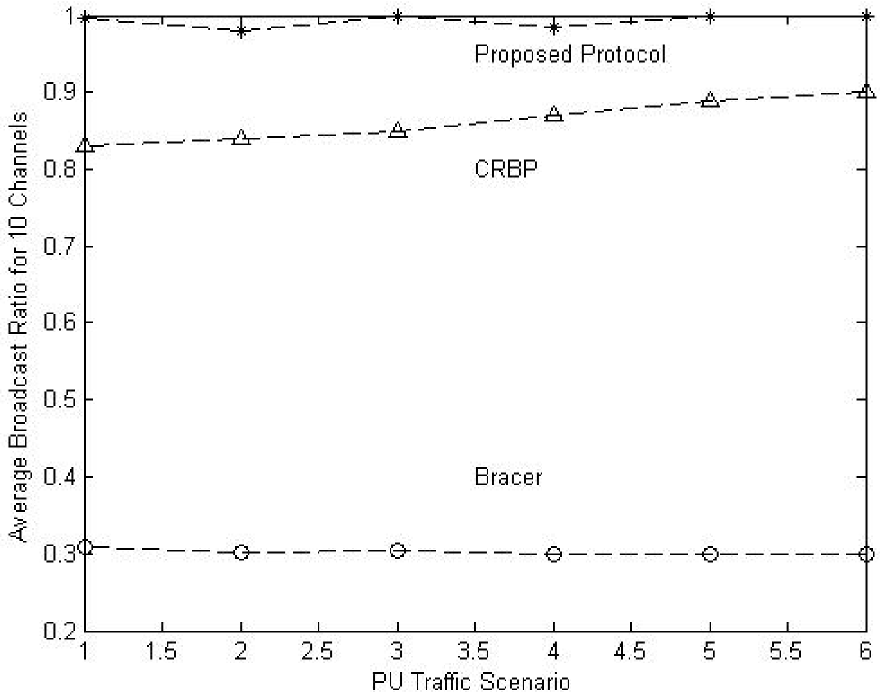

Figure 10.15: Broadcast Ratio for six PU traffic scenarios and ten channels

The broadcast ratio, i.e., the percentage of the sender's generated packets that reach the receiver node for each hop, is measured, as well as the mean delay, the overhead, i.e., the rate of outgoing and incoming bits (bits/bits) in a node, and the collision rate. The broadcast ratio and overhead measurements in experiments justify the difference in mean delay for various PU traffic scenarios and various data packet lengths as well; A priori broadcasting path establishment, allows rapid broadcasting in a PU environment. As traffic comes in bursts, the updates interval of channel conditions are long enough not to affect the protocol's performance.

10.8. CONCLUSION

The proposed Broadcast Protocol achieves local optimums in channel sensing and bit rate maximization without global information. Collision avoidance at receiver's side is ensured saving energy and resources for the network. An optimal Machine learning Scheme predicts the best channel availability for broadcasting avoiding collisions and minimizing CCC hopping due to PUs' arrival which is energy consuming. The network nodes can be unmovable but due to fast reclustering the protocol can be applied to movable nodes. Fast reclustering is feasible via relegation of computations to the cluster and its neighboring clusters level. The proposed protocol outperforms existing literature which supports Collision avoidance at receiver's side and provides QoS without degradation.

Chapter 11

SECURITY ISSUES IN COGNITIVE RADIO NETWORK AND CLOUD

Coordination without Collaboration in Imperfect Games: the Primary User Emulation Attack Example

In cognitive radio networks, an adversary transmits signals with characteristics that emulate those of primary users to prevent secondary users from transmitting. Such an attack is called a primary user emulation (PUE) attack. In this research work [141], a game theoretical framework is proposed to study the primary user emulation attack (PUEA) on cognitive radio nodes as a game of imperfect information between the Secondary Users (SUs) who do not exchange game information between them against the adversaries generating the PUEA and to define optimal strategies with minor computational demands. When the SU challenges the PU Emulator successfully, updating the information on a Cloud-based database enables the rest of the network to know the identity of the PUE. As the game evolves, the grand coalition of the secondary users acts as one without collaboration against the PU Emulator playing a winning strategy. The performance of the game for optimal strategies is equal to the performance of the collaborative methods for PUEA detection.

11.1 Introduction

Cognitive radio technology was introduced to answer the spectrum scarcity problem by enabling an unused or under-utilized spectrum to be used by users who are not licensed (secondary users-SUs) whenever the licensed users (primary users-PUs) vacate the spectrum. Although the SUs must periodically sense the spectrum, find the best spectrum band, dynamically access the spectrum - Dynamic Spectrum Access (DSA) and vacate it within a certain time upon the return of the primary user, the sensing mechanisms for PU detection do not guarantee a 100% accuracy. This vulnerability makes the cognitive network prone to Denial of Service (DoS) attacks, namely, Primary User Emulation Attacks (PUEAs). The selfish PUEA behavior is studied, i.e., when the adversaries do not act maliciously but want to gain the spectrum selfishly.

Actually, the scheme that describes the coexistence with the primary network fall into three classes: Underlay, Overlay and Interweave. In the underlay approach, simultaneous secondary and primary transmissions are allowed as long as the interference level at the primary user side remains acceptable. In the overlay approach, primary users share knowledge of their signal codebooks and messages with the cognitive users. Finally in the interweave approach, cognitive users sense the spectrum in different dimensions to find the abundant spectrum gaps. Hybrid schemes using a combination of the aforementioned approaches improve the efficiency of spectrum sharing and maximize the transmission rate once a spectrum opportunity is detected.

Due to the nature of dynamic spectrum access, the CR network became vulnerable to attacks by hostile users regarding all theits main functionalities such as spectrum sensing, spectrum mobility, spectrum sharing and spectrum management. The typical attacks on CR networks may include Primary User Emulation Attacks, Denial of Service (DoS) attacks, system penetration, repudiation, spoofing, authorization violation, malware infection, and data modification. These attacks cause potential threats to the information confidentiality, integrity and availability of the CR network. The Primary User Emulation Attack is considered here.

This paper introduces a method beginning from an original imperfect game of non-partial observations of the players without collaboration/cooperation that eventually evolves to a perfect game with coordination between the players such that they make the same decisions without exchanging messages and then apply the formation to PUEA Detection problem. The PUEs will have a serious penalty for PU Emulation, if detected by the PU. The grand coalition of the SUs achieves coordination as the game evolves and acts as one SU player - without collaboration - who plays a zero-sum game with the PUE. It is considered one arrival of PUE each time. Perfect recall is also considered, i.e., the nodes are aware of all of their past actions and observations. The optimal strategy of the zero-sum game is calculated, and the value of the game is also calculated. Upon successful detection of a PUE a Cloud-based database is updated such that the rest of the network knows the identity of the attacker. The SU nodes connect to the Cloud-based database periodically.

The real PUE transmission probability is eliminated over the range of 0.5% to 1.3% for the PUE optimal strategy, the per SU basis high values up to 99%, while the *PUE detection negative* reaches 6%. The rest of the paper is organized as follows. Sections I and II are an introduction to the work reported in this paper and related work on PUE Attack, respectively. Section III is a thorough description of the system model, particularly subsection A, which is a presentation of Information Tracking in Games. Subsection B is a presentation of Epistemic Unfolding with Knowledge Sets and subsection C introduces the new game of imperfect information, which evolves, while playing, to a game of perfect information based on Information Tracking and Epistemic Unfolding with Knowledge Sets. The new game is applied to the PUE problem, which is solved, and optimal strategies are computed. The results for optimal strategies are similar to the collaborative method results for PUE Detection.

11.2 RELATED WORK

In [142], the authors study imperfect games and introduce the constraints for a safety game based only on the observations of the players, but they do not define best strategies. Best strategies and perfect coordination construction are introduced in [143] for imperfect games of players with partial observations - the observations of the game by the SUs are not partial. This limitation is overcome by combining both [142] and [143], extending them such that a new type of game is introduced that is not dependent on the states of the game but on the knowledge sets (knowledge gained) states that are extracted by the analysis of the game according to [142] and then by applying the Deterministic Finite Automaton of Knowledge states to play a winning strategy.

Most studies on PUE Detection are location-based and use collaboration among the SU nodes. In [144], the authors compare the transmission origin with the previous known-PU position, and we identify similar approaches in [145], [146]. A coordinated decision is reached in [147] and in [148], [149] the position of the PUE is estimated. In [150], the authors use the phase noise of a local oscillator as a fingerprint to differentiate the incumbent signals from the attacking ones. Exploiting the collaboration between the nodes and the detection results reaches 99%. In [151], the signal activity pattern of the PU is used to detect a Primary User Emulation Attack. Coordination between one-hop nodes is used for PUE Detection in COOPON that reaches 87% for successful detection [152]. In [153], a two-level database-assisted detection approach is proposed to detect PUE attacks. Collaboration is the parameter that contributes more in detection [10].

In [154], the PUE Detection is formulated as a game, and a belief factor is introduced to learn the state of the primary user that is compared to a Bayesian belief estimation. The former achieves PU detection approximately 95.55%-95.29%, and the latter achieves PU detection approximately 83.57%-82.21%. The belief factor is updated with the information gathered by policy nodes, i.e., not real-time. The game theory is used to detect the selfish attacks [155] in the system. Yu-Wei Chan et al. [156] describe the payoff problems between the users. In [157], the authors present a constant sum differential game approach to mitigate the PUE attack. Based on the assumption that the PUE attacker has less energy than the PUs, they look for the optimal sensing strategy of SU. The Nash equilibrium solution is obtained. The authors in [158] formulate a non-zero-sum game with incomplete information for selfish and malicious PUE attacks without coordination to be achieved between the SU players at some point with no schedule for network parameter update while playing. In [159], they neither use collaboration nor past-PUE log information, and they achieve probability detection and false alarm probabilities equal to 90% and 10%, respectively. A Cloud service for strong centralized trust management is introduced in [160].

This paper proposes a model for achieving coordination without collaboration in imperfect game systems with non-partial observations, something that holds for Cognitive Radio Network. This model is introduced in this paper and is later applied in the well-known PUE Attack Detection problem in a non-cooperative Cognitive Radio Network. To the best of our knowledge, this paper is the first to introduce coordination without collaboration between SUs in a CRN for handling PUEA. The system has high performance. The secondary nodes must follow the same strategy based on the well-known penalties and gains that depend on the network conditions and are retrieved periodically from the Cloud database.

11.3 SYSTEM MODEL

11.3.1. Distributed Games and Information Tracking

In [142], the authors address the fundamental problem in distributed systems of decomposing a global winning strategy such that the individual agents operate on the information they can access. The information tracking on game graphs of games with imperfect information and particularly the unwrapping of the information sets K_i in a graph game with finite tracking is presented. The authors decide on a deterministic finite automaton construction of information sets that satisfies winning conditions on a game graph, and they add a choice function $s_i(K)$, thus implementing a distributed winning strategy. The analysis does not include optimal strategies.

A game with perfect information is a game where a player knows the state of the play at any stage. If the player does not, we speak of a game with imperfect information. Imperfect information arises naturally in computational models as an effect of locality of components, internal variables, privacy constraints, or incomplete specifications. One highly non-trivial issue regarding uncertainty in computational systems is whether the different players have the means to synchronize their moves. The general approach of solving games with imperfect information in the synchronous setting is the power-set construction proposed in for solving games for one player against nature [142].

11.3. 2. Perfect Coordination in Imperfect Games

In [142], the authors transform an n-player game G with imperfect information into a two-player zero-sum game $G_+{}^+$ with perfect information and define the best strategies such that the grand coalition in G has a winning strategy against nature if, and only if, the first player has a winning strategy in $G+$; winning strategies of the first player in $G+$ can be translated uniformly into joint winning strategies of the grand coalition in G and vice versa. To describe the knowledge acquired by the players during a play, they use epistemic models. An epistemic model over G is a Kripke structure K = (K, $(Pv)\ v \in V, (\sim i)i < n)$ where $(Pv)\ v \in V$ is a transition of K, and each $\sim i$ is an equivalence relation on K such that, for all $k, k' \in$ K, $if\ k \sim i\ k'$, then $vk \sim i\ vk'$, with υ_k denoting the unique element from V such that $k \in Pvk$.

11.3.4. Epistemic Unfolding with Knowledge Sets

This paper proposes a system for solving an imperfect game $\mathcal{G}$ in which players initially may pass through states of perfect information. The epistemic unfolding [142] is extended, and best strategies are defined. There are two phases for reaching the solution. In the first phase, the initial game graph G is unraveled, and the tracking of G is extracted to identify, if possible, and compute the Knowledge Sets and a finite-state automaton and, consequently, the distributed winning strategy. In the second phase, we compute the Kripke structures of the Knowledge Sets, and we perform epistemic unfolding in the new game in which the states are the Knowledge Sets of the G. We transform the game then to an equivalent one and inquire whether it is possible for the grand coalition to play a game of perfect information where

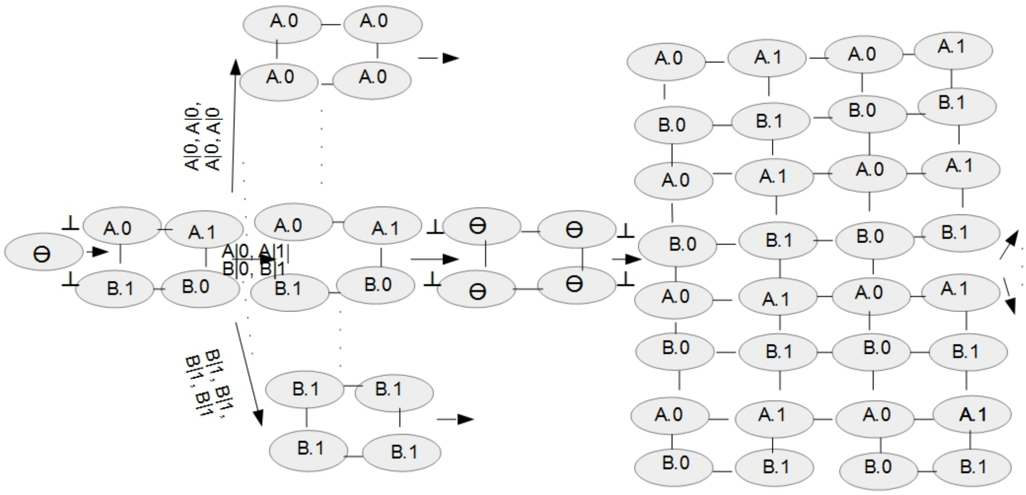

Figure 11.1: Epistemic Unfolding of an imperfect information game with Player 1's observations {A,B} and Player 2's observations {0,1}.

all players play a winning strategy and act as one, i.e., they are coordinated without cooperation, i.e., message exchange.

It is necessary to provide some definitions for the imperfect information games, as well as several theorems and lemmas that have been considered as preliminaries for the epistemic unfolding with knowledge set solving of a game with imperfect information.

We consider a game of n players against nature. We consider a set $A^i$of actions available to player i and a set of observations B^i for player $i. A$ is the set of action profiles and B the set of observation profiles. Next, a game graph is a structure $G =$ $(V, \Delta, (\beta i)\ i < n$ with V the set of positions, Δ the move relationship $\Delta \subseteq V \times A \times V$ and an observation function $\beta^i: V \longrightarrow B^i$ for each player $i < n$. G is a game tree if (V, Δ) is a tree. A play π starting from initial position $v_0 \in V$ in G is an infinite sequence of actions and positions $\pi = v_0, \alpha_0, v_1, v_1, \dots$ where $(v_l, \alpha, v_{l+1}) \in \Delta$, for all $l \geq 0$. We can extend observations to $\beta^i(\pi) = \beta^i(v_0), \beta^i(v_1), \dots$ Thus, a strategy for a player i is a function $s^i: (VA) * V \longrightarrow A^i$ such that $s^i(\pi) = s^i(\pi')$ for plays π, π' if $\beta^i(\pi) =$ $\beta^i(\pi')$. A play π follows strategy $s^i \in S^i$ if $\alpha_l^i = s^i(v_0, \alpha_0, v_1, \dots, \alpha_{l-1}, v_l)$ for every $l \geq 0$.

A winning condition over a game graph G is a set $W \subseteq (VA)^\omega$ of plays. A game $\mathcal{G}$ consists of its game graph and a winning condition. A play π is winning if $\pi \subseteq W$. A strategy s^I is a winning strategy if all outcomes are winning. A coloring function $(G, \Delta, (\beta^i)_{i<n}, \gamma)$ is available for games such that we can say that a coloring is observable by player i if $\beta^i(v) \neq \beta^i(v')$. Then, the coloring holds that $\gamma(v) \neq \gamma(v')$. A safety game is a game with two colors observable to all players $\gamma: V \longrightarrow$ $\{safe, notsafe\}$ such that $W = \{safe^\omega\}$, i.e., a play π is winning if it avoids all "$notsafe$" colored positions. A *bisimulation* between two game graphs G and G' is a binary relation $Z \subseteq V \times V'$ that preserves the colors and the observations. If two game trees T and T′ are bisimilar, then the games (T, W) and $(T', W)$are equivalent for every winning condition W. The *unravelling* of a game graph G from a position v_0 is a game tree $T(G, v_0)$ where the set of positions consists of all initial plays G, v_0, the move relationship consists of edges (π, α, π') for all plays $\pi = v_0, \alpha_0, \dots, v_l$ and $\pi' =$ $v_0, \alpha_0, \dots, v_l, \alpha_l, v_{l+1}$with $\alpha_l = \alpha$, the observation function of Player i maps every play $v_0, \alpha_0, \dots, v_l$ to $\beta^i(v_l)$, and the coloring function maps every $v_0, \alpha_0, \dots, v_l$ to $\gamma^i(v_l)$. Therefore, the projection $T(G, v_0) \longmapsto G, v_0$ sending every initial play to its last position defines a bisimulation between $T(G, v_0)$ and G, v_0. Extending this projection to entire plays allows us to view any winning condition W over a game graph as a winning condition over its unravelling and speak of $(T(G, v_0), W)$ as the unravelling of the game (G, v_0, W) [142].

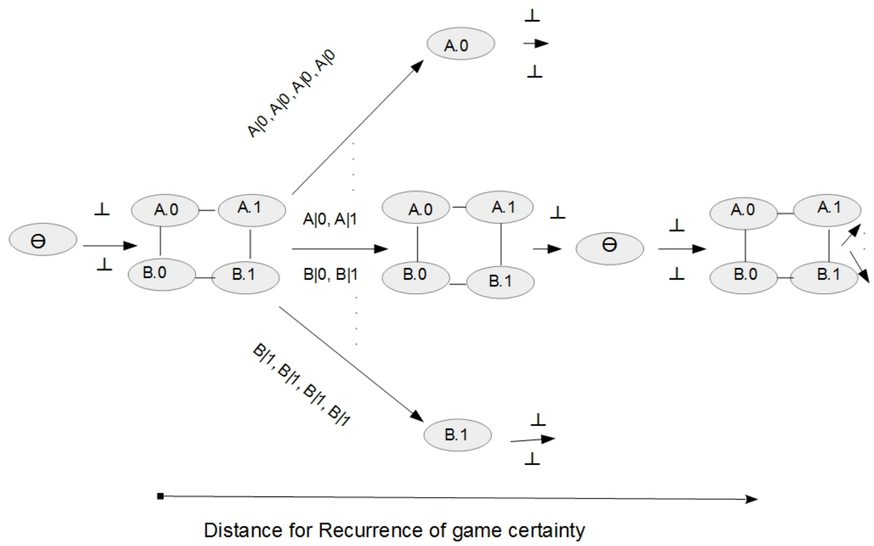

Figure 11.2: Epistemic Unfolding of an imperfect information game with Player 1's observations {A,B} and Player 2's observations: Computation of Tr ' $core$ {0,1}.

The *indistinguishability* relation of Player i on game tree $\mathcal{T} = (T, \Delta, (\beta^i)_{i<n}$ is defined as

$\pi \sim^i \pi'$ if $a^i(\pi) = \alpha^i(\pi')$ and $\beta^i(\pi) = \beta^i(\pi')$.

The indistinguishability relation of Player i on game graph G, v_0 is his indistinguishability relation on the unravelling of G, v_0 [142]. The indistinguishability relation on a game tree $\mathcal{T}$ satisfies perfect recall. The extensive form $Ext(G, v_0)$ of a game graph G, v_0 is the extensive form obtained by unravelling the game graph from the initial position v_0 and expanding the game graph with the indistinguishability relations of all players on the unravelling [142].

We consider a game tree $\mathcal{T} = (T, \Delta, (\beta^i)_{i<n}, \gamma)$ and the $\simeq$maximal bisimulation relationship over its expansion $(\mathcal{T}, (\sim^i)_{i\leq n})$ with the indistinguishability relations of all players. The *tracking* $Tr(\mathcal{T})$ of $\mathcal{T}$ is a game graph $G = (V\ \ , \Delta', (\beta'^i)_{i<n}, \gamma')$ with positions that correspond to the equivalence classes of $\simeq$, $\Delta' := \{[\pi], a, [\pi']: (\tau, a, \tau') \in \Delta$

for any $\tau \simeq \pi$ and $\tau' \simeq \pi'\}, \beta'^{i}([\pi]) = \beta^{i}(\pi), \gamma'([\pi]) = \gamma(\pi)$ and initial position that corresponds to the root of the $\mathcal{T}$. The tracking of a game graph is the tracking of its unravelling, and each game is equivalent to its tracking [2].

We must define knowledge set $\mathcal{K}^{i}$ also as a partition induced by $\approx^{i}$ in $Ext(\mathcal{G}, v_0)$. Thus, the $\mathcal{K}^{i}(\pi)$ of a play π is a unique set $\mathcal{K} \in \mathcal{K}^{i}$ with $\pi \in \mathcal{K}$ that reflects the knowledge the player must acquire to play a safety game on $\mathcal{G}, v_0$. Then, by expanding the knowledge set from the extensive form to the tracking of the game by setting as $\mathcal{K}^{i}(v)$ $t$he set $\mathcal{K}(\pi)$ for any play ending at v so that a player observes its current position to be sufficient. For all initial plays π, τ ending at the same node in $Tr(G, v_0)$, we have $\mathcal{K}^{i}(\pi) = \mathcal{K}^{i}(\tau)$ [142].

For every extensive game, if the grand coalition has a winning strategy, then it has a winning strategy such that $s^{i}(x) = s^{i}(y)$ whenever $x \approx^{i} y$ for all $i < n$.

If the tracking of a game is finite, then there is according to [142] a finite-state automaton over $\mathrm{A}^{i} \times \mathrm{B}^{i}$ for every player i that recognizes the knowledge set $\mathcal{K}(\pi)$ of any initial play $\pi = v_0, \alpha_0, v_1, \alpha_1, \ldots, \alpha_l, v_l$ for the action-observation sequence $\alpha_0^{i}, \beta^{i}(v_1), \alpha_1^{i}, \beta^{i}(v_2), \ldots, \alpha_{l-1}^{i}, \beta^{i}(v_i)$. If we add a choice function to the finite-state automaton $s^{i}(\mathcal{K})$ at every state $\mathcal{K} \in \mathcal{K}^{i}$, then we have a distributed winning strategy.

As soon as we have computed the finite-state automaton of the initial game of imperfect information $\mathcal{G}$, we will compute the Kripke structures of the Knowledge Sets that have been computed in phase one. Kripke structures hold all the information obtained by the players to play a safety game each time, i.e., to reach a winning condition.

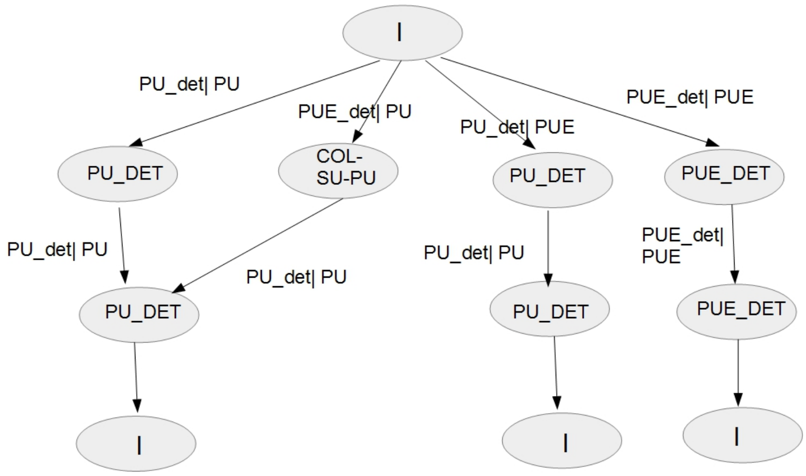

Figure 11.3: Game tree when there are no collisions between the PU-PUE

An epistemic model of a game $\mathcal{G}$ is a Kripke structure $\mathfrak{K} = (\mathbb{K}, (P_\upsilon)_{\upsilon\in\mathsf{V}} \ ,(\sim^i)_{\iota<\nu})$ where $(P_\upsilon)_{\upsilon\in\mathsf{V}}$ is a partition of $\mathbb{K}$ and each $\sim^i$ is an equivalence relationship on $\mathbb{K}$ such that for all $k_1, k'_1 \in \mathbb{K}$ if $k_1 \sim^i k'_1$, then $\upsilon_{k_1} \sim^i \upsilon_{k'_1}$ with υ_{k_1}denotes the unique element from V such that $k_1 \in P_{\upsilon_{\kappa_1}}$.

$\mathfrak{K}$ will connect with $\sim \cup = \cup_i \sim i$. A function f is an homorphism from $\mathfrak{K}$ to $\mathfrak{K}'$ for

$\mathfrak{K}' = (\mathbb{K}', (P'_\upsilon)_{\upsilon\in\mathsf{V}} \ , (\sim'^i)_{i<n}$ if $P_\upsilon(k_1) \Longrightarrow P'_\upsilon(f(k_1)$

and $k_1 \sim^i k'_1 \Longrightarrow f(k_1) \sim'^i f(k'_1)$, the models $\mathfrak{K} \approx^1 \mathfrak{K}'$ are homomorphically equivalent. and the composition of homomorphisms is homomorphism.

The $core$ of an epistemic model $\mathfrak{K}$ is a $'$: $\mathfrak{K} \approx^1 \mathfrak{K}'$ with the minimal number of elements, and the $core$ is unique up to homomorphism. To present the full knowledge that the players have at a certain stage of a play, we unfold the game $\mathcal{G}$ and at the same time retain the information in the Kripke structures of an epistemic model.

If $(\alpha_{k_1})_{k_1\in\mathbb{K}}$ be a tuple of actions $a_{k_1} \in A$ compatible with the players' knowledge, i.e., for every $i < n$ and for all $k_1, k'_1 \in \mathbb{K}$ with $k_1 \sim^i k_{1,}$ $(\alpha_{k_1})_i = (\alpha_{k'_1})_i$.

By updating

$Update(\mathfrak{K}, (a_{k'_1})_{k_1 \in \mathbb{K}}) \coloneqq (\mathbb{K}', (P_\upsilon)_{\upsilon \in V}, (\sim^\iota)_{\iota<n}$

where $\mathbb{K}' = \{k_1\upsilon | k_1 \in \mathbb{K}, k_1 \in P_\psi, (\psi, a_{k_1}\upsilon) \in \Delta\}$,

$P_\upsilon = \{k_1\upsilon | \ k_1\upsilon \in \mathbb{K}'\}, \qquad k_1\upsilon \sim^i k'_1\upsilon' \Leftrightarrow k_1 \sim^i_{\mathfrak{K}} k'_1, \upsilon \sim^i_G \upsilon'$

The epistemic successor of $Next(\mathfrak{K}, (\alpha_{k_1})_{k \in \mathbb{K}})$ consists of the $\sim \cup$ connected components of $Update\ (\mathfrak{K}, (\alpha_{k_1})_{k_1 \in \mathbb{K}})$. The initial element is the trivial structure $\{\upsilon_0, \mathfrak{K}_0 = (\{\upsilon_0\}, (P_\upsilon)_{\upsilon \in V,} (\sim^i)_{i<n}, P_{\upsilon_0} = \{\upsilon_0\}, P_\psi = \emptyset, \psi \neq \upsilon_0, \ \sim^i = \{(\upsilon_0, \upsilon_0)\}$. Therefore, with the epistemic unfolding, what we get is a game:

$Tr'(G) \coloneqq (V^t, \Delta^t, (\sim^i)_{i<n}, W^t)$

- where V^t is the set of all epistemic models $\mathfrak{K}$ over G with $\mathbb{K} \subseteq V^*$
- $\Delta^t = \{(\mathfrak{K}, (\alpha_{k_1})_{k_1 \in \mathbb{K}}, \mathfrak{K}' |\ (\alpha_{k_1})_{k_1 \in \mathbb{K}} \in \ A^{|\mathbb{K}|}, \mathfrak{K}' \in Next(\ \mathfrak{K}, (\alpha_{k_1})_{k_1 \in \mathbb{K}})\}$
- $\mathfrak{K}_0, \mathfrak{K}_1, \ldots \in W^t$ if and only if for each sequence $\pi = k_{1_0}, k_{1_1}, ..$ where $k_{1_l} \in \mathfrak{K}_l$, $\quad k_{1_{l+1}} = k_{1_l}\upsilon$ for some υ with $(\upsilon_{k_{1_l}}, \alpha, \upsilon \in \Delta$ for some $\alpha, \upsilon_{k_{1_0}}, \upsilon_{k_{1_1}} \ldots. \in W.$

The winning condition for $Tr'(G)$ requires that all paths through the sequence of Kripke structures be winning in the original game. In Figure 1, an example of epistemic unfolding is shown. The grand coalition has a winning strategy in the original game $\mathcal{G}, \upsilon_0$ if and only if the grand coalition has a winning strategy in $Tr'(\mathcal{G}), \mathfrak{K}_0$ [142]. If the image of homomorphism in this tracking is the $core$, i.e., the minimum number of elements, and we replace the repeated structures by their $core$, we obtain $Tr'_{core(\mathcal{G})}$, which is a game with perfect information.

Starting from the game $\mathcal{G}$ with observable winning conditions, i.e., when a player reaches the winning condition, all the others will be informed, we get the game $Tr'_{core(\mathcal{G})}$, and we solve the perfect information game $Tr'\_core(\mathcal{G})$ instead (an example of Tr'_core is shown in Figure 11.2).

The knowledge-sets $\mathcal{K}^i$ are the full descriptions of the knowledge that players have at a certain stage of the play while the observations $\beta^i(\upsilon)$ of the player are not.

We define the Kripke structure based on the Knowledge Sets computed in phase one as follows:

$\mathfrak{K} = (\mathbb{K}, (P_{\mathcal{K}^i})_{\mathcal{K}^i \in \mathcal{K}, (\sim^i)_{\iota<n}})$ where $(P_{\mathcal{K}^i})_{\mathcal{K}^i \in \mathcal{K}}$ is a partition $\mathbb{K}$, and each $\sim^i$ is an equivalence relationship on $\mathbb{K}$ such that for all $k_1, k'_1 \in \mathbb{K}$ if $k_1 \sim^i k'_1, then$ $\mathcal{K}^i{}_{k_1} \sim^i \mathcal{K}^i{}_{k'_1}$ with $\mathcal{K}^i{}_{k_1}$denoting the unique element from $\mathcal{K}$ such that $k_1 \in P_{\mathcal{K}^i{}_{k_1}}$.

We perform the epistemic unfolding and compute the $Tr'(\mathcal{G}^{\mathcal{K}})$. The Kripke structures of the knowledge sets of the players hold the knowledge of the current state of the game, and $Tr'(\mathcal{G}^{\mathcal{K}})$ is thus a game of perfect information, i.e.:

$$\sim^i = \{(\mathfrak{K}, \mathfrak{K}) | \mathfrak{K} \in V^t\}$$

The winning condition for $Tr'(\mathcal{G}^{\mathcal{K}})$ requires that all paths through the sequence of the Kripke structures be winning in the original game $\mathcal{G}^{\mathcal{K}}$ that holds as the finite-state automaton assures a winning condition.

If the wining conditions are observable in the initial game $\mathcal{G}$, i.e., it is a safety game with two colors observable to all players $\gamma: \mathrm{V} \quad \longrightarrow \{safe, notsafe\}$ such that $W = \{safe^{\omega}\}$, then it holds that $\gamma: \mathcal{K} \longrightarrow \{safe, notsafe\}$ such that $W = \{safe^{\omega}\}$. Since epistemic models are connected $\sim \cup$, and the coloring is constant for a position $\mathfrak{K} \in Tr'(\mathcal{G}^{\mathcal{K}})$, we have $\gamma(\mathfrak{K})\ and\ \mathfrak{K}_0\mathfrak{K}_1 \dots \mathfrak{K}_r \in W^t$ if and only if $\gamma(\mathfrak{K}_1)\gamma(\mathfrak{K}_2) \dots \in W$.

Let us consider a winning strategy of the grand coalition in $\mathcal{G}^{\mathcal{K}}$, $s = s_0 s_1 \dots s_{n-1}$ and a play $\pi^t = \mathfrak{K}_0\mathfrak{K}_1 \dots \dots$ in $Tr'(\mathcal{G}^{\mathcal{K}})$ consistent with the strategy $\sigma^t = \sigma_0^t \sigma_1^t \dots \sigma_{n-1}^t$ with $\sigma^t(\pi^t) = (\alpha_{k_1})_{k_1 \in \mathfrak{K}_r}, \alpha_{k_1} = \sigma(k_1)$ for every $k_1 \in \mathbb{K}$ and $\rho = k_{1_0} k_{1_1} \dots$

any path through structures in π^t such that π^t follows strategy $\sigma^t = \sigma^0 \sigma^1 \dots \sigma^{n-1}$ and $k_{1_i} = \mathcal{K}_0\mathcal{K}_1 \ldots \mathcal{K}_i$

.

so that $\mathcal{K}_0\mathcal{K}_1 \dots \mathcal{K}_i$ is historically consistent with s, and if $\mathcal{K}_0\mathcal{K}_1 \dots \in W$, then $\pi^t \in W^t$ and $\sigma^t$is a winning strategy. If σ^t is a winning strategy over $Tr'(\mathcal{G})$, we construct each history-s $\pi = \mathcal{K}_0\mathcal{K}_1 \dots \mathcal{K}_r$ in $\mathcal{G}^{\mathcal{K}}$ such that $\zeta(\pi) = \mathfrak{K}_0\mathfrak{K}_1 \dots \mathfrak{K}_r$ is consistent with σ^t. Then, any finite prefix $\mathcal{K}_0\mathcal{K}_1 \dots \mathcal{K}_l$ is also a path through π^t of the form $k_{1_0} k_{1_1} \dots . k_{1_l}$ and extends to the whole π. As π^t is consistent with σ^t, which is a winning strategy, $\pi^t \in W^t$ and consequently $\pi \in W$.

The grand coalition has also a winning strategy in $Tr'\_core(\mathcal{G}^{\mathcal{K}})$. If $\pi^{core} = \mathcal{L}_0\mathcal{L}_1 \dots$ is a play in $Tr'\_core(\mathcal{G}^{\mathcal{K}})$ consistent with strategy s^{core}, there is homomorphism $v_r: \mathcal{L}_r \longrightarrow \mathfrak{K}_{r.}$ such that it is consistent with s^{core}. The sequence of history $\mu(\pi^{core}), \mu(\mathcal{L}_0), \mu(\mathcal{L}_0\mathcal{L}_1), \ldots$ yields a play $\mathfrak{K}_0\mathfrak{K}_1 \ldots$. in $Tr'(\mathcal{G}^{\mathcal{K}})$. If $\pi = l_0 l_1$ with $l_r \in L_r, l_{r+1} = core(l_r\mathcal{K})$ and for $\mathcal{K}$ with $(\mathcal{K}_{lr}, \alpha, \mathcal{K}) \in \Delta$ for some α. The homomorphism $v_r(l_r) \in \mathbb{K}_r$ so that $\gamma(\mathcal{K}_{l0})\gamma(\mathcal{K}_{l1}) \ldots = \gamma(\mathfrak{K}_0)\gamma(\mathfrak{K}_1) \ldots$ and as $\mathfrak{K}_0\mathfrak{K}_1 \ldots \in W^{core}$ then $\gamma(\mathcal{K}_{l0})\gamma(\mathcal{K}_{l1}) \ldots \in W$ and π^{core} is winning and s^{core} a winning strategy for the grand coalition. The reverse also holds.

As a consequence, during the second phase, we compute $Tr'\_core(\mathcal{G}^{\mathcal{K}})$, and as it is finite because of the finite-state automaton, we solve this game of perfect information instead; we solve a two-player game, i.e., the grand coalition of players against nature. The $core$ element holds perfect knowledge of the game, so it is a stage of certainty that the equivalent of the $\mathcal{G}^{\mathcal{K}}$ game passes through.

A distributed game of imperfect information is transformed to a perfect game, and players become synchronized. Each player i based on his observations can decide about his current knowledge set $\mathcal{K}^i$ for playing a safety game, i.e., $\mathcal{K}^i$ is sufficient knowledge of the state of the game of player *i* based on his history.

Then, the best strategies are defined by solving the two-player zero-sum game (the grand coalition acts as one player and the second player is nature). The deterministic finite automaton reassures finite tracking of $Tr'\_core\ (\mathcal{G}^{\mathcal{K}})$ and the winning condition in the epistemic model.

The important task is to identify isomorphic Kripke structures in the game $Tr'\_core(\mathcal{G}^{\mathcal{K}})$. As soon as the isomorphic Kripke structures are identified, the game Tr'_core is a finite game with perfect information. Likewise, games on graphs with the property that every cycle passes through a perfect-information state have recurring certainty, i.e., the uncertainty of players regarding the current state is temporary and vanishes after a finite number of rounds, i.e., the period of uncertainty equals the distance in $Tr'\_core(\mathcal{G}^{\mathcal{K}})$ of $core$ recurrence [2].

11.3.5. PUE Detection Game with no collisions between PU and PUE

This research work considers the PU Emulator Detection as a distributed game of n players - the SUs - with imperfect information about the state of the game and the actions of the other players for each channel. The SUs can connect to the Internet and a Cloud-based database. Many PUs/PUEs could be in a channel. The SUs define the same strategy based on the well-known network constraints that are stored in the Cloud and upon hearing a transmission, the system covers both cases of static and mobile users, act *{PU_Detection|PUE_Detection}* and come to the corresponding state *{PU_DET,PUE_DET}*. The PUE is supposed to transmit with probability *q=1-PUtransmission_probability*. The SUs differentiate the PU or PUE transmissions from the SU signals. The channel upon PU or PUE arrival comes to states *PU_TRANSMIT, PUE_TRANSMIT (not PU_TRANSMIT)*, and the SU will choose either to free the channel if his observations are of *PU_DET* or stay *(PUE_DET)*. When an SU chooses to stay and PU transmits and then causes collision to PU and the state of the channel is *COLSU_PU*, the SU can vacate the channel within a predefined interval for the network as soon as he realizes the PU presence. When the SU chooses to stay and PUE transmits, the channel comes to state *COLSU_PUE*, and the PUE leaves the channel as his intention is to gain spectrum. When a PUE is challenged, the SU knows that it wins. If the PUE transmits and PU arrives, then the channel comes to state COLPU_PUE, and the SU knows then that it was the PUE transmitting and the newcomer is the PU who stays in the channel. On PU arrival, PUE eventually leaves the channel; PUE will have a serious penalty. If the PUE is detected, he leaves the channel but another PUE may arrive.

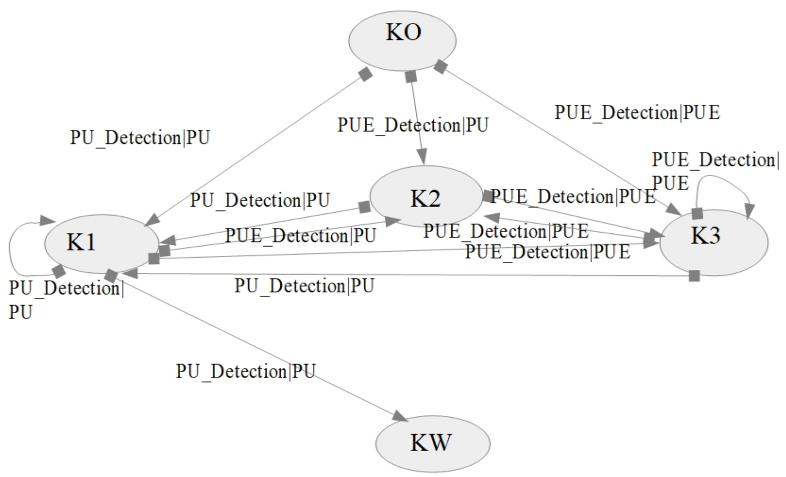

Figure 11.4: Deterministic automaton of the knowledge sets when there are no collisions between the PU-PUE

Following the section C analysis, the game tree is constructed as it appeared in Figure 11. 3. The state *I* corresponds to the *Idle Channel* and when a transmission begins, the SU plays his strategy. As shown in Figure 11. 3, the game tree has two levels for each round of the game. Each round corresponds to a high energy transmission. In the game graph, under the indistinguishability, the equivalent games form the knowledge sets $K1, K2, K3, K4$ (Figure 11.4). The initial knowledge set is *K0*, and the terminating knowledge set is *KW*.

The deterministic finite automaton is constructed by the knowledge sets *Ki*, which become the states of the game and the action/observations of the SU as the transitions shown in Figure 11.4. We must decide upon the best strategies. The deterministic finite automaton assures winning conditions. The initial state of automaton is $K0$ and the final state is *Kw*, the winning state. The $K1$ state corresponds to the case where the PUE is not detected and takes advantage of the spectrum. The SU is aware of the existence of the PUE but still vacates the spectrum. The *K2* state of the automaton corresponds to the PU detection certainty and *K3* to PUE detection certainty. The K4 knowledge set corresponds to total awareness as the PU and PUE are identified. (As the state transition proceeds in the deterministic finite automaton, the knowledge of the game evolves).

In the Kripke structures of *Ki* as described in section C, the isomorphic Kripke structures are extracted. The tracking is finite. As soon as the isomorphic Kripke structures are extracted, the game is a perfect game, and the uncertainty of players regarding the current state is temporary and vanishes after a finite number of rounds. The transitions in the tree of Kripke structures is restricted by the DFA that assures winning conditions. The uncertainty of the players is focused on the cases when they observe that PU is present, and their actions are *PU Detection*. Then, the two-player (the grand coalition-one SU against nature, i.e., PUE) zero sum game is solved for defining the best strategies. A zero-sum game is the one where the sum of the payoffs of the players equals zero.

The grand coalition acts as a super-player and the zero-sum game is based on the states $\{K1, K2, K3\}$. Whenever the SU finds an opportunity for transmission, then he gains the spectrum $G1$. There is a penalty C for SU interference to the PU and a penalty Pn for PUE emulation. The interference penalty implies that the SU will be discouraged with regard to transmissions. The attack gain of the PUE (causes SU-confusion) is C'.

According to the graphical solution, we must define *p* such that the SU maximize his guaranteed average winnings, and the 2xN zero-sum game thus involves solving a 2x2 zero-sum game. If there is an element *a ij* at the game matrix 2x2 of the zero-sum game now $A\ ij$ such that the SU player can win at least *a ij* by choosing row *i* and the player PUE can keep her loss at most *a ij* by playing column *j*, it is a saddle point. If in the matrix *A*, $a_{11} > a_{12}, a_{12} < a_{22}, a_{22} > a_{21}\ and\ a_{21} < a_{11}$, there is no saddle point, then we solve by finding equalizing strategies. If the SU chooses the first row with probability p (i.e., uses the mixed strategy $(p, 1-p)$), we equate his average return when PUE uses columns 1 and 2, i.e., $a_{11}\,p + a_{21}\,(1 - p) = a_{12}\,p + a_{22}\,(1 - p)\ (I)$. We solve the equation for *p*. If the PUE chooses the first column with probability q (i.e., uses the mixed strategy *(q, 1−q)),* we equate her average return when SU uses rows 1 and 2, $a_{11}\,q + a_{12}\,(1 - q) = a_{21}\,q + a_{22}\,(1 - q)(II)$. We solve the equation for *q*. *(I)=(II)=v* is the value of the game when playing optimal strategies.

There is no saddle point in the PUEA zero-sum-game, and there is an optimal strategy $(p, 1-p)$ for the SU and $(q, 1-q)$ for the PUE, and the value of the game will be v by finding equalizing strategies. If the SU wants to maximize his average winnings, he has to play *PUE_Detection* with probability p and *PU_Detection* with probability $1-p$. If the PUE wants to minimize his average loses, he must attack with probability q and not attack with probability $(1 - q)$.

	K1	K2	K3
PUE_Detection	G+Pn	-C-C’	G+Pn
PU_Detection	-C’-G	C	-C’-G

Table 11.1: Zero-sum game for SU with no collisions between PU-PUE

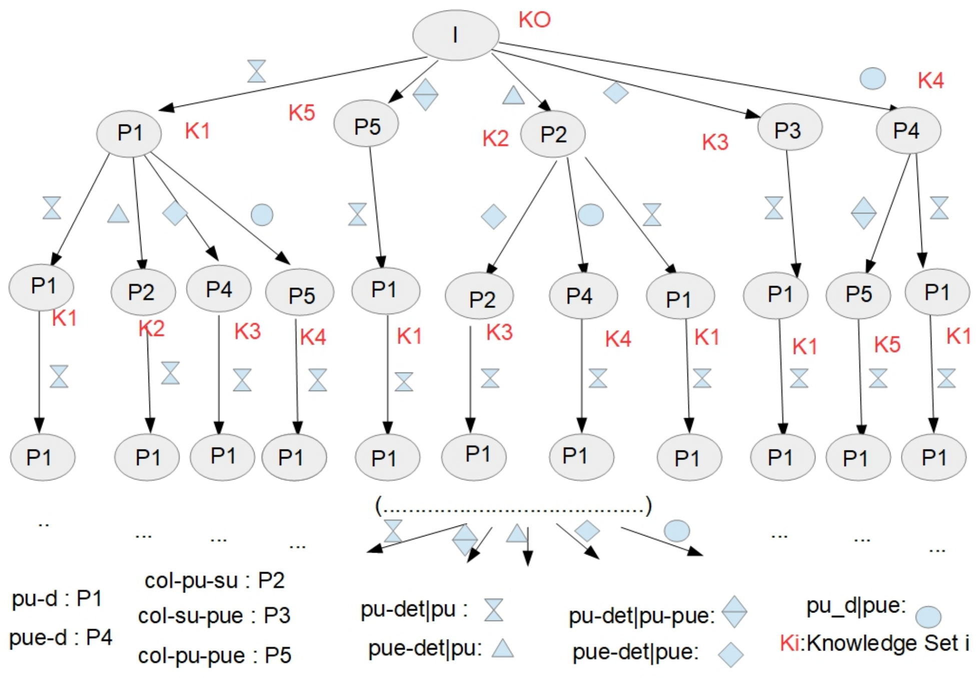

Figure 11.5: States of the games and the knowledge sets K_i when there are collisions between PU and PUE

The 2x3 zero sum game is solved by the 2x2 zero-sum game of columns K1K2. We can say that the critical state is K1 as this state represents uncertainty, and the SU can either be aggressive and play *PUE_detection* and earn $Pn + G$ or play *PU_detection* and remain in the uncertainty with payoff $-C' - G$. Applying equalizing strategies, we get p and q:

$$p = \frac{C + C' + G}{Pn + 2(C + C' + G)} (III)$$

$$q = (2C + C')/(Pn + 2(C + C\text{^}' + G))(IV)$$

As the zero-sum game is a repeated game, we must consider probability δ, i.e., the probability that the game will continue and 1-δ, the probability that the game will end in the next stage. If the SU starts the game from uncertainty and plays *PUE_detection*, the game will come to a state of certainty and then will start again in an uncertainty state, etc. Thus, the overall payoff v1 if the SU plays aggressively, i.e., PUE_detection would be

$$payoff1 = \frac{G + Pn - C - C'}{1 + \delta} + \frac{G + Pn - C - C'}{1 + \delta}\delta + \\ + \frac{G + Pn - C - C'}{1 + \delta}\delta^2 + \cdots = \\ = (G + Pn - C - C')\frac{1}{1 - \delta}(V)$$

If the SU starts playing from uncertainty and plays PU detection continually, then it will remain in uncertainty and his payoff will be:

$$payoff2 = \frac{C - C' - G}{1 + \delta} + \frac{C - C' - G}{1 + \delta}\delta +$$

$$+\frac{C - C' - G}{1 + \delta}\delta + \cdots . = (C - C' - G)\frac{1}{1 - \delta}(VI)$$

For the SU to have the incentives to continue playing, the constraints below must hold:

$$payoff1 > payoff2 \Rightarrow \frac{G + Pn - C - C''}{1 - \delta} \\ > \frac{C - C' - G}{1 - \delta} \Rightarrow G + Pn > 2C \qquad (VII)$$

Similarly, if the SU is in uncertainty and decides to play *PU_detection* and from then on be aggressive, the payoff would be:

$$payoff3 = \frac{C - C' - G}{1 + \delta} + \frac{G + Pn - C - C'}{1 + \delta}\delta +$$

$$+\frac{G + Pn - C - C'}{1 + \delta}\delta^2 + \cdots =$$

$$= \frac{C - C' - G}{1 + \delta} + \frac{G + Pn - C - C'}{1 + \delta} * \frac{\delta}{1 - \delta}\ (VIII)$$

If the SU is in uncertainty and plays *PUE_detection* once and then changes his strategy and plays PU_detection, the payoff would be:

$$payoff4 = \frac{G + Pn - C - C'}{1 + \delta} + \frac{C - C' - G}{1 + \delta}\delta +$$

$$+ \frac{C - C' - G}{1 + \delta}\delta^2 + \cdots =$$

$$= \frac{G + Pn - C - C'}{1 + \delta} + \frac{C - C' - G}{1 + \delta} * \frac{\delta}{1 - \delta}(IIX)$$

We expect SU to have incentives to change his initial strategy *PU_detection* and be more aggressive, i.e., play *PUE_detection*. If the SU plays *PUE_detection* at the beginning, the inequality must hold:

$$payoff3 > payoff4 \Rightarrow \delta > \frac{Pn + 2G - 2C}{2Pn + 4G - 4C}(IX)$$

The total payoff of the game thus will be the sum of the four possible outcomes of the game. Some constraints can also be considered on the parameters of the game: $C > G1: (VIII)$. This constraint makes the SU avoid interference with the PU, $Pn > G1$: (IX). The network forces the PUE not to emulate the PU, $Pn > C'$: (X). This constraint makes the PUE launch attacks but not be detected by the PU. $C' > G: (XI)$, this constraint makes the PUE have incentives to launch attacks.

The parameters above that depend on the network conditions and govern the strategies of the game are stored at the Cloud database to which the SU nodes connect periodically to update their game parameters. At the Cloud, an optimization of the game payoff is performed as shown below:

Maximize SUs

payoff =payoff1+payoff2+payoff3+payoff4=

$$= (G + Pn - C - C') * \frac{1}{1-\delta} + (C - C' - G) *$$

$$* \frac{1}{1-\delta} + \frac{C - C' - G}{1+\delta} + \frac{G + Pn - C - C'}{1+\delta} * \frac{\delta}{1-\delta} +$$

$$+ \frac{G + Pn - C - C'}{1+\delta} + \frac{C - C' - G}{1+\delta} * \frac{\delta}{1-\delta}$$

$$Subject\ to\colon\ C < G, C' < Pn$$
$$G < C, G < Pn$$
$$\delta < 1, \qquad 2C < Pn + G$$

$$\frac{Pn + 2G - 2C}{2Pn + 4G - 4C} < \delta$$

The optimal solution, i.e., the values of network parameters, is delivered to the SU nodes. The SUs can differentiate the PU/PUE signals from other SU signals, but they do not know whether each one is a truly licensed use due to Primary User Emulation.

11.3.6. PUE Detection Game with collisions between PU and PUE

We consider that PU and PUE may collide, e.g., if PUE transmits and PU arrives. In that case, the game tree is shown in Figure 11.5, the deterministic automaton in Figure 6, and the game payoffs in Table 11.2.

	K1	K2	K3	K4	K5
PUE Detection	-C'-C	-C-C'	Pn+G	Pn+G	-C
PU Detection	-C'	-C'	-C'-G	-C'-G	C'

Table 11.2: Zero-sum game for SU with collision between PU and PUE

We solve the 2x5 zero-sum game of Table 11.2 graphically, and we get the 2x2 zero-sum game of the 2nd and 3rd columns that give the same solution by applying equalizing strategies as (III) and (IV) for p and q.

$$p = \frac{C + C' + G}{Pn + 2(C + C' + G)} (III)$$

$$q = \frac{2C + C\prime}{Pn + 2(C + C' + G)} \text{(IV)}$$

If the game starts from an uncertainty state and the strategy of the SU is to always play *PU_detection*, then his payoff will be:

$$payoff5 = \frac{C - G}{1 + \delta} + \frac{C - G}{1 + \delta}\delta + \frac{C - G}{1 + \delta}\delta^2 + \cdots =$$

$$= \frac{C - G}{1 + \delta} * \frac{1}{1 - \delta} (XII)$$

If the game starts from uncertainty and the strategy of the SU is to always play *PUE_detection*, the payoff of the game will be:

$$payoff6 =$$

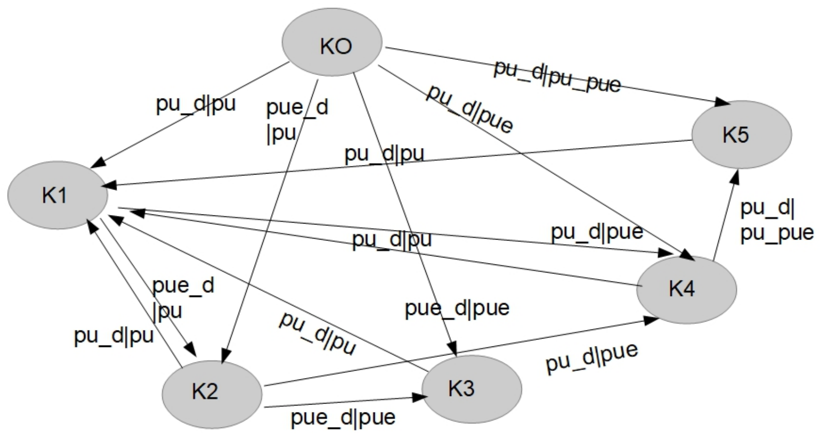

Figure 11.6: Deterministic automaton of the Knowledge Sets for the game when there are collisions between PU-PUE

$$= \frac{G + Pn - 2C - C'}{1 + \delta} + \frac{G + Pn - 2C - C'}{1 + \delta}\delta +$$

$$+ \frac{G + Pn - 2C - C'}{1 + \delta}\delta^2 + \cdots =$$

$$= \frac{G + Pn - 2C - C'}{1 + \delta}\frac{1}{1 - \delta}(XIII)$$

If the game starts from an uncertainty state and the strategy of the SU is to play *PU_detection* once and then always play *PUE_detection*, then the payoff will be:

$$payoff7 = \frac{C - G}{1 + \delta} + \frac{G + Pn - 2C - C'}{1 + \delta}\delta +$$

$$+\frac{G+Pn-2C-C'}{1+\delta}\delta^2+\cdots=$$

$$=\frac{C-G}{1+\delta}+\frac{G+Pn-2C-C'}{1+\delta}\frac{\delta}{1-\delta}(XIV)$$

If the game starts from an uncertainty state and the strategy of the SU is to play *PUE_detection* once and then always play PU_detection, then the payoff will be

$$payoff8=\frac{G+Pn-2C-C'}{1+\delta}+\frac{C-G}{1+\delta}\delta+$$

$$+\frac{C-G}{1+\delta}\delta^2+\cdots=\frac{G+Pn-2C-C'}{1+\delta}+\frac{C-G}{1+\delta}*$$

$$*\frac{\delta}{1-\delta}(XV)$$

If we want SU to have incentives to play the game, the following inequalities must hold:

$$payoff6>payoff5\ \ whcih\ holds\ (XVI)$$

and

$$payoff7>payoff8\Rightarrow$$

$$\Rightarrow\frac{C-G}{1+\delta}+\frac{G+Pn-2C-C'}{1+\delta}\frac{\delta}{1-\delta}$$

$$>\frac{G+Pn-2C-C'}{1+\delta}+\frac{C-G}{1+\delta}*\frac{\delta}{1-\delta}\Rightarrow$$

$$\Rightarrow \delta > \frac{2G + Pn - C - C'}{4G + 2Pn - 5C - 2C'} (XVII)$$

If (XVII) does not hold, then SU had better stop playing *PU_Detection* for the rest of the game.

The parameters above that depend on the network conditions and govern the strategies of the game are stored at the Cloud database to which the SU nodes connect periodically to update their game parameters. At the Cloud, the optimal solution of the game is computed:

Maximize SU's

Payoff =payoff5+payoff6+payoff7+payoff8=

$$= \frac{C - G}{1 + \delta} * \frac{1}{1 - \delta} + \frac{G + Pn - 2C - C'}{1 + \delta} \frac{1}{1 - \delta} + \frac{C - G}{1 + \delta}$$

$$+ \frac{G + Pn - 2C - C'}{1 + \delta} \frac{\delta}{1 - \delta} + \frac{G + Pn - 2C - C'}{1 + \delta}$$

$$+ \frac{C - G}{1 + \delta} * \frac{\delta}{1 - \delta} \quad (XVI)$$

Subject to $C<G$, $C'<Pn$

$G<C$, $G<Pn$

$\delta<1$,

$$\frac{2G + Pn - C - C'}{4G + 2Pn - 5C - 2C'} < \delta$$

11.3.6. SIMULATION RESULTS

The simulation was conducted in OMNET with the PU and PUE packets being of equal size, i.e., 50000 bits, for five SUs. The PU and PUE traffic follows exponential distributions. The parameters used for the simulation for the proposed protocol are *Pn=20, G=1, C=5, C'=2* and for equalizing strategies, the optimal strategy for PUE|PU is *q|(1-q)~0.33|0.67* and for the SUs, the optimal strategy solution is *p|(1-p)~0.22|0.78*. The tests included the measurement of some metrics such as *PU_Detection Positive, PUE_Detection_Positive, PUE_Detection_Negative*.

The probability *PU_Detection_Positive* equals the number of times that each SU played *PU_Detection* and he was right, divided by the total number of times the PU transmitted. The probability *PUE_Detection_Positive* equals the number of times each SU played *PUE_Detection* and he was right divided by the number of times PUE transmitted. The probability *PUE_Detection_Negative* equals the number of times each SU played *PUE_Detection*, and it was PU transmitting, divided by the total number of times the PUE transmitted. For the comparative study, the [159] was selected. In [159], there is a Network Management entity that could receive the results of all SUs acting as one player against the PUE and therefore can be considered to be a cooperative model.

In [159], the PUE does not know PU traffic as in the proposed protocol. For the Nash Equilibrium computation of [159], it was considered that a) the network, i.e., the SUs, can always utilize the spectrum released by the PUE detection, and b) the penalty to the PUE is high for emulation. Therefore, the strategies computed showed that when the PU transmission probability drops to 0.5 and less, the PUE stops performing attacks, and the network management entity stops defending the network.

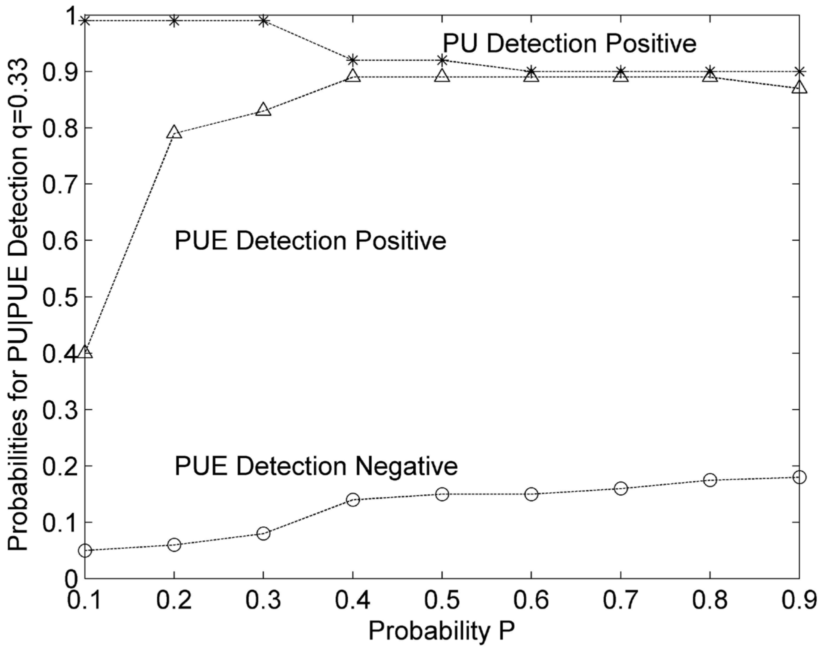

Figure 11.7: Detection probabilities for PUE optimal strategy for the proposed protocol

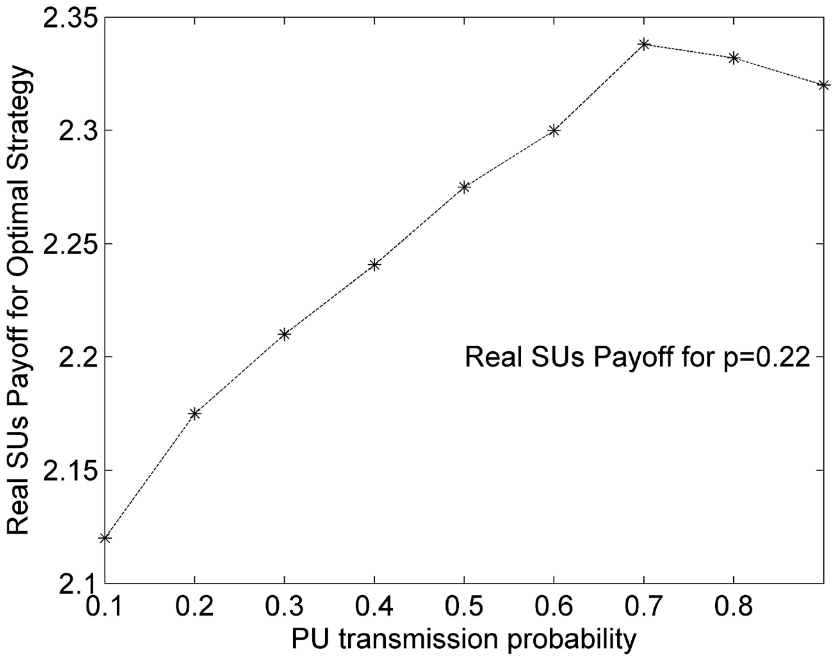

Figure 11.8: Real payoffs for the SUs for p=0.22 (optimal strategy) for the proposed protocol

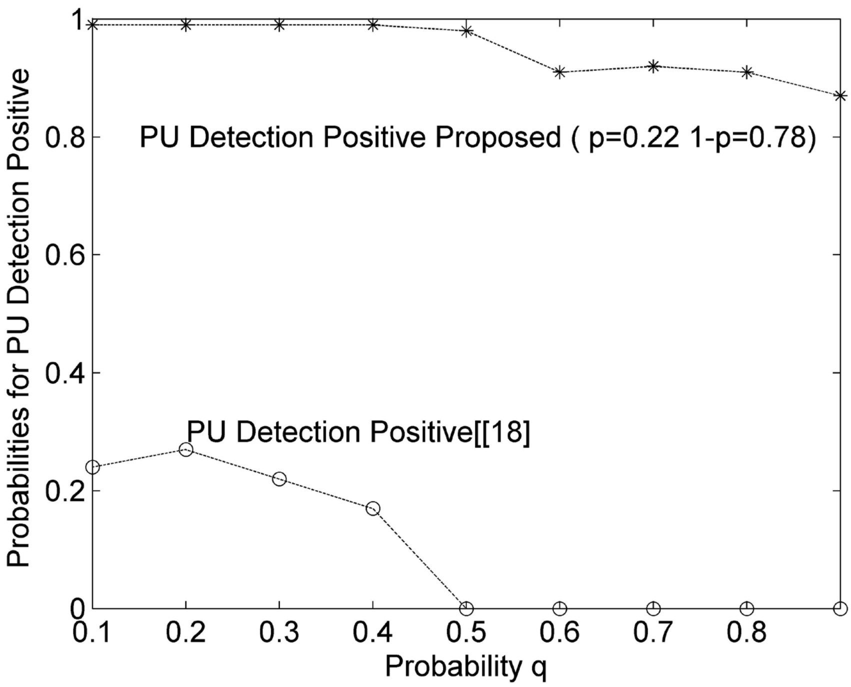

Figure 11.9a: PU detection positive for SU following optimal strategy in the proposed protocol and SU playing Nash Equilibrium in [18]

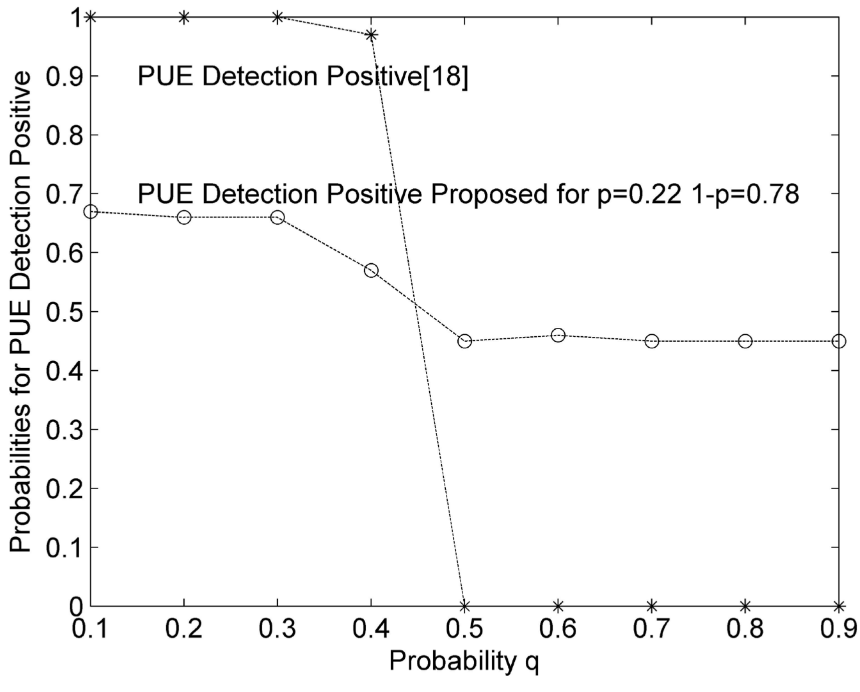

Figure 11.9b: PUE detection positive for SU following optimal strategy in the proposed protocol and SU playing Nash Equilibrium in [18]

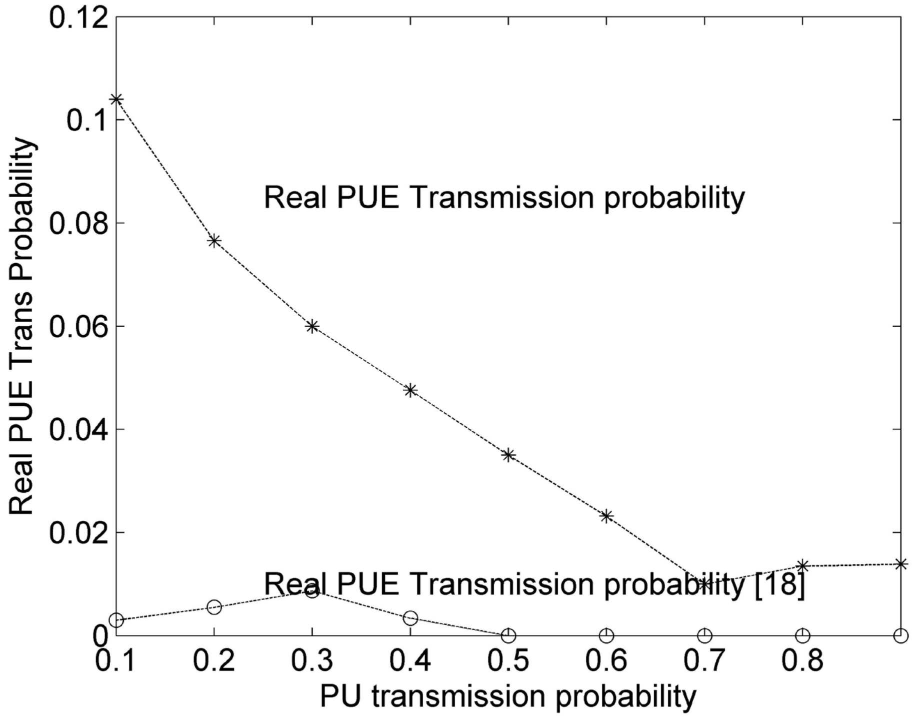

Figure 11.11: Real PUE transmission probability during the game for PUE-optimal strategy for the proposed protocol

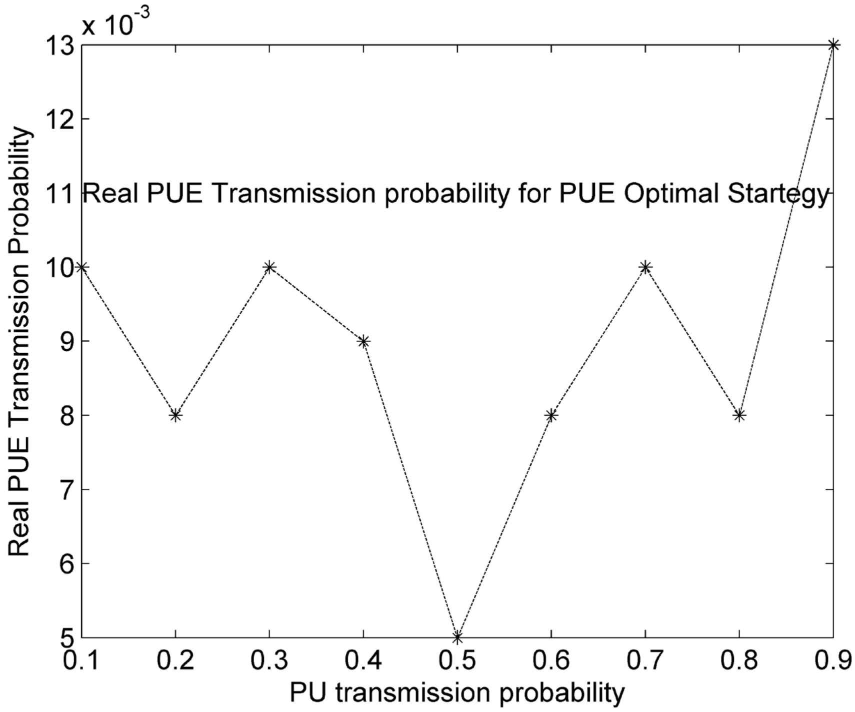

Figure 11.10: Real PUE transmission probability for SU following optimal strategy in the proposed protocol and SU playing Nash Equilibrium in [18]

In the first experiment (Figure 11.7), the PUE plays optimal strategies *0.33|0.66*, and the values of PUE|PU Detection versus the probability *p* of SU playing *PUE_Detection* are shown. The *PU_Detection_Positive* is 98% for *p*=0.1,0.2,0.3 and then decreases by increasing the *p* while q=0.33. There is more chance for misdetection and false alarm, i.e., that is why *PUE_Detection_Negative* increases. The *PUE_Detection_Positive* increases as there is more chance to detect the PUE when the SU becomes more aggressive and plays *PUE_Detection* more often. The *PUE_Detection_Negative* reaches 5%. In the second experiment (Figure 11.9), the SU plays optimal strategy *0.22|0.78,* and the PU|PUE detection probabilities versus the probability q of PUE attacking are presented. Now, the *PU_Detection_Positive* reaches 99% and the *PU_Detection_Positive* decreases as q increases. The SU, by playing *PUE_Detection* with probability 0.22, misses more PUE transmissions as q increases. The *PUE_Detection_Negative* increases as q increases because the SU becomes more confused by the PUE attacks while remaining a relatively low challenging probability of 0.22. The SU plays a winning strategy with the support of the deterministic finite automaton so the *PU_Detection_Positive* and *PUE_Detection_Positive* are high, but the *PUE_Detection_Negative* reaches 5%. In [19], the network management entity plays more aggressively at NE strategies so that the PUE detection probabilities (Figure 11.9a and Figure 11.9b) are good but collide with the PU according to *PU_Detection_Positive*, which is a reason for penalty for the Cognitive Radio Network.

When the players choose optimal strategies, the results are like the results of the cooperative methods, which use message exchange for PUE attack detection.

The real payoff for all SUs versus the PU transmission probability is shown in Figure 11.8 and is almost stable, taking values between 2.11 and 2.31. The real PUE transmission probability is eliminated despite the continuous arrival of PUEs to the network versus the PU transmission probability, when the SUs follow optimal strategy as shown in Figure 11.10. This probability is much lower than the *PUE_Detection_Positive* because the latter is estimated on a per SU basis, i.e., another SU may detect the PUE and so free the network of the PUE attack. The minimum value corresponds to the PUE optimal strategy, i.e., q=0.33 that is eliminated to 1%. Finally, the real PUE transmission probability versus the detection probability p, when the PUEs follow optimal strategy, is shown in Figure 11.11. Although the PUEs keep arriving one after another, the penalty Pn implies a backoff period for the PUEs, and the real PUE transmission probability is eliminated to the range [0.5%…1.3%], i.e., similar to the results of [19] for real PUE transmission probability. The system has a good response to the PU Emulation Attack as the coordinated SUs play a safety game from the beginning that assures winning condition and must decide upon the best strategy for optimal results.

11.3.7. CONCLUSIONS

This paper defined a new model of a game of imperfect information and applied it to the PUE Attack problem. As the game evolves, the SUs act as a grand coalition that achieves synchronization - all SUs make the same decisions without collaboration, i.e., without message exchange. To the best of our knowledge, this study is the first that addresses coordination without collaboration in the PUEA detection problem with results familiar to collaborative methods. Eventually, all SUs act as a super-user who plays a zero-sum safety game with the PUE and defines the optimal strategy. The uncertainty of players regarding the current state is temporary and vanishes after a finite number of rounds. Upon successful PUE detection, the PUE identity is stored in the Cloud. The proposed system has high performance, and the results are similar to the performance of cooperative methods applied for PUE Attack Detection. In the future, research will be conducted on malicious nodes detection in the CRN.

Chapter 12

WIDEBAND SUB-NYQUIST SAMPLING IN COGNITIVE RADIO NETWORK

Multiscale Decision Making Scheme for wideband spectrum sensing with sub-Nyquist sampling in CRN and fading channels

Cognitive Radio (CR) is a key technology in next generation Wireless Networks. This research work [161] proposes a multiscale decision making scheme for wideband sensing with sub-Nyquist sampling in Cognitive Radio Networks (CRNs) and fading channels. The proposed scheme estimates the ability of each SU in the cooperative network to provide an accurate sensing decision in severe fading and shadowing conditions and proceeds in a selective sensing schedule based on machine learning and the achieved Nash Equilibrium. The channel conditions are considered varying. The scheme makes optimal decisions and has high performance in terms of accuracy and overhead.

12.1. INTRODUCTION

Spectrum sensing is an essential task in improving spectrum utilization efficiency and is a key issue in the Cognitive Radio Networks. There are basically two basic spectrum sensing techniques among the cognitive radio users: cooperative and non-cooperative sensing. Cooperative spectrum is more effective than non-cooperative sensing. However, cooperative sensing implies that there will be either a fusion center to receive the SUs' sampling reports and reach a global decision based on a fusion rule or there would be intense direct message exchange between the SUs. In the former case, there are two options in current literature i.e. the soft decision and hard decision process where the SUs send only hard one-bit decisions to the fusion center. Soft decision solutions require signal acquisition, processing, energy consumption and transmission overhead. Hard decision schemes are easier to implement and they require less processing and transmission cost but they are less efficient than soft decision schemes.

Sub-Nyquist wideband sensing elaborates fewer channels' sensing which make it appropriate for cognitive radio networks while blind sub-Nyquist sampling recovers the signal based on the jointly sparse nature of multiband signals [162]. In literature, they have been introduced many cooperative soft decision schemes [163] [164] [165] [166] which handle cooperative sensing in terms of perfect or imperfect CSI, optimization of the decision's threshold, optimal number of SUs participating in the decision. Some hard decision schemes are [167] [168] which again examine the previous network parameters, too. The authors in [162] consider sub-Nyquist sampling.

This research work proposes a two-step multiscale decision-making scheme for cooperative sub-Nyquist wideband sensing of fading channels in Cognitive Radio Networks. The fusion center collects the samples of the SUs and updates a weight metric matrix which estimates the ability of each SU per sub-band to provide accurate sensing outcome about the Primary User's (PU's) presence in the Cognitive Network. A hierarchically interaction model between two agents i.e. the local and global agents respectively is assigned to each SU per sub-band reaching Nash Equilibrium when the local and global metric (reward) coincide. Then this SU is selected for participating in the sensing of the particular sub-band in the second step. The scheme provides optimal results. The fusion center can be cloud-assisted in its signal processing. To the best of the authors' knowledge, there is no other reference that introduces a hard decision process with enhanced performance to the soft decision process's level and which considers fading channels, and sub-Nyquist sampling. The proposed scheme learns the fading conditions of the SUs and proceeds to accurate predictions about the fading conditions that each SU is prone to experience. Thus the fusion center evaluates the SUs' ability to contribute to spectrum sensing.

The rest of the chapter is organized as follows: in section II, the system and network model is presented, in section III, the proposed scheme is analyzed and the evaluation process is provided in section IV.

12.2. SYSTEM AND NETWORK MODEL

The paper considers a cooperative wideband spectrum sensing in a cognitive radio network with a fusion center and secondary users SUs, which share the same spectrum with a PU network. In cognitive radio the signal sampling should be as fast as possible, even with high dimensional signals so to reduce the processing time and accelerate the scanning process. Compressive Sensing (CS) is a sampling paradigm which states that it is feasible, with overwhelming probability that a signal is reconstructed based on samples taken but with far fewer samples than those dictated by the traditional well-established Nyquist criterion stating that for accurate signal reconstruction one must adjust sampling rate to be at least twice the highest frequency present in the mathematical expression of the signal. The main benefit introduced by leveraging CS in cognitive radio systems is the ability to sense the same frequency band with fewer samples than those dictated by the traditional methods or a wider frequency band with the same number of samples. With no prior information about the band locations, blind sub-Nyquist sampling is implemented at each SU to estimate the active channel locations.

For a number of narrowband channels L, multicoset sampling is considered at each SU by taking non-uniform samples at the time instants $t = (mL + ci)T$, where p is the number of parallel cosets $i = 1..p;\ m \in \mathbb{Z}, and\ 1/T = fs$ is the Nyquist sampling rate. The sampling pattern is defined as the set $C = \{c_i\}^p$ of p integers selected from the range $1 \ldots L - 1$. A multi-coset sub-Nyquist sampling is introduced in [2]. A random number generator which runs at the fusion center creates the sampling patterns which are sent to the SUs of the network.

As sub-Nyquist sampling is more prone to channel degradation, cooperative sensing arises as a solution [2]. Each SU experiences different fading and shadowing conditions that consequently affect their ability to make a decision about PUs' presence in the spectrum. Although the SUs listen to the same PUs, they produce different sensing outcomes due to fading and shadowing.

Each time the fusion center, based on the sample v_s received from the J SUs for each narrowband channel i updates its table $\mathbf{Z_s}$ accordingly:

$$\boldsymbol{Z_s} = [\boldsymbol{v_s}[1]^T \ldots. \boldsymbol{v_s}[L]^T] \quad (1)$$

where

$$\boldsymbol{v_s}[\boldsymbol{i}]^{\boldsymbol{T}} = \left[\boldsymbol{v}_{\boldsymbol{s}}^{(\boldsymbol{1})}[i]^T \ \boldsymbol{v}_{\boldsymbol{s}}^{(\boldsymbol{2})}[i]^T \ldots.. \boldsymbol{v}_{\boldsymbol{s}}^{(\boldsymbol{J})}[i]^T\right] \quad (2)$$

is the vector with elements the $\boldsymbol{v}_{\boldsymbol{s}}^{(\boldsymbol{j})}[i]^T$ the sampling output of SU j for narrowband channel i. Samples for each sub-channel from more than one SU will be reported to the fusion center so there will be more than one sampling reports for each sub-band each time. Not all of the J SUs will participate in each $\boldsymbol{v}_{\boldsymbol{s}}^{(\boldsymbol{j})}[i]^T$ in sub-Nyquist sampling. The SUs which will participate in $\boldsymbol{v}_{\boldsymbol{s}}^{(\boldsymbol{j})}[i]^T$ are those whose sampling pattern includes the sub-band i according to random number generator distribution and each SU senses only p sub-bands. However, all the sub-bands will be sensed by more than one SU, if the sub-Nyquist sampling ratio is ensured.

The vector $\boldsymbol{v_s}[i]^T$ will be used when all SU report their samples. For the original signal reconstruction the normalized Mean Squared Error (MSE) estimation which is shown below:

$$MSE = \frac{\|X_{RECONSTRUCTED} - X_{ORIGINAL}\|}{\|X_{ORIGINAL}\|} \qquad (3)$$

Where $X_{RECONSTRUCTED}$,$X_{ORIGINAL}$ the reconstructed and the original signal respectively.

The proposed scheme considers that in the first step the necessary SUs'samples of sub-band sensing arrive at the fusion center which will be used by the proposed scheme for the normalized MSE estimation of samples corresponding to narrow bands sensing. The normalized MSE error of the sensing of each SU per channel will be used further as input in a decision making model. It takes as inputs the samples of the SUs and provides as outputs the metrics describing the capability of each SU to perform accurate sensing in each narrow band because of the fading conditions he experiences and selects the SU with the best metric for each narrow band.

During the first step the scheme needs as inputs the SUs' samples to compute the metrics and prepare the second hard decision phase. As soon as the metrics reach a predefined value or the number of iterations is reached, the network proceeds to step two where the selected SUs send one-bit-hard decisions about the PUs presence at the narrow channels. The Hard decision scheme is easy to implement and is not computationally intensive. The performance of the hard decision phase is superior to hard decisions schemes as its performance is equivalent to soft-decisions scheme. Optimal decisions and optimal rewards are achieved. However, the fusion center has to monitor network's performance and trigger the sub-Nyquist sampling as network conditions change. As the proposed scheme provides metrics that predict the changes in the fading conditions that each SU experience at each channel both in first and the second step the fading conditions at each channel are considered as varying.

12.3. PROPOSED WIDEBAND SPECTRUM SENSING SCHEME

Multipath fading channels are considered where the signal degradation is mainly concentrated on amplitude and we consider the normalized error estimation of SU's sample for each narrow channel as follows:

$$Error_i^j = \frac{\left\| x_i^0 - x_i^j \right\|}{\left\| x_i^0 \right\|} \tag{4}$$

Where x_i^j is the signal sample received by the SU j for narrowband channel i and x_i^0 is the original signal for channel i and $Error_i^j$ is the normalized error of sensing of SU j for channel i. We consider the two agent model problem who has to make decisions which influence each other rewards and probabilities of decisions outcomes according to multiscale decision theory [168]. Each agent does not know the other's agent's decisions. A two-agent case analysis is presented in [169].

The network performs sub-Nyquist sampling for n times and each time the fusion center collects the reports of the SUs. For each SU estimates the normalized error according to (4) at each time n. The fusion center at each time n knows the normalized error of each SU and the minimum normalized error reported by all SUs and with those values plays a two agent game for each SU where the local agent updates the reward for the SU according to his normalized error report and the global agent updates the reward with respect the best normalized error reported by some SU which participated in the sub-Nyquist sampling at time n.

The Nash Equilibrium of the game is considered and the optimal coefficients are estimated for the decision scheme to make optimal decisions. If an SU experienced the minimum normalized error at time n, the fusion center will assign his normalized error to the best local error and if this is the best normalized error reported for the particular narrow band, the fusion center will assign his normalized error to the global error value for the particular narrow band. The coefficients of the games estimate the impact that the local error reporting will have to the global narrow band's error estimation which then select the SU with the best global normalized reports in period of n times.

As the fading conditions that each SU experiences will affect the normalized error of his sample, the fusion center during n times learns the SUs that experience the least fading conditions and selects them for reporting at the corresponding narrow bands.

We consider for each SU there exist two agents one making decisions on the SU's j best local error metric based on $Error$ for channel i until time n $bestlocal_i^j(n)$ and the second agent makes decisions based on the comparison of the local $Error_i^j(n)$ with the current best outcome between SUs for channel i at time n. At each point n at time the agents seek a decision which makes them switch to state $s_i^{j,n}$and choose and action $\alpha_i^{j,n}$ with probability $p_i^{j,n}\left(s_i^{j,n+1}\middle|s_j^{i,n},\alpha_j^{i,n}\right)$.

The action space of the local agent includes two actions according to the feedback he receives from the environment which are {Update_Best_Local, Not_Update_Best_Local} = $\{\alpha_i^{local,j,1},\alpha_i^{local,j,2}\}$ and the corresponding states are {Local_Update, Not_Local_Update}=$\{s_i^{local,j,1},s_i^{local,j,2}\}$. For the global agent associated with SU j the action space includes the actions based on the environments feedback i.e. the $Error$ computation for all SUs in channel i, {Update_Best_Global, Not_Update_Best_Global}= $\{\alpha_i^{global,j,1},\alpha_i^{global,j,2}\}$ i.e. update the global value if the $Error$ of the SU is lower than that of the current MSE of all SUs for channel i and the corresponding state space is {Update_Global, Not_Update_Global} = $\{s_i^{global,j,1},s_i^{global,j,2}\}$.

$$if\ Error_i^j(n) < bestlocal_i^j(n)\ then\ bestlocal_i^j(n) = Error_i^j(n) \quad (5)$$

$$if\ Error_i^j(n) < global_i\ (n)\ then\ global_i\ (n) = Error_i^j(n)$$
(6)

$Bestlocal_i^j(n)$ is the lowerst error occurred for SU j at channel i until time n. $global_i\ (n)$ is the lowest error $Error_i^j(n)$ occurred for any SU at channel i at time n. There are positive/negative rewards associated with each state for each agent. The initial rewards for each agent are:

$$r_{1,n+1}^{locl}\left(s_{i,n+1}^{locl,j,1}\right) = \rho_{i,n}^{locl,j,1}, \quad (7)$$

$$r_{1,n+1}^{locl}\left(s_{i,n+1}^{locl,j,2}\right) = \rho_{i,n}^{locl,j,2} \quad (8)$$

$$r_{1,n+1}^{globl}\left(s_{i,n+1}^{globl,j,1}\right) = \rho_{i,n}^{globl,j,1}, \quad (9)$$

$$r_{2,n+1}^{globl}\left(s_{i,n+1}^{globl,j,2}\right) = \rho_{i,n}^{globl,j,2} \quad (10)$$

The initial state-dependent transition probabilities for global agent are:

$$p\left(s_{i,n+1}^{globl,j,1}\middle|s_{i,n}^{globl,j,1}, \alpha_i^{globl,j,1}\right) = \alpha_i^{globl,j,1,k} \quad (11)$$

$$p\left(s_{i,n+1}^{globl,j,2}\middle|s_{i,n}^{globl,j,1}, \alpha_i^{globl,j,1}\right) = 1 - \alpha_i^{globl,j,1,k} \quad (12)$$

$$p\left(s_{i,n+1}^{globl,j,2}\middle|s_{i,n}^{globl,j,2}, \alpha_i^{globl,j,2}\right) = \alpha_i^{globl,j,2,k} \quad (13)$$

$$p\left(s_{i,n+1}^{globl,j,1}\middle|s_{i,n}^{globl,j,2}, \alpha_i^{globl,j,2}\right) = 1 - \alpha_i^{globl,j,2,k} \quad (14)$$

For the local agent are:

$$p\left(s_{i,n+1}^{,loclj,1}\middle|s_{i,n}^{locl,j,1}, \alpha_i^{locl,j,1}\right) = \alpha_i^{locl,j,1,k} \quad (15)$$

$$p\left(s_{i,n+1}^{locl,j,2}\middle|s_{i,n}^{locl,j,1}, \alpha_i^{locl,j,1}\right) = 1 - \alpha_i^{locl,j,1,k} \quad (16)$$

$$p\left(s_{i,n+1}^{locl,j,2}\middle|s_{i,n}^{locl,j,2}, \alpha_i^{locl,j,2}\right) = \alpha_i^{locl,j,2,k} \quad (17)$$

$$p\left(s_{i,n+1}^{locl,j,1}\middle|s_{i,n}^{locl,j,2}, \alpha_i^{locl,j,2}\right) = 1 - \alpha_i^{glocl,j,2,k} \quad (18)$$

The final transition probability of global agent depends on the local agents decisions. This is expressed as:

$$p\left(s_{i,final,n+1}^{globl,j,v}\middle|s_{i,n}^{globl,j,k}, \alpha_i^{globl,j,m}, s_{i,n+1}^{locl,j,l}\right) = p\left(s_{i,final,n+1}^{globl,j,v}\middle|s_{i,n}^{globl,j,k}, \alpha_i^{globl,j,m}\right) + f(s_{i,n+1}^{globl,j,k}|s_{i,n+1}^{locl,j,l}) \quad (19)$$

Then the influence function f is considered as:

$$f\left(s_{i,n+1}^{global,j,k}\middle|s_{i,n+1}^{local,j,l}\right) = \begin{cases} c_n \text{ } if \text{ } k = l \\ -c_n \text{ } if \text{ } k \neq l \end{cases} \quad (20)$$

The meaning of the coefficient c_n is that state Local_Update increases the probability of state Global_Update and reduces the probability of state Not_Global_Update. The final reward w_{ij} for SU j for local agents' decisions would depend partially to the decision of the global agent and the decision of the local agent:

$$\begin{aligned} w_{ij}(n+1) &= r^{locl,final}\left(s_{i,n+1}^{globl,j,k} \middle| s_{i,n+1}^{locl,j,l}\right) = \\ &= c_{1,n} * r\left(s_{i,n+1}^{locl,j,l}\right) + c_{2,n} * r\left(s_{i,n+1}^{globl,j,k}\right) = \\ &= c_{1,n} * \rho_{l,n}^{locl} + c_{2,n} * \rho_{k,n}^{globl} = \\ &= c_{1,n} * \rho_{l,n}^{locl} + (1 - c_{1,n}) * \rho_{k,n}^{globl} \\ & c_{1,n}, c_{2,n} \in (0,1) \end{aligned} \tag{21}$$

The reward for the global agent would be:

$$r\left(s_{i,n+1}^{globl,j,k}\right) = c_{1,n}\rho_{k,n}^{globl} \tag{22}$$

$$\rho_{l,n}^{locl} = bestlocal_{ij,l}^{n} - w_{ij}(n) \tag{23}$$

$$\rho_{k,n}^{globl} = bestglobal_{ij,k}^{n} - w_{ij}(n) \tag{24}$$

The following assumptions hold:

$$\rho_{1,n}^{locl} < \rho_{2,n}^{locl}, \rho_{1,n}^{globl} < \rho_{2,n}^{globl} \tag{25}$$

The expected reward for local agent of an SU for a period n is given by:

$$\begin{aligned} &\mathbb{E}\left(r_{final,n}^{locl} \middle| s_{i,n}^{globl}, s_{j,n}^{locl}, \alpha_{f,n}^{locl}, \alpha_{m,n}^{globl}\right) \\ &= \sum_{k=1}^{2}\sum_{l=1}^{2} r_{final,n}^{locl}\left(s_{k,n+1}^{globl}, s_{l,n+1}^{locl}\right) * p_n^{local}\left(s_{l,n+1}^{locl} \middle| s_{j,n}^{locl}, \alpha_{f,n}^{locl}\right) \\ &\quad * p_{final,n}^{globl}\left(s_{k,n+1}^{globl} \middle| s_{i,n}^{globl}, s_{l,n+1}^{locl}, \alpha_{m,n}^{globl}\right) \end{aligned} \tag{26}$$

The cumulative reward for local agent would be:

$$r_{final(n)}^{locl}\left(s_{i,1}^{globl}, s_{j,1}^{locl}\right) = \sum_{t=1}^{N-1} r_{final,n}^{locl}\left(s_{k,n+1}^{globl}, s_{l,n+1}^{locl}\right), \quad n = 1..(n-1) \qquad (27)$$

The expected cumulative reward for local agent for SU will be:

$$\begin{aligned}\mathbb{E}\left(r_{final(n)}^{locl} | s_{i,n}^{globl}, s_{j,n}^{locl}, \alpha_{m,n}^{globl} \alpha_{f,n}^{locl}\right) \\ = \mathbb{E}\left(r_{final,n}^{locl} | s_{i,n}^{globl}, s_{j,n}^{locl}, \alpha_{m,n}^{globl} \alpha_{f,n}^{locl}\right) \\ + \sum_{k=1}^{2}\sum_{l=1}^{2}\begin{pmatrix} p_n\left(s_{k,n+1}^{globl}, s_{l,n+1}^{locl} | s_{i,n}^{globl}, s_{j,n}^{locl}, \alpha_{m,n}^{globl} \alpha_{f,n}^{locl}\right) * \\ \mathbb{E}^*\left(r_{final(n)}^{locl} | s_{i,n}^{globl}, s_{j,n}^{locl}\right)\end{pmatrix}\end{aligned} \qquad (28)$$

Where

$$\begin{aligned}p_n\left(s_{k,n+1}^{globl}, s_{l,n+1}^{locl} | s_{i,n}^{globl}, s_{j,n}^{locl}, \alpha_{m,n}^{globl} \alpha_{f,n}^{locl}\right) \\ = p_n\left(s_{l,n+1}^{locl} | s_{j,n}^{locl}, \alpha_{f,n}^{locl}\right) p_{final,n}^{globl}\left(s_{k,n+1}^{globl} | s_{i,n}^{globl}, s_{l,n+1}^{locl}, \alpha_{m,n}^{globl}\right)\end{aligned} \qquad (29)$$

The two agents reach a Nash equilibrium in their decisions when the $Error_i^j(n)$ updates both $bestlocal_i^j(n)$, $global_i\,(n)$. Then the rewards are minimized. The inequalities below hold:

$$\mathbb{E}\left(r_{final(n)}^{locl} | s_{i,n}^{globl}, s_{j,n}^{locl}, \alpha_{1,n}^{globl} \alpha_{1,n}^{locl}\right) \leq \mathbb{E}\left(r_{final(n)}^{locl} | s_{i,n}^{globl}, s_{j,n}^{locl}, \alpha_{1,n}^{globl} \alpha_{2,n}^{locl}\right) \qquad (30)$$

$$\mathbb{E}\left(r_{final(n)}^{locl} | s_{i,n}^{globl}, s_{j,n}^{locl}, \alpha_{1,n}^{globl} \alpha_{1,n}^{locl}\right) \leq \mathbb{E}\left(r_{final(n)}^{locl} | s_{i,n}^{globl}, s_{j,n}^{locl}, \alpha_{2,n}^{globl} \alpha_{1,n}^{locl}\right) \qquad (31)$$

$$\mathbb{E}\left(r_{final(n)}^{locl} | s_{i,n}^{globl}, s_{j,n}^{locl}, \alpha_{1,n}^{globl} \alpha_{1,n}^{locl}\right) \leq \mathbb{E}\left(r_{final(n)}^{locl} | s_{i,n}^{globl}, s_{j,n}^{locl}, \alpha_{2,n}^{globl} \alpha_{2,n}^{locl}\right) \qquad (32)$$

Applying the inequalities to the expected reward and after computations, three conditions for the coefficients are derived which evolve as the agents operate in time as shown in Table 1 in APPENDIX 1.

The three conditions are applied at each step when the network defines the value of the coefficients based on the updated each time probabilities and rewards. For the coefficients $c_{1,n}$ selection of the scheme, the maximum value of $c_{1,n}$will be selected to reflect that the agents seek local and global optima non-cooperatively.

The fusion learns the fading conditions of each SU and then selects for each sub-band the SU whose weighted error metric w_{ij} is the lower. The first phase lasts as long as the weight matrix is stabilized i.e. a small number of iterations and then the hard decision phase occurs.

12.4. EVALUATION

The proposed scheme is evaluated with MATLAB simulations and 10 sub-bands with the same bandwidth. The sub-Nyquist sampling ratio was chosen as $\alpha = p/L = 4/10$ and the p was the number of distict integers for the sampling pattern.

Rayleigh and Nakagami fading channels were considered. Some experimental data does not fit well into either Rayleigh or Rician distributions. Thus, a more general fading distribution was developed whose parameters can be adjusted to fit a variety of empirical measurements. This distribution is called the Nakagami fading distribution which is parameterized by Pr and the fading parameter m. For $m = 1$ the distribution reduces to Rayleigh fading. For $m = (K+1)^2/(2K+1)$ the distribution is approximately Rician fading with parameter K. For $m = 1$ we get no fading [171]. Thus, the Nakagami distribution can model Rayleigh and Rician distributions, as well as more general ones. Note that some empirical measurements support values of the m parameter less than one, in which case the Nakagami fading causes more severe performance degradation than Rayleigh fading [171].

The simulated signal is generated as shown in the APPENDIX 2.

In Figure 12.1, the experiments with Rayleigh fading channels for 20, 30,40, 50 SUs and the fading conditions are continually changing for each SU and each sub-channel where the number of multi-paths were chosen between 5 and 16 randomly. A benchmarking soft decision process based on the MSE estimator is used for comparison. The MSE is considered in [163], too. For the benchmarking soft decision process, if the MSE was below 0.01 then it was considered that the sensing was accurate.

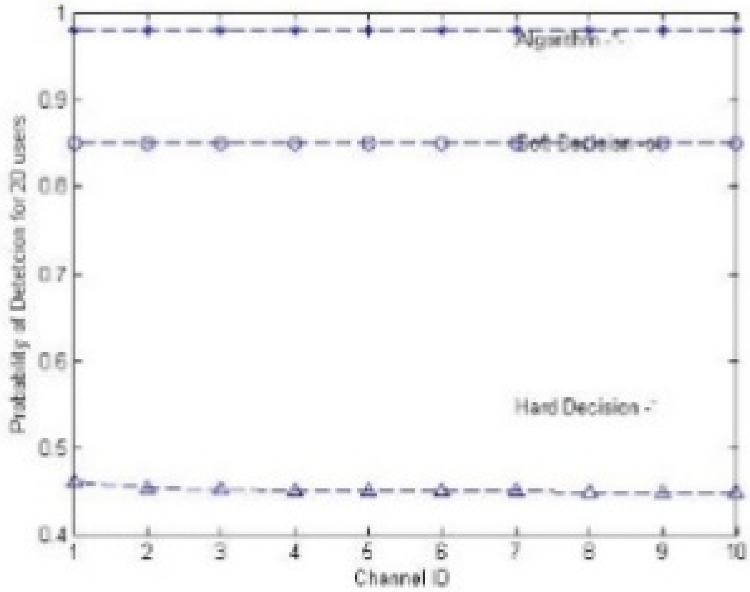

20 users

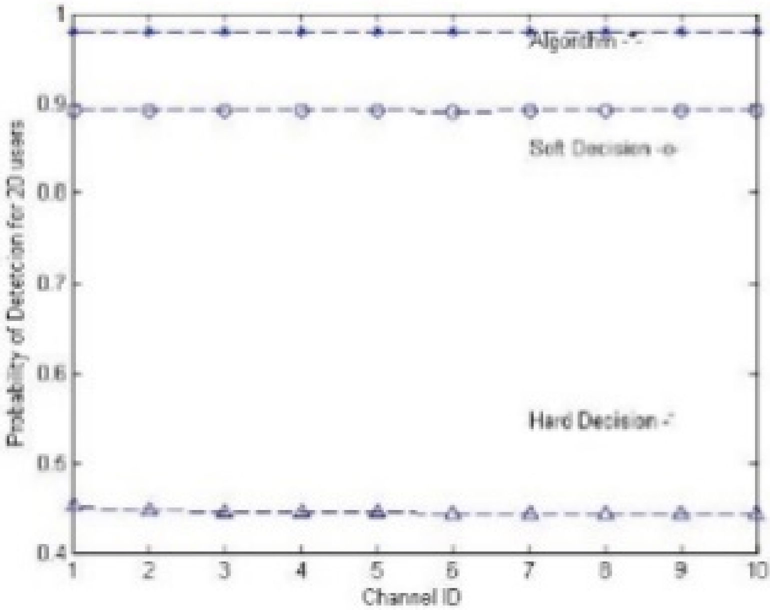

30 users

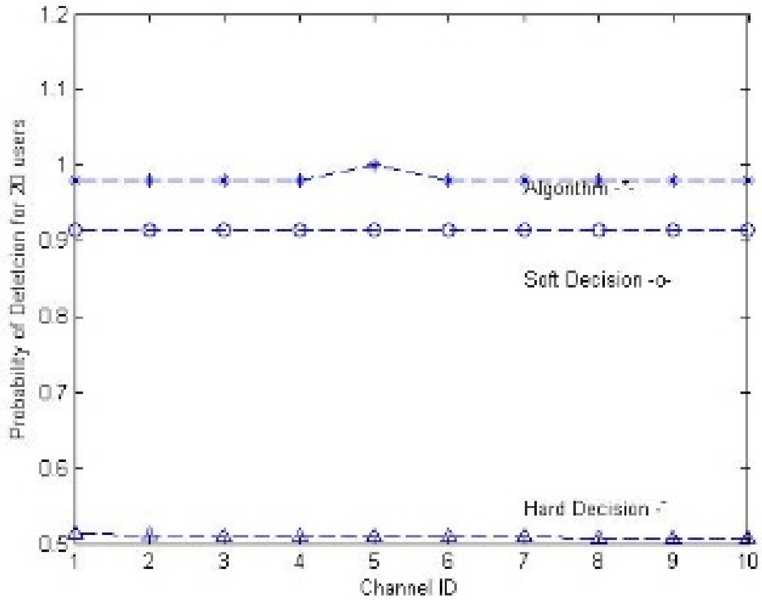

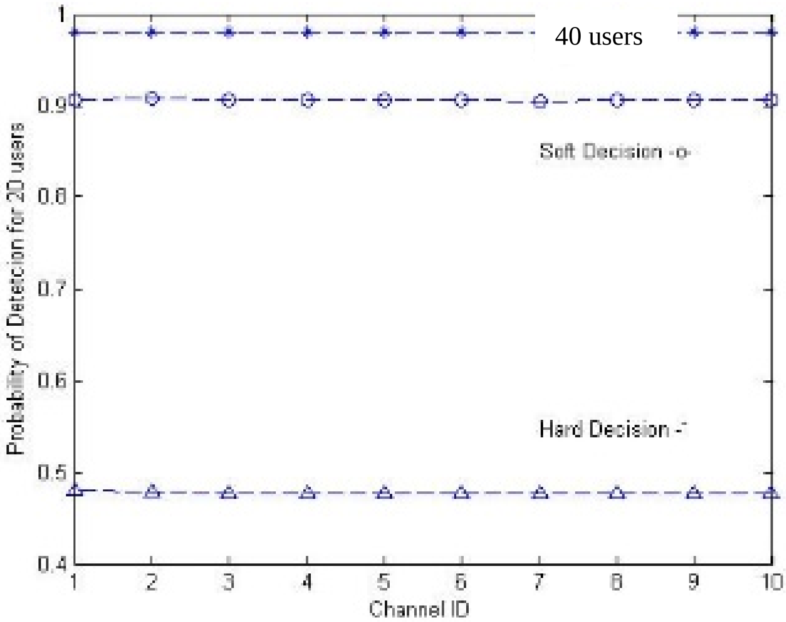

50 users

Figure 12.1. Detection Probability for 20,30,40,50 SUs and Rayleigh channels

The scheme exceeds performance of soft decision scheme where all the SUs participate in the decision process and so they degrade the outcome as the fading is intensive for most of them whilst the proposed scheme selects the SUs for participating in the sensing decision outcome which experience least fading and they are most likely to keep experience least fading conditions (Figure 12.2, Figure 12.3). The results are the same for all the channels because fading conditions were uniformly distributed random variables for the SUs per sub-band and for all sub-bands the fading parameters were the same. Parameter $c1$ was set to 0.9. For Nakagami fading channels conditions change continually, too. The proposed scheme's performance for the Nakagami case stabilizes to 0.9 (Figure 12.4).

(a)

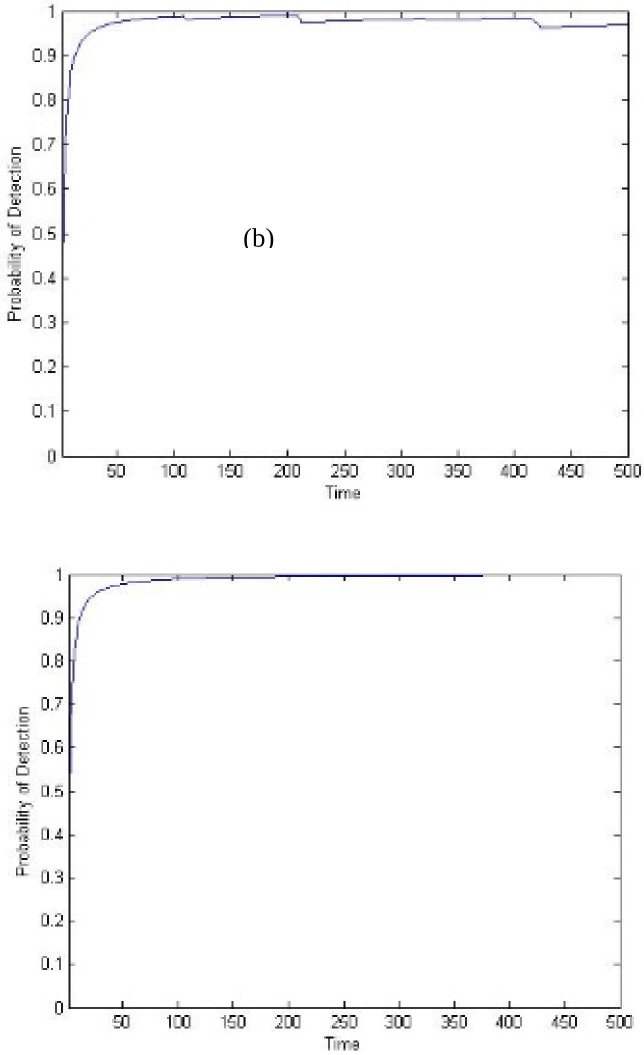

Figure 12.2. Detection Probability for Rayleigh channels a)the Soft Decision and b) Proposed Scheme versus time

(a) (b)

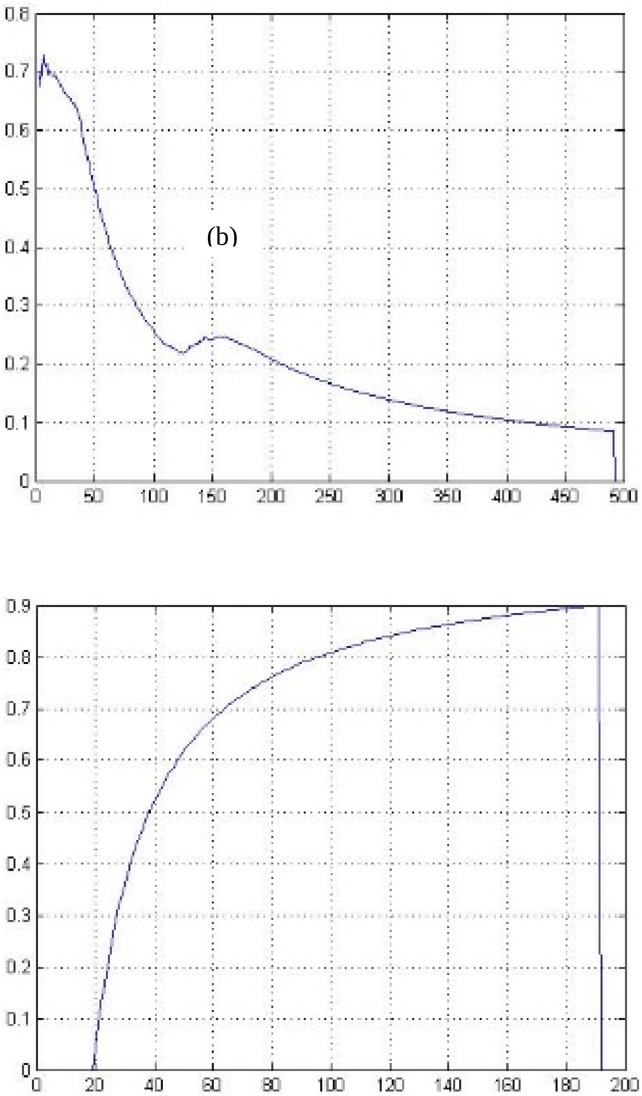

Figure 12.3. Detection Probability for Nakagami channels a) Soft Scheme and) Proposed Scheme versus time

The threshold rule for benchmark hard decision scheme was set as:

$$\|x_i^j\| > \|x_i^0 - x_i^j\| \qquad (33)$$

Nakagami experiments' parameters were $M = 3$ and m were chosen randomly and continually as $m = 3,4,5,6,7$.

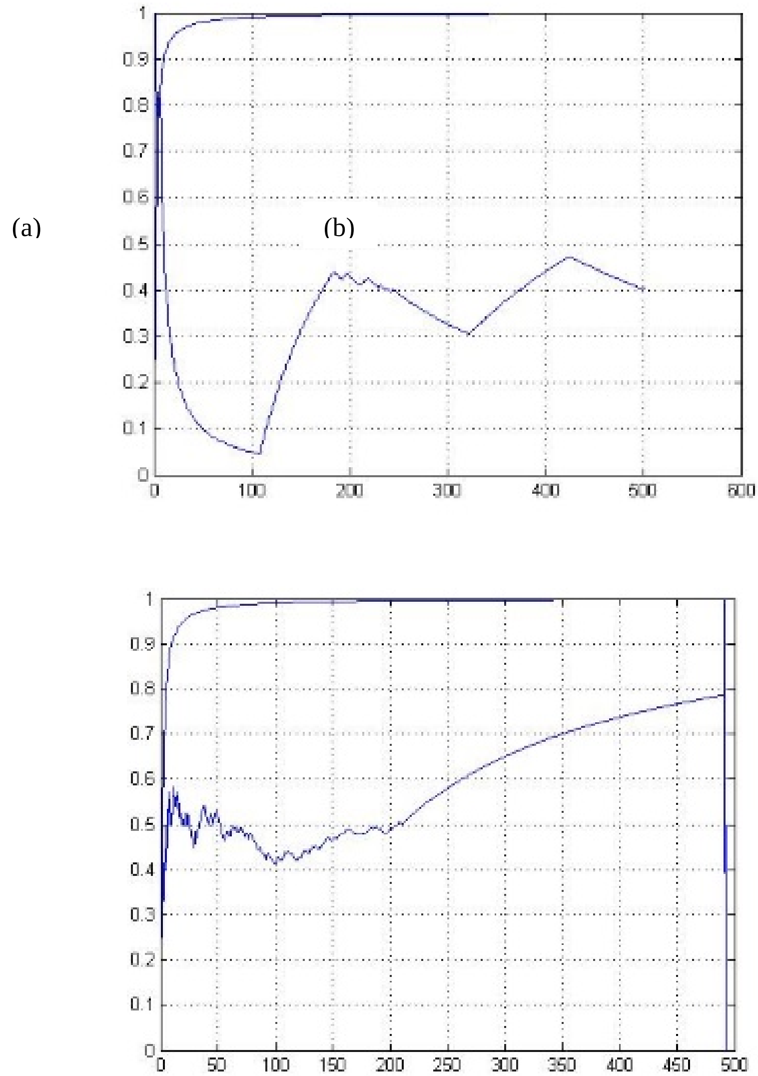

Figure 12.4. Detection Probability for a) Rayleigh and b) Nakagami channels for the Proposed scheme and benchmark Hard Decision Scheme versus time

For Rayleigh channels the Hard decision scheme performance is within 0.4-0.5 whilst for the proposed scheme the performance is excellent (Fig.3). In Nakagami fading channels the Hard decision scheme stabilizes to 0.8 whilst the proposed scheme reaches 0.99 (Fig.3). The Proposed Scheme selects efficiently the SUs which participate in the decision making process and outperforms even soft decision scheme for the highly fading channels that were encountered in the experiments.

12.5. Conclusion

In this paper a multiscale decision making scheme for wideband sensing in CRN and fading channels is proposed. The proposed scheme estimates the ability of each SU in the cooperative network to provide an accurate sensing decision and proceeds in a SU selective optimal sensing schedule for a hard decision scheme establishment which is easy to implement, not computationally intensive and exhibited high performance. The scheme supports the sub-Nyquist sampling which is sensitive to the interference the SUs experience at each sub-band. The fading conditions are considered continually varying for each SU at each sub-band. The evaluation results outperform MSE benchmark and they demonstrate the efficiency of the scheme in terms of performance, processing, transmission overhead and energy, although we considered highly fading channels.

Chapter 13

ENHANCED SIGNAL PROCESSING FOR COGNITIVE RADIO NETWORK AND CLOUD

AN OPTIMAL FILTER WITH KALMAN-LIKE FILTERING OF PARTICLES FOR NON-LINEAR STATE ESTIMATION

The state estimation problem can apply on various systems and applications such as signal processing and position tracking. This research work [172] considers a non-linear dynamic system with Gaussian noises and introduces a novel optimal filter namely a combination of an optimal Kalman-like filter which cooperates with a Particle filter to improve state estimation performance. The Proposed Filter refines the results of Particle Filtering for increased accuracy in state estimation. The novel optimal filter is evaluated with a well-studied system equation example and outperforms amongst others Particle filter and Kalman filter with fewer number of particles.

13.2. INTRODUCTION

In a dynamic process there are restrictions imposed to the measurements which have to be considered each time in order the system to proceed to reliable state estimations such as noise. Well-known probabilistic algorithms, such as Kalman Filter (KF) [173] and Particle Filter (PF) [173] [174] include noisy behavior in their models and depend on the estimation of the posterior density of the state vector by means of the Bayes rule.

In this paper the problem of refining the estimation of the non-linear dynamic system's state provided by Particle Filtering is considered. The paper introduces a novel filter where the Gaussian noisy measurements pass through efficient parameterized PF and KF-like filters in sequence to improve the accuracy of state estimation. The novel filter requires less particles than the PF filter which reduces complexity significantly.

13.2. RELATED WORK

In a dynamic system the state space model includes a hidden state from which partial information is obtained by observations [176]. In the Bayesian framework, this is done by computing or approximating the posterior distribution $p(x_k|z_{1:k})$ for the state vector x_k providing the observations $z_{1:k}$ at that time k. Nonlinear filtering for discrete time nonlinear state models infers hidden state x_k based on the observations z_k.

The Kalman filter which combines knowledge state techniques and recursive algorithms unfolds in two basic steps: a) prediction which is assisted by the dynamic model and b) correction where the observed measurements are used in order for the error covariance of the sensor to be reduced as we had an optimal sensor.

In Kalman filter both the process and measurement noise are Gaussian and uncorrelated [177]. If the noise is not Gaussian but suffer of heavy tails then solutions have been introduced in literature [177][178]. Non-Gaussian noises for Kalman filtering are considered in [9]. Kalman Filter also does not support time-correlation. The authors in [180] study time-correlated measurement processes.

Particle filtering for non-linear model has better performance than Extended Kalman filter i.e. approaches the posterior density with more accuracy however the increased performance is achieved via an increased number of particles which increase significantly the computational load.

Particle Filter (PF) approaches non-linear and non-Gaussian state estimation [181] [182]. The PF is a Bayes filter particularization where the posterior density is discretized and is more accurate than EKF or other Bayes filters such as Monte Carlo. However the computational load of this Bayes filter is lower than others which make it appropriate for real time applications. The authors in [183] consider dependent noise processes. When the state space can be partitioned such that PF can be applied to a reduced state space partition and then a Kalman filter can be applied at each particle which "provides the conditional distribution of linear states x_k^l conditioned over the trajectory of non-linear states $x_{1:k}^n$ and the past observations"[185a] [185] and the filter is known as Marginilized Particle Filter or Rao-Blackwellized particle filter and the reduction of the state variance appears in [185]. The authors in [177a] consider the cases where the observation likehood $p(z_k|x_k)$ is multimodal or heavy-tailed or the the state space is very large and the state transition pdf is broad because when the state transition is narrow even if the observation likehood is multimodal, the optimal importance density i.e. the density for generating the samples such that the variance of weights of the samples is reduced, is unimodal. So, the authors propose an importance density conditioning on the states where observation likehood is unimodal.

The chapter is organized as follows: section III.A describes the particle filter part of the filter and the parameters estimation excluded of the particle filtering processing which will be the inputs for the next phase. Section III.B proposes the enhanced Kalman filter. The enhanced Kalman filter's state estimation will be the final estimation of the Proposed Filter. In Section IV the performance of the Proposed Filter is illustrated .

13.2. PROPOSED FILTER

A. The Particle Filter Part of the Proposed Filter

The Proposed Filter considers the non-linear system model :

$$x_{k+1} = f^0(x_k, v_k^0) = f^{0\prime}(x_k) + v_k^0 \quad (1)$$

$$z_k = h^0(x_k, w_k^0) = h^{0\prime}(x_k) + w_k^0 \quad (2)$$

Where v_k^0 is a stochastic noise process with known probability desnity function and w_k^0 additive measurement noise.

A stochastic process is a Markov process if $p(x_{k+1}|x_k, x_{k-1} \dots) = p(x_{k+1}|x_k)$ and the state is Markov process if the state noise v_k^0 is white in the strict sense i.e. all the $\{v_k^0\}$ are independent of each other. Then the state pdf is given by Chapman-Kolmogorov equation:

$$p(x_{k+1}) = \int p(x_{k+1}|x_k) p(x_k) \quad (3)$$

And the $p(x_{k+1}|x_k)$ is determined by $p(v_k^0)$. If both v_k^0 and w_k^0 are and independent of the initial state then the x_k, z_k are Gaussian signals and if v_k^0 is white in strict sense and independent of the initial state x_0 then the model is a Gauss-Markov model and these hold for both a non-linear and a linear model. Then z is given by $g(z_k|x_k)$.

In filtering the Bayesian approach for the state estimation is to compute the posterior density of the state given the observation $p(x_k|z_{1:k})$ where $z_{1:k}$ denotes al the observations from time 1 to k. Because of the Markov property it holds that $p(x_{k+1}|x_{1:k}, z_{1:k}) = p(x_{k+1}|x_k)$ and $g(z_k|x_{1:k}, z_{1:k-1}) = g(z_k|x_k)$ [4].

The particle generation $\{x_{0:k}^i, w_k^i\}_{i=1}^N$ i.e. N samples per state $x_{0:k}$ is a random measure of the true posterior density $p(x_{0:k}|z_{0:k})$. [4] where w_k^i the weight associated with each sample $x_{0:k}^i$.

The model in (1) (2) is a non-linear Gauss-Markov model. The non-linear model passes through a particle filtering and the posterior density $p(x_k|z_{1:k})$ is estimated. In the same time the the state variance of the particles i.e. the error of the samples and the second order variance are estimated for each state x_k which then pass as inputs to the second level of the proposed filter of the Kalman-like filtering to extract the imposed error. The output of the Kalman-like filter is the output of the Proposed filter providing more accurate estimations of the state of the non-linear dynamic system.

One of the most important decisions on particle filtering is the choice of the importance density $q(.)$ which is the probability density with which the samples are generated such that the samples provided the importance density is a weighted approximation to the posterior density $p(x_k|z_k)$:

$$p(x_k|z_k) = \sum_{i=1}^{N} w^i \delta(x_k - x_k^i)$$

Where x_k^i is the ith sample/particle, w^i is the weight for the ith sample and $\delta()$ is the Dirac function. The optimal importance density reduces the variance of w^i given the x_{k-1}^i whatever sample is produced of:

$$q_{opt}\left(x_k \middle| x_{k-1}^i, z_k\right) = p\left(x_k \middle| x_{k-1}^i, z_k\right)$$

Thus the weights are updated according to:

$$w_k^i \propto w_{k-1}^i p\left(x_k \middle| x_{k-1}^i, z_k\right) = w_{k-1}^i \int p(z_k|x'_k) p\left(x'_k \middle| x_{k-1}^i\right) dx'_k$$

Where

$$p\left(x_k \middle| x_{k-1}^i\right) = STP\left(x_k \middle| x_{k-1}^i\right)$$

$STP(.)$ is the state transition prior density. However solving with this distribution and estimating the inregral is not possible with a few exceptions. For this reason sub-optimal approximations are considered for the proposal density such as the prior $p(x_k|x_{k-1}^i)$ known and as bootstrap filter or SIR filter.

One common problem in particle filtering is that gradually most of the particles will have negligible weights and then the process of resampling takes place to select those particles with the higher weights. This is the *degeneracy* phenomenon. The negligible weights of particles imply that a lot of computational effort is not dedicated to the posterior estimation. A common measure of the degeneracy phenomenon is the effective sample size:

$$N_{eff} = \frac{N}{1+Var(w_k^i)}$$

A $N_{eff} = 1$ implies that all N samples have equal weights and contribute equally to the posterior estimation. When N_{eff} is small resampling selects the samples with the higher weights.

If the state space region where the observation likelihood density $g(z_k|x_k)$ is significant is small comparing to the state space where the prior $p(x_k|z_{k-1})$ is significant then there will a large number of those samples which will be assigned negligible weights and thus will be discarded by resampling [175a]. This way the samples nearby the likelihood states will be selected repeatedly whilst the other will be discarded [175a]. Thus, the diversity of particles will be eliminated and this problem is known as *sample improverishment*. Although the weights of the selected samples by resampling will have small variance the probability density of the covariance of the samples will not be normal. The second order covariance of the samples then will provide the necessary information hidden in tails. Besides the N_{eff} , the pdf of the covariance of particles for each dimension of the state space is a measure of the success of the design of the particular particle filter, too.

The paper considers a L-dimension state space model and SIR filter where the selection of the importance density is sub-optimal i.e. the prior. For each state space dimension, the samples are generated by generating a sample of the process noise which is Gaussian $\boldsymbol{v}_{k-1}^{0,i} \sim \mathcal{N}(\boldsymbol{v}_{k-1}^{0}, Q)$, Q is the covariance of the v_k^0 ,and then setting $X_{P,k}^i = f^{0\prime}\left(X_{P,k-1}^i, \boldsymbol{v}_{k-1}^{0,i}\right)$ [172]. As resampling is applied at each stage $w_{k-1}^i = \frac{1}{N}$, where N the number of samples, the samples are accepted based on the:

$$W_k^i = g\left(Z_{p,k}|X_{P,k}^i\right)$$

For the vectors $X_{P,k}^i, Z_{p,k}, \boldsymbol{v}_{k-1}^0,\ \boldsymbol{v}_{k-1}^{0,i}$of the $L-$space model.

This process “explores the state space without knowledge of observations and thus is sensitive to outliers” [173]. The aforementioned importance density performs well when the noise is not high. The proposed filter aims to employ sub-optimal importance density and reduced number of particles without performance degradation.

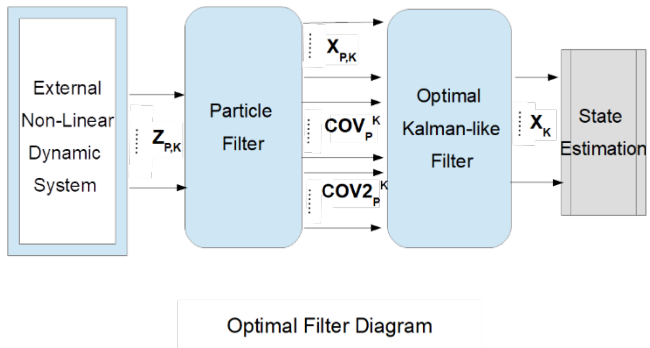

Figure 13.1: The Optimal Filter Diagram

SIR Particle Algorithm[TutorialParticle]
$[\{x_k^i, w_k^i\}_{i=1}^{N_p}] = SIR[\{x_k^i, w_k^i\}_{i=1}^{N_s}, z_{P,k}]$
FOR $i = 1 : N_p$
Draw x_k^i from $p(x_{P,k}|x_{p,k-1}^i)$
Calculate $w_k^i = p(z_{p,k}|x_{p,k}^i)$
END FOR
Calculate total weight t=SUM$\{[w_k^i]\}_{i=1}^{N_s}$
FOR i=1 : N_p
Normalise $w_k^i = \frac{w_k^i}{t}$
END FOR
Resample
RESAMPLE($\{x_{p,k}^i, w_k^i\}_{i=1}^{N_p}$)
//
///////
$x_{p,k}^i$ is the ith particle of state x_k
w_k^i is the weight of $x_{p,k}^i$ particle
N_p the number of particles for each state
$x_{P,k}|$ is the state estimate of the particle for epoch k
$z_{p,k}$ the initial measurement of the non-linear

Figure 13.2: The SIR Particle Algorithm as defined in [3]

For a Gaussian signal $z_{P,k}$ the $p\left(z_{P,k}\middle|x_{p,k}^i\right) = \mathcal{N}\left(z_{P,k}, h^{0'}\left(x_{p,k}^i\right), R\right)$ where R is the covariance of w_k^0 and Q is the covariance of the v_k^0 and x_k is the state estimation of particle filtering $x_{p,k}$. The particle can be generated by producing a random vector v_k^0 and then computing $x_k^i = f^{0'}\left(x_{p,k-1}^i\right) + v_{k-1}^{0,i}$ [173]. The particle at each epoch k that fits to the measurement best will be chosen as the state estimation of particle filtering for the epoch k. So, particles at each epoch given the initial non-linear model, are uncorrelated-i.e. there is no linear relation between them-and their difference i.e. the error of each particle, are uncorrelated between each other and the particles.

The posterior density of the state given the observation $p(x_k|z_{1:k})$ can be expressed in relation to the particle error as follows:

$$p(x_k|z_{1:k}) = \sum_{i=1}^{N} w_k^i \delta(x_k - x_{p,k}^i) = \sum_{i=1}^{N} w_k^i \delta(e_k^{P,i}) \xLeftrightarrow{w_k^i = p(z_{P,k}|x_{p,k}^i)} \sum_{i=1}^{N} p(z_{P,k}|x_{p,k}^i)\delta(e_k^{P,i}) \quad (6)$$

Where $e_k^{P,i}$ is the error of sample $x_{p,k}^i$.

$$\sum_{i=1}^{N} p(z_{P,k}|x_k^i)\delta(e_k^{P,i}) = e_k^P \quad (7)$$

As the samples at each dimension are generated as:

$\boldsymbol{v}_{k-1}^{0,i} \sim \mathcal{N}(\boldsymbol{v}_{k-1}^{0}, Q)$ and then setting $x_{P,k}^i = f^{0\prime}(x_{P,k-1}^i, \boldsymbol{v}_{k-1}^{0,i})$ we have :

$$p(x_{p,k}|z_{p,1:k}) = \sum_{i=1}^{N} w_k^i \delta(x_k - x_{p,k}^i)$$

$$= \sum_{i=1}^{N} w_k^i \delta(x_{p,k} - f^{0\prime}(x_{p,k-1}^i) - v_{k-1}^{0,i})$$

$$= \sum_{i=1}^{N} w_k^i \delta(f^{0\prime}(x_{p,k-1}) + v_{k-1}^{0} - f^{0\prime}(x_{p,k-1}^i) - v_{k-1}^{0,i}) =$$

$$= \sum_{i=1}^{N} w_k^i \delta([f^{0\prime}(x_{p,k-1}) - f^{0\prime}(x_{p,k-1}^i)] + [v_{k-1}^{0} - v_{k-1}^{0,i}])$$

$$\left(by\ definition\ w_k^i = w_{k-1}^i p(z_{P,k}|x_{p,k}^i)\right)$$

$$= \sum_{i=1}^{N} p(z_{P,k}|x_{p,k}^i) w_{k-1}^i \delta([f^{0\prime}(x_{p,k-1}) - f^{0\prime}(x_{p,k-1}^i)] + [v_{k-1}^{0} - v_{k-1}^{0,i}])$$

$$= \sum_{i=1}^{N} p(z_{P,k}|x_{p,k}^i) w_{k-1}^i \delta([f^{0\prime}(x_{p,k-1}) - f^{0\prime}(x_{p,k-1}^i)] + [v_{k-1}^{0} - v_{k-1}^{0,i}])$$

$$= \sum_{i=1}^{N} p(z_{P,k}|x_{p,k}^i) w_{k-1}^i \delta([f^{0\prime}(x_{p,k-1}) - f^{0\prime}(x_{p,k-1}^i)] + [v_{k-1}^{0} - v_{k-1}^{0,i}])$$

$$= \sum_{i=1}^{N} p\left(z_{P,k} \middle| x_{p,k}^{i}\right) \frac{1}{N} \delta\left(f^{0\prime}\left(x_{p,k-1}\right) - f^{0\prime}\left(x_{p,k-1}^{i}\right)\right) + \sum_{i=1}^{N} \frac{\left[v_{k-1}^{0} - v_{k-1}^{0,i}\right]}{N} p\left(z_{P,k} \middle| x_{p,k}^{i}\right)$$

$$\xRightarrow{f^{0\prime}\left(x_{p,k-1}\right) - f^{0\prime}\left(x_{p,k-1}^{i}\right) = e_k^{\widehat{P,\iota}}}$$

$$p\left(x_{p,k} \middle| z_{p,1:k}\right) = \sum_{i=1}^{N} \frac{1}{N} p\left(z_{P,k} \middle| x_{p,k}^{i}\right) e_k^{\widehat{P,\iota}} + \sum_{i=1}^{N} \frac{\left(v_{k-1}^{0} - \mathcal{N}(\boldsymbol{v}_{k-1}^{0}, Q)\right)}{N} p\left(z_{P,k} \middle| x_{p,k}^{i}\right)$$

$$= \sum_{i=1}^{N} \frac{1}{N} p\left(z_{P,k} \middle| x_{p,k}^{i}\right) e_k^{\widehat{P,\iota}} + \frac{\mathcal{N}(0,Q)}{N} \sum_{i=1}^{N} \frac{1}{N} p\left(z_{P,k} \middle| x_{p,k}^{i}\right)$$

$$\xRightarrow{w_k^i = p\left(z_{P,k} \middle| x_{p,k}^{i}\right)\ at\ SIR}$$

$$\xRightarrow{\sum_{I=1}^{N} w_k^i = 1\ by\ definition\ of\ weights}$$

$$p\left(x_{p,k} \middle| z_{p,1:k}\right) = \frac{1}{N} \sum_{i=1}^{N} p\left(z_{P,k} \middle| x_{p,k}^{i}\right) e_k^{\widehat{P,\iota}} + \frac{\mathcal{N}(0,Q)}{N} \rightarrow$$

The probability of accepting a sample at SIR is

$$p\left(z_{P,k} \middle| x_{p,k}^{i}\right) = \mathcal{N}\left({z_{P,k}}^{i}, h^{0\prime}(x_{p,k}^{i}), R\right)$$

$$\rightarrow p\left(x_{p,k} \middle| z_{p,1:k}\right) = \frac{1}{N} \sum_{i=1}^{N} \mathcal{N}\left({z_{P,k}}^{i}, h^{0\prime}(x_{p,k}^{i}), R\right) e_k^{\widehat{P,\iota}} + \frac{\mathcal{N}(0,Q)}{N} \quad (8)$$

As the generation of the ith particle is a Gaussian signal and given the assumptions about particle filtering as appear in [174], the following equations hold :

$$p\left(x_k \middle| z_{P,1:k}\right) = \frac{1}{N}\sum_{i=1}^{N} \mathcal{N}\left(z_{P,k}{}^{i}, h^{0\prime}(x_k^i), R\right) \widehat{e_k^{P,\iota}} + \frac{\mathcal{N}(0,Q)}{N}$$

$$= \frac{1}{N}\sum_{i=1}^{N}\left[\mathcal{N}\left(z_{P,k}{}^{i}, h^{0\prime}(x_{P,k}^i), R\right) - \mathcal{N}\left(z_{P,k}, h^{0\prime}\left(x_{P,k}\right), R\right) + \mathcal{N}\left(z_{P,k}, h^{0\prime}\left(x_{P,k}\right), R\right)\right]\widehat{e_k^{P,\iota}}$$

$$+ \frac{\mathcal{N}(0,Q)}{N} =$$

$$\frac{1}{N}\sum_{i=1}^{N}\left[\mathcal{N}\left(z_{P,k}{}^{i}, h^{0\prime}(x_{p,k}^i), R\right) - \mathcal{N}\left(z_{P,k}, h^{0\prime}(x_{p,k}), R\right)\right]\widehat{e_k^{P,\iota}}$$

$$+ \frac{1}{N}\sum_{i=1}^{N}\left[\mathcal{N}\left(z_{P,k}, h^{0\prime}\left(x_{p,k}\right), R\right)\right]\widehat{e_k^{P,\iota}} + \frac{\mathcal{N}(0,Q)}{N} = \frac{1}{N}\sum_{i=1}^{N}\left[\mathcal{N}\left(z_{P,k}{}^{i}\right.\right.$$

$$\left.\left. - z_{P,k}, h^{0\prime}(x_{p,k}^i) - h^{0\prime}(x_{p,k}), R + R\right)\right]\widehat{e_k^{P,\iota}}$$

$$+ \frac{1}{N}\sum_{i=1}^{N}\left[\mathcal{N}\left(z_{P,k}, h^{0\prime}(x_{p,k}), R\right)\right]\widehat{e_k^{P,\iota}} + \frac{\mathcal{N}(0,Q)}{N}$$

$$\xRightarrow{e_{z,k}{}^{i} = h^{0\prime}(x_k^i) - h^{0\prime}(x_k) \text{ is the observation error of particle}}$$

$$p\left(x_{p,k} \middle| z_{p,1:k}\right) = \tfrac{1}{N}\textstyle\sum_{i=1}^{N}\left[\mathcal{N}\left(e_{z,k}{}^{i}, 2R\right)\right]\widehat{e_k^{P,\iota}} + \tfrac{1}{N}\textstyle\sum_{i=1}^{N}\left[\mathcal{N}\left(z_{P,k}, h^{0\prime}(x_{p,k}), R\right)\right]\widehat{e_k^{P,\iota}} +$$

$$\tfrac{\mathcal{N}(0,Q)}{N} = \tfrac{1}{N}\textstyle\sum_{i=1}^{N}\left[\mathcal{N}\left(e_{z,k}{}^{i}, 2R\right)\right]\widehat{e_k^{P,\iota}} + \mathcal{N}\left(z_{P,k}, h^{0\prime}(x_{p,k}), R\right)\tfrac{1}{N}\textstyle\sum_{i=1}^{N}\widehat{e_k^{P,\iota}} + \tfrac{\mathcal{N}(0,Q)}{N}$$

$$\xRightarrow{\widehat{e_k^{P,\iota}} = \left(e_k^{P,i} - \left(v_{k-1}^{0} - v_{k-1}^{0,i}\right)\right)} \tfrac{1}{N}\textstyle\sum_{i=1}^{N}\left[\mathcal{N}\left(e_{z,k}{}^{i}, 2R\right)\right]e_k^{P,\iota} -$$

$$\tfrac{1}{N}\textstyle\sum_{i=1}^{N}\left[\mathcal{N}\left(e_{z,k}{}^{i}, 2R\right)\mathcal{N}(0,Q)\right] + \tfrac{1}{N}\left(\textstyle\sum_{i=1}^{N}\mathcal{N}\left(z_{P,k}, h^{0\prime}\left(x_{p,k}\right), R\right)e_k^{P,\iota}\right) -$$

$$\textstyle\sum_{i=1}^{N}\mathcal{N}\left(z_{P,k}, h^{0\prime}(x_{p,k}), R\right)\tfrac{\mathcal{N}(0,Q)}{N} + \tfrac{\mathcal{N}(0,Q)}{N} \Longrightarrow \left\langle \textstyle\sum_{i=1}^{N}\tfrac{\mathcal{N}(0,Q)}{N} = \sqrt{Q}\right\rangle \Longrightarrow p\left(x_{p,k} \middle| z_{p,1:k}\right) =$$

$$\textstyle\sum_{i=1}^{N}\mathcal{N}\left(e_{z,k}{}^{i}, 2R\right)\textstyle\sum_{i'=1}^{N}\tfrac{1}{N}e_k^{P,\iota} - \textstyle\sum_{i\neq i'}\mathcal{N}\left(e_{z,k}{}^{i}, 2R\right)\tfrac{1}{N}e_k^{P,i'} -$$

$\frac{1}{N}\sum_{i=1}^{N}\left[\mathcal{N}\left(e_{z,k}{}^{i},2R\right)\mathcal{N}(0,Q)\right]+\mathcal{N}\left(z_{P,k},h^{0\prime}\left(x_{p,k}\right),R\right)\frac{1}{N}\sum_{i=1}^{N}e_k^{P,\iota}\ -$

$\sqrt{Q}\mathcal{N}\left(z_{P,k},h^{0\prime}(x_{p,k}),R\right)+\frac{\mathcal{N}(0,Q)}{N}$(9)

(9) $\Rightarrow p\left(x_{p,k}\middle|z_{p,1:k}\right)=$

$$\mathcal{N}\left(z_{P,k},h^{0\prime}\left(x_{p,k}\right),R\right)\left[\frac{1}{N}\sum_{i=1}^{N}e_k^{P,\iota}-\sqrt{Q}\right]$$

$$+\frac{1}{N}\left[\sum_{i=1}^{N}\mathcal{N}\left(e_{z,k}{}^{i},2R\right)\sum_{i'=1}^{N}e_k^{P,\iota}-\sum_{i\neq i'}\mathcal{N}\left(e_{z,k}{}^{i},2R\right)e_k^{P,i'}\right]$$

$$+\frac{\mathcal{N}(0,Q)}{N}\left[1-\sum_{i=1}^{N}\mathcal{N}\left(e_{z,k}{}^{i},2R\right)\right] \qquad (10)$$

Equation (10) implies that by applying brute force sampling i.e. $N\rightarrow\infty$ the term :

$$\frac{1}{N}\sum_{i=1}^{N}e_k^{P,\iota}$$

Represents the covariance of the particle filter as the samples will participate equally to the state estimate at epoch k. Then if the covariance of the filter equals the process noise standard deviation then the SIR particle filter does not depend on the measurement but rather at the errors of the particles $e_k^{P,\iota}$, the observation errors of the particles $e_{z,k}{}^{i}$ and their covariance.

There is no linear relation between the particles at each epoch k because of the initial non-linear model and the particle generation process and as a result both the particles and the errors between the particles are uncorrelated. Furthermore, the errors generated for particles i and j at epoch k and n respectively are uncorrelated, i.e. the covariance is zero.

The posterior density is computed via the particle algorithm SIR in evaluation (Figure 13.2).

In this paper the evaluation of the proposed filter was performed on target tracking and the covariance and second order covariance of the particles which have been generated at each epoch was computed as appears below:

$P_{k|k-1}=COVARIANCE(x_k)=cov_k^P$

$$= \sum_{i=1}^{N_s} w_{k|k-1}^{i} \left(x_k^i - \hat{x}_{P,k|k-1}\right)\left(x_k^i - \hat{x}_{P,k|k-1}\right)^T$$

$$\hat{x}_{k|k-1} = x_{P,k} = \sum_{i=1}^{N_s} w_{k|k-1}^{i} x_k^i \quad (11)$$

The second order covariance at each epoch is computed as the expected value of:

$$\left(\frac{1}{\binom{N_s}{2}} \sum_{\{i,j\}} \left[\frac{1}{2}\left(x_i - x_j\right)^2 - cov_k^P\right]\right)^2 (12)$$

The above estimation yields three types of outer products terms which eventually lead to the equation below:

$$Var(S^2) = cov2_k^P = \frac{\mu_4}{N_s} - \frac{cov_k^P(N_s-3)}{N_s(N_s-1)} \quad (13)$$

And where μ_4 is the fourth central moment of x estimated as

$$\mu_4 = \sum_{i=1}^{N_s} \frac{\left(x - x_k^i\right)^4}{N_s}. \quad (14)$$

The covariance and second order covariance of the particle process for each sample will be the noise parameters of the Kalman-like filter. The covariance is a metric of how well the particle filtering achieved the required diversity of particles which should follow normal distribution and any difficiencies to meet this goal of particle filtering will be hidden in the tails that appear and covariance will not be sufficient so the second order covariance is a metric for this and overcoming the error of the posterior density estimate of the particle filtering implies to encounter the second order covariance of particle generation.

B. The Kalman-like Filter

The general Kalman filter provides optimal solutions for linear models as it minimizes the Mean Square Error (MSE) of the Kalman filter process error. Kalman Filter is an optimal solution for extracting noise.

The Proposed Kalman-like filter considers the model:

$$X_{k+1} = \Phi X_k + W_k \quad (15)$$

$$Z_{p,k} = H X_k + V_k \quad (16)$$

Where **Φ=I** and **H=I** and

$$w_k = e_k^P + cov_k^P, \qquad v_k = cov_k^P \ (17)$$

And the covariances of w_k and v_k are not stationary but estimated for each epoch k:

$W_k = cov_k^P + cov2_k^P$ and $V_k = cov2_k^P$ (18)

The w_k reflects all the uncertainty regarding the external system state estimation which was performed during particle filtering [184]. The w_k is a centered Gaussian random signal and it is defined entirely by its covariance. The covariance of the process noise is not stationary. The $\{w_k\}$ and $\{v_k\}$ are white in the strict sense so the linear scalar system is a Gauss-Markov model which should correct the estimation of the Bayesian posterior density of the particle filtering based on the estimated particle generation failure metric which are the covariance and second order covariance. The x_k , Hx_k is the state and measurement matrices. The error of the filter process i.e. the difference of the state estimate and the real state, if $\hat{x}_k$ is the estimated state and x_k itself is then:

$f(e_k) = f(x_k - \hat{x}_k)$ (19)

A good choice of an error function should be positive and increase monotonically [176]. The square error function satisfies those prerequisite and given that we consider a period of time, the MSE function is a good metric:

$e_k = \mathbb{E}[e_k^2]$ (20)

The filter process error covariance:

$P_k^K = \mathbb{E}[e_k e_k^T] = \mathbb{E}[e_k^2] = \mathbb{E}[(x_k - \hat{x}_k)(x_k - \hat{x}_k)^T]$ (21)

If the prior estimate of the $\hat{x}_k$ gained by the system is the $\hat{x}_k{}'$ then we have:

$\hat{x}_k = \hat{x}_k{}' + K_k(z_k - H\hat{x}_k{}') = \hat{x}_k{}' + K_k(H\hat{x}_k + v_k - H\hat{x}_k{}')$(22)

Where K_k is the filter's gain at epoch k.

The uncertainty of the state estimate as computed through the particle filtering is passed as the error in both the state estimate and measurement of the Kalman-like filter. However the state estimate uncertainty is increased with both the covariance and second order covariance of the error whilst the second order covariance of the error constitute the noise considered for the measurement. The second order covariance provides information which is hidden in tails that is why it is encountered in the proposed filter. The covariance and second order covariance of the particle filter are chi-square variables and according to central limit theorem for the large number of particles they follow the normal distribution.

The probability of likelihood $p(z_k|\hat{x}_k)$ has to be maximized and as the noise remain Gaussian, the maximum likelihood for the filter is given by:

$$p(z_k|\hat{x}_k) = K_k exp\left(-\frac{(z_k - \hat{x}_k)^2}{cov2_k^P}\right)$$

$$= K_k exp\left(-\frac{\left(x_{p,k} - \hat{x}_k\right)^2}{cov2_k^P}\right) \Rightarrow p\left(x_{p,k}\middle|\hat{x}\right)$$

$$= \prod_k K_k exp\left(-\frac{\left(x_{p,k} - \hat{x}_k\right)^2}{cov2_k^P}\right) \Rightarrow logp\left(x_{p,k}\middle|\hat{x}\right) = \frac{1}{2}\sum_k\left(\frac{\left(x_{p,k} - \hat{x}_k\right)^2}{cov2_k^P}\right) + C \quad (23)$$

The (23) implies that a state estimation $\hat{x}_k$ is computed based on the $x_{p,k}$ and the fact that the estimated error covariance and second order covariance of the error $cov2_k^P$ affected the initial $x_{p,k}$ estimation.The driving function of (23) is the Mean Square Error and can be applied if $x_{p,k}$ is a Gaussian signal- which holds as the particle filtering generates Gaussian signals -and then the MSE provides the $\hat{x}$ that maximizes the $p\left(x_{p,k}\middle|\hat{x}\right)$. The $\hat{x}$ will be the state estimate approximation of the initial non-linear dynamic model (1) (2) with the error inhered by the particle filtering and extracted by the proposed Kalman-like filter. If the scalar model extracts the second order covariance implications i.e. the metric that shows the inability of the particle filtering implementation to achieve the normal distribution in particle generation.

The conditions for Kalman-like filter process to be unbiased provided that the noise is centered, are shown below :

$$\begin{aligned}
\dot{e_k} &= \Phi x_k + w_k - \Phi_f \hat{x}_k - K_k(Hx_k + v_k) \\
&= (\Phi - K_k H)x_k + w_k - \Phi_f \hat{x}_k - K_k v_k \\
&= (\Phi - K_k H)e_k - \left(\Phi - K_k H - \Phi_f\right)\hat{x}_k + w_k - K_k v_k \Rightarrow \\
&\mathbb{E}[\dot{e_k}] = (\Phi - K_k H)\mathbb{E}[e_k] - \left(\Phi - K_k H - \Phi_f\right)\mathbb{E}[\hat{x}_k] + \mathbb{E}[w_k] - K_k\mathbb{E}[v_k]
\end{aligned}$$

(24)

Then the $\lim_{t\to\infty} \mathbb{E}[\dot{e_k}] = 0$ for $\forall\mathbb{E}[\hat{x}_k]$ if and only

$\Phi - K_k H = I - K_k = \Phi_f$ and $\Phi - K_k H = I - K_k$ should be stable (25)

Then the following equations hold:

$$(19)\&\ (20) \Rightarrow \dot{e_k} = (I - K_k)e_k + [I \quad -K_k]\begin{bmatrix} w_k \\ v_k \end{bmatrix} \quad (26)$$

Then $\mathbb{E}\left[\begin{bmatrix} w_k \\ v_k \end{bmatrix}\left[w_{k+l}{}^T \quad v_{k+l}{}^T\right]\right] = \begin{bmatrix} W & 0 \\ 0 & V \end{bmatrix}\delta_l$ with δ_l =1 if l =0 and 0 elsewhere (27)

The covariance matrix in (27) has this form because the error during particles generation for epoch k is independent to the error generated at epoch l since the error of particles is uncorrelated:

$$\mathbb{E}[w_k \quad v_{k+l}] = 0 \qquad (28)$$

Moreover the covariance matrices W and V are positive semidefinite and diagonal. And the Kalman-like filter process error covariance evolves as:

$$P_k^K = \mathbb{E}[e_k e_k^T] = \mathbb{E}[e_k^2] = \mathbb{E}[(x_k - \hat{x}_k)(x_k - \hat{x}_k)^T] \quad (29)$$

$$(26)\&(29) \longrightarrow \dot{P_k^K} = (I - K_k)P_k^K + P_k^K(I - K_k)^T + W + K_k V {K_k}^T \qquad (30)$$

If $(I - K_k)$ stable then then process error covariance matrix P_k^K is positive definite and $W + K_k V {K_k}^T$ is positive semidefinite. (30) is Lyapunov equation [185] [186] and if $(I - K_k)$ stable then $\dot{P_k^K} = 0$ for each epoch k. So, the system is stable at each epoch. The general unique solution to the general Lyapunov equation is (30):

$$AP + PA^T + Q = 0 \qquad (31)$$

$$P = \int_0^\infty e^{At} Q e^{A^T t} dt \quad (32)$$

So, the solution to (30) iff $(I - K_k)$ is Voltera-Lyapunov stable (i.e. strongly stable and D-stable) for each epock k is given by:

$$\dot{P_k^K} = \int_0^\infty e^{(I - \dot{K_k})t} \left(W + K_k V {K_k}^T\right) e^{(I - K_k)^T t} dt \ \ (33)$$

If a matrix A is Voltera-Lyapunov stable then for P symmetric positive, each matrix (A-αI) for every α >0 is a Voltera-Lyapunov stable as:

$$\begin{aligned} &AP + PA^T = Q_1 (negative\ definite)\ and\ A\ is\ negative\ stable \\ &\qquad\qquad \longrightarrow (\mathrm{A} - \alpha\mathrm{I})P + P(\mathrm{A} - \alpha\mathrm{I})^T \\ &= AP - \alpha IP + PA - \alpha P = AP + PA - 2\alpha P = Q_1 - 2\alpha P \\ &\qquad\qquad < 0\ \ and\ (\mathrm{A} - \alpha\mathrm{I})\ negative\ stable \longrightarrow \\ &(\alpha I - A)P + P\,(\alpha I - A)^T = -AP - PA + 2\alpha P = -Q_1 + 2\alpha P (positive\ definite) \\ &\qquad\qquad \longrightarrow\ (34) \end{aligned}$$

Then $(\alpha I - A)\ positive\ stable$ [14]

So, K_k positive semidefinite should follow within the unit cycle (35)

To minimize the trace of $\dot{P_k^K}$ which represents the Mean Square Error, we differentiate w.r.t. K_k and get the trace :

$$\frac{\partial\left(trace\dot{P_k^K}\right)}{\partial K_k} = -2P_k^K + 2K_k V = 0 \Longrightarrow K_k = P_k^K V^{-1} \ \ (36)$$

(36) provides the relations between the filter’s gain and the process error covariance.

From (36) as P_k^K is a covariance matrix is symmetric positive semidefinite and V symmetric positive semidefinite, V^{-1} exists and is positive semidefinite [187] [188], Theorem 2.2.], too. Then K_k positive semidefinite and the matrix $(I - K_k)$ is negative definite as for ∀ non zero vector of real numbers : $z^T K_k z \geq 0$. Then $(I - K_k)$ is negative definite i.e.

∀ non zero vector of real numbers z :

$$z^T(I - K_k)z < 0 \longrightarrow z^T z - z^T K_k z < 0 \longrightarrow z^T z - z^T z - z^T K_k z < 0 - z^T z < 0 \longrightarrow -z^T K_k z < 0 \longrightarrow z^T K_k z > 0, which\ holds\ \longrightarrow$$
$$(I - K_k)$$

is negative define and has negative eigenvalues,so Lyapunov equation (30)holds

If we want to express the process error covariance w.r.t to the prior estimate of the filter $P_k^{K'}$ for the P_k^K we have to substitute $\hat{x}_k$ in (16) with the prior estimate $\hat{x}_k{}'$:

$$\dot{P_k^K} = \mathbb{E}[(x_k - \hat{x}_k)(x_k - \hat{x}_k)^T] =$$
$$= \mathbb{E}[[(I - K_k H)(x_k - \hat{x}_k{}') - K_k v_k)][(I - K_k H)(x_k - \hat{x}_k{}') - K_k v_k)]^T] \quad (37)$$

$x_k - \hat{x}_k{}'$ is the error of the prior estimate. As the state variable is scalar for the proposed Kalman-like filter, we have for the prior error that the state x_k of the primary non-linear dynamic system will be corrected/extracted by the innovation (i.e. $y - \hat{y}$ where $\hat{y} = H\hat{x}_k$) of the proposed Kalman-like filter.

$$(37) \longrightarrow \dot{P_k^K} = (I - K_k H)\mathbb{E}[(x_k - \hat{x}_k{}')(x_k - \hat{x}_k{}')^T](I - K_k H)^T$$
$$+K_k \mathbb{E}[v_k v_k{}^T]K_k{}^T - (I - K_k H)\mathbb{E}[(x_k - \hat{x}_k{}')v_k]K_k{}^T$$
$$-K_k \mathbb{E}[v_k(x_k - \hat{x}_k{}')](I - K_k H)^T \xrightarrow{(23)}$$
$$\dot{P_k^K} = (I - K_k H)\mathbb{E}[(x_k - \hat{x}_k{}')(x_k - \hat{x}_k{}')^T](I - K_k H)^T$$
$$+K_k \mathbb{E}[v_k v_k{}^T]K_k{}^T = P_k^{K'} - P_k^{K'} K_k{}^T - K_k P_k^{K'} + K_k\left(P_k^{K'} + V\right)K_k{}^T \quad (38)$$

As we want to minimize the trace $\dot{P_k^K}$ we differientate w.r.t. to K_k again and we get the equation of filter's gain:

$$\frac{\partial\left(trace\dot{P_k^K}\right)}{\partial K_k} = -2P_k^{K'} + 2K_k P_k^{K'} + 2K_k V = 0 \Longrightarrow K_k = P_k^{K'}\left(P_k^{K'} + V\right)^{-1} \quad (39)$$

As long as V is a positive semidefinite matrix the K_k remains within the unit circle, so it is stable. Substituting (39) to (38) provides the estimate of the process error covariance w.r.t. to prior error covariance:

$$\dot{P}_k^K = (I - K_k) P_k^{K'} \quad (40)$$

So, (40) estimates the proposed filter's error covariance at each epoch k which is the estimated noise to the initial state of the non-linear dynamic system, i.e. with higher accuracy than particle filtering taking into account the information that is hidden in the tails and it is not represented by covariance. The proposed filter then discards all the $cov2_k^P$ second order covariance effects. The control for the stability of the system is assured at each epoch k.

Although the proposed filter reduces variance, it must be assured that there is an acceptable lower bound to average Mean Square Error and such a metric is the Cramer Rao Lower Bound (CRLB). The CRLB depends on the model and not on the implementation and as soon as it is reachable an optimal algorithm attaines CRLB and the error variance of its estimates coincides with CRLB and the estimates are provided by maximum likelihood approach. The performance of particle filter is bounded by CRLB theoretically [184] but achieving optimal MSE requires a very large number of particles which is impractical. A recusrsive computation of CRLB is given by Riccati equation [184] for covariance of the error of the nonlinear particle filtering of the initial non-linear system for an unbiased estimator:

$$P_k^{CRLB} = P'^{CRLB}_{k-1} - P'^{CRLB}_{k-1} H^{0^T}(x_k^0) \left(H^0(x_k^0) P'^{CRLB}_{k-1} H^{0^T}(x_k^0) + R_k \right)^{-1} H^0(x_k^0) P'^{CRLB}_{k-1} \quad (41)$$

$$P'^{CRLB}_{k+1} = F(x_k^0) P_k^{CRLB} F^T(x_k^0) + G(x_k^0) Q_k G^T(x_k^0) \quad (42)$$

Given the initial non-linear system (1) and (2) :

$$F(x_k^0) = \left.\frac{\partial f^0(x_k, v_k^0)}{\partial x_k}\right|_{x_k = x_k^0, v_k^0 = 0} (43)$$

$$G(x_k^0) = \left.\frac{\partial f^0(x_k, v_k^0)}{\partial v_k}\right|_{x_k = x_k^0, v_k^0 = 0} (44)$$

$$H^0(x_k^0) = \left.\frac{\partial h^0(x_k)}{\partial x_k}\right|_{x_k = x_k^0} (45)$$

$$COV(w_k^0) = R_k,\, COV(v_k^0) = Q_k,\, COV(x_1^0) = P_0^{CRLB}, (46)$$

For the scalar system (7) (8) of the Kalman-like filter which considers Gaussian signals and as long as the signals remain Gaussian, the following equations hold:

$$p(x_{k+1} | x_k, W_k) = \mathcal{N}(x_k, W_k) \quad (47)$$

$$p(z_k | x_k, V_k) = \mathcal{N}(x_k, V_k) \quad (48)$$

The following equation provides the logarithm of Gaussian function:

$$\ln \mathcal{N}(\mu, P) = -\frac{1}{2}\ln 2\pi - \frac{1}{2}\ln P - \frac{1}{2P}(x-\mu)^2 \quad (49)$$

Then the Fisher Information Matrix (FIM) J_k^{-1} [19] [20] of the Kalman-like filter is given by:

$$\boldsymbol{J_{k=}} K_{k+1}^{k+1} - K_{k+1}^{k+1,k}\left(J_k + K_{k+1}^{k} + L_k^k\right)^{-1} K_{k+1}^{k,k+1} \quad (50)$$

Where K_{k+1}^{k+1}, $K_{k+1}^{k+1,k}$, K_{k+1}^{k} , $(K_{k+1}^{k,k+1} is\ the\ traspose\ of\ K_{k+1}^{k+1,k})$, L_k^k are estimated as [18]:

$$K_{k+1}^{k} = \mathbb{E}_{x_{k+1}}\left[-\nabla_{x_k}\left[\nabla_{x_k} \ln p(x_{k+1}|x_k)\right]^T |x_k\right] = W_k^{-1} \quad (51)$$
$$K_{k+1}^{k,k+1} = \mathbb{E}_{x_{k+1}}\left[-\nabla_{x_{k+1}}\left[\nabla_{x_k} \ln p(x_{k+1}|x_k)\right]^T |x_k\right] = -W_k^{-1} \quad (52)$$
$$K_{k+1}^{k+1} = \mathbb{E}_{x_{k+1}}\left[-\nabla_{x_{k+1}}\left[\nabla_{x_{k+1}} \ln p(x_{k+1}|x_k)\right]^T |x_k\right] = W_k^{-1} \quad (53)$$
$$L_k^{k} = \mathbb{E}_{z_k}\left[-\nabla_{x_k}\left[\nabla_{x_k} \ln p(z_k|x_k)\right]^T |x_k\right] = V_k^{-1} \quad (54)$$

By substituting (45), (46), (47), (48) in (44), the inverse of the FIM is given by:

$$\boldsymbol{J_{k+1}} = W_{\boldsymbol{k}} - W_k^{-1}\left(J_k + W_k^{-1} + V_k^{-1}\right)^{-1} W_k^{-1} \quad (55)$$

The Riccati equation for P_k^K [190]coincides with equation (49) where $J_k = P_k^{K^{-1}}$ which implies that the Kalman-like filter is optimal i.e. achieves Cramer Rao bound but as the inputs of the Kalman-like filter is the state estimation of particle filtering the bound reached then depends on how well the particle algorithm describes the initial non-linear system.

Finally, the update equations of the optimal proposed discrete Kalman-like filter evolve as follows:

Description	Equation
Enhanced Kalman Gain	$K_k = \dfrac{P_k^{K'}}{P_k^{K'} + cov2_k^P}$
Update State Estimate	$\hat{x}_k = \hat{x}_k{}' + K_k(z_k - H\hat{x}_k{}')$
Update Process Covariance	$P_k^K = P_k^{K'}(I - K_k H)$
Project into k+1	$\hat{x}_{k+1}{}' = \Phi\hat{x}_k = \hat{x}_k$ $P_{k+1}^{K}{}' = P_k^K + (cov_k^P + cov2_k^P)$

Table 13.2: The Proposed Kalman-like Filter recursive equations for state estimation

As the proposed Kalman-like filter minimizes the MSE of the output of Particle filter where the noise is considered as the error of the Particle filter estimation i.e. it is optimal. Besides, the e_k^P, cov_k^P for each sample are estimated from the particle filtering algorithm so the additional computations per sample are the (14) and (13) increasing the computational load by $\mathcal{O}(n)$ per sample.

Proposed Filter:
Input: measurements $z_{p,i}$ $i = 1 : N_s$
FOR $i = 1 : N_s$
{ $(x_{p,i}, e_i^P, cov_i^P)$ =Particle($z_{p,i}$)}
FOR $i = 1 : N_s$
{ Calculate $cov2_i^P$}
$z_k = x_p$
FOR $k = 1 : N$
{
$\hat{x}_k{}' = \Phi\hat{x}_{k-1} = \hat{x}_{k-1}$
$P_k^{K'} = P_{k-1}^K + (cov_{k-1}^P + cov2_{k-1}^P)$

$$K_k = \frac{P_k^{K'}}{P_k^{K'} + cov2_k^P}$$

$\hat{x}_k = \hat{x}_k{}' + K_k(z_k - H\hat{x}_k{}')$
}

Figure 13.3: The Algorithm for the Proposed Filter

13.4. EVALUATION

The evaluation of the proposed optimal filter was implemented in Javascript and was performed with the most common Particle filter i.e. SIR Particle Algorithm for the non-linear system equation and the position tracking problem [173] :

$$f(x_{k-1}, k) = \frac{x_{k-1}}{2} + \frac{25x_{k-1}}{x_{k-1}{}^2+1} + 8\cos(1.2k) \quad (56)$$

And $x_k = f(x_{k-1}, k) + v_{k-1}$.

The trajectories were passed to the particle filter and then the particle filter estimations passed through as new trajectories to the Kalman-like filter. The measurements were considered Gaussian noise measurements with covariance Q=10 and R=1 which means that the noise is high for the particular system. The proposed filter was compared to a) the

Particle filter b) the Kalman-like filter c) a combined filter where the Kalman-like filter was applied to the particles of each sample x_k and a mean filter in terms of Euclidean distance. The normality of both the cov_k^P and $cov2_k^P$ was evaluated as they are the noise inputs for the Kalman-like filter. The normality of covariance cov_k^P was verified for 200 samples and 500 particles per sample (Fig. 3) and 200 samples and 1500 particles per sample (Figure 13.4) and the Euclidean distances are presented.

As it can be seen when the number of particles is not large the covariance of the SIR filter as implemented –which does not describe system (56) well- for the input system model preserves the bell curve but when the number of particles is large i.e. 1500 particles per sample the covariance curve becomes more skewed i.e. approaches more a Chi-variable and with sharper peak due the increased number of particles. As a result, the performance of the whole proposed filter degrades. As it can be seen from Figure 13.3, the curve is wide which implies that there is more information hidden in tails and covariance is not sufficient to describe the noise. In Figure 13.4 the curve becomes more skewed because with the increasing number of particles the diversity does not increase. That is to say, the covariance does not provide accurate estimates as there is information hidden in tails so the second order covariance has to be encountered.

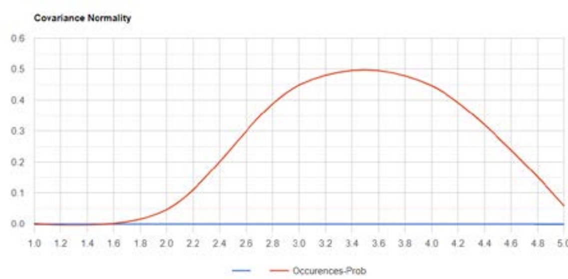

Compare Average Euclidean Distances of Filters

```
average Euclidean distance of Z is: 7.542
average Euclidean distance of Kalman Filter is: 6.970
average Euclidean distance of Particle Filter is: 7.648
average Euclidean distance of   Kalman at Particles is: 7.075
average Euclidean distance of  Proposed Filter is: 5.353
```

Figure 13.3: The covariance curve and the Euclidean distances for 500 samples and 500 particles per sample

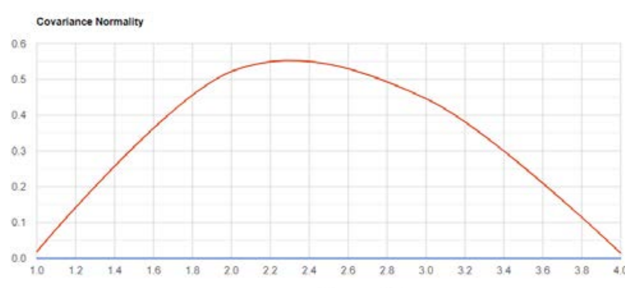

Compare Average Euclidean Distances of Filters

```
average Euclidean distance of Z is: 7.989
average Euclidean distance of Kalman Filter is: 7.384
average Euclidean distance of Particle Filter is: 8.007
average Euclidean distance of   Kalman at Particles is: 7.408
average Euclidean distance of  Proposed Filter is: 5.636
```

Figure 13.4: The covariance curve and the Euclidean distances for 500 samples and 1500 particles per sample

The covariance depends on the SIR Particle filter performance which is sensitive to outliers and the importance density does not perform well in high noise.

The performance of all the filters for 200 samples and 500 particles per sample are shown in Figure 13.5, Figure 13.6, Figure 13.7, Figure 13.8, Figure 13.9.

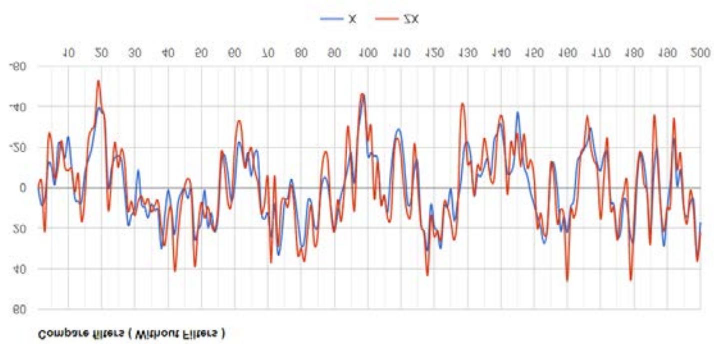

Figure 13.5: The measurement of non-linear dynamic model

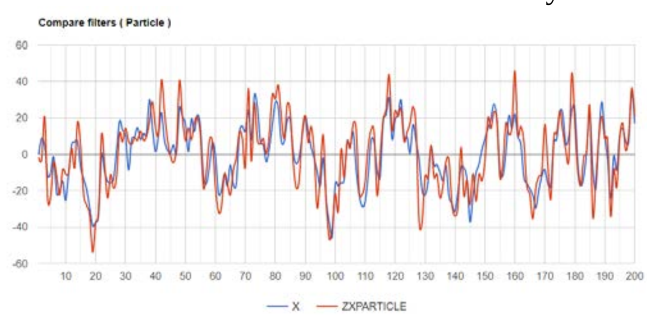

Figure 13.6: The Particle Filtering for 200 samples/500 particles

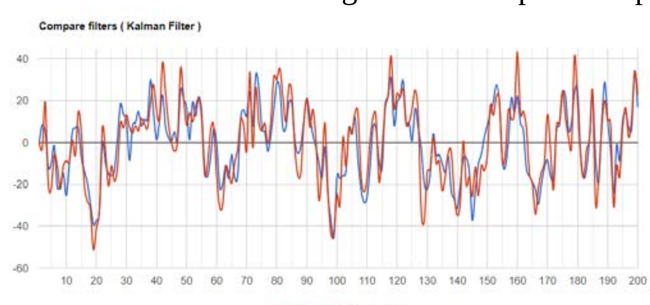

Figure 13.7: The Kalman Filtering for 200 samples

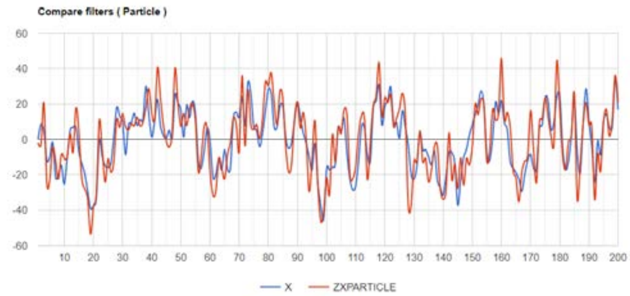

Figure 13.8: The Kalman Filter applied to the particles of each sample (200 sample/500 particles)

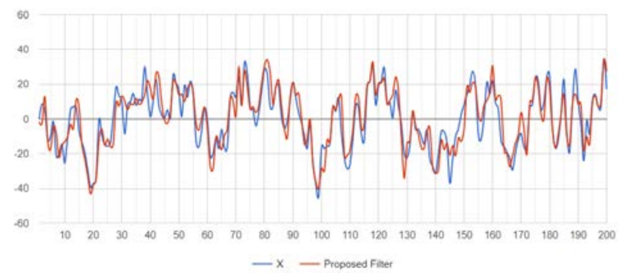

Figure 13.9: The Proposed Filtering for 200 samples and 500 particles.

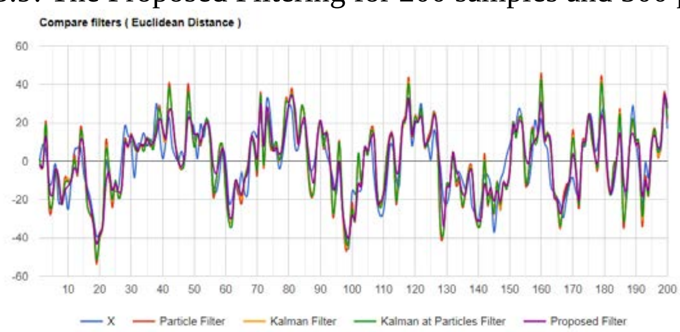

Figure 13.10: All the filters for 200 samples and 500 particles

The Euclidean distance was computed for all the filters and four cases a) 200 samples and 500 particles (Figure 13.11) b) 200 samples and 1000 particles (Figure 13.12), c)500 samples and 500 particles (Figure 13.13 d) 500 samples and 1000 particles (Figure 13.14). From Figure 13.11, Figure 13.12, Figure 13.13, Figure 13.14 it can be seen that an increase in the number of particles degrades the performance of the proposed filter because as it was implemented with the particular adjuvant SIR algorithm which does not provide the necessary particle diversity for the specific non-linear dynamic system (56) of the evaluation. However, the proposed filter adsorbs this dificiency and provides more accurate estimates. An increase in the number of samples does not increase significantly the performance and the covariance of the noise of the Kalman-like filter is estimated per sample, i.e the proposed filter operates equally for a larger and smaller number of samples.

Compare Average Euclidean Distances of Filters

```
average Euclidean distance of Z is: 7.831
average Euclidean distance of Kalman Filter is: 7.265
average Euclidean distance of Particle Filter is: 7.901
average Euclidean distance of   Kalman at Particles is: 7.351
average Euclidean distance of  Proposed Filter is: 5.587
```

Figure 13.11: The Euclidean distances for 200 samples and 500 particles

Compare Average Euclidean Distances of Filters

```
average Euclidean distance of Z is: 8.474
average Euclidean distance of Kalman Filter is: 7.751
average Euclidean distance of Particle Filter is: 8.434
average Euclidean distance of   Kalman at Particles is: 7.730
average Euclidean distance of  Proposed Filter is: 5.869
```

Figure 13.12: The Euclidean distances for 200 samples and 1000 particles

Compare Average Euclidean Distances of Filters

```
average Euclidean distance of Z is: 8.007
average Euclidean distance of Kalman Filter is: 7.389
average Euclidean distance of Particle Filter is: 8.040
average Euclidean distance of   Kalman at Particles is: 7.435
average Euclidean distance of  Proposed Filter is: 5.739
```

Figure 13.13: The Euclidean distances for 500 samples and 500 particles

Compare Average Euclidean Distances of Filters

```
average Euclidean distance of Z is: 8.011
average Euclidean distance of Kalman Filter is: 7.432
average Euclidean distance of Particle Filter is: 8.039
average Euclidean distance of   Kalman at Particles is: 7.454
average Euclidean distance of  Proposed Filter is: 6.153
```

Figure 13.14: The Euclidean distances for 500 samples and 1000 particles

The Cramer Rao Lower Bound (CRLB) is a performance bound which is computed on true trajectory and depends on the model and not on the particle filtering implementation. The CRLB was estimated with (41) and (42) and the results for the Average MSE of all the filters for the simulation and a) 200 samples and 500 particles (Figure 13.15), 200 samples and 1000 particles (Figure 13.16), c) 500 samples and 500 particles (Figure 13.17), d) 500 samples and 1000 particles (Figure 13.18) are shown below. The CRLB can be computed on true trajectory so can be estimated in simulations or when the ground truth is available from a reference system [177].

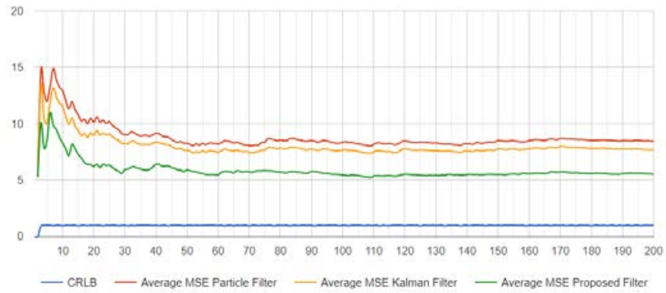

Figure 13.15: The CRLB and Average MSEs for all the filters and 200 samples and 500 particles

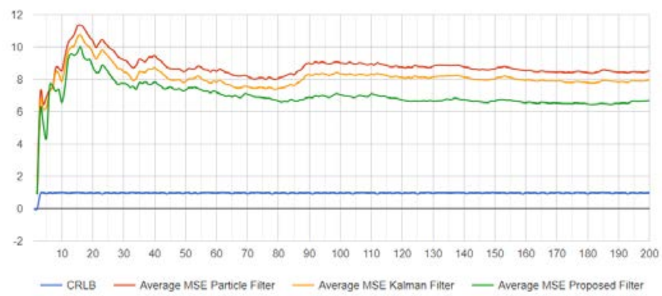

Figure 13.16: CRLB and Average MSEs for all filters and 200 samples and 1000 particles

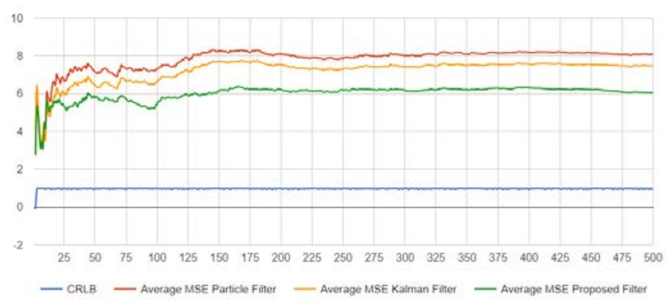

Figure 13.17: CRLB and Average MSEs for all filters and 500 samples and 500 particles

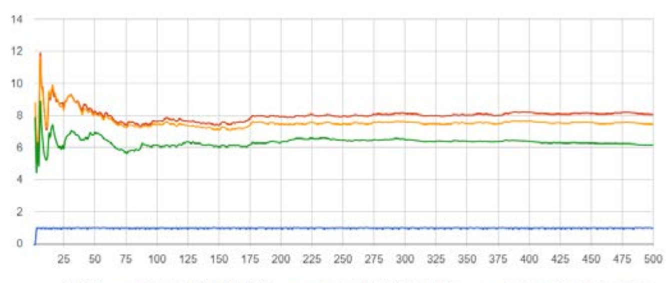

Figure 13.18: CRLB and Average MSEs for all filters and 500 samples and 1000 particles

The evaluation of the proposed filter encountered a common and simple to implement particle algorithm as it is not in scope of this paper to exploit the optimal performance of particle filtering but the opposite i.e. to overcome its deficiencies such as the large number of particles which increase tremendously the computational load or the difficulties of implementing more complex particle algorithms. The SIR algorithm as implemented was not meeting the demands of the noisy system which was examined, so a performance divergence of the optimal theoretical particle filtering performance was expected. The proposed Kalman-like filter with limited computations can overcome any particle filtering performance degradation e.g. in Fig.15 the particle filtering achieves Average MSE around 7.5 and the Kalman-like filter improves it to 5 when the estimated CRLB is 1. Not only that but the Kalman-like Filter achieves optimal performance, i.e. minimizes the MSE, with even with fewer samples and particles which decreases the computational load whilst remains optimal performance.

13.5. Conclusion

An optimal filter for state estimation is introduced which combines a proposed optimal Kalman-like filter stage part with a Particle filter part stage for a non-linear dynamic system model with Gaussian noises. The proposed filter refines the Particle Filtering results based on the estimated error and error covariance of particles per sample and requires a small number of particles whilst overcomes deficiencies in particle algorithm, thus achieves higher performance with fewer particles and less complex algorithms. The proposed filter achieves higher accuracy and outperformed Kalman and Particle Filters during evaluation with a noisy and well-studied model example applied to tracking problem even with a simple particle algorithm and fewer number of particles.

Chapter 14

MASSIVE MIMO TECHNOLOGY FOR COGNITIVE RADIO NETWORK

MASSIVE MIMO FOR CRN WITH IMPERFECT CSI AND NON-RECIPROCAL CHANNELS

The performance of linearly precoded time division duplex Multi User-Multiple Input Multiple Output (MIMO) OFDM Cognitive Radio Network under imperfect CSI and non-reciprocal channels (NRC) covering transceiver frequency response non-reciprocity and antenna mutual coupling mismatches at the Secondary Network Base Station (BS), Secondary User Equipment (UE) and between the secondary network and the Primary Users is studied in this research work [192]. Zero-Forcing and MMSE precoding are considered for the downlink and detailed signal and system models are derived. Channel non-reciprocity is analyzed for the downlink transmission and closed-form analytical expressions are derived for performance degradation regarding the effective signal to interference plus noise ratios and corresponding channel capacity. Those expressions are further used for channel estimation period optimization so to increase network's performance.

14.1 INTRODUCTION

Massive MultipleInputMultipleOutput (MIMO) systems and Cognitive Radio Network are key technologies for the future 5G Network realization [11] [193]. In Massive MIMO the Base Station (BS) employs an array of large number of antennas N that can serve simultaneously K user equipments (UEs) on the same time-frequency resource with N>>K. The need for intense and accurate sensing made Multiple Input Multiple Output (MIMO) technology appropriate for Cognitive Radio. Cognitive radio answers the spectrum scarcity problem arising with the growth of usage of wireless networks and mobile services by exploiting the underutilized licensed spectrum.

Time Division Duplexing (TDD) systems provide the advantage of acquiring CSI at transmitter without the need for dedicated feedback signaling as in Frequency Division Duplexing (FDD) [193]. The downlink (DL) channel estimation is based on uplink pilots relying on the reciprocity of DL and UL channels and thus the resources required are proportional to the UE i.e. K and not N.

However, DL and UL channels are not reciprocal in practice due to differences between the frequency responses (FR) of transmitter and receiver chains of individual transceiver and mutual coupling effects between the antenna elements [194] [195].

Channel non-reciprocity in massive MIMO systems is studied at [194] [195] [196] [197] [198].

Furthermore, for CSI estimation in TDD systems the reporting period has to be divided into two phases: the first phase devoted to channel estimation and the second is the transmission phase. There is a trade-off between the length of the training sequence and transmission period as the time of channel learning will affect the efficiency of the system. An optimization of the training period as well the optimal number of K UEs is proposed for mimimun mean square error (MMSE) and zero-forcing (ZF) linear precoding. MMSE precoding aims at each transmitted antenna is constrained and ZF precoding is a technique which aims at the canceling out interuser interference at each user.

Although MIMO systems as well as imperfect CSI and channel non-reciprocity have been studied so far, current literature on Massive MIMO systems in CRN is not extensive. The authors in [199] propose precoding adaptation for imperfect CSI. In [200] the minimum mean square error is studied for imperfect CSI in full-duplex MIMO systems in Cognitive Radio Networks (CRNs). The minimization problem of transmit power for MIMO CRN under imperfect CSI is studied [201] and imperfect CSI for both SU and PU is under consideration in [202] so they propose an opportunistic beamforming to minimize feedback. The authors in [203] consider and MIMO OFDM CRN with non-interfering channels and they propose a game for rate optimization. The exact outage probability expressions and expression of outage probability for high SINR are derived in [204]. Optimal beamforming for energy optimization, imperfect CSI and perfect and imperfect PU's precoding is proposed in [205]. [206] optimize precoding. All the previous works may consider imperfect CSI, they do not encounter non-reciprocity CRN channels due to transceiver FR and antenna mutual coupling mismatches, their impact on the signal and system characteristics is not analyzed along with precoding, channel learning period and number of UEs optimization. In this paper, detailed signal and system models are derived. Not only that but a comparative study of MMSE and ZF precoding in terms of achievable rate and SINR as well as performance degradation due to channel non-reciprocity are also presented.

The rest of the paper is organized as follows: the section I is a presentation of the system under consideration, section II introduces imperfect CSI and non-channel reciprocity in massive MIMO CRN for MMSE and ZF precoding, section III optimizes the systems performance in terms of channel learning period and number of UEs.

Section IV is a comparative study of the two precoding schemes in terms of capacity and SINR. Finally, section V discusses the performance degradation due to channel non-reciprocity. In the notation used throughout the paper includes $(.)^T$ which denotes the transpose operation and $(.)^H$ denotes the Hermitian transpose.

14.2 SYSTEM MODEL

We consider Multi User -MIMO CRN with K users each one equipped with Nυ antennas . The Secondary Base Station (SBS) is equipped with an antenna array of N elements. The Primary Network operates with a Primary Base Station (PBS) equipped with an antenna array of Np elements. For both networks non-reciprocal channels are considered and the acquired Channel State Information is imperfect. The effective physical channels linking the devices include also all the transceivers and antennas used in the transmitting and receiving devices. There are mismatches between the frequency responses (FRs) of transmitter (TX) and receiver (RX) chains of any individual transceiver, as well as further mutual coupling effects between the antenna elements in multi-antenna devices. TDD multi-user (MU) MIMO-OFDM downlink transmissions are considered. During DL transmission, OFDM waveforms are constructed using N – point IFFT preceded by proper sub-carrier level precoding and stream multiplexing. In this paper, we analyze and characterize the joint impacts of channel non-reciprocity due to transceiver FR and antenna mutual coupling mismatches on precoded TDD multiuser (MU) MIMO-OFDM downlink transmission.

Both MMSE and ZF precoding are considered for the downlink. The BS can use linear detection schemes to reduce the decoding complexity. However, these schemes have lower detection reliability compared with ML detection. There is always a tradeoff between complexity and system performance which vanishes as the number of BS antennas grow large and then linear detectors are nearly-optimal [207], [208]. We assume MMSE precoding which is the optimal precoding for MU- MIMO and aims to a constrained the transmitted power by each antenna. In ZF precoding, the multiuser interference is completely nulled out by projecting each stream onto the orthogonal space of the interuser interference.

Where **H** denotes the frequency domain channel matrix KXN of representing the transfer functions of the K users to the BS and **Hp** denotes the channel matrix between the SBS and PUs. The BS will use the channel matrix estimate and in particular the transpose $\mathbf{H^T}$ to process the signals before transmitting them to the K users. Physical propagation channel matrices are denoted with **H** while the corresponding effective channel matrices are denoted with $\overline{\mathbf{H}}$ which incorporates transmit chains' frequency responses, transmitter and receiver antenna coupling effects, and receiver chains' frequency responses. The estimated channel matrix is denoted by $\widehat{\mathbf{H}.}$ **N** is the additive white Gaussian noise. We assume that the BS uses linear precoding and the precoding matrix is **W**, the data symbol vector be **x** and such that $\mathbb{E}\{|x_k|^2\} = 1$.

The channel estimation phase optimizes the beamforming transmission and the longer that be the better estimation of the channel matrix we would have. On the other hand, the longer the channel estimation phase would decrease the global system bandwidth. A good estimate of CSI reporting duration would then increase the system performance. We assume that the secondary and primary network agree on non-overlapping CSI reporting periods. We assume imperfect CSI for the SU-PU channels, too.

14.3 CSI Estimation and Channel Non-Reciprocity

The SBS starts by transmitting a training sequence of length $M = \frac{aT}{T_s}$ data units, where T is the TDD frame period, α is the proportion devoted to training phase and Ts is the training symbol time. The SBS transmits a predefined training sequence $\mathbf{C_i}$ which are orthogonal with $\mathbf{C^H C} = \mathrm{M}\,\mathbf{Id}$. The K users then report the training sequence to the base station and **H** is the NxK channel matrix between the the K users and the base station. The elements of **H** are i.i.d. variables with zero mean and unit variance. If the K users transmit power is Pu then the received pilot matrix at the base station is **Y**, then the estimated channel matrix at the BS is:

$$\mathbf{Y} = \sqrt{Pu}\mathbf{HC^T} + \mathbf{N} \quad (1)$$

Where **N** is additive Gaussian noise with zero mean and unit variance. The channel matrix can be estimated at the SBS by $\mathbf{Y_H}$:

$$\widehat{\mathbf{Y_H}} = \frac{\sqrt{Pu}}{M}\mathbf{H}\mathbf{C}^{\mathbf{T}}\mathbf{C}^{*} + \frac{1}{M}\mathbf{N}\mathbf{C}^{*} = \frac{\sqrt{Pu}}{M}\mathbf{H} + \frac{1}{M}\mathbf{N}\mathbf{C}^{*} = \frac{\sqrt{Pu}}{M}\mathbf{H} + \mathbf{Np} \quad \mathbf{(2)}$$

The elements of $\mathbf{NC^*}$ matrix are i.i.d. Gaussian with zero mean and unit variance. Let us consider the k column of the above equation which are independent with each other:

$$\widehat{\mathbf{h_k}} = \frac{\sqrt{Pu}}{M}\mathbf{h_k} + \boldsymbol{n_k} \quad \mathbf{(3)}$$

For MMSE channel estimation we want to find the channel matrix that minimizes the mean square error:

$$\widehat{\mathbf{h_k}} = \arg min\,\mathbb{E}\left\{\left\|\widehat{\mathbf{h_k}} - \mathbf{h_k}\right\|^2\right\} = argmin\mathbb{E}\left\{\frac{\left(\sqrt{Pu}-M\right)^2}{Pu}\|\boldsymbol{h_k}\|^{\mathbf{2}} + \frac{1}{\mathrm{Pu}}\|\mathbf{n_k}\|^2 - 2\left(\sqrt{Pu} - M\right)\mathbf{h_k}^T\mathbf{n_k}\right\} \Longrightarrow \mathbf{y_k} = \frac{\left(\sqrt{Pu}-M\right)^2}{Pu}\mathbf{h_k} + \frac{1}{Pu}\mathbf{n_k} \quad \mathbf{(4)}$$

According to Lindeberg-Levy central limit theorem as $\mathbf{h_k^T}, \mathbf{n_k}$ are i.i.d. variables with zero mean and variances $\boldsymbol{\sigma^2_{h_k}\sigma^2_{n_k}}$ $\frac{\mathbf{1}}{\boldsymbol{n}}\mathbf{h_k^T n_k} \rightarrow \boldsymbol{\mathcal{CN}}\left(\mathbf{0}, \boldsymbol{\sigma^2_{h_k}\sigma^2_{n_k}}\right), \boldsymbol{n} \longrightarrow \infty$

The transmitted vector channels would be $\mathbf{s} = \mathbf{H^T W x}$ where $\mathbf{H^T}$ the effective downlink channel matrix and the average transmission power of the transmission vector would be:

$$\mathbb{E}\{\|\mathbf{s}\|^2\} = \mathrm{tr}(\mathbf{W^T W}) = P_{transmision} \quad (5)$$

The received signal then at the K users in the secondary network would be:

$$\mathbf{y} = \mathbf{H^T W x} + \mathbf{N} \quad \mathbf{(6)}$$

The Mean Square Error then would be:

$$\varepsilon = \mathbb{E}\{\|\beta\mathbf{y} - \mathbf{x}\|^2\} = \mathbb{E}\{\|\beta\mathbf{H^T W x} + \beta\mathbf{N} - \mathbf{x}\|^2\} \quad (7)$$

Where β is the Wiener filter. Then, we form in the optimization problem below:

$$[\mathbf{W}, \beta] = \arg\min \varepsilon \quad (8)$$

$$subject\ to: \|\mathbf{s}\|^2 \leq P_{max} \quad (9)$$

Where $Pmax$ is the maximum power allowed to the secondary network so that the interference caused to the primary massive MIMO network by the secondary massive MIMO network is accepted. We apply the Lagrangian method in the optimization problem and we get:

$$\mathcal{L}(W,\beta,\lambda) = \mathbb{E}\{\|\beta y - x\|^2\} - \lambda(s^H s - P_{max}) \rightarrow \frac{\partial \mathcal{L}(W,\beta,\lambda)}{\partial W} =$$

$$= \frac{\partial\left(\beta^2 \frac{\left(\sqrt{Pu}-M\right)^4}{Pu^2} H^* H^T W^H W^T x^H x^T - \lambda x^H W^H W^T x^T - \beta \frac{\left(\sqrt{Pu}-M\right)^2}{Pu} H^* W^H x^H x^T - \lambda P_{max}\right)}{\partial W}$$

$$= 0 \rightarrow$$

$$\mathrm{W_{MMSE}} = \frac{1}{\beta}\frac{\left(\sqrt{\mathrm{Pu}}-\mathrm{M}\right)^2}{\mathrm{Pu}} \mathrm{H}^* \left(\frac{\left(\sqrt{\mathrm{Pu}}-\mathrm{M}\right)^4}{\mathrm{Pu}^2}\mathrm{H^T H^*} + \frac{\lambda}{\beta^2}\mathrm{I_K}\right)^{-1} (10)$$

From the power constraint (9) we have got:

$$\mathrm{W^H W^T} = \mathrm{P_{max}} \Longrightarrow \frac{1}{\beta^2}\frac{\left(\sqrt{\mathrm{Pu}}-\mathrm{M}\right)^4}{\mathrm{Pu}^2}\mathrm{H^T H^*}\left(\frac{\left(\sqrt{\mathrm{Pu}}-\mathrm{M}\right)^4}{\mathrm{Pu}^2}\mathrm{H^T H^*} + \frac{\lambda}{\beta^2}\mathrm{I_K}\right)^{-2} = P_{max}$$

$$\Longrightarrow \beta = \frac{\left(\sqrt{\mathrm{Pu}}-\mathrm{M}\right)^2}{\mathrm{Pu}}\sqrt{\frac{\mathrm{tr}\left(\mathrm{H^T H^*}\left(\frac{\left(\sqrt{\mathrm{Pu}}-\mathrm{M}\right)^4}{\mathrm{Pu}^2}\mathrm{H^T H^*} + \frac{\lambda}{\beta^2}\mathrm{I_K}\right)^{-2}\right)}{\mathrm{P_{max}}}} (11)$$

For $\mu = \frac{\lambda}{\beta^2}$ we want to minimize $\varepsilon\big(\mathrm{W}(\mu), \beta(\mu)\big) \longrightarrow \mu = \frac{\mathrm{trI_K}}{\mathrm{P_{max}}} = \frac{\mathrm{K}}{\mathrm{P_{max}}}$ (12)

Then **W** and β are given by the equations below:

$$\mathrm{W_{MMSE}} = \frac{1}{\beta}\frac{\left(\sqrt{\mathrm{Pu}}-\mathrm{M}\right)^2}{\mathrm{Pu}}\mathrm{H}^*\left(\frac{\left(\sqrt{\mathrm{Pu}}-\mathrm{M}\right)^4}{\mathrm{Pu}^2}\mathrm{H^TH^*}+\frac{\mathrm{K}}{\mathrm{P_{max}}}\mathrm{I_K}\right)^{-1} =$$

$$\frac{\sqrt{P_{max}}}{\sqrt{\mathrm{tr}\left(\mathrm{H^TH^*}\left(\frac{\left(\sqrt{\mathrm{Pu}}-\mathrm{M}\right)^4}{\mathrm{Pu}^2}\mathrm{H^TH^*}+\frac{\mathrm{K}}{\mathrm{P_{max}}}\mathrm{I_K}\right)^{-2}\right)}}\mathrm{H}^*\left(\frac{\left(\sqrt{\mathrm{Pu}}-\mathrm{M}\right)^4}{\mathrm{Pu}^2}\mathrm{H^TH^*}+\frac{\mathrm{K}}{\mathrm{P_{max}}}\mathrm{I_K}\right)^{-1} \quad (13)$$

$$\beta = \frac{\left(\sqrt{\mathrm{Pu}}-\mathrm{M}\right)^2}{\mathrm{Pu}}\sqrt{\frac{\mathrm{tr}\left(\mathrm{H^TH^*}\left(\frac{\left(\sqrt{\mathrm{Pu}}-\mathrm{M}\right)^4}{\mathrm{Pu}^2}\mathrm{H^TH^*}+\frac{\mathrm{K}}{\mathrm{P_{max}}}\mathrm{I_K}\right)^{-2}\right)}{\mathrm{P_{max}}}} \quad (14)$$

The matrix $\Lambda = \left(\frac{\left(\sqrt{\mathrm{Pu}}-\mathrm{M}\right)^4}{\mathrm{Pu}^2}\mathrm{H^TH^*}+\frac{\mathrm{K}}{\mathrm{P_{max}}}\mathrm{I_K}\right)^{-1}$ is diagonal.

However, in practice, the *effective physical channels* linking the devices include also all the transceivers and antennas used in the transmitting and receiving devices and mismatches between the FRs of TX and RX chains of any individual transceiver exist, as well as further mutual coupling effects between the antenna elements in multiantenna devices. The resulting effective downlink (DL) and uplink (UL) channels are thus not reciprocal anymore and performance degradation is expected in any system that is building on the reciprocity assumption [Yaning]. However, as depicted in Figure 14.1 and Figure 14.2, the *effective DL and UL channels* are generally cascades of transceivers and antenna mutual coupling at TX side, physical propagation channels, and antenna mutual coupling and transceivers at RX side:

$$\overline{\mathbf{H_{DL}}} = \mathbf{A_{UR}CU_R\widehat{H_{DL}}C_{BT}A_{BT}} \quad (15)$$

$$\overline{\mathbf{H_{UL}}} = \mathbf{A_{BR}C_{BR}\widehat{H_{DL}}C_{UT}A_{UT}} \quad (16)$$

$$\mathbf{A_{BS,T}} = \mathbf{diag}\{\mathbf{a_{BS,T,1}}, \mathbf{a_{BS,T,2}}, \dots, \mathbf{a_{BS,T,K}}\} \quad (17)$$

$$\mathbf{A_{BS,R}} = \mathbf{diag}\{\mathbf{a_{BS,R,1}}, \mathbf{a_{BS,R,2}}, \dots, \mathbf{a_{BS,R,K}}\} \tag{18}$$

$$\mathbf{A_{U,T}} = \mathbf{diag}\{\mathbf{A_{U,T,1}}, \mathbf{A_{U,T,2}}, \dots, \mathbf{A_{U,T,K}}\} \tag{19}$$

$$\mathbf{A_{U,R}} = \mathbf{diag}\{\mathbf{A_{U,R,1}}, \mathbf{A_{U,R,2}}, \dots, \mathbf{A_{U,R,K}}\} \tag{20}$$

$$\mathbf{A_{U,T,L}} = \mathbf{diag}\{\mathbf{a_{U,T,1}}, \mathbf{a_{U,T,2}}, \dots, \mathbf{a_{U,T,K}}\} \tag{21}$$

$$\mathbf{A_{U,R,l}} = \mathbf{diag}\{\mathbf{a_{U,R,1}}, \mathbf{a_{U,R,2}}, \dots, \mathbf{a_{U,R,K}}\} \tag{22}$$

Where α_i is the frequency response of TX, RX at the k transceiver at the BS or at the UE and $C_i(k)$ are the mutual coupling matrices at the UE and the BS respectively.

The *effective UL channels* can now be written, in terms of *effective DL channels*, as:

$$\mathbf{\overline{H}_{UL}} = \mathbf{A_B C_B \overline{H}_{DL}}^{\mathbf{T}} \mathbf{C_U A_U} \tag{23}$$

$$\mathbf{\overline{H}_{UL,l}} = \mathbf{A_B C_B \overline{H}_{DL,l}}^{\mathbf{T}} \mathbf{C_l A_l} \tag{24}$$

Where $A_B = A_{B,T}^{-1} A_{B,R}$, $A_U = A_{U,T}^{-1} A_{U,R}$, $C_B = C_{B,T} C_{B,R}^{-1}$, $A_l = A_{l,T}^{-1} A_{l,R}$, $C_l = C_{l,T} C_{l,R}^{-1}$. In [18], as a practical example, a fairly simple and widely-used coupling model is established where the circuit-level coupling matrix is of the form $C = (Z_A + Z_T)(\boldsymbol{Z} + Z_T I_N)^{-1}$ where the parameters *ZA* and *ZT* and the elements of the matrix **Z** depend on the impedances of the antenna elements and the associated transceiver circuits [19]. In this paper, to simplify the notations and the presentation, the diagonal elements of mutual coupling matrices are assumed to be normalized to 1. Then the estimated downlink channel matrix would be:

$$\mathbf{\widehat{\overline{H}}_{DL}} = \mathbf{\overline{H}_{UL}^T} = \mathbf{A_U^T C_U^T \overline{H}_{DL} C_B^T A_B^T} = \mathbf{G_U \overline{H}_{DL} G_B} =$$

$$(\mathbf{G'_U} + \mathbf{I})^{-1}\overline{\mathbf{H}}_{\mathbf{DL}}(\mathbf{G'_B} + \mathbf{I})^{-1} \tag{25}$$

Where $\mathbf{G'_U} = \mathbf{G_U^{-1}} - \mathbf{I}, \mathbf{G'_B} = \mathbf{G_B^{-1}} - \mathbf{I}$.

We assume that the primary network is MU-MIMO network of L users communicating with the primary BS. $\mathbf{H_P^T}, \mathbf{W_P}, \mathbf{x_P}$ are the transpose fading coefficients matrix of the primary network, the precoding matrix of the primary network and the data symbol vector of the primary network respectively, $\mathbf{C_{p,B}^T A_{p,B}^T}$ are the mutual coupling matrices of the primary BS and the frequency-responses of TX transceiver at the BS side :

$$\begin{aligned}\widehat{\overline{\mathbf{H}}}_{\mathbf{p,DL}} = \widehat{\overline{\mathbf{H}}}_{\mathbf{p}} = \mathbf{A_U^T C_U^T} \overline{\mathbf{H}}_{\mathbf{p,DL}} \mathbf{C_{p,B}^T A_{p,B}^T} = \\ = \mathbf{G_U} \overline{\mathbf{H}}_{\mathbf{DL}} \mathbf{G_{p,B}} = (\mathbf{G'_U} + \mathbf{I})^{-1}\overline{\mathbf{H}}_{\mathbf{DL}}(\mathbf{G'_{p,B}} + \mathbf{I})^{-1}\end{aligned} \tag{26}$$

We assume the primary network uses the same precoding and the primary and secondary network agree on non-overlapping CSI estimating periods.

14.3.1 IMPERFECT CSI AND MMSE PRECODING

For imperfect CSI and MMSE precoding we have:

$$\widehat{\mathrm{W}}_{\mathrm{MMSE,DL}} = \frac{1}{\beta}\frac{\left(\sqrt{\mathrm{Pu}} - \mathrm{M}\right)^2}{\mathrm{Pu}}\widehat{\overline{H_{DL}}}^{*}\left(\frac{\left(\sqrt{\mathrm{Pu}} - \mathrm{M}\right)^4}{\mathrm{Pu}^2}\widehat{\overline{\mathrm{H}_{DL}}}^{\mathrm{T}}\widehat{\overline{\mathrm{H}_{DL}}}^{*} + \frac{\mathrm{K}}{\mathrm{P_{max}}}\mathrm{I_K}\right)^{-1} =$$

$$= \frac{\sqrt{P_{max}}}{\sqrt{\mathrm{tr}\left(\widehat{\overline{\mathrm{H}_{DL}}}^{\mathrm{T}}\widehat{\overline{\mathrm{H}_{DL}}}^{*}\left(\frac{\left(\sqrt{\mathrm{Pu}} - \mathrm{M}\right)^4}{\mathrm{Pu}^2}\widehat{\overline{H_{DL}}}^{\mathrm{T}}\widehat{\overline{H_{DL}}}^{*} + \frac{\mathrm{K}}{\mathrm{P_{max}}}\mathrm{I_K}\right)^{-2}\right)}}\widehat{\overline{H_{DL}}}^{*}\left(\frac{\left(\sqrt{\mathrm{Pu}} - \mathrm{M}\right)^4}{\mathrm{Pu}^2}\widehat{\overline{H_{DL}}}^{\mathrm{T}}\widehat{\overline{H_{DL}}}^{*} + \frac{\mathrm{K}}{\mathrm{P_{max}}}\mathrm{I_K}\right)^{-1}$$

(27)

$$\beta == \frac{\left(\sqrt{\mathrm{Pu}} - \mathrm{M}\right)^2}{\mathrm{Pu}} \sqrt{\frac{\mathrm{tr}\left(\widehat{H_{DL}}^{\mathrm{T}} \widehat{H_{DL}}^{*} \left(\frac{\left(\sqrt{\mathrm{Pu}} - \mathrm{M}\right)^4}{\mathrm{Pu}^2} \widehat{H_{DL}}^{\mathrm{T}} \widehat{H_{DL}}^{*} + \frac{\mathrm{K}}{\mathrm{P_{max}}} \mathrm{I_K}\right)^{-2}\right)}{\mathrm{P_{max}}}}$$

(28)

The received signal from user K users after considering the interference coefficients and the interference coefficients of the L-users primary MU-MIMO network plus the noise which is i.i.d with zero mean and unit variance is given by the equation below for imperfect CSI:

$$\boldsymbol{Y} = \mathbf{W_R^H \overline{H}_{DL} \widehat{W}_{DL} x} + \mathbf{W_R^H} \sum_{l=1, i \neq k}^{K} \mathbf{\overline{H}_{DL} \widehat{W}_{DL} x} + \mathbf{W_R^H W_R^H} \sum_{l=1}^{L} \mathbf{\overline{H}_p \widehat{W}_{DL} x} + \mathbf{W_R^H N} = \mathbf{W_R^H G_U^{-1} \widehat{\overline{H}}_{DL} G_B^{-1} \widehat{W}_{MMSE,DL} x} + \mathbf{W_R^H} \sum_{l=1, i \neq k}^{K} \mathbf{G_U^{-1} \widehat{\overline{H}}_{DL} G_B^{-1} \widehat{W}_{MMSE,p} x}_{\boldsymbol{p}} + \mathbf{W_R^H} \sum_{l=1}^{L} \mathbf{G_{p,U}^{-1} \widehat{H}_p G_{p,B}^{-1} \widehat{W}_{MMSE,p} x}_{\boldsymbol{p}} + \mathbf{W_R^H N}$$

(29)

We can obtain that the first term provides the signal free of Inter User Interference (IUI) and that we have to consider only ISI at the UE. The second implies that BS calibration would suffice despite FR and mutual coupling mismatches at the UE. The fourth term shows that calibration at the SBS would eliminate IUI from other UEs. The third term shows that we have to encounter ISI at the other UEs. At the same time, PBS calibration would suffice for the secondary UE to receive a signal without IUI from the PU and then with a filter at the receiver cancellation would be feasible. In general ISI cancelation at the UE would be applied with the receiver's filter.

$$
= \mathbf{W_R^H G_U^{-1} \widehat{\widehat{H}}_{DL} G_B^{-1}} \frac{\sqrt{\mathrm{P_{max}}}}{\sqrt{\mathrm{tr}\left(\widehat{\mathbf{H_{DL}}}^{\mathbf{T}}\widehat{\mathbf{H_{DL}}}^{*}\left(\frac{\left(\sqrt{\mathrm{Pu}}-\mathrm{M}\right)^{4}}{\mathrm{Pu}^{2}}\widehat{\mathbf{H_{DL}}}^{\mathbf{T}}\widehat{\mathbf{H_{DL}}}^{*}+\frac{\mathrm{K}}{\mathrm{P_{max}}}\mathrm{I_K}\right)^{-2}\right)}} \widehat{\mathbf{H_{DL}}}^{*}\left(\frac{\left(\sqrt{\mathrm{Pu}}-\mathrm{M}\right)^{4}}{\mathrm{Pu}^{2}}\widehat{\mathbf{H_{DL}}}^{\mathbf{T}}\widehat{\mathbf{H_{DL}}}^{*}\right.
$$

$$
\left.+\frac{\mathrm{K}}{\mathrm{P_{max}}}\mathrm{I_K}\right)^{-1}\mathbf{x}
$$

$$
+\sum_{i=1, i\neq k}^{K} \mathbf{W_R^H G_U^{-1} \widehat{\widehat{H}}_{DL} G_B^{-1}} \frac{\sqrt{\mathrm{P_{max}}}}{\sqrt{\mathrm{tr}\left(\widehat{\mathbf{H_{DL}}}^{\mathbf{T}}\widehat{\mathbf{H_{DL}}}^{*}\left(\frac{\left(\sqrt{\mathrm{Pu}}-\mathrm{M}\right)^{4}}{\mathrm{Pu}^{2}}\widehat{\mathbf{H_{DL}}}^{\mathbf{T}}\widehat{\mathbf{H_{DL}}}^{*}+\frac{\mathrm{K}}{\mathrm{P_{max}}}\mathrm{I_K}\right)^{-2}\right)}} \widehat{\mathbf{H_{DL}}}^{*}\left(\frac{\left(\sqrt{\mathrm{Pu}}-\mathrm{M}\right)^{4}}{\mathrm{Pu}^{2}}\widehat{\mathbf{H_{DL}}}^{\mathbf{T}}\widehat{\mathbf{H_{DL}}}^{*}\right.
$$

$$
\left.+\frac{\mathrm{K}}{\mathrm{P_{max}}}\mathrm{I_K}\right)^{-1}\mathbf{x}
$$

$$
+\mathbf{W_R^H}\sum_{l=1}^{L} \mathbf{G_{p,U}^{-1} \widehat{\widehat{H}}_p G_{p,B}^{-1}} \frac{\sqrt{\mathrm{P_{max}}}}{\sqrt{\mathrm{tr}\left(\widehat{\mathbf{H_p}}^{\mathbf{T}}\widehat{\mathbf{H_p}}^{*}\left(\frac{\left(\sqrt{\mathrm{Pu}}-\mathrm{M}\right)^{4}}{\mathrm{Pu}^{2}}\widehat{\mathbf{H_p}}^{\mathbf{T}}\widehat{\mathbf{H_p}}^{*}+\frac{\mathrm{K}}{\mathrm{P_{max}}}\mathrm{I_K}\right)^{-2}\right)}} \widehat{\mathbf{H_p}}^{**}\left(\frac{\left(\sqrt{\mathrm{Ppu}}-\mathrm{M}\right)^{4}}{\mathrm{Pu}^{2}}\widehat{\mathbf{H_p}}^{\mathbf{T}}\widehat{\mathbf{H_p}}^{*}\right.
$$

$$
\left.+\frac{\mathrm{K}}{\mathrm{P_{pmax}}}\mathrm{I_K}\right)^{-1}\mathbf{x}_{\boldsymbol{p}} + \mathbf{W_R^H N}
$$

$$
= \beta_U \mathbf{W_R^H G_U^{-1}} \boldsymbol{\Lambda x} + \beta_U \mathbf{W_R^H G_U^{-1} \widehat{\widehat{H}}_{DL}} (\boldsymbol{G'_B}) \widehat{\mathbf{H_{DL}}}^{*} \boldsymbol{\Lambda x} + \sum_{i\neq k}^{K} \beta_U \mathbf{W_R^H G_U^{-1}} \boldsymbol{\Lambda x}
$$

$$
+ \sum_{i\neq k}^{K} \beta_U \mathbf{W_R^H G_U^{-1} \widehat{\widehat{H}}_{DL}} (\boldsymbol{G'_B}) \widehat{\mathbf{H_{DL}}}^{*} \boldsymbol{\Lambda x} + \beta_p \mathbf{W_R^H} \sum_{l=1}^{L} \mathbf{G_U^{-1} \widehat{\widehat{H}}_p} \boldsymbol{\Lambda x}
$$

$$
+ \beta_p \mathbf{W_R^H} \sum_{l=1}^{L} \mathbf{G_U^{-1} \widehat{\widehat{H}}_p} \left(\boldsymbol{G'_{p,B}}\right) \widehat{\mathbf{H_p}}^{*} \boldsymbol{\Lambda_p x_p} + \mathbf{W_R^H N} \tag{30}
$$

14.4. THE LMMSE FILTER FOR MMSE PRECODING

We consider LMMSE filter for the receiver to cancel interference from both the secondary and primary network, so we have:

$$\mathbf{W_R^H} = \left(\left(\overline{\mathbf{H}}_{\mathbf{DL}} \widehat{\mathbf{W}}_{\mathbf{DL}}\right)\left(\overline{\mathbf{H}}_{\mathbf{DL}} \widehat{\mathbf{W}}_{\mathbf{DL}}\right)^{H} + \boldsymbol{\Sigma_a} \right)^{-1} \overline{\mathbf{H}}_{\mathbf{DL}} \widehat{\mathbf{W}}_{\mathbf{DL}}$$

$$= \left(\left(\overline{\mathbf{H}}_{\mathbf{DL}} \widehat{\mathbf{W}}_{\mathbf{DL}} \widehat{\mathbf{W}}_{\mathbf{DL}}{}^{\boldsymbol{H}} \overline{\mathbf{H}}_{\mathbf{DL}}{}^{\boldsymbol{H}} \right) + \boldsymbol{\Sigma_a} \right)^{-\mathbf{1}} \overline{\mathbf{H}}_{\mathbf{DL}} \widehat{\mathbf{W}}_{\mathbf{DL}}$$

$$= \left(\left(\beta_U \mathbf{G_U^{-1}} \widehat{\overline{\mathbf{H}}}_{\mathbf{DL}} \mathbf{G_B^{-1}} \widehat{\overline{\mathbf{H}_{\mathbf{DL}}}}^{*} \boldsymbol{\Lambda} \left(\beta_U \widehat{\mathbf{W}}_{\mathbf{DL}} \widehat{\overline{\mathbf{H}_{\mathbf{DL}}}}^{*} \boldsymbol{\Lambda} \right)^{\boldsymbol{H}} \left(\mathbf{G_U^{-1}} \widehat{\overline{\mathbf{H}}}_{\mathbf{DL}} \mathbf{G_B^{-1}} \right)^{\boldsymbol{H}} \right) \right.$$

$$\left. + \boldsymbol{\Sigma_a} \right)^{-\mathbf{1}} \beta_U \mathbf{G_U^{-1}} \widehat{\overline{\mathbf{H}}}_{\mathbf{DL}} \mathbf{G_B^{-1}} \widehat{\overline{\mathbf{H}_{\mathbf{DL}}}}^{*} \boldsymbol{\Lambda}$$

$$= \left(\beta_U \mathbf{G_U^{-1}} \widehat{\overline{\mathbf{H}}}_{\mathbf{DL}} (\mathbf{G_B'} + \boldsymbol{I}) \widehat{\overline{\mathbf{H}_{\mathbf{DL}}}}^{*} \boldsymbol{\Lambda} \left(\beta_U \mathbf{G_U^{-1}} \widehat{\overline{\mathbf{H}}}_{\mathbf{DL}} (\mathbf{G_B'} + \boldsymbol{I}) \widehat{\overline{\mathbf{H}_{\mathbf{DL}}}}^{*} \boldsymbol{\Lambda} \right)^{\boldsymbol{H}} \right.$$

$$\left. + \boldsymbol{\Sigma_a} \right)^{-\mathbf{1}} \beta_U \mathbf{G_U^{-1}} \widehat{\overline{\mathbf{H}}}_{\mathbf{DL}} (\mathbf{G_B'} + \boldsymbol{I}) \widehat{\overline{\mathbf{H}_{\mathbf{DL}}}}^{*} \boldsymbol{\Lambda}$$

$$= \left(\mathbf{G_U^{-1}} \boldsymbol{\Lambda} \left(\mathbf{G_U^{-1}} \widehat{\overline{\mathbf{H}}}_{\mathbf{DL}} (\mathbf{G_B'}) \widehat{\overline{\mathbf{H}_{\mathbf{DL}}}}^{*} \boldsymbol{\Lambda} \right)^{\boldsymbol{H}} + \mathbf{G_U^{-1}} \widehat{\overline{\mathbf{H}}}_{\mathbf{DL}} (\mathbf{G_B'}) \widehat{\overline{\mathbf{H}_{\mathbf{DL}}}}^{*} \boldsymbol{\Lambda} \left(\mathbf{G_U^{-1}} \boldsymbol{\Lambda} \right)^{\boldsymbol{H}} \right.$$

$$+ \beta_U \mathbf{G_U^{-1}} \widehat{\overline{\mathbf{H}}}_{\mathbf{DL}} (\mathbf{G_B'}) \widehat{\overline{\mathbf{H}_{\mathbf{DL}}}}^{*} \boldsymbol{\Lambda} \left(\beta_U \mathbf{G_U^{-1}} \widehat{\overline{\mathbf{H}}}_{\mathbf{DL}} (\mathbf{G_B'}) \widehat{\overline{\mathbf{H}_{\mathbf{DL}}}}^{*} \boldsymbol{\Lambda} \right)^{\boldsymbol{H}}$$

$$\left. + \boldsymbol{\Sigma_a} \right)^{-\mathbf{1}} \beta_U \mathbf{G_U^{-1}} \widehat{\overline{\mathbf{H}}}_{\mathbf{DL}} \mathbf{G_B^{-1}} \widehat{\overline{\mathbf{H}_{\mathbf{DL}}}}^{*} \boldsymbol{\Lambda} \tag{31}$$

For $k_i \ll 1$ and $\beta_i \ll 1$ we have :

$$\boldsymbol{\Sigma_a} = \sqrt{Pu}\, k_1\, \overline{\mathbf{H}}_{\mathbf{DL}} \boldsymbol{diag}\left(\widehat{\mathbf{W}}_{\mathbf{DL}} \widehat{\mathbf{W}}_{\mathbf{DL}}{}^{\boldsymbol{H}} \right) \overline{\mathbf{H}}_{\mathbf{DL}}{}^{\boldsymbol{H}} + \beta_1 \sqrt{Pu}\, \boldsymbol{diag}\left(\overline{\mathbf{H}}_{\mathbf{DL}} \widehat{\mathbf{W}}_{\mathbf{DL}} \widehat{\mathbf{W}}_{\mathbf{DL}}{}^{\boldsymbol{H}} \overline{\mathbf{H}}_{\mathbf{DL}}{}^{\boldsymbol{H}} \right)$$

$$+ \quad \eta_1 \sum_{\boldsymbol{l \neq i}}^{\boldsymbol{L}} \left[\overline{\mathbf{H}}_{\mathbf{p}} \left(\widehat{\mathbf{W}}_{\mathbf{p}} \widehat{\mathbf{W}}_{\mathbf{p}}{}^{\boldsymbol{H}} + k_1 \boldsymbol{diag}\left(\widehat{\mathbf{W}}_{\mathbf{p}} \widehat{\mathbf{W}}_{\mathbf{p}}{}^{\boldsymbol{H}} \right) \right) \overline{\mathbf{H}}_{\mathbf{p}}{}^{\boldsymbol{H}} \right]$$

$$+ \beta_1 \eta_1 \sum_{\boldsymbol{l \neq i}}^{\boldsymbol{L}} \left[\boldsymbol{diag}\left(\overline{\mathbf{H}}_{\mathbf{p}} \widehat{\mathbf{W}}_{\mathbf{p}} \widehat{\mathbf{W}}_{\mathbf{p}}{}^{\boldsymbol{H}} \overline{\mathbf{H}}_{\mathbf{p}}{}^{\boldsymbol{H}} \right) \right]$$

$$+ \quad \eta_2 \sum_{\boldsymbol{k \neq i}}^{\boldsymbol{K}} \left[\overline{\mathbf{H}}_{\mathbf{DL}} \left(\widehat{\mathbf{W}}_{\mathbf{DL}} \widehat{\mathbf{W}}_{\mathbf{DL}}{}^{\boldsymbol{H}} + k_2 \boldsymbol{diag}\left(\widehat{\mathbf{W}}_{\mathbf{DL}} \widehat{\mathbf{W}}_{\mathbf{DL}}{}^{\boldsymbol{H}} \right) \right) \overline{\mathbf{H}}_{\mathbf{DL}}{}^{\boldsymbol{H}} \right]$$

$$+ \beta_2 \eta_2 \sum_{\boldsymbol{k \neq i}}^{\boldsymbol{K}} \left[\boldsymbol{diag}\left(\overline{\mathbf{H}}_{\mathbf{DL}} \widehat{\mathbf{W}}_{\mathbf{DL}} \widehat{\mathbf{W}}_{\mathbf{DL}}{}^{\boldsymbol{H}} \overline{\mathbf{H}}_{\mathbf{DL}}{}^{\boldsymbol{H}} \right) \right] + \boldsymbol{I}$$

(32)

14.3.2 IMPERFECT CSI AND ZF PRECODING

For imperfect CSI and ZF precoding we have:

$$\widehat{\mathbf{W}}_{\mathbf{ZF,DL}} = \widehat{\overline{\mathbf{H}_{\mathbf{DL}}}}^{\mathbf{H}} \left(\widehat{\overline{\mathbf{H}_{\mathbf{DL}}}} \ \ \widehat{\overline{\mathbf{H}_{\mathbf{DL}}}}^{\mathbf{H}} \right)^{-1} \tag{33}$$

The received signal from K users after considering the interference and the interference of the L-users primary MU-MIMO network plus the noise which is i.i.d with zero mean and unit variance is given by the equation below for imperfect CSI:

$$\begin{aligned}
\boldsymbol{Y} = {} & \mathbf{W}_{\mathbf{R}}^{\mathbf{H}} \overline{\mathbf{H}}_{\mathbf{DL}} \widehat{\mathbf{W}}_{\mathbf{DL}} \mathbf{x} + \sum_{i \neq k}^{K} \mathbf{W}_{\mathbf{R}}^{\mathbf{H}} \overline{\mathbf{H}}_{\mathbf{DL}} \widehat{\mathbf{W}}_{\mathbf{DL}} \mathbf{x} + \mathbf{W}_{\mathbf{R}}^{\mathbf{H}} \sum_{l=1}^{L} \overline{\mathbf{H}}_{\mathbf{p}} \widehat{\mathbf{W}}_{\mathbf{p}} \mathbf{x}_{\mathbf{p}} + \mathbf{W}_{\mathbf{R}}^{\mathbf{H}} \mathbf{N} \\
& = \mathbf{W}_{\mathbf{R}}^{\mathbf{H}} \mathbf{G}_{\mathbf{U}}^{-1} \widehat{\overline{\mathbf{H}}}_{\mathbf{DL}} \mathbf{G}_{\mathbf{B}}^{-1} \widehat{\mathbf{W}}_{\mathbf{ZF,DL}} \mathbf{x} + \sum_{i \neq k}^{K} \mathbf{W}_{\mathbf{R}}^{\mathbf{H}} \mathbf{G}_{\mathbf{U}}^{-1} \widehat{\overline{\mathbf{H}}}_{\mathbf{DL}} \mathbf{G}_{\mathbf{B}}^{-1} \widehat{\mathbf{W}}_{\mathbf{ZF,DL}} \mathbf{x} \\
& + \mathbf{W}_{\mathbf{R}}^{\mathbf{H}} \sum_{l=1}^{L} \mathbf{G}_{\mathbf{p,U}}^{-1} \widehat{\overline{\mathbf{H}}}_{\mathbf{p}} \mathbf{G}_{\mathbf{p,B}}^{-1} \widehat{\mathbf{W}}_{\mathbf{p,ZF}} \mathbf{x}_{\boldsymbol{p}} + \mathbf{W}_{\mathbf{R}}^{\mathbf{H}} \mathbf{N} \\
& = \mathbf{W}_{\mathbf{R}}^{\mathbf{H}} \mathbf{G}_{\mathbf{U}}^{-1} \widehat{\overline{\mathbf{H}}}_{\mathbf{DL}} \mathbf{G}_{\mathbf{B}}^{-1} \widehat{\overline{\mathbf{H}_{\mathbf{DL}}}}^{\mathbf{H}} \left(\widehat{\overline{\mathbf{H}_{\mathbf{DL}}}} \ \ \widehat{\overline{\mathbf{H}_{\mathbf{DL}}}}^{\mathbf{H}} \right)^{-1} \mathbf{x} \\
& + \sum_{i \neq k}^{K} \mathbf{W}_{\mathbf{R}}^{\mathbf{H}} \mathbf{G}_{\mathbf{U}}^{-1} \widehat{\overline{\mathbf{H}}}_{\mathbf{DL}} \mathbf{G}_{\mathbf{B}}^{-1} \widehat{\overline{\mathbf{H}_{\mathbf{DL}}}}^{\mathbf{H}} \left(\widehat{\overline{\mathbf{H}_{\mathbf{DL}}}} \ \ \widehat{\overline{\mathbf{H}_{\mathbf{DL}}}}^{\mathbf{H}} \right)^{-1} \mathbf{x} \\
& + \mathbf{W}_{\mathbf{R}}^{\mathbf{H}} \sum_{l=1}^{L} \mathbf{G}_{\mathbf{,U}}^{-1} \widehat{\overline{\mathbf{H}}}_{\mathbf{p}} \mathbf{G}_{\mathbf{p,B}}^{-1} \widehat{\overline{\mathbf{H}_{\mathbf{DL}}}}^{\mathbf{H}} \left(\widehat{\overline{\mathbf{H}_{\mathbf{DL}}}} \ \ \widehat{\overline{\mathbf{H}_{\mathbf{DL}}}}^{\mathbf{H}} \right)^{-1} \mathbf{x}_{\boldsymbol{p}} + \mathbf{W}_{\mathbf{R}}^{\mathbf{H}} \mathbf{N} =
\end{aligned}$$

$$
\begin{aligned}
&= \mathbf{W_R^H G_U^{-1} \hat{\hat{H}}_{DL} \widehat{\overline{H_{DL}}}^H \left(\widehat{\overline{H_{DL}}} \;\; \widehat{\overline{H_{DL}}}^H\right)^{-1} x + W_R^H G_U^{-1} \hat{\hat{H}}_{DL}} \boldsymbol{G'_B} \mathbf{\widehat{\overline{H_{DL}}}^H \left(\widehat{\overline{H_{DL}}} \;\; \widehat{\overline{H_{DL}}}^H\right)^{-1} x} \\
&\quad + \sum_{i \neq k}^{K} \mathbf{W_R^H G_U^{-1} \hat{\hat{H}}_{DL} \widehat{\overline{H_{DL}}}^H \left(\widehat{\overline{H_{DL}}} \;\; \widehat{\overline{H_{DL}}}^H\right)^{-1} x} \\
&\quad + \sum_{i \neq k}^{K} \mathbf{W_R^H G_U^{-1} \hat{\hat{H}}_{DL}} \boldsymbol{G'_B} \mathbf{\widehat{\overline{H_{DL}}}^H \left(\widehat{\overline{H_{DL}}} \;\; \widehat{\overline{H_{DL}}}^H\right)^{-1} x} \\
&\quad + \mathbf{W_R^H} \sum_{l=1}^{L} \mathbf{G_{,U}^{-1} \hat{\hat{H}}_p \widehat{\overline{H_p}}^H \left(\widehat{\overline{H_p}} \;\; \widehat{\overline{H_p}}^H\right)^{-1} x}_{\boldsymbol{p}} + \\
&\quad + \mathbf{W_R^H} \sum_{l=1}^{L} \mathbf{G_{,U}^{-1} \hat{\hat{H}}_p G'}_{\boldsymbol{p}} \mathbf{\widehat{\overline{H_p}}^H \left(\left(\widehat{\overline{H_p}} \;\; \widehat{\overline{H_p}}^H\right)\right)^{-1} x}_{\boldsymbol{p}} + \mathbf{W_R^H N}
\end{aligned}
\tag{34}
$$

If both the secondary and primary networks adapt ZF precoding, we come to the same conclusions for non-reciprocity as in MMSE precoding.

14.3.2.1 THE LMMSE FILTER FOR ZF PRECODING

We consider LMMSE filter for the receiver to cancel interference from both the secondary and primary network too, so we have:

$$\mathbf{W}_{\mathbf{R}}^{\mathbf{H}} = \left((\overline{\mathbf{H}}_{\mathbf{DL}} \widehat{\mathbf{W}}_{\mathbf{DL}})(\overline{\mathbf{H}}_{\mathbf{DL}} \widehat{\mathbf{W}}_{\mathbf{DL}})^{H} + \boldsymbol{\Sigma_a} \right)^{-1} \overline{\mathbf{H}}_{\mathbf{DL}} \widehat{\mathbf{W}}_{\mathbf{DL}}$$

$$= \left(\left(\overline{\mathbf{H}}_{\mathbf{DL}} \widehat{\mathbf{W}}_{\mathbf{DL}} \widehat{\mathbf{W}}_{\mathbf{DL}}{}^{H} \overline{\mathbf{H}}_{\mathbf{DL}}{}^{H} \right) + \boldsymbol{\Sigma_a} \right)^{-\mathbf{1}} \overline{\mathbf{H}}_{\mathbf{DL}} \widehat{\mathbf{W}}_{\mathbf{DL}}$$

$$= \left(\left(\mathbf{G}_{\mathbf{U}}^{-\mathbf{1}} \widehat{\overline{\mathbf{H}}}_{\mathbf{DL}} \boldsymbol{G'_B} \widehat{\overline{\mathbf{H}_{\mathbf{DL}}}}^{\mathbf{H}} \left(\widehat{\overline{\mathbf{H}_{\mathbf{DL}}}} \; \widehat{\overline{\mathbf{H}_{\mathbf{DL}}}}^{\mathbf{H}} \right)^{-\mathbf{1}} \left(\mathbf{G}_{\mathbf{U}}^{-\mathbf{1}} \widehat{\overline{\mathbf{H}}}_{\mathbf{DL}} \boldsymbol{G'_B} \widehat{\overline{\mathbf{H}_{\mathbf{DL}}}}^{\mathbf{H}} \left(\widehat{\overline{\mathbf{H}_{\mathbf{DL}}}} \; \widehat{\overline{\mathbf{H}_{\mathbf{DL}}}}^{\mathbf{H}} \right)^{-\mathbf{1}} \right)^{H} \right) + \boldsymbol{\Sigma_a} \right)^{-\mathbf{1}} \mathbf{G}_{\mathbf{U}}^{-\mathbf{1}} \widehat{\overline{\mathbf{H}}}_{\mathbf{DL}} \boldsymbol{G'_B} \widehat{\overline{\mathbf{H}_{\mathbf{DL}}}}^{\mathbf{H}} \left(\widehat{\overline{\mathbf{H}_{\mathbf{DL}}}} \; \widehat{\overline{\mathbf{H}_{\mathbf{DL}}}}^{\mathbf{H}} \right)^{-\mathbf{1}} \tag{35}$$

For k_i<<1 and β_i<<1 we have :

$$\begin{aligned} \boldsymbol{\Sigma_a} = {} & \sqrt{Pu}\, k_1\, \overline{\mathbf{H}}_{\mathbf{DL}} \boldsymbol{diag}\left(\widehat{\mathbf{W}}_{\mathbf{DL}} \widehat{\mathbf{W}}_{\mathbf{DL}}{}^{H} \right) \overline{\mathbf{H}}_{\mathbf{DL}}{}^{H} + \beta_1 \sqrt{Pu}\, \boldsymbol{diag}\left(\overline{\mathbf{H}}_{\mathbf{DL}} \widehat{\mathbf{W}}_{\mathbf{DL}} \widehat{\mathbf{W}}_{\mathbf{DL}}{}^{H} \overline{\mathbf{H}}_{\mathbf{DL}}{}^{H} \right) \\ & + \eta_1 \sum_{k \neq i}^{L} \left[\overline{\mathbf{H}}_{\mathbf{p}} \left(\widehat{\mathbf{W}}_{\mathbf{p}} \widehat{\mathbf{W}}_{\mathbf{p}}{}^{H} + k_1 \boldsymbol{diag}\left(\widehat{\mathbf{W}}_{\mathbf{p}} \widehat{\mathbf{W}}_{\mathbf{p}}{}^{H} \right) \right) \overline{\mathbf{H}}_{\mathbf{p}}{}^{H} \right] \\ & + \beta_1 \eta_1 \sum_{k \neq i}^{L} \left[\boldsymbol{diag}\left(\overline{\mathbf{H}}_{\mathbf{p}} \widehat{\mathbf{W}}_{\mathbf{p}} \widehat{\mathbf{W}}_{\mathbf{p}}{}^{H} \overline{\mathbf{H}}_{\mathbf{p}}{}^{H} \right) \right] \\ & + \eta_2 \sum_{k \neq i}^{K} \left[\overline{\mathbf{H}}_{\mathbf{DL}} \left(\widehat{\mathbf{W}}_{\mathbf{DL}} \widehat{\mathbf{W}}_{\mathbf{DL}}{}^{H} + k_2 \boldsymbol{diag}\left(\widehat{\mathbf{W}}_{\mathbf{DL}} \widehat{\mathbf{W}}_{\mathbf{DL}}{}^{H} \right) \right) \overline{\mathbf{H}}_{\mathbf{DL}}{}^{H} \right] \\ & + \beta_2 \eta_2 \sum_{k \neq i}^{K} \left[\boldsymbol{diag}\left(\overline{\mathbf{H}}_{\mathbf{DL}} \widehat{\mathbf{W}}_{\mathbf{DL}} \widehat{\mathbf{W}}_{\mathbf{DL}}{}^{H} \overline{\mathbf{H}}_{\mathbf{DL}}{}^{H} \right) \right] + \boldsymbol{I} \end{aligned} \tag{36}$$

We next quantify the relative achievable rate performance under MMSE and ZF precoding schemes. The asymptotic behavior of this relative achievable rate performance for large number of antennas, a non-asymptotic comparison of the achievable SINRs at the m-th antenna in the UE side between MMSE and ZF precoding schemes under NRC and in order to quantify the SINR degradation under nonreciprocal channels with respect to ideal reciprocal channel reference case, we define a metric.

In above, the second term of primary and secondary signals consist of the desired streams while the first term is mostly inter-user-interference.

We want to maximize the achievable bit rate for each user kth so from Shannon's theorem we have:

$$R_{MMSE} = \mathbb{E}\{\log_2(1 + SINR_{MMSE})\} = (36)$$

Equation (36) appears in APPENDIX 3 of Chapter 14.

We can solve the convex optimization below select the proper training period with α.

$$maximize_{\alpha,K}\ R_{MMSE}$$

$$subject\ to{:}\ Intereference_{SU-TO-PU} = tr\left(\left(\left(\mathbf{G}_{,\mathbf{U}}^{-1}\widehat{\widehat{\mathbf{H}}}_{\mathbf{p}}\mathbf{G}'_{\boldsymbol{p}}\right)\left(\mathbf{G}_{,\mathbf{U}}^{-1}\widehat{\widehat{\mathbf{H}}}_{\mathbf{p}}\mathbf{G}'_{\boldsymbol{p}}\right)_{\mathbf{p}}^{\boldsymbol{H}}\right)\beta_U\overline{\widehat{\mathbf{H}_{\mathbf{DL}}}}^{*}\boldsymbol{\Lambda}\right) < Interference_{threshold} \quad (37)$$

For imperfect CSI and ZF precoding we have:

$$\widehat{\mathbf{W}}_{\mathbf{ZF,DL}} = \overline{\widehat{\mathbf{H}_{\mathbf{DL}}}}^{\mathbf{H}}\left(\overline{\widehat{\mathbf{H}_{\mathbf{DL}}}}\ \ \overline{\widehat{\mathbf{H}_{\mathbf{DL}}}}^{\mathbf{H}}\right)^{-\mathbf{1}} \quad (38)$$

The received signal from user k after considering the interference coefficients of the other (K-1) users and the interference coefficients of the L-users primary MU-MIMO network plus the noise which is i.i.d with zero mean and unit variance is given by the equation below for imperfect CSI:

$$\boldsymbol{Y} = \mathbf{W_R^H \overline{H}_{DL} \widehat{W}_{DL} x} + \sum_{i\neq k}^{K} \mathbf{W_R^H \overline{H}_{DL} \widehat{W}_{DL} x} + \mathbf{W_R^H} \sum_{l=1}^{L} \mathbf{\overline{H}_p \widehat{W}_p x_p} + \mathbf{W_R^H N}$$

$$= \mathbf{W_R^H G_U^{-1} \hat{\hat{H}}_{DL} G_B^{-1} \widehat{W}_{ZF,DL} x} + \sum_{i\neq k}^{k} \mathbf{W_R^H G_U^{-1} \hat{\hat{H}}_{DL} G_B^{-1} \widehat{W}_{ZF,DL} x}$$

$$+ \mathbf{W_R^H} \sum_{l=1}^{L} \mathbf{G_{p,U}^{-1} \hat{\hat{H}}_p G_{p,B}^{-1} \widehat{W}_{p,ZF} x}_{\boldsymbol{p}} + \mathbf{W_R^H N}$$

$$= \mathbf{W_R^H G_U^{-1} \hat{\hat{H}}_{DL} G_B^{-1} \widehat{\overline{H_{DL}}}^H} \left(\widehat{\overline{\mathbf{H_{DL}}}} \ \widehat{\overline{\mathbf{H_{DL}}}}^{\mathbf{H}} \right)^{-1} \mathbf{x}$$

$$+ \sum_{i\neq k}^{K} \mathbf{W_R^H G_U^{-1} \hat{\hat{H}}_{DL} G_B^{-1} \widehat{\overline{H_{DL}}}^H} \left(\widehat{\overline{\mathbf{H_{DL}}}} \ \widehat{\overline{\mathbf{H_{DL}}}}^{\mathbf{H}} \right)^{-1} \mathbf{x}$$

$$+ \mathbf{W_R^H} \sum_{l=1}^{L} \mathbf{G_{,U}^{-1} \hat{\hat{H}}_p G_{p,B}^{-1} \widehat{\overline{H_p}}^H} \left(\widehat{\overline{\mathbf{H_p}}} \ \widehat{\overline{\mathbf{H}_{\boldsymbol{p}}}}^{\mathbf{H}} \right)^{-1} \mathbf{x}_{\boldsymbol{p}} + \mathbf{W_R^H N} =$$

$$= \mathbf{W_R^H G_U^{-1} \hat{\hat{H}}_{DL} \widehat{\overline{H_{DL}}}^H} \left(\widehat{\overline{\mathbf{H_{DL}}}} \ \widehat{\overline{\mathbf{H_{DL}}}}^{\mathbf{H}} \right)^{-1} \mathbf{x} + \mathbf{W_R^H G_U^{-1} \hat{\hat{H}}_{DL} G_B' \widehat{\overline{H_{DL}}}^H} \left(\widehat{\overline{\mathbf{H_{DL}}}} \ \widehat{\overline{\mathbf{H_{DL}}}}^{\mathbf{H}} \right)^{-1} \mathbf{x}$$

$$+ \sum_{i\neq k}^{K} \mathbf{W_R^H G_U^{-1} \hat{\hat{H}}_{DL} \widehat{\overline{H_{DL}}}^H} \left(\widehat{\overline{\mathbf{H_{DL}}}} \ \widehat{\overline{\mathbf{H_{DL}}}}^{\mathbf{H}} \right)^{-1} \mathbf{x}$$

$$+ \sum_{i\neq k}^{K} \mathbf{W_R^H G_U^{-1} \hat{\hat{H}}_{DL} G_B' \widehat{\overline{H_{DL}}}^H} \left(\widehat{\overline{\mathbf{H_{DL}}}} \ \widehat{\overline{\mathbf{H_{DL}}}}^{\mathbf{H}} \right)^{-1} \mathbf{x}$$

$$+ \mathbf{W_R^H} \sum_{l=1}^{L} \mathbf{G_{,U}^{-1} \hat{\hat{H}}_p \widehat{\overline{H_p}}^H} \left(\widehat{\overline{\mathbf{H_p}}} \ \widehat{\overline{\mathbf{H_p}}}^{\mathbf{H}} \right)^{-1} \mathbf{x}_{\boldsymbol{p}} + \mathbf{W_R^H} \sum_{l=1}^{L} \mathbf{G_{,U}^{-1} \hat{\hat{H}}_p G'}_{\boldsymbol{p}} \mathbf{\widehat{\overline{H_p}}^H} \left(\widehat{\overline{\mathbf{H_p}}} \ \widehat{\overline{\mathbf{H_p}}}^{\mathbf{H}} \right)^{-1} \mathbf{x}_{\boldsymbol{p}}$$

$$+ \mathbf{W_R^H N}$$

(39)

We want to maximize the achievable bit rate for each user kth so from Shannon's theorem we have:

$$R_{ZF} = \mathbb{E}\{\log_2(1 + SINR_{ZF})\} = (40)$$

(40)

Equation (40) appears in APPENDIX 5 of Chapter 14.

We can solve the convex optimization below select the proper training period with α.

$$maximize_{\alpha,K}\ R_{ZF}$$

$$subject\ to{:}\ Intereference_{SU-TO-PU} = tr\left(\left(\left(\mathbf{G}_{,\mathbf{U}}^{-1}\widehat{\widehat{\mathbf{H}}}_{\mathbf{p}}\mathbf{G'}_{\boldsymbol{p}}\right)\left(\mathbf{G}_{,\mathbf{U}}^{-1}\widehat{\widehat{\mathbf{H}}}_{\mathbf{p}}\mathbf{G'}_{\boldsymbol{p}}\right)_{\mathbf{p}}^{\boldsymbol{H}}\right)\beta_{U}\overline{\widehat{\mathbf{H}_{\mathbf{DL}}}}^{*}\boldsymbol{\Lambda}\right) < Interference_{threshold} \tag{41}$$

This a convex optimization problem that the MU-MIMO Cognitive Radio Network can solve with the cloud assistance.

We next quantify the relative achievable rate performance under MMSE and ZF precoding schemes. The asymptotic behavior of this relative achievable rate performance for large number of antennas, a non-asymptotic comparison of the achievable SINRs at the m-th antenna in the UE side between MMSE and ZF precoding schemes under NRC and in order to quantify the SINR degradation under nonreciprocal channels with respect to ideal reciprocal channel reference case, we define a metric.

For large scale MIMO the channel vectors are nearly orthogonal and $\mathbf{H}\mathbf{H}^{\mathbf{T}} = \mathbf{H}^{\mathbf{T}}\mathbf{H} = \frac{\xi}{r}\mathbf{I}$, $\xi = \sum_{i=1}^{r}\lambda_i$ where λi the eigenvalues of **H,** $\mathbf{H}^{\mathbf{T}}$: The diagonal Λ matrix and β would be computed as shown below:

$$\beta_{\upsilon} == \frac{\left(\sqrt{\mathrm{Pu}}-\mathrm{M}\right)^2}{\mathrm{Pu}}\sqrt{\frac{\mathrm{tr}\left(\widehat{H_{DL}}^{\mathrm{T}}\widehat{H_{DL}}^{*}\left(\frac{\left(\sqrt{\mathrm{Pu}}-\mathrm{M}\right)^4}{\mathrm{Pu}^2}\widehat{H_{DL}}^{\mathrm{T}}\widehat{H_{DL}}^{*}+\frac{\mathrm{K}}{\mathrm{P_{max}}}\mathrm{I_K}\right)^{-2}\right)}{\mathrm{P_{max}}}} =$$

$$= \frac{\left(\sqrt{\mathrm{Pu}}-\mathrm{M}\right)^2}{\mathrm{Pu}}\sqrt{\frac{\mathrm{tr}\left(\left(\left(\left(\frac{\left(\sqrt{\mathrm{Pu}}-\mathrm{M}\right)^4}{\mathrm{Pu}^2}+\frac{\mathrm{K}}{\mathrm{P_{max}}}\right)\mathrm{I_K}\right)^{-2}\right)\right)}{\mathrm{P_{max}}}}$$

(42)

$$\Lambda = \left(\frac{\left(\sqrt{\mathrm{Pu}}-\mathrm{M}\right)^4}{\mathrm{Pu}^2}\mathrm{H^T H^*}+\frac{\mathrm{K}}{\mathrm{P_{max}}}\mathrm{I_K}\right) = \left(\left(\frac{\xi}{r}\frac{\left(\sqrt{\mathrm{Pu}}-\mathrm{M}\right)^4}{\mathrm{Pu}^2}+\frac{\mathrm{K}}{\mathrm{P_{max}}_{\mathrm{K}}}\right)\mathbf{I}\right)^{-1^{-1}}$$

(43)

So, the performance of each precoding for Massive MIMO can be estimated by the following equation:

$$\lim_{N\to\infty}\frac{R_{MMSE}}{R_{ZF}} = \frac{(1-\alpha)\log_2(1+SNR_{MMSE})}{(=(1-\alpha)\log_2(1+SNR_{ZF})}$$

(44)

So we have :

$$\lim_{N\to\infty} SINR_{MMSE} = (45) =$$

(45)

Where $V_1 = \frac{\xi}{r}\frac{\left(\sqrt{\mathrm{Pu}}-\mathrm{M}\right)^2}{\mathrm{Pu}}\sqrt{\frac{\mathrm{K}}{\mathrm{P_{max}}}}$, $V_2 = \frac{\xi}{r}\frac{\left(\sqrt{\mathrm{Pu}}-\mathrm{M}\right)^4}{\mathrm{Pu}^2}+\frac{\mathrm{K}}{\mathrm{P_{max}}_{\mathrm{K}}}$, $V_3 = \frac{\left(\sqrt{\mathrm{Pu}}-\mathrm{M}\right)^4}{\mathrm{Pu}^2}+\frac{\mathrm{K}}{\mathrm{P_{max}}}$, $V = \frac{V_1}{V_2 V_3}$

(46)

$$\lim_{N\to\infty} SINR_{ZF} = (47)$$

(47)

$$\frac{\lim_{N\to\infty} SINR_{MMSE}}{\lim_{N\to\infty} SINR_{ZF}} = (48)$$

(48)

Equations (44), (45), (46), (47), (48) appear in APPENDIX 7 of Chapter 14.

The performance of the MMSE system comparing to ZF system depends on the value of variables V, $\frac{\xi}{rV_2}$. The selection of those system parameters would make MMSE to outperform ZF precoding in terms of SINR and capacity.

14.4 SYSTEM DEGRADATION DUE TO NON-RECIPROCITY

The system performance degradation due to channel non-reciprocity for both precodings can be retrieved by the factor *d* below:

$$d_{MMSE} = \frac{SINR_{MMSE-REC} - SINR_{MMSE-NON-REC}}{SINR_{MMSE-REC}} \qquad (49)$$

$$\lim_{N\to\infty} SINR_{MMSE-REC}$$

$$= \frac{\left|\beta_U \mathbf{W_R^H}\widehat{\mathbf{H}}_{\mathbf{DL}}\widehat{\mathbf{H_{DL}}}^* \boldsymbol{\Lambda}\right|^2}{\mathbf{W_R^H}\mathbf{W_R} + \sum_{k\neq i}^{K}\left(\left(\beta_U \mathbf{W_R^H}\widehat{\mathbf{H}}_{\mathbf{DL}}\widehat{\mathbf{H_{DL}}}^* \boldsymbol{\Lambda}\right)\left(\beta_U \mathbf{W_R^H}\widehat{\mathbf{H}}_{\mathbf{DL}}\widehat{\mathbf{H_{DL}}}^* \boldsymbol{\Lambda}\right)^{\boldsymbol{H}}\right) + \sum_{l=1}^{L}\left(\left(\beta_U \mathbf{W_R^H}\widehat{\mathbf{H}}_{\mathbf{p}}\widehat{\mathbf{H_p}}^* \boldsymbol{\Lambda_p}\right)\left(\beta_U \mathbf{W_R^H}\widehat{\mathbf{H}}_{\mathbf{p}}\widehat{\mathbf{H_p}}^* \boldsymbol{\Lambda_p}\right)^{\boldsymbol{H}}\right)}$$

$$= \frac{V\left|\mathbf{W_R^H}\right|^2}{\mathbf{W_R^H}\mathbf{W_R} + \boldsymbol{V}\sum_{i\neq k}^{K}\left|\mathbf{W_R^H}\widehat{\mathbf{H}}_{\mathbf{DL}}\widehat{\mathbf{H_{DL}}}^*\right|^2 + \sum_{l=1}^{L}\left(\left(\beta_p \mathbf{W_R^H}\widehat{\mathbf{H}}_{\mathbf{p}}\widehat{\mathbf{H_p}}^* \boldsymbol{\Lambda_p}\right)\left(\beta_p \mathbf{W_R^H}\widehat{\mathbf{H}}_{\mathbf{p}}\widehat{\mathbf{H_p}}^* \boldsymbol{\Lambda_p}\right)^{\boldsymbol{H}}\right)}$$

$$= \frac{V\left|\mathbf{W_R^H}\right|^2}{\mathbf{W_R^H}\mathbf{W_R} + \boldsymbol{V}\sum_{k\neq i}^{K}\left|\mathbf{W_R^H}\widehat{\mathbf{H}}_{\mathbf{DL}}\widehat{\mathbf{H_{DL}}}^*\right|^2 + V_P L\left|\mathbf{W_R^H}\widehat{\mathbf{H}}_{\mathbf{p}}\widehat{\mathbf{H_p}}^*\right|^{\mathbf{2}}} =$$

(50)

$$\lim_{N\to\infty} SINR_{MMSE-NON-REC} = (51)$$

(51)

The eqations (50), (51) for MMSE degradation appear in APPENDIX 5 of Chapter 14.

For ZF precoding system performance degradation is given below:

$$d_{ZF} = \frac{SINR_{ZF-REC} - SINR_{ZF-NON-REC}}{SINR_{ZF-REC}}$$

$$\lim_{N\to\infty} SINR_{ZF-REC} = \frac{\left|\mathbf{W_R^H}\right|^2}{\mathbf{W_R^H}\mathbf{W_R} + \sum_{k\neq i}^{K}\left|\mathbf{W_R^H}\right|^2 + \frac{\boldsymbol{\xi}}{\boldsymbol{r}}\sum_{l=1}^{L}\left(\left(\mathbf{W_R^H}\widehat{\mathbf{H}}_{\mathbf{p}}\widehat{\mathbf{H_p}}^{\mathbf{H}}\right)\left(\mathbf{W_R^H}\widehat{\mathbf{H}}_{\mathbf{p}}\widehat{\mathbf{H_p}}^{\mathbf{H}}\right)^{\boldsymbol{H}}\right)}$$

(52)

$$\lim_{N\to\infty} SINR_{ZF-NON-REC=}(53)$$

(53)

The equations (52), (53) for ZF degradation appear in APPENDIX 6 of Chapter 14.

14.4. CONCLUSION

This research work studied the performance of linearly precoded time division duplex Multi User-Multiple Input Multiple Output (MIMO) OFDM Cognitive Radio Network under imperfect CSI and non-reciprocal channels (NRC) covering transceiver frequency response non-reciprocity and antenna mutual coupling mismatches at the Secondary Network Base Station (BS), Secondary User Equipment (UE) and between the secondary network and the Primary Users is studied in this research work [1]. ZF and MMSE precoding are considered. Since perfect CSI is difficult to achieve [210], and although the study of Massive MIMO in CRN for non-reciprocal channels currently starts to attract the interest of research community e.g. machine learning and generic models [211], this research work studied and introduced closed-form expressions for performance degradation regarding the effective signal to interference plus noise ratios and corresponding channel capacity is essential for channel estimation period optimization so to increase network's performance.

Chapter 15

RADIO ENVIRONMENT MAPS FOR 5G COGNITIVE RADIO NETWORK AND CLOUD ENHANCEMENT

RADIO ENVIRONMENT MAPS FOR 5G CRN

Radio Environment Maps (REMs) have been introduced as a powerful tool in Cognitive Radio Networks to manage inter-transmitter interference. In the evolution of 5G heterogeneous ecosystem REMs are forced to be transformed to a more powerful tool hosting the diverse needs of an immense network. This research work [223] reviews REMs and proposes an enhanced REM architecture for integration in the 5G network.

15.1 INTRODUCTION

Cognitive Radio technology was introduced to answer the spectrum scarcity problem by utilizing the unoccupied spectrum in time, frequency and space [11]. In Cognitive Radio Networks the unlicensed users also called and secondary users may occupy the spectrum if the licensed users also called primary users are not transmitting and if the interference they cause to the primary network is below a certain threshold. Secondary users can sense the spectrum for transmitting opportunities non-cooperatively or cooperatively. Many protocols have been introduced for CRNs for both scenarios with the cooperative schemes to achieve higher accuracy in most cases.

Radio Environment Maps concept was introduced to cooperatively collect, store and share information amongst the network users regarding the transmitter locations, spectrum usage maps, spectrum usage statistics in time and space, probabilistic models [224] and manage interference [225] [226]. Moreover REMs were introduced as more powerful tools to support CRN in its Cognitive Cycle of Radio Environment Awareness [227].

The immense 5G network would integrate a vast number of heterogeneous networks supporting an increasingly diverse set of services, applications and users from mobile users to IoT. In the meantime, on the quest for offloading the 5G users from spectrum management and thus reducing computation and energy consumption, REM arise as a collaborative tool residing in the network which efficient design would overcome the overhead required for its update and increase overall network's performance.

15.2 The REM Concept

REM was first introduced by [228] as an integrated database (Figure 15.1) that would store information locally or globally regarding spectrum usage, primary and secondary users transmission patterns, available channels, interference levels.

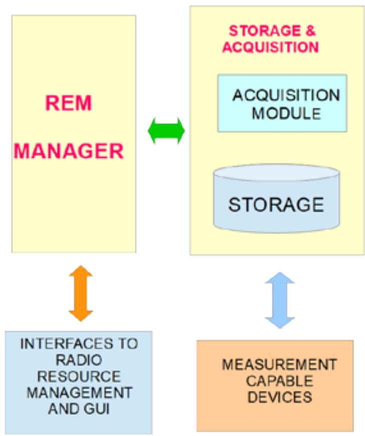

Figure 15.1: The Basic REM Structure

The basic REM architecture consists of the REM storage and Acquisition module which is responsible of collecting the reports of the measurement capable devices (MCDs) which can reconfigure and store the raw measurement data as well the output of the REM processes. The REM storage is a knowledge-based repository with spectrum occupancy information, the REM Manager is responsible for all the processing and REM generation and maintenance whilst the control application utilizes the REM information.

REM supports various CR applications such as i) hierarchical spectrum access, ii) spectrum sharing iii) intra-operator radio resource management iv) dedicated spectrum monitoring which is essential e.g. for intelligent transport systems, self-organizing networks [229] v) interference management. On the other hand the information stored in the the REM storage and acquisition module can be classified as long term information which is updated slowly or short information which is updated more frequently [229].

The REM construction consists of exploiting the reports received by the Measurement Capable Devices and the estimations of the signal levels in the areas where there no MCDs. The accuracy of the REM depends on the i) resolution ii) the quality of data iii) the construction method iv) the REM data update period. If the information stored in the REM is out-dated then the whole network's performance degrades.

The REM construction methods fall in three classes namely i) the direct methods (interpolation based) (Figure 15.2), ii) indirect (localization and propagation based) (Figure 15.3) iii) hydrid methods. In direct methods spatial interpolation is applied to the spatial RF- maps of the measured signals on a neighborhood basis. The most well-known direct methods are Inverse Distance Weighted (IDW), Nearest Neighbors (NN), splines, Natural Neighbors (NNI), modified Spepard's, Kriging, Gradient plus Inverse Distance Squared (GIDS). A survey on REM construction methods can be found in [229].

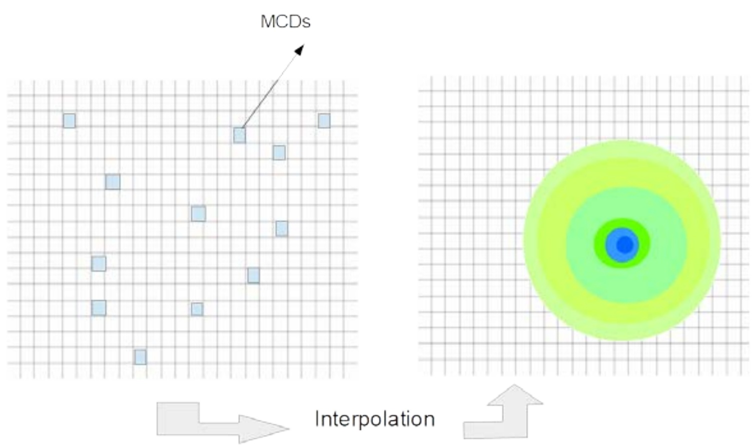

Figure 15.2: Direct RF-REM construction

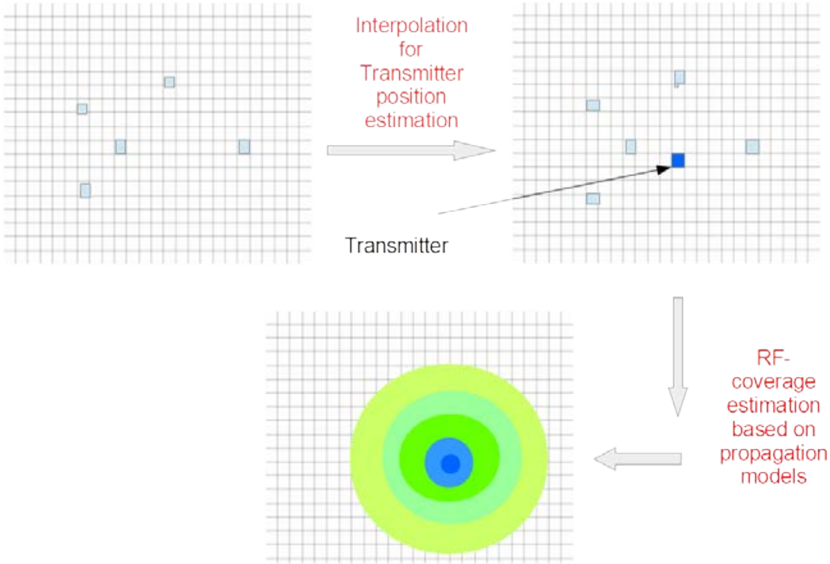

Figure 15.3: Indirect RF-REM construction

In indirect methods interpolation is applied to estimate the transmitter location and then the transmitter parameters and propagation models provided, the RF coverage at each pixel is estimated using the propagation model. There are two basic indirect methods i) LiVE and ii) SNR-aided method [8]. In LiVE method the received RF signal of the available MCDs are collected and then a propagation model is used to estimate the transmitter power and location in a least square optimization problem. The propagation model that would be selected is essential for this method. The SNR-aided method based on the angle of arrival (AoA), SNR data fusion and a propagation model constructs the REM around the transmitter [230]. In [231] an indirect self-tuning method was proposed. In [232] a hybrid approach combining transmitter localization and interpolation applied for urban Line of Site (LoS) and Non Line of Site (NLoS) environments. Transmitter localization methods have higher accuracy than interpolation methods in general. The authors in [233] propose a distributed Kalman filter to estimate position, velocity and power of transmitter. In [234] the Kriging interpolation method is improved and the model was evaluated in urban areas.

15.3 REM IN 5G

REM construction is a complex process integrating the transmitters' information, propagation models selection, interpolation methods selection, exploiting the available MCDs capabilities, mobility, the RF coverage maps, the cognitive radio spectrum management and in the same time perceiving the past experience into the Cognitive Radio Cycle of observing the environment, orienting, planning, designing, acting. Not only that but other issues have to be considered such as spectrum sharing policies, national and cross-border regulations, operator and cross-operator policies which govern the spectrum management process.

In the necessity of a layered REM model was exploited at [235] and at [231] in a heterogeneous LTE architecture of macrocells and femtocells based on the coverage maps. In [234] a study of application of REM in urban areas is presented addressing the issues that affect the RF-coverage in urban areas such as location, interference, fading, time.

In the vast heterogeneous 5G network the REM deployment should keep up-to-date the long and short term information in order to efficiently support the network and maintain the data rates, latency, QoE required levels of performance.

Thus, the following aspects arise:

- REM deployment close to network nodes to handle fast changing information, receive the MCDs reports, react to the local RF environment situations exploiting local powerful nodes or the RAN.
- REM deployment not close to network nodes to handle slowly changing information which can reside in the core network and the cloud.
- REM deployment to handle mobility
- REM deployment to handle cooperation between heterogeneous networks
- REM deployment to handle inter-operator functionality

The issues which will arise each time e.g. the intensive interpolation processing, the transmitter localization, a change in the number of available MCDs, a change in the propagation model would be pass to the REM in the core network or the cloud or be handled locally on a periodic basis, on demand or as emergencies.

In [11] the authors propose a REM architecture aligned with the RAN virtualization concept which considers Network Function Virtualization and an SDN- 5G network. Network Function Virtualization allows the network resources to be seen as pool of virtual resources that can be managed by physical or virtual operators. The SDN controller forces the decisions to the network. The proposed architecture mainly consists of the abstraction models such as interference maps which are used for short-term spectrum management, the REM and repository of regulations. The Spectrum Manager Application (SMA) will receive the information of the abstraction models which eventually will pass to REM and will be used on demand. The SMA will rely on different databases and the REM.

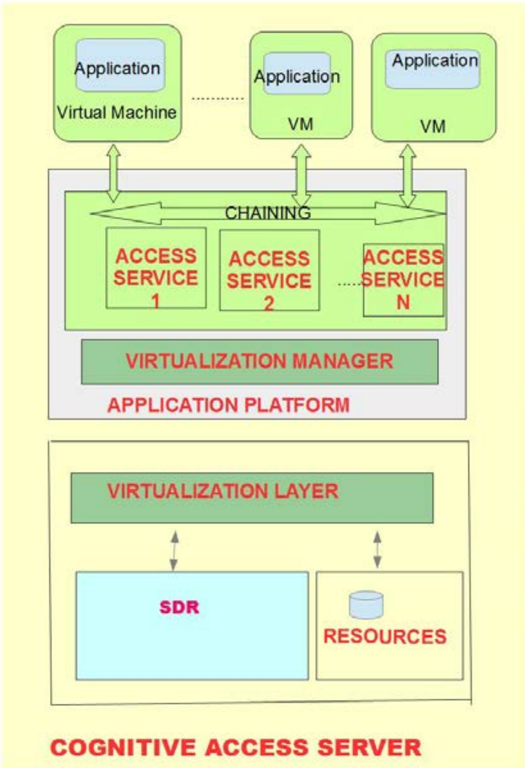

Figure 15.4: The Cognitive Access Server for the REM Deployment

Network Function Virtualization and SDN networks can be supportive in REM deployment. In [11] the cognitive radio functionality is offloaded at the Radio Access

Network (RAN) or at the local powerful nodes in the form of access services provision for the Cognitive Radio Network by virtualizing the lower layer's functionality and resources and leveraging the connection to the core network and the Cloud connection. Lower layer Cognitive Radio Services and applications on the Edge Computing would increase capabilities not only within the RAN but within local mobile network on a peer-to-peer basis for access and backhauling. In the latter case, ad-hoc networks or vehicles would leverage powerful local nodes allowing them to be self-organized [11]. REM as a chained-service would benefit of the proposed architecture deployment as the MCDs would pass their reports to more powerful nodes and the REM deployment will be served by the proposed architecture in [11] (Figure 15.4 and Figure 15.5). However, as REM management encompasses national, regional and inter-operator policies and regulations, the necessity for new services arise for cross-operator, cross-border operability, QoE provision. For this reason an enhancement of the architecture [11] is proposed.

15.4 Enhanced REM Deployment

In order the REM deployment to respond to 5G challenges the provision of enhanced and abstract services on the top of the NFV chained services [11] arise. So, the NFV chained-services abstraction layer would be the basis for new abstract services composition. On the top of service orchestration layer would provide entries to the new services taking also into account the policies, regulations, required level of performance and security issues. The abstract layers would allow operability between the heterogeneous networks, mobile nodes, cross-operators, QoS and QoE assurance as will make feasible the sharing and processing of virtual resources across the immense 5G network (Figure 15.6).

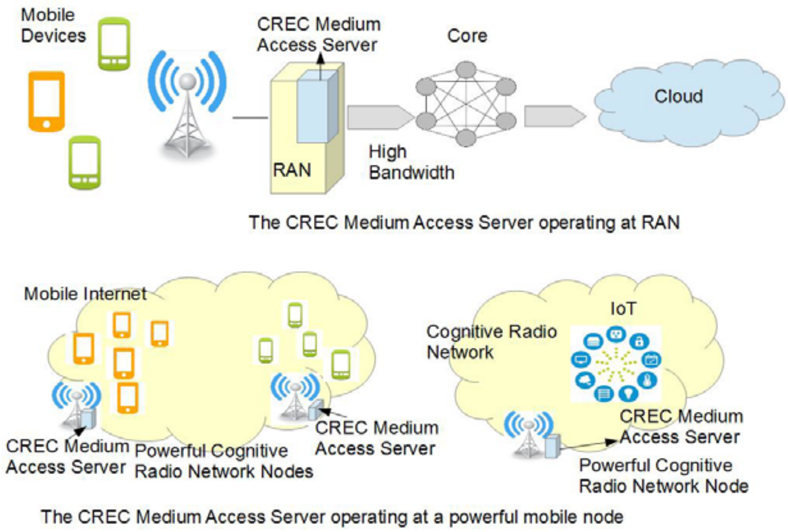

Figure 15.5: Cognitive Access Server deployment for the REM

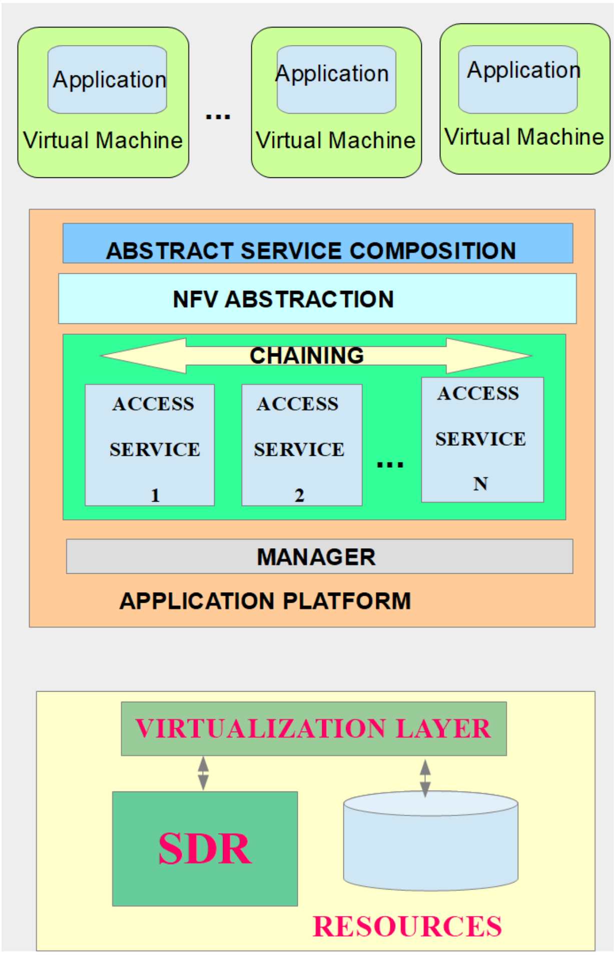

Figure 15.6: The Enhanced Cognitive Access Server for the REM deployment

Abstract service scenarios would exploit the radio elements, radio scene, environment and trigger the chaining of NFV services applicable for each operator, heterogeneous network etc. Concerning the Abstract Radio Environment Maps services, they would specify amongst others different REM construction method for each network or operator, araise mobility support, define REM update frequency, REM image processing for information extraction, QoE, data mining for cloud storage, define the number of MCDs, and consider policies and regulations. The Abstarct REM Services Composition would ensure transparency for heterogeneous networks, cross-operator, cross-border etc. The architecture would be enabled within the SDN context.

15.5 CONCLUSION

The research work discusses the various issues of Radio Environment Maps construction and application and proposes the architecture [11] based on NFV and SDN network and an enhanced architecture of [11] for REM deployment in the 5G heterogeneous network, cross-operator, cross-border. The proposed architecture takes into consideration the creation of new abstract services for cross-operator, cross-network operability and high level of QoE required in the immense and diverse 5G ecosystem.

CONCLUSION

COGNITIVE RADIO NETWORK AND COGNITIVE RADIO NETWORK CLOUD

The necessity of lower layers services and applications conceptualization and abstraction up to the seven layer OSI stack within the Cognitive Radio Cycle is the main issue that this dissertation manifests whilst providing algorithms for responding to diverse issues within the Cognitive Radio Network and Cognitive Radio Network Cloud.

Demanding tasks could be off-loaded to powerful nodes locally allowing the local network to be self-organized. Self-organizing Cognitive Radio Networks in an immense heterogeneous wireless network along with Dynamic Spectrum Access, Management and Control Mitigation on demand or not on demand to respond to network needs in real time and on the fly can be realized with high level abstraction and conceptualization of Cognitive Medium Access Control and SDR Services and Abstract Cognitive Medium Access Control and SDR Services integration and deployment on all the OSI layers, cross-platform and cross-network, cross-operator. Central coordination would be applicable for triggering local nomad network to be self-organized, as well for hand-off or for meeting QoE, radio network performance, institutional metrics.

Most of the research work presented in this dissertation has been published and the rest is considered for submission.

A new mathematic method of mathematic game unfolding is introduced i.e. a new mathematic method for generating games without coordination and a corresponding mathematic game model as an application of the proposed mathematic method to for the Cognitive Radio Network and Cognitive Radio Cloud Security was introduced. Other mathematic game reaching Nash Equilibriums also were introduced. Deterministic automata and Machine Learning were also introduced as well as other mathematic formulas applicable to the corresponding network protocols, mathematic models for steady-state-Lyapunov filtering algorithm for enhanced CRN-SDR signal processing and mathematic formulas for Non-Reciprocal Channels in Massive MIMO CRN were also introduced in this dissertation.

This dissertation contributes to the Cognitive Radio research field by introducing a novel concept and a reference architecture for Cognitive Radio Medium Access Control and SDR as a Service and Application conseptualisation and abstraction utilizing the Cognitive Radio Network Cloud and allowing self-organized clusters to operate in a dynamic manner allowing nomadic lower layers Services and Application clustering and providing the CRN and CRNC with the desired transparency which is considered as the basis for the 5G, 6G , Space-Air-Ground-Sea integrated communication and wireless tactile network evolution . Mathematic methods and mathematic formulas have been introduced for a number of diverse CRNC problems, too.

$$(27) \rightarrow \frac{1}{c_{1,n}} \geq 1 + \frac{\left(a_{j.1.n}^{glo} + c_n - 2a_{j.1.n}^{glo}c_n - a_{j.1.n}^{glo}a_{i.1.n}^{lo} - a_{j.1.n}^{glo}a_{i.2.n}^{lo}\right)\rho_{1.n}^{lo} + \left(2a_{j.2.n}^{glo}a_{i.1.n}^{lo} - a_{j.1.n}^{glo}a_{i.1.n}^{lo} - a_{j.1.n}^{glo}a_{i.2.n}^{lo} + a_{j.1.n}^{glo}a_{i.2.n}^{lo} - 1 - c_n\right)\rho_{2.n}^{lo}}{\left(2\alpha_{j,1,n}^{glo}a_{i.1.n}^{lo} - a_{i.1.n}^{lo} - c_n\right)\rho_{1.n}^{glo} + \left(1 + 2\alpha_{j.1.n}^{glo} + \alpha_{i.2.n}^{lo} + \alpha_{j.2.n}^{glo} - 2\alpha_{j.1.n}^{glo}\right)\rho_{2.n}^{glo}}$$

$$(28) \rightarrow \frac{1}{c_{1,n}} \geq 1 + \frac{\left(2\alpha_{j.1.t}^{g;o}\alpha_{i.1.t}^{lo} + 2\alpha_{j.1.t}^{glo}c_t + \alpha_{i.2.t}^{lo} - \alpha_{j.1.t}^{glo} - \alpha_{i.1.t}^{lo} - c_t\right)\rho_{1.t}^{lo} + \left(1 + \alpha_{j.1.t}^{glo}\alpha_{i.1.t}^{lo} + \alpha_{j.1.t}^{glo}\alpha_{i.2.t}^{lo} + c_t - 2\alpha_{j.1.t}^{glo}c_t - \alpha_{i.2.t}^{lo} - \alpha_{j.1.t}^{glo} - \alpha_{j.2.t}^{glo}\right)\rho_{2.t}^{lo}}{\left(1 + c_t - 2\alpha_{j.1.t}^{glo}\alpha_{\iota.1.\tau}^{lo} - 2\alpha_{j.2.t}^{glo}c_t - \alpha_{j.2.t}^{glo}\right)\rho_{1.t}^{glo} + \left(3\alpha_{i.2.t}^{lo} + 2\alpha_{j.2.t}^{glo}c_t - 2 - 2\alpha_{j.1.t}^{glo}c_t - \alpha_{j.1.t}^{glo} - \alpha_{j.1.t}^{glo}\alpha_{i.2.t}^{lo}\right)\rho_{2.t}^{glo}}$$

$$(29) \rightarrow \frac{1}{c_{1,n}} \geq 1 + \frac{\left(1 + \alpha_{j.1.t}^{glo}\alpha_{i.1.t}^{lo} + 2\alpha_{j.1.t}^{glo}\alpha_{i.2.t}^{lo} + \alpha_{j.1.t}^{glo}c_t + \alpha_{j.2.t}^{glo}\alpha_{i.2.t}^{lo} - 2\alpha_{j.1.t}^{glo} - 2\alpha_{i.2.t}^{lo} - \alpha_{j.2.t}^{glo}c_t\right)\rho_{1.t}^{lo} + \left(1 + 3\alpha_{j.1.t}^{glo}\alpha_{i.2.t}^{lo} + \alpha_{j.1.t}^{glo}\alpha_{\iota.1.\tau}^{\lambda o} - 2\alpha_{j.1.t}^{glo} - 2\alpha_{i.2.t}^{lo}\right)\rho_{2.t}^{lo}}{\left(2\alpha_{j.1.t}^{glo} - 2\alpha_{j.1.t}^{glo}\alpha_{i.2.t}^{lo} - 2\alpha_{j.1.t}^{glo}\alpha_{i.1.t}^{lo} - \alpha_{j.1.t}^{glo}c_t\right)\rho_{1.t}^{glo} + \left(4\alpha_{i.2.t}^{lo} + c_t + \alpha_{j.1.t}^{glo} - 3\alpha_{j.1.t}^{glo}\alpha_{i.2.t}^{lo} - \alpha_{j.2.t}^{glo}\alpha_{i.2.t}^{lo} - \alpha_{j.1.t}^{glo}c_t - 2\right)\rho_{2.t}^{glo}}$$

Table 1: The conditions derived for the proposed scheme

APPENDIX 2

The code in Matlab for the simulated generated signal in Rayleigh fading conditions.

```
Ts=1/Fs;
S1o=1;
So=16;
fd=100;
tstart=0;
tend=2;
%t=[tstart:Ts:tend];
wm=2*pi*fd;                        %Maximum shift
fm=wm/(2*pi);                      %Doppler shift
S=2*(2*So+1);
X1co=(1.414*cos(wm*t));
X1so=0;



wm=2*pi*fd;                        %Maximum shift
fm=wm/(2*pi);                      %Doppler shift
S=2*(2*So+1);
Xco=(1.414*cos(wm*t));
Xso=0;



for n=1:1:So
A(n)=(2*pi*n)/S;                %Azimuthal angles
wn(n)=wm*cos(A(n));
O(n)=(pi*n)/(So+1);
sum3=sum3+(cos(O(n)).*cos(wn(n)*t));
sum4=sum4+(cos(wn(n)*t).*sin(O(n)));
end
Xc=2*sum3+Xco;
Xs=2*sum4+Xso;
sig2=(1/sqrt(2*So+1))*(Xc+j*Xs);
```

The code in Matlab for the simulated generated signals in Nakagami fading conditions.

```
M1=3;
m1=3;
M=3;
m=3;
gpsk=(sin(pi/M))^2;
gamasr_dB=[1:0.1:50];
gpsk1=(sin(pi/M1))^2;
u=1;


m=randi([3 7],1,1);

gamasr(h)=10.^(gamasr_dB(h)/10);
alfa(h)=sqrt((gpsk.*gamasr(h)/m)/(1+(gpsk.*gamasr(h)/m)))*cot(pi/M);
K(h)=(1/pi)*sqrt((gpsk.*gamasr(h)/m)/(1+gpsk.*gamasr(h)/m));


suma1=0;
for k=0:(m-1)
 suma1=suma1 +(factorial(2*k)/(factorial(k)^2))*1/(4*(1+(gpsk.*gamasr(h)/m))^k);
 end;


suma2=0;
for k=1:(m-1)
for i=1:k
T(i)=(factorial(2*k)/(factorial(k)^2))/(factorial(2*(k-i))/(((factorial(k-i))^2)*(4^i)*(2*(k-
i)+1)));
BR(i)=T(i)*(cos(atan(alfa(h))))^(2*(k-i)+1);
end;
suma2=suma2+BR(i)/(1+gpsk.*gamasr(h)/m)^k;
end;
 Ps(h)=((M-1)/M)-K(h)*((pi/2+atan(alfa(h)))*suma1+sin(atan(alfa(h))*suma2));
Pb(h)=Ps(h)/log2(M);


sig2=Pb(h);
```

APPENDIX 3

$$R_{MMSE} = \mathbb{E}\{\log_2(1 + SINR_{MMSE})\} = (36)$$

$$= \mathbb{E}\left\{ \log_2\left(1 + \frac{(1-\alpha)\left|\beta_U \mathbf{W_R^H G_U^{-1}} \boldsymbol{\Lambda}\right|^2}{\mathbf{W_R^H W_R} + \left|\beta_U \mathbf{W_R^H G_U^{-1} \widehat{\widehat{H}}_{DL}} (\boldsymbol{G'_B}) \widehat{\mathbf{H_{DL}}}^* \boldsymbol{\Lambda}\right|^2 + \sum_{i\neq k}^{K} \left|\beta_U \mathbf{W_R^H G_U^{-1}} \boldsymbol{\Lambda}\right|^2 + \sum_{i\neq k}^{K} \left|\beta_U \mathbf{W_R^H G_U^{-1} \widehat{\widehat{H}}_{DL}} (\boldsymbol{G'_B}) \widehat{\mathbf{H_{DL}}}^* \boldsymbol{\Lambda}\right|^2 + \sum_{l=1}^{L} \left|\beta_\upsilon \mathbf{W_R^H G_U^{-1} \widehat{\widehat{H}}_p} \widehat{\mathbf{H_p}}^* \boldsymbol{\Lambda_p}\right|^2 + \sum_{l=1}^{L} \left|\beta_\upsilon \mathbf{W_R^H G_U^{-1} \widehat{\widehat{H}}_p} (\boldsymbol{G'_{p,B}}) \widehat{\mathbf{H_p}}^* \boldsymbol{\Lambda_p}\right|^2}\right)\right\}$$

$$= \mathbb{E}\left\{ \log_2\left(1 + \frac{(1-\alpha)\left|\beta_U \mathbf{W_R^H} \boldsymbol{\Lambda}\right|^2}{\mathbf{W_R^H W_R} + \left|\beta_U \mathbf{W_R^H G_U^{-1} \widehat{\widehat{H}}_{DL}} (\boldsymbol{G'_B}) \widehat{\mathbf{H_{DL}}}^* \boldsymbol{\Lambda}\right|^2 + \sum_{i\neq k}^{K} \left|\beta_U \mathbf{W_R^H G_U^{-1}} \boldsymbol{\Lambda}\right|^2 + \sum_{i\neq k}^{K} \left|\beta_U \mathbf{W_R^H G_U^{-1} \widehat{\widehat{H}}_{DL}} (\boldsymbol{G'_B}) \widehat{\mathbf{H_{DL}}}^* \boldsymbol{\Lambda}\right|^2 + + \sum_{l=1}^{L} \left|\beta_\upsilon \mathbf{W_R^H G_U^{-1} \widehat{\widehat{H}}_p} \widehat{\mathbf{H_p}}^* \boldsymbol{\Lambda_p}\right|^2 + \sum_{l=1}^{L} \left|\beta_\upsilon \mathbf{W_R^H G_U^{-1} \widehat{\widehat{H}}_p} (\boldsymbol{G'_{p,B}}) \widehat{\mathbf{H_p}}^* \boldsymbol{\Lambda_p}\right|^2}\right)\right\}$$

$$R_{ZF} = \mathbb{E}\{\log_2(1 + SINR_{ZF})\} = (40) =$$

$$= \mathbb{E}\left\{ (1-\alpha)\ \log_2\left(1 + \frac{\left|\mathbf{W_R^H G_U^{-1} \widehat{\widehat{H}}_{DL}} \widehat{\mathbf{H_{DL}}}^{\mathbf{H}} \left(\widehat{\mathbf{H_{DL}}} \ \ \widehat{\mathbf{H_{DL}}}^{\mathbf{H}}\right)^{-1}\right|^2}{\mathbf{W_R^H W_R} + \left|\mathbf{W_R^H G_U^{-1} \widehat{\widehat{H}}_{DL}} \boldsymbol{G'_B} \widehat{\mathbf{H_{DL}}}^{\mathbf{H}} \left(\widehat{\mathbf{H_{DL}}} \ \ \widehat{\mathbf{H_{DL}}}^{\mathbf{H}}\right)^{-1}\right|^2 + \mathbf{W_R^H} \sum_{I\neq k}^{K} \left|\mathbf{G_U^{-1} \widehat{\widehat{H}}_{DL}} \widehat{\mathbf{H_{DL}}}^{\mathbf{H}} \left(\widehat{\mathbf{H_{DL}}} \ \ \widehat{\mathbf{H_{DL}}}^{\mathbf{H}}\right)^{-1}\right|^2 + \sum_{i\neq k}^{K} \left|\mathbf{W_R^H G_U^{-1} \widehat{\widehat{H}}_{DL}} \boldsymbol{G'_B} \widehat{\mathbf{H_{DL}}}^{\mathbf{H}} \left(\widehat{\mathbf{H_{DL}}} \ \ \widehat{\mathbf{H_{DL}}}^{\mathbf{H}}\right)^{-1}\right|^2 + \sum_{l=1}^{L} \left|\mathbf{W_R^H G_{,U}^{-1} \widehat{\widehat{H}}_p} \widehat{\mathbf{H_p}}^{\mathbf{H}} \left(\widehat{\mathbf{H_p}} \ \ \widehat{\mathbf{H_p}}^{\mathbf{H}}\right)^{-1}\right|^2 + \sum_{l=1}^{L} \left|\mathbf{W_R^H G_{,U}^{-1} G_{,U}^{-1} \widehat{\widehat{H}}_p G'_{\mathit{p}}} \widehat{\mathbf{H_p}}^{\mathbf{H}} \left(\widehat{\mathbf{H_p}} \ \ \widehat{\mathbf{H_p}}^{\mathbf{H}}\right)^{-1} \mathbf{x}_p\right|^2}\right)\right\}$$

APPENDIX 4

$$\lim_{N\to\infty}\frac{R_{MMSE}}{R_{ZF}}=\frac{(1-\alpha)\log_2(1+SNR_{MMSE})}{(1-\alpha)\log_2(1+SNR_{ZF})}=$$

$$=\frac{(1-\alpha)\log_2\left(1+\frac{\left|\mathbf{W_R^H}\mathbf{G_U^{-1}}V\right|^2}{\mathbf{W_R^H}\mathbf{W_R}+V\left|\mathbf{W_R^H}\frac{\xi}{r}\mathbf{G_U^{-1}}\widehat{\widehat{\mathbf{H}}}_{\mathbf{DL}}(\boldsymbol{G'}_{\boldsymbol{B}})\overline{\widehat{\mathbf{H}}_{\mathbf{DL}}}^{*}\boldsymbol{\Lambda}\right|^2+\sum_{i\neq k}^{K}\left|\mathbf{W_R^H}\mathbf{G_U^{-1}}V\right|^2+\sum_{i\neq k}^{K}V\left|\mathbf{W_R^H}\frac{\xi}{r}\mathbf{G_U^{-1}}\widehat{\widehat{\mathbf{H}}}_{\mathbf{DL}}(\boldsymbol{G'}_{\boldsymbol{B}})\overline{\widehat{\mathbf{H}}_{\mathbf{DL}}}^{*}\boldsymbol{\Lambda}\right|^2+\sum_{l=1}^{L}\left|\beta_p\mathbf{W_R^H}\mathbf{G_U^{-1}}\widehat{\widehat{\mathbf{H}}}_{\mathbf{p}}\overline{\widehat{\mathbf{H}}_{\mathbf{p}}}^{*}\boldsymbol{\Lambda_p}\right|^2+\beta_p\sum_{l=1}^{L}\left|\frac{\boldsymbol{\xi_\pi}}{\boldsymbol{r_\pi}}\mathbf{W_R^H}\mathbf{G_U^{-1}}\widehat{\widehat{\mathbf{H}}}_{\mathbf{p}}(\boldsymbol{G'}_{\boldsymbol{p}})\overline{\mathbf{H}_{\mathbf{p}}}\boldsymbol{\Lambda_p}\right|^2}\right)}{(1-\alpha)\log_2\left(1+\frac{\left|\mathbf{W_R^H}\mathbf{G_U^{-1}}\widehat{\widehat{\mathbf{H}}}_{\mathbf{DL}}\overline{\widehat{\mathbf{H}}_{\mathbf{DL}}}^{\mathbf{H}}\left(\overline{\widehat{\mathbf{H}}_{\mathbf{DL}}}\ \ \overline{\widehat{\mathbf{H}}_{\mathbf{DL}}}^{\mathbf{H}}\right)^{-1}\right|^2}{\mathbf{W_R^H}\mathbf{W_R}+\left|\mathbf{W_R^H}\mathbf{G_U^{-1}}\widehat{\widehat{\mathbf{H}}}_{\mathbf{DL}}\boldsymbol{G'}_{\boldsymbol{B}}\overline{\widehat{\mathbf{H}}_{\mathbf{DL}}}^{\mathbf{H}}\left(\overline{\widehat{\mathbf{H}}_{\mathbf{DL}}}\ \ \overline{\widehat{\mathbf{H}}_{\mathbf{DL}}}^{\mathbf{H}}\right)^{-1}\right|^2+\mathbf{W_R^H}\sum_{l\neq k}^{K}\left|\mathbf{G_U^{-1}}\widehat{\widehat{\mathbf{H}}}_{\mathbf{DL}}\overline{\widehat{\mathbf{H}}_{\mathbf{DL}}}^{\mathbf{H}}\left(\overline{\widehat{\mathbf{H}}_{\mathbf{DL}}}\ \ \overline{\widehat{\mathbf{H}}_{\mathbf{DL}}}^{\mathbf{H}}\right)^{-1}\right|^2+\sum_{i\neq k}^{K}\left|\mathbf{W_R^H}\mathbf{G_U^{-1}}\widehat{\widehat{\mathbf{H}}}_{\mathbf{DL}}\boldsymbol{G'}_{\boldsymbol{B}}\overline{\widehat{\mathbf{H}}_{\mathbf{DL}}}^{\mathbf{H}}\left(\overline{\widehat{\mathbf{H}}_{\mathbf{DL}}}\ \ \overline{\widehat{\mathbf{H}}_{\mathbf{DL}}}^{\mathbf{H}}\right)^{-1}\right|^2+\sum_{l=1}^{L}\left|\mathbf{W_R^H}\mathbf{G_{,U}^{-1}}\widehat{\mathbf{H}}_{\mathbf{p}}\overline{\widehat{\mathbf{H}}_{\mathbf{p}}}^{\mathbf{H}}\left(\overline{\widehat{\mathbf{H}}_{\mathbf{p}}}\ \ \overline{\widehat{\mathbf{H}}_{\mathbf{p}}}^{\mathbf{H}}\right)^{-1}\right|^2+\sum_{l=1}^{L}\left|\mathbf{W_R^H}\mathbf{G_{,U}^{-1}}\widehat{\mathbf{H}}_{\mathbf{p}}\mathbf{G'}_{\boldsymbol{p}}\overline{\widehat{\mathbf{H}}_{\mathbf{p}}}^{\mathbf{H}}\left(\overline{\widehat{\mathbf{H}}_{\mathbf{p}}}\ \ \overline{\widehat{\mathbf{H}}_{\mathbf{p}}}^{\mathbf{H}}\right)^{-1}\right|^2}\right)}$$

(44)

$$\lim_{N\to\infty}SINR_{MMSE}=\frac{V\left|\mathbf{W_R^H}\mathbf{G_U^{-1}}\right|^{\mathbf{2}}}{\mathbf{W_R^H}\mathbf{W_R}+V\left|\mathbf{W_R^H}\mathbf{G_U^{-1}}\widehat{\widehat{\mathbf{H}}}_{\mathbf{DL}}(\boldsymbol{G'}_{\boldsymbol{B}})\overline{\widehat{\mathbf{H}}_{\mathbf{DL}}}^{*}\right|^2+\sum_{i\neq k}^{K}\left|\mathbf{W_R^H}\mathbf{G_U^{-1}}V\right|^2+\sum_{i\neq k}^{K}V\left|\mathbf{W_R^H}\frac{\xi}{r}\mathbf{G_U^{-1}}\widehat{\widehat{\mathbf{H}}}_{\mathbf{DL}}(\boldsymbol{G'}_{\boldsymbol{B}})\overline{\widehat{\mathbf{H}}_{\mathbf{DL}}}^{*}\boldsymbol{\Lambda}\right|^2++V_P L\left|\mathbf{W_R^H}\mathbf{G_U^{-1}}\widehat{\widehat{\mathbf{H}}}_{\mathbf{p}}\overline{\widehat{\mathbf{H}}_{\mathbf{p}}}^{*}\right|^{\mathbf{2}}+\frac{\boldsymbol{\xi_p}}{\boldsymbol{r_p}V_{p_2}}\sum_{l=1}^{L}\left|\mathbf{W_R^H}\mathbf{G_U^{-1}}\ \widehat{\widehat{\mathbf{H}}}_{\mathbf{p}}(\boldsymbol{G'}_{\boldsymbol{p}})\overline{\widehat{\mathbf{H}}_{\mathbf{p}}}^{*}\right|^2}$$

(45)

Where $V_1=\frac{\xi}{r}\frac{\left(\sqrt{\mathrm{Pu}}-\mathrm{M}\right)^2}{\mathrm{Pu}}\sqrt{\frac{\mathrm{K}}{\mathrm{P_{max}}}}$, $V_2=\frac{\xi}{r}\frac{\left(\sqrt{\mathrm{Pu}}-\mathrm{M}\right)^4}{\mathrm{Pu}^2}+\frac{\mathrm{K}}{\mathrm{P_{max}}_{\mathrm{K}}}$, $V_3=\frac{\left(\sqrt{\mathrm{Pu}}-\mathrm{M}\right)^4}{\mathrm{Pu}^2}+\frac{\mathrm{K}}{\mathrm{P_{max}}}$, $V=\frac{V_1}{V_2V_3}$

$$\lim_{N\to\infty} SINR_{ZF}$$

$$= \frac{\left|\mathbf{W}_\mathbf{R}^\mathbf{H}\mathbf{G}_\mathbf{U}^{-1}\right|^2}{\mathbf{W}_\mathbf{R}^\mathbf{H}\mathbf{W}_\mathbf{R} + \left|\mathbf{W}_\mathbf{R}^\mathbf{H}\mathbf{G}_\mathbf{U}^{-1}\widehat{\mathbf{H}}_\mathbf{DL}\boldsymbol{G'}_{\boldsymbol{B}}\widehat{\widehat{\mathbf{H}}_\mathbf{DL}}^\mathbf{H}\left(\widehat{\widehat{\mathbf{H}}_\mathbf{DL}}\ \ \widehat{\widehat{\mathbf{H}}_\mathbf{DL}}^\mathbf{H}\right)^{-1}\right|^2 + \mathbf{W}_\mathbf{R}^\mathbf{H}\sum_{l\neq k}^{K}\left|\mathbf{G}_\mathbf{U}^{-1}\widehat{\mathbf{H}}_\mathbf{DL}\widehat{\widehat{\mathbf{H}}_\mathbf{DL}}^\mathbf{H}\left(\widehat{\widehat{\mathbf{H}}_\mathbf{DL}}\ \ \widehat{\widehat{\mathbf{H}}_\mathbf{DL}}^\mathbf{H}\right)^{-1}\right|^2 + \sum_{i\neq k}^{K}\left|\mathbf{W}_\mathbf{R}^\mathbf{H}\mathbf{G}_\mathbf{U}^{-1}\widehat{\mathbf{H}}_\mathbf{DL}\boldsymbol{G'}_{\boldsymbol{B}}\widehat{\widehat{\mathbf{H}}_\mathbf{DL}}^\mathbf{H}\left(\widehat{\widehat{\mathbf{H}}_\mathbf{DL}}\ \ \widehat{\widehat{\mathbf{H}}_\mathbf{DL}}^\mathbf{H}\right)^{-1}\right|^2 + \sum_{l=1}^{L}\left|\mathbf{W}_\mathbf{R}^\mathbf{H}\mathbf{G}_\mathbf{U}^{-1}\ \widehat{\mathbf{H}}_\mathbf{p}\widehat{\widehat{\mathbf{H}}_\mathbf{p}}^\mathbf{H}\left(\widehat{\widehat{\mathbf{H}}_\mathbf{p}}\ \ \widehat{\widehat{\mathbf{H}}_\mathbf{p}}^\mathbf{H}\right)^{-1}\right|^2 + \sum_{l=1}^{L}\left|\mathbf{W}_\mathbf{R}^\mathbf{H}\mathbf{G}_\mathbf{U}^{-1}\ \widehat{\mathbf{H}}_\mathbf{p}\mathbf{G'}_{\boldsymbol{p}}\widehat{\widehat{\mathbf{H}}_\mathbf{p}}^\mathbf{H}\left(\widehat{\widehat{\mathbf{H}}_\mathbf{p}}\ \ \widehat{\widehat{\mathbf{H}}_\mathbf{p}}^\mathbf{H}\right)^{-1}\right|^2}$$

$$= \frac{\left|\mathbf{W}_\mathbf{R}^\mathbf{H}\mathbf{G}_\mathbf{U}^{-1}\right|^2}{\mathbf{W}_\mathbf{R}^\mathbf{H}\mathbf{W}_\mathbf{R} + \left|\mathbf{W}_\mathbf{R}^\mathbf{H}\mathbf{G}_\mathbf{U}^{-1}\widehat{\mathbf{H}}_\mathbf{DL}\boldsymbol{G'}_{\boldsymbol{B}}\widehat{\widehat{\mathbf{H}}_\mathbf{DL}}^\mathbf{H}\widehat{\widehat{\mathbf{H}}_\mathbf{DL}}^{\mathbf{H}^{-1}}\widehat{\widehat{\mathbf{H}}_\mathbf{DL}}^{-1}\right|^2 + \mathbf{W}_\mathbf{R}^\mathbf{H}\sum_{l\neq k}^{K}\left|\mathbf{G}_\mathbf{U}^{-1}\widehat{\mathbf{H}}_\mathbf{DL}\widehat{\widehat{\mathbf{H}}_\mathbf{DL}}^\mathbf{H}\left(\widehat{\widehat{\mathbf{H}}_\mathbf{DL}}\ \ \widehat{\widehat{\mathbf{H}}_\mathbf{DL}}^\mathbf{H}\right)^{-1}\right|^2 + \sum_{i\neq k}^{K}\left|\mathbf{W}_\mathbf{R}^\mathbf{H}\mathbf{G}_\mathbf{U}^{-1}\widehat{\mathbf{H}}_\mathbf{DL}\boldsymbol{G'}_{\boldsymbol{B}}\widehat{\widehat{\mathbf{H}}_\mathbf{DL}}^\mathbf{H}\left(\widehat{\widehat{\mathbf{H}}_\mathbf{DL}}\ \ \widehat{\widehat{\mathbf{H}}_\mathbf{DL}}^\mathbf{H}\right)^{-1}\right|^2 \sum_{l=1}^{L}\left|\mathbf{W}_\mathbf{R}^\mathbf{H}\ \mathbf{G}_\mathbf{U}^{-1}\widehat{\mathbf{H}}_\mathbf{p}\widehat{\widehat{\mathbf{H}}_\mathbf{p}}^\mathbf{H}\left(\widehat{\widehat{\mathbf{H}}_\mathbf{p}}\ \ \widehat{\widehat{\mathbf{H}}_\mathbf{p}}^\mathbf{H}\right)^{-1}\right|^2 + \sum_{l=1}^{L}\left|\mathbf{W}_\mathbf{R}^\mathbf{H}\mathbf{G}_\mathbf{U}^{-1}\widehat{\mathbf{H}}_\mathbf{p}\mathbf{G'}_{\boldsymbol{p}}\widehat{\widehat{\mathbf{H}}_\mathbf{p}}^\mathbf{H}\left(\widehat{\widehat{\mathbf{H}}_\mathbf{p}}\ \ \widehat{\widehat{\mathbf{H}}_\mathbf{p}}^\mathbf{H}\right)^{-1}\right|^2}$$

$$= \frac{\left|\mathbf{W}_\mathbf{R}^\mathbf{H}\mathbf{G}_\mathbf{U}^{-1}\right|^2}{\mathbf{W}_\mathbf{R}^\mathbf{H}\mathbf{W}_\mathbf{R} + \left|\mathbf{W}_\mathbf{R}^\mathbf{H}\mathbf{G}_\mathbf{U}^{-1}\ \widehat{\mathbf{H}}_\mathbf{DL}\boldsymbol{G'}_{\boldsymbol{B}}\widehat{\widehat{\mathbf{H}}_\mathbf{DL}}^{-1}\right|^2 + \mathbf{W}_\mathbf{R}^\mathbf{H}\sum_{l\neq k}^{K}\left|\mathbf{G}_\mathbf{U}^{-1}\widehat{\mathbf{H}}_\mathbf{DL}\widehat{\widehat{\mathbf{H}}_\mathbf{DL}}^\mathbf{H}\left(\widehat{\widehat{\mathbf{H}}_\mathbf{DL}}\ \ \widehat{\widehat{\mathbf{H}}_\mathbf{DL}}^\mathbf{H}\right)^{-1}\right|^2 + \sum_{i\neq k}^{K}\left|\mathbf{W}_\mathbf{R}^\mathbf{H}\mathbf{G}_\mathbf{U}^{-1}\widehat{\mathbf{H}}_\mathbf{DL}\boldsymbol{G'}_{\boldsymbol{B}}\widehat{\widehat{\mathbf{H}}_\mathbf{DL}}^\mathbf{H}\left(\widehat{\widehat{\mathbf{H}}_\mathbf{DL}}\ \ \widehat{\widehat{\mathbf{H}}_\mathbf{DL}}^\mathbf{H}\right)^{-1}\right|^2 + L\frac{\boldsymbol{\xi_p}}{\boldsymbol{r_p}}\left|\mathbf{W}_\mathbf{R}^\mathbf{H}\ \mathbf{G}_\mathbf{U}^{-1}\widehat{\mathbf{H}}_\mathbf{p}\widehat{\widehat{\mathbf{H}}_\mathbf{p}}^\mathbf{H}\right|^2 + \frac{\boldsymbol{\xi_p}}{\boldsymbol{r_p}}\sum_{l=1}^{L}\left|\mathbf{W}_\mathbf{R}^\mathbf{H}\mathbf{G}_\mathbf{U}^{-1}\ \widehat{\mathbf{H}}_\mathbf{p}\mathbf{G'}_{\boldsymbol{p}}\widehat{\widehat{\mathbf{H}}_\mathbf{p}}^{-1}\right|^2}$$

(47)

$$\frac{\lim_{N\to\infty} SINR_{MMSE}}{\lim_{N\to\infty} SINR_{ZF}} = \frac{V\mathbf{W}_\mathbf{R}^\mathbf{H}\mathbf{W}_\mathbf{R} + V\left|\mathbf{W}_\mathbf{R}^\mathbf{H}\mathbf{G}_\mathbf{U}^{-1}\ \widehat{\mathbf{H}}_\mathbf{DL}\boldsymbol{G'}_{\boldsymbol{B}}\widehat{\widehat{\mathbf{H}}_\mathbf{DL}}^{-\mathbf{1}}\right|^2 + \sum_{k\neq i}^{K}V\left|\mathbf{W}_\mathbf{R}^\mathbf{H}\mathbf{G}_\mathbf{U}^{-1}\widehat{\mathbf{H}}_\mathbf{DL}\widehat{\widehat{\mathbf{H}}_\mathbf{DL}}^{*}\right|^2 + \sum_{k\neq i}^{K}V\left|\mathbf{W}_\mathbf{R}^\mathbf{H}\mathbf{G}_\mathbf{U}^{-1}\widehat{\mathbf{H}}_\mathbf{DL}(\boldsymbol{G'}_{\boldsymbol{B}})\widehat{\widehat{\mathbf{H}}_\mathbf{DL}}^{*}\right|^2 + VL\frac{\boldsymbol{\xi_p}}{\boldsymbol{r_p}}\left|\mathbf{W}_\mathbf{R}^\mathbf{H}\ \mathbf{G}_\mathbf{U}^{-1}\widehat{\mathbf{H}}_\mathbf{p}\widehat{\widehat{\mathbf{H}}_\mathbf{p}}^{*}\right|^{\mathbf{2}} + V\frac{\boldsymbol{\xi_p}}{\boldsymbol{r_p}}\sum_{l=1}^{L}\left|\mathbf{W}_\mathbf{R}^\mathbf{H}\mathbf{G}_\mathbf{U}^{-1}\ \ \widehat{\mathbf{H}}_\mathbf{p}(\boldsymbol{G'}_{\boldsymbol{p}})\widehat{\widehat{\mathbf{H}}_\mathbf{p}}^{*}\right|^2}{\mathbf{W}_\mathbf{R}^\mathbf{H}\mathbf{W}_\mathbf{R} + V\left|\mathbf{W}_\mathbf{R}^\mathbf{H}\mathbf{G}_\mathbf{U}^{-1}\widehat{\mathbf{H}}_\mathbf{DL}(\boldsymbol{G'}_{\boldsymbol{B}})\widehat{\widehat{\mathbf{H}}_\mathbf{DL}}^{*}\right|^2 + \sum_{k\neq i}^{K}V\left|\mathbf{W}_\mathbf{R}^\mathbf{H}\mathbf{G}_\mathbf{U}^{-1}\widehat{\mathbf{H}}_\mathbf{DL}\widehat{\widehat{\mathbf{H}}_\mathbf{DL}}^{*}\right|^2 + \sum_{k\neq i}^{K}V\left|\mathbf{W}_\mathbf{R}^\mathbf{H}\mathbf{G}_\mathbf{U}^{-1}\widehat{\mathbf{H}}_\mathbf{DL}(\boldsymbol{G'}_{\boldsymbol{B}})\widehat{\widehat{\mathbf{H}}_\mathbf{DL}}^{*}\right|^2 + V_pL\frac{\boldsymbol{\xi_p}}{\boldsymbol{r_p}}\left|\mathbf{W}_\mathbf{R}^\mathbf{H}\ \mathbf{G}_\mathbf{U}^{-1}\widehat{\mathbf{H}}_\mathbf{p}\widehat{\widehat{\mathbf{H}}_\mathbf{p}}^{*}\right|^{\mathbf{2}} + \frac{\mathbf{1}}{V_{p2}}\frac{\boldsymbol{\xi_p}}{\boldsymbol{r_p}}\sum_{l=1}^{L}\left|\mathbf{W}_\mathbf{R}^\mathbf{H}\mathbf{G}_\mathbf{U}^{-1}\ \ \widehat{\mathbf{H}}_\mathbf{p}(\boldsymbol{G'}_{\boldsymbol{p}})\widehat{\widehat{\mathbf{H}}_\mathbf{p}}^{*}\right|^2}$$

(48)

APPENDIX 5

$$\lim_{N\to\infty} SINR_{MMSE-REC} = \frac{\left|\beta_U \mathbf{W_R^H}\widehat{\widehat{\mathbf{H}}}_{\mathbf{DL}}\widehat{\overline{\mathbf{H_{DL}}}}^{*}\boldsymbol{\Lambda}\right|^2}{\mathbf{W_R^H}\mathbf{W_R} + \sum_{\boldsymbol{k\neq i}}^{\boldsymbol{K}}\left(\left(\beta_U \mathbf{W_R^H}\widehat{\widehat{\mathbf{H}}}_{\mathbf{DL}}\widehat{\overline{\mathbf{H_{DL}}}}^{*}\boldsymbol{\Lambda}\right)\left(\beta_U \mathbf{W_R^H}\widehat{\widehat{\mathbf{H}}}_{\mathbf{DL}}\widehat{\overline{\mathbf{H_{DL}}}}^{*}\boldsymbol{\Lambda}\right)^{\boldsymbol{H}}\right) + \sum_{\boldsymbol{l=1}}^{\boldsymbol{L}}\left(\left(\beta_U \mathbf{W_R^H}\widehat{\widehat{\mathbf{H}}}_{\mathbf{p}}\widehat{\overline{\mathbf{H_p}}}^{*}\boldsymbol{\Lambda_p}\right)\left(\beta_U \mathbf{W_R^H}\widehat{\widehat{\mathbf{H}}}_{\mathbf{p}}\widehat{\overline{\mathbf{H_p}}}^{*}\boldsymbol{\Lambda_p}\right)^{\boldsymbol{H}}\right)}$$

$$= \frac{V\left|\mathbf{W_R^H}\right|^2}{\mathbf{W_R^H}\mathbf{W_R} + \boldsymbol{V}\sum_{i\neq k}^{K}\left|\mathbf{W_R^H}\widehat{\widehat{\mathbf{H}}}_{\mathbf{DL}}\widehat{\overline{\mathbf{H_{DL}}}}^{*}\right|^2 + \sum_{\boldsymbol{l=1}}^{\boldsymbol{L}}\left(\left(\beta_p \mathbf{W_R^H}\widehat{\widehat{\mathbf{H}}}_{\mathbf{p}}\widehat{\overline{\mathbf{H_p}}}^{*}\boldsymbol{\Lambda_p}\right)\left(\beta_p \mathbf{W_R^H}\widehat{\widehat{\mathbf{H}}}_{\mathbf{p}}\widehat{\overline{\mathbf{H_p}}}^{*}\boldsymbol{\Lambda_p}\right)^{\boldsymbol{H}}\right)} = \frac{V\left|\mathbf{W_R^H}\right|^2}{\mathbf{W_R^H}\mathbf{W_R} + \boldsymbol{V}\sum_{k\neq i}^{K}\left|\mathbf{W_R^H}\widehat{\widehat{\mathbf{H}}}_{\mathbf{DL}}\widehat{\overline{\mathbf{H_{DL}}}}^{*}\right|^2 + V_P L\left|\mathbf{W_R^H}\widehat{\widehat{\mathbf{H}}}_{\mathbf{p}}\widehat{\overline{\mathbf{H_p}}}^{*}\right|^{\mathbf{2}}} =$$

(50)

$$\lim_{N\to\infty} SINR_{MMSE-NON-REC}$$

$$= \frac{V\left|\mathbf{W_R^H}\mathbf{G_U^{-1}}\right|^{\mathbf{2}}}{\mathbf{W_R^H}\mathbf{W_R} + V\left|\mathbf{W_R^H}\mathbf{G_U^{-1}}\widehat{\widehat{\mathbf{H}}}_{\mathbf{DL}}(\boldsymbol{G'}_{\boldsymbol{B}})\widehat{\overline{\mathbf{H_{DL}}}}^{*}\right|^2 + + \sum_{i\neq k}^{K}\left|\mathbf{W_R^H}\mathbf{G_U^{-1}}V\right|^2 + \sum_{i\neq k}^{K} V\left|\mathbf{W_R^H}\frac{\xi}{r}\mathbf{G_U^{-1}}\widehat{\widehat{\mathbf{H}}}_{\mathbf{DL}}(\boldsymbol{G'}_{\boldsymbol{B}})\widehat{\overline{\mathbf{H_{DL}}}}^{*}\boldsymbol{\Lambda}\right|^2 + \sum_{l=1}^{L}\left|\beta_p \mathbf{W_R^H}\mathbf{G_U^{-1}}\widehat{\widehat{\mathbf{H}}}_{\mathbf{p}}\widehat{\overline{\mathbf{H_p}}}^{*}\boldsymbol{\Lambda_p}\right|^2 V_P L\left|\mathbf{W_R^H}\mathbf{G_U^{-1}}\widehat{\widehat{\mathbf{H}}}_{\mathbf{p}}\widehat{\overline{\mathbf{H_p}}}^{*}\right|^{\mathbf{2}} + \frac{\boldsymbol{\xi_p}}{\boldsymbol{r_p}V_{p_2}}\sum_{l=1}^{L}\left|\mathbf{W_R^H}\mathbf{G_U^{-1}}\ \widehat{\widehat{\mathbf{H}}}_{\mathbf{p}}(\boldsymbol{G'}_{\boldsymbol{p}})\widehat{\overline{\mathbf{H_{DL}}}}^{*}\right|^2}$$

(51)

APPENDIX 6

$$\lim_{N\to\infty} SINR_{ZF-REC}$$

$$= \frac{\left|\mathbf{W}_{\mathbf{R}}^{\mathbf{H}}\hat{\hat{\mathbf{H}}}_{\mathbf{DL}}\overline{\widehat{\mathbf{H}_{\mathbf{DL}}}}^{\mathbf{H}}\left(\overline{\widehat{\mathbf{H}_{\mathbf{DL}}}}\ \ \overline{\widehat{\mathbf{H}_{\mathbf{DL}}}}^{\mathbf{H}}\right)^{-1}\right|^{2}}{\mathbf{W}_{\mathbf{R}}^{\mathbf{H}}\mathbf{W}_{\mathbf{R}} + \sum_{k\neq i}^{K}\left(\left(\mathbf{W}_{\mathbf{R}}^{\mathbf{H}}\hat{\hat{\mathbf{H}}}_{\mathbf{DL}}\overline{\widehat{\mathbf{H}_{\mathbf{DL}}}}^{\mathbf{H}}\left(\overline{\widehat{\mathbf{H}_{\mathbf{DL}}}}\ \ \overline{\widehat{\mathbf{H}_{\mathbf{DL}}}}^{\mathbf{H}}\right)^{-1}\right)\left(\mathbf{W}_{\mathbf{R}}^{\mathbf{H}}\hat{\hat{\mathbf{H}}}_{\mathbf{DL}}\overline{\widehat{\mathbf{H}_{\mathbf{DL}}}}^{\mathbf{H}}\left(\overline{\widehat{\mathbf{H}_{\mathbf{DL}}}}\ \ \overline{\widehat{\mathbf{H}_{\mathbf{DL}}}}^{\mathbf{H}}\right)^{-1}\right)^{H}\right) + \sum_{l=1}^{L}\left(\left(\mathbf{W}_{\mathbf{R}}^{\mathbf{H}}\hat{\hat{\mathbf{H}}}_{\mathbf{p}}\overline{\widehat{\mathbf{H}_{\mathbf{DL}}}}^{\mathbf{H}}\left(\overline{\widehat{\mathbf{H}_{\mathbf{DL}}}}\ \ \overline{\widehat{\mathbf{H}_{\mathbf{DL}}}}^{\mathbf{H}}\right)^{-1}\right)\left(\mathbf{W}_{\mathbf{R}}^{\mathbf{H}}\hat{\hat{\mathbf{H}}}_{\mathbf{p}}\overline{\widehat{\mathbf{H}_{\mathbf{DL}}}}^{\mathbf{H}}\left(\overline{\widehat{\mathbf{H}_{\mathbf{DL}}}}\ \ \overline{\widehat{\mathbf{H}_{\mathbf{DL}}}}^{\mathbf{H}}\right)^{-1}\right)^{H}\right)}$$

$$= \frac{\left|\mathbf{W}_{\mathbf{R}}^{\mathbf{H}}\right|^{2}}{\mathbf{W}_{\mathbf{R}}^{\mathbf{H}}\mathbf{W}_{\mathbf{R}} + \sum_{k\neq i}^{K}|\mathbf{W}_{\mathbf{R}}^{\mathbf{H}}|^{2} + \frac{\boldsymbol{\xi}}{\boldsymbol{r}}\sum_{l=1}^{L}\left(\left(\mathbf{W}_{\mathbf{R}}^{\mathbf{H}}\hat{\hat{\mathbf{H}}}_{\mathbf{p}}\overline{\widehat{\mathbf{H}_{\mathbf{p}}}}^{\mathbf{H}}\right)\left(\mathbf{W}_{\mathbf{R}}^{\mathbf{H}}\hat{\hat{\mathbf{H}}}_{\mathbf{p}}\overline{\widehat{\mathbf{H}_{\mathbf{p}}}}^{\mathbf{H}}\right)^{H}\right)}$$

(52)

$$\lim_{N\to\infty} SINR_{ZF-NON-REC=}$$

$$= \frac{\left|\mathbf{W}_{\mathbf{R}}^{\mathbf{H}}\mathbf{G}_{\mathbf{U}}^{-\mathbf{1}}\right|^{2}}{\mathbf{W}_{\mathbf{R}}^{\mathbf{H}}\mathbf{W}_{\mathbf{R}} + \left|\mathbf{W}_{\mathbf{R}}^{\mathbf{H}}\mathbf{G}_{\mathbf{U}}^{-\mathbf{1}}\ \hat{\hat{\mathbf{H}}}_{\mathbf{DL}}\boldsymbol{G'}_{\boldsymbol{B}}\overline{\widehat{\mathbf{H}_{\mathbf{DL}}}}^{*}\right|^{2} + \mathbf{W}_{\mathbf{R}}^{\mathbf{H}}\sum_{I\neq k}^{K}\left|\mathbf{G}_{\mathbf{U}}^{-\mathbf{1}}\hat{\hat{\mathbf{H}}}_{\mathbf{DL}}\overline{\widehat{\mathbf{H}_{\mathbf{DL}}}}^{\mathbf{H}}\left(\overline{\widehat{\mathbf{H}_{\mathbf{DL}}}}\ \ \overline{\widehat{\mathbf{H}_{\mathbf{DL}}}}^{\mathbf{H}}\right)^{-\mathbf{1}}\right|^{2} + \sum_{i\neq k}^{K}\left|\mathbf{W}_{\mathbf{R}}^{\mathbf{H}}\mathbf{G}_{\mathbf{U}}^{-\mathbf{1}}\ \hat{\hat{\mathbf{H}}}_{\mathbf{DL}}\boldsymbol{G'}_{\boldsymbol{B}}\overline{\widehat{\mathbf{H}_{\mathbf{DL}}}}^{*}\right|^{2} + L\left|\mathbf{W}_{\mathbf{R}}^{\mathbf{H}}\ \mathbf{G}_{\mathbf{U}}^{-\mathbf{1}}\hat{\hat{\mathbf{H}}}_{\mathbf{p}}\overline{\widehat{\mathbf{H}_{\mathbf{DL}}}}^{\mathbf{H}}\right|^{\mathbf{2}} + \sum_{l=1}^{L}\left|\mathbf{W}_{\mathbf{R}}^{\mathbf{H}}\mathbf{G}_{\mathbf{U}}^{-\mathbf{1}}\ \hat{\hat{\mathbf{H}}}_{\mathbf{p}}\mathbf{G'}_{\boldsymbol{p}}\overline{\widehat{\mathbf{H}_{\mathbf{DL}}}}^{-\mathbf{1}}\right|^{2}}$$

(53)

ABBREVIATIONS

Angle of Arrival (AoA)

Best Linear Ubiased Estimator (BLUE)

Channel State Information (CSI)

Cluster Heads (CH)

Cognitive Radio Edge Computing (CREC)

Cognitive Radio Medium Access Control (CRMAC)

Cognitive Radio Network (CRN)

Cognitive Radio Network Cloud (CRNC)

Cognitive Radio Sensor Networks (CRSNs)

Common Control Channel (CCC)

Compressive Sensing (CS)

Cramer Rao Lower Bound (CRLB)

Denial of Service (DoS)

Dynamic Spectrum Access (DSA)

Fast Fourier transform (FFT)

Faster-Than-Nyquist (FTN)

First Come First Served (FCFS)

Fisher Information Matrix (FIM)

Gateway nodes (GTW)

Gradient plus Inverse Distance Squared (GIDS)

Heterogeneous Cognitive Networks (HCN)

Inter User Interference (IUI)

Inverse Distance Weighted (IDW)

Kalman Filter (KF)

Line of Site (LoS)

Massive Multiple-Input/Multiple-Output (Massive MIMO)

Maximal Ratio Combining (MRC)

Mean Square Error (MSE)

Measurement Capable Devices (MCDs)

Minimum Mean Square Error (MMSE)

Mobile-edge Computing (MEC)

Multi-Radio Access Technologies (RAT)

Natural Neighbors (NNI)

Nearest Neighbors (NN)

Network Base Station (BS)

Network Functions Virtualization (NFV)

Non Line of Site (NLoS)

Non-Orthogonal-Multiple Access (NOMA)

Non-Reciprocal Channels (NRC)

Open Systems Interconnection (OSI)

Particle Filter (PF)

Primary Base Station (PBS)

Primary User Emulation (PUE)

Primary User Emulation Attack (PUEA)

Primary Users (PUs)

Quality of Experience (QoE)

Quality of Service (QoS)

Radio Access Network (RAN)

Radio Environment Maps (REMs)

Receiver (RX)

Secondary Base Station (SBS)

Secondary Users (SUs)

Signal to Interference Noise Ratio (SINR)

Signal-to-Noise Ratio (SNR)

Software Defined Radio (SDR)

Software Defined Radio (SDR)

Software Defined Systems (SDS)

Software Defined Systems (SDS)

Software Defined Wireless Sensor Network (CSDWSN)

Spectrum Manager Application (SMA)

Transmission Time Interval (TTI)

Transmitter (TX)

User Equipment (UE)

Virtual Machines (VMs)

Wavelet Packet Transform (WPT)

Zero-Forcing (ZF)

REFERENCES

[1]S.Haykin, “Cognitive radio:brain-empowered wireless communications”, IEEE Journal on Selected Areas in Communications, vol.23, no 2,pp 201-220,2005

[2]R.V.Prasad, P.Pawlczak, J.A.Hoffmeyer, H.S.Berger, “Cognitive functionality in next generation wireless networks: standardization efforts”, IEEE Communications Magazine, vol.46, no 4, pp. 72-78, 2008.

[3]S.Jeng, C.Tsung, F.Chang, “ WLAN smart antenna with Bluetooth interference reduction”, IET Communications, vol.2 , no.8, pp.1098-1107, 2008

[4]Q.Zhao, B.M.Sandler, “A Survey of dynamic spectrum access”, IEEE Signal Processing Magazine, vol.24, no.3, pp 79-89, 2007

[5]Q.Phang, V.C.M.Leung, “Channel clustering and probabilistic channel visiting techniques for WLAN interference mitigation in Bluethooth services”, IEEE Transactions on Electromagnetic Compatibility, vol.49, no.4, pp. 914-923, 2007

[6]B.A.Fette, B.Fette, Cognitive Radio Technology, Newnes, 2006

[7]T.C.Clancy, “Achievable capacity under the interference temperature mode”, in Proceedings of IEEE International Conference on Computer Communications(INFOCOM), May 2007, pp.794-802

[8]E.Hossain, D.Niyato, Z.Han, Dynamic Spectrum Access and Management in Cognitive Radio Networks, Cambridge University Press, 2009

[9]A.Sahai, N.Hoven, R.Tandra, “Some foundamental limits in cognitive radio”, Proccedings of Alletron Conference on Communications , Control and Computing, October 2004

[10]M.J.Marcus, P.Kodolzy,A.Lippman, “ Reclaiming the vast wasteland: why unlicensed use of white space in TV bands will not cause interference to DTV viewers”, New America Foundation: Wireless Future Program, Report 2005

[11] I.Kakalou, K. E. Psannis, P. Krawiec, R. Badea, Cognitive Radio Network and Network Service Chaining towards 5G: challenges and requirements, IEEE Communications, November 2017 vol. 55, issue: 11, pp. 145-151.

[12] J. Mitola, G. Q. Maguire, Jr., "Cognitive radio: making software radios more personal," *IEEE Personal Communications Magazine*, vol. 6, no.4, 1999, pp. 13–18.

[13] H.D. Thai, Lee C., D. Niyato, P. Wang, A Survey of Mobile Cloud Computing: Architecture, Applications and Approaches, *Wireless Communications and Mobile Computing* vol.13, no.18, 2013, pp.1587-1611

[14] C.H. Co, D. H. Huang, S.-H. Wu, Cooperative Spectrum Sensing in TV White Spaces: When Cognitive Radio Meets Cloud, *Workshop on Cloud Computing, IEEE INFOCOM 2011*, 2011, pp.683-688

[15] B.Y. Reddy, Solving Hidden Terminal Problem in Cognitive Networks using Cloud Technologies, *Proc. 6th International Conference on Sensor Technologies and Applications,* 2012, pp.235-240.

[16] I. Kakalou, G. Papadimitriou, P. Nikopolitidis, P.G. Sarigianidis, M.S. Obaidat, A Reinforcing Learning-based Cognitive MAC Protocol, *IEEE International Conference on Communications (ICC 2015),* London, UK, 2015, pp.5608-5613

[17] D.B. Rawat, S. Shetty, K. Raza, Game Theoretic Dynamic Spectrum Access in Cloud-based Cognitive Radio Networks, *Proc. IEEE International Conference on Cloud Engineering 2014* , 2014, pp.586-591.

[18] D.B. Rawat, ROAR: An Architecture for Real-time Opportunistic Spectrum Access in Cloud-assisted Cognitive Radio Networks, *Proc. 13th IEEE Annual Consumer Communications & Networking Conference 2016*, Las Vegas, NV, USA, 2016.

[19] D.B. Rawat, S. Reddy, N. Sharma, B.B. Bista, S. Shetty, Cloud-Assisted GPS-driven Dynamic Spectrum Access in Cognitive Radio Vehicular Networks for transportation Cyber Physical Systems, *Proc. IEEE Wireless Communications and Networking Conference 2015,* New Orleans, LA, USA, 2015.

[20] F. Ge, H. Lin, A. Khajeh, C. Jason Chiang, A. M. Eltawil, C. W. Bostian, W.C. Feng, and R. Chadha, "Cognitive Radio Rides on the Cloud," in *Proc. Military Communications Conference (MILCOM) 2011*, 2011, pp.1448.

[21] H. Lin et al., “MOON: MapReduce on opportunistic environments,” in *the Proc. ACM International Symposium on High Performance Distributed Computing (HPDC) 2010*, Chicago, IL, USA, 2010, pp.95-106.

[22] S.-H. Wu, H.-L. Chao, C.H. Ko, S.-R. Mo, C.-T. Jiang, T.-L. Li, C.-C. Cheng, and C.-F. Liang, “A cloud model and concept prototype for cognitive radio networks,” *IEEE Wireless Communications,* vol. 19, no. 4, 2012, pp. 49–58.

[23] D. Huang, S.-H. Wu, and P.-H. Wang, Cooperative Radio Source Positioning and Power Map Reconstruction: A Sparse Bayesian Learning Approach, *IEEE Transactions on Vehicular Technology,* vol.64, no.6, 2015, pp. 2318-2332.

[24] S.Y. Chang, H.C. Wu, Adaptive Antenna Selection by Parallel QR-Factorization for Cognitive Radio Cloud Network, *Proc. IEEE GLOBECOM 2014, Cognitive Radio and Networks Symposium,* Austin TX, USA, 2014, pp.882-887.

[25] A. Gupta, R.K. Jha, A Survey of 5G Network: Architecture and Emerging Technologies, *IEEE Access,* vol.3, 2015, pp. 1206-1232.

[26] I. Kakalou, K. Psannis, S. K. Goudos, T. V. Yioultsis, N. V. Kantartzis, Y. Ishibasi, Radio Environment Maps for 5G Cognitive Radio Network, International Conference on Modern Circuits and Systems Technologies, Thessaloniki, Greece, 13-15 May 2019.

[27] Wireless Innovation Forum

[28] Ioanna Kakalou, Danai Papadopoulou,Theofanis Xifilidis, Kostas Psannis, Katherine Siakavara, Sotirios K.Goudos, , Yuataka Ishibashi, A Survey On Spectrum Sensing Algorithms for Cognitive Radio Networks, IEEE, International Conference on Modern Circuits and Systems Technologies (MOCAST) on Electronics and Commuications, 7 - 9 May 2018, Thessaloniki, Greece.

[29] K. P. Rainer Stone, "Differential Evolution (DE) for Continuous Function Optimization (an algorithm by Kenneth Price and Rainer Storn)," [Online]. Available: http://www1.icsi.berkeley.edu/~storn/code.html.

[30] L. Xu, H. Fang, Z. Lin,, Evolutionarily stable opportunistic spectrum access in cognitive radio networks, IET Commun., 2016, Vol. 10, Iss. 17, pp. 2290–2299

[31] M. Saeedzarandi, Optimization of Multiband Sensing -Time-Adaptive Detection in Cognitive Radio Networks Using Artificial Immune Algorithm, 2nd Conference on Swarm Intelligence and Evolutionary Computation (CSIEC2017)

[32] M. Bkassiny, S. K. Jayaweera, Robust, Non-Gaussian Wideband Spectrum Sensing in Cognitive Radios, IEEE Transactions on Wireless Communications, Vol. 13, Issue 11, pp. 6410 – 6421

[33] H. Li, X. Xing, J. Zhu, X. Cheng, K. Li, R. Bie, T. Jing, Utility-Based Cooperative Spectrum Sensing Scheduling in Cognitive Radio Networks, IEEE Transactions on Vehicular Technology, Vol. 66, Issue 1, pp. 645 – 655

[34] P.C. Ng, Optimization of Spectrum Sensing for Cognitive Sensor Network using Differential Evolution Approach in Smart Environment, 2015 IEEE 12th International Conference on Networking, Sensing and Control

[35] X-L. Huang, , F. Hu, J. Wu, Member, H.-H. Chen, G. Wang, T. Jiang, Intelligent Cooperative Spectrum Sensing via Hierarchical Dirichlet Process in Cognitive Radio Networks, IEEE Journal on Selected Areas in Communications, Vol. 33, Issue 5, pp. 771 – 787

[36] B.Li, S. Li, A. Nallanathan, Y. Nan, C. Zhao, Z. Zhou, Deep Sensing for Next-Generation Dynamic Spectrum Sharing: More Than Detecting the Occupancy State of Primary Spectrum, IEEE Transanctions on Communications, VOL. 63, NO. 7, JULY 2015

[10] F. Gao, J. Li, Tao Jiang, W. Chen, Sensing and Recognition When Primary User Has Multiple Transmit Power Levels, IEEE Transanctions on Signal Processing, VOL. 63, NO. 10, MAY 15, 2015

[37] A. Salman, I. M. Qureshi, K. Sultan, S. Saeed, Joint spectrum sensing for detection of primary users using cognitive relays with evolutionary computing, IET Communications 2015 Vol.9, Issue 13, pp. 1643 – 1648

[38] I. Hwang, J. W. Lee, Cooperative Spectrum Sensing with Quantization Combining over Imperfect Feedback Channels, IEEE Transactions on Signal Processing 2017 Vol. 65, Issue 3, 721 -732

[39] A. Tsakmalis, S. Chatzinotas, B. Ottersten, Interference Constraint Active Learning with Uncertain Feedback for Cognitive Radio Networks, IEEE Transactions on Wireless Communications 2017, Vol. 16, Issue 7, pp. 4654 – 4668

[40] H. Wu, F. Yao, Y. Chen; Y. Liu; T. Liang, Multibit-QuantizationBased Collaborative Spectrum Sensing Scheme for Cognitive Sensor Networks, IEEE Access 2017 Vol.5 pp. 25207 – 25216

[41] D.L. Donoho, "Compressed Sensing", IEEE Trans. Inf. Theory, vol.52, no.4, pp.1289-1306, Apr. 2006.

[42] Z. Zhang, S. Member, Y. Xu, S. Member, A survey of sparse Representation: Algorithms and applications, IEEE Access 2015490–530.

[43] S. Foucart, Hard threshol pursuit: An algorithm for compressive sensing, SIAM J. Numer. Anal. 49 (6) (2011) 2543–2563.

[44] D. Cohen, Y. C. Eldar, "Sub-Nyquist Cyclostationary Detection for Cognitive Radio", IEEE Transactions on Signal Processing, vol. 65, issue 11, pp. 3004-3019, June 2017

[45] D. Cohen and Y. C. Eldar, "Sub-Nyquist Sampling for Power Spectrum Sensing in Cognitive Radios: A Unified Approach", IEEE Transactions on Signal Processing, vol. 62, issue 15, pp. 3897-3910, August 2014.

[46] K. Cicho´n, et al. "Energy- efficient cooperative spectrum sensing: a survey", IEEE Com. Sur. & Tut., vol.18, no.3, pp. 1861- 1886, 2016.

[47] M.Thoppian, S.Venkatesan, R.Prakash, and R.Chandrasekaran, "MAC-layer scheduling in cognitive radio based multi-hop wireless networks", Proceedings of IEEE International Symposium on a World of Wireless, Mobile and Multimedia Networks(WoWMoM),

[48] A-C.Hsu, D.S.L. Weit, C.C.J. Kuo, " A cognitive MAC protocol using statistical channel allocation for wireless ad-hoc networks", Proceedings of Wireless Communications and Networking Conference(WCNC) March 2007, pp.105-110.

[49] C.Doerr, M.Neufeld, J.Fifield, T.Weingart, D.Sicker, D.Grunwald, "Multi-MAC-an adaptive MAC framework for dynamic radio networking", Proceedings of

IEEE International Symposium on New Frontiers in Dynamic Spectrum Access Networks(DySPAN), November 2005, pp.548-555.

[50] T.Chen, H.Zhang, G.M.Maggio, I.Chlamtac, “CogMesh: acluster-based cognitive radio network”, Proceedings of IEEE International Symposium in Dynamic Spectrum Access Networks, April 2007, pp.168-178.

[51] H.Sui, X.Zhang, “CREAM-MAC: An Efficient Cognitive Radio EnAbledMultiChannel MAC Protocol for Wireless Networks”, Proceedings of IEEE International Symposium on A World of Wireless, Mobile and Multimedia Networks, 2008,pp.1-8

[52] SL Wu, CY Lin, YC Tseng, JP Sheu, A new multi-channel MAC protocol with on-demand channel assignment for multi-hop mobile ad hoc networks, IEEE DySPAN, Maryland, USA,2005, pp. 203–213

[53] SJ Yoo, H Nan, TI Hyon, DCR-MAC: distributed cognitive radio MAC protocol for wireless ad hoc networks. Wirel Commun Mobile Comput. 9(5), 2009,pp.631–653

[54]J Jia, Q Zhang, X Shen, HC-MAC: A Hardware-Constrained Cognitive MACfor Efficient Spectrum Management. IEEE J Sel Areas Commun. 26(1),2008,pp.106–117

[55] HAB Salameh, MM Krunz, O Younis, Cooperative adaptive spectrum sharingin cognitive radio networks. IEEE/ACM Trans Netw. 18(4),2010,pp. 1181–1194

[56] X Wang, A Wong, PH Ho, Stochastic Medium Access for Cognitive Radio AdHoc Networks. IEEE J Sel Areas Commun. 29(4),2011, pp. 770–783

[57] Brandon F.Lo, “A survey of common control channel design in cognitive radio networks”,Elsevier Physical Communication, Vol 4, 1, 2011, pp. 26-39

[58]Papadimitriou GI, Pomportis AS, “On the use of learning auto-mata in medium access control of single-hop lightwave Networks” Elsevier Computer Communications,vol.23,2000,pp.783-792

[59] Ioanna Kakalou, Kostas Psannis, Katherine Siakavara, Sotirios K.Goudos, , Yuataka Ishibashi SDN-based QoS Provisioning and Interference Management in

Heterogeneous CRN , International Conference on Modern Circuits and Systems Technologies, , Thessaloniki, Greece, 7-9 May 2018

[60] Duan L., Gao L., and Huang J., “Cooperative spectrum sharing: a contract-based approach,” Mobile Computing, IEEE Transactions on, vol. 13, no. 1, pp. 174–187, 2014.

[61] Zubow A., Doring M., Chwalisz M., Wolisz A.,(2015) “An SDN-Approach to Spectrum Brokerage in Infrastructure-based Cognitive Radio Networks”, *IEEE DySPAN 2015*

[62] Lien S-Y.,Lin Y-Y., Chen K-C., (2011)“Cognitive and Game-Theoretical Radio Resource Management for Autonomous Femtocells with QoS Guarantees”, IEEE Transactions on Wireless Communications, vol.10, no.7, 2011

[63] Moon S., LeAnh T., Kazmi A.S.M., Oo T.Z., Hong C-S., (2015)“SDN-based Optimal User Association and Resource Allocation in Heterogenous Cognitive Networks”, IEICE 2015

[64] Urgaonkar R., Neely M.J.,(2012) “Opportunistic Cooperation in Cognitive Femtocel Networks”, IEEE Journal on Selected Areas in Communications (JSAC), vol. 30, no. 3, pp. 607-616, 2012.

[65] Jararweh Y., Al-Ayyoub M., Doulat A., (2015)“Software Defined Cognitive Radio Framework : Design and Evaluation” International Journal of Grid and High Performance Computing (IJGHPC) 2015

[66] Namal S., Ahmad I., Jokinen M., Gurtov A., Ylianttila M., “SDN Core for Mobility between Cognitive Radio and 802.11 Networks”, IEEE Eighth International Conference on Next Generation Mobile Appls, Services and Technologies (NGMAST) 2014.

[67] D. Zhao, M. Zhu, and M. Xu, “Leveraging sdn and openflow to mitigate interference in enterprise wlan,” Journal of Networks, vol. 9, no. 6, pp. 1526–1533, 2014.

[68] Ioanna Kakalou, and Kostas Psannis, Sustainable and Efficient Data collection in Cognitive Radio Sensor Networks, IEEE Transactions on Sustainable Computing, vol.4, issue 1, pp.29-38 , Jan-March 2019

[69] Z. Fu, X. Wu, C. Guan, X. Sun, and K. Ren, “Toward efficient multi-keyword fuzzy search over encrypted outsourced data with accuracy improvement,” IEEE Transactions on Information Forensics and Security, vol. 11, no. 12, pp. 2706–2716, 2016.

[70] K.Gai, M.Qiu, Z.Ming, H.Zhao, L.Qiu, “Spoofing-Jamming Attack Strategy using Optimal Power Distributions in Wireless Smart Grid”, IEEE Transactions on Smart Grid, vol. 8, issue 5, pp.2431-2439, September 2017.

[71] Y.-J. Ren, J. Shen, J. Wang, J. Han, and S.-Y. Lee, “Mutual verifiable Provable data auditing in public cloud storage,” Journal of Internet Technology, vol. 16, no. 2, pp. 317–323, 2015.

[72] Y. Zhang, X. Sun, and B. Wang, “Efficient algorithm for k-barrier coverage based on integer linear programming,” China Communications, vol. 13, no. 7, pp. 16–23, 2016.

[73]M. Zhao, Y. Yang, and C. Wang, “Mobile data gathering with load balanced clustering and dual data uploading in wireless sensor networks,” IEEE Transactions on Mobile Computing, vol. 14, no. 4, pp. 770–785, 2015.

[74] C.Nevala, “Mobility Management for software defined wireless sensor networks”, Thesis Malardaren University, Sweden, 25-5-2016.

[75] K.Gai, M.Qiu, H.Zhao, “Energy-aware task assignment for mobile cyber-enabled applications in heterogeneous cloud computing”, J. on Parallel and Distributed Computing, vol. 111 pp.126-135, 2018.

[76] K.Gai, L.Qiu, M.Chen, H.Zhao, M.Qiu, “SA-EAST: security aware efficient data transmission for ITS in Mobile Heterogeneous Cloud Computing”, ACM Transactions on Embedded Computing Systems”, vol.6, no.2, January 2017.

[77] C.Nevala, “Mobility Management for software defined wireless sensor networks”, Thesis Malardaren University, Sweden, 25-5-2016.

[78] T. Luo, H.-P. Tan, and T. Q. S. Quek, “Sensor OpenFlow: Enabling software-defined wireless sensor networks,” IEEE Commun. Lett., vol. 16, no. 11, pp. 1896–1899, Nov. 2012.

[79]Zheng D, Miyasaki T., Guo S., Tsukahara T., Kitamichi J., Hayashi T., (2013) “Evolution of Software Defined Sensor Networks” 2013 IEEE 9th International Conf. on Mobile Ad-Hoc and Sensor Networks

[80] Zheng D., Miyasaki T., Guo S., Tsukahara T., Kitamichi J., Hayashi T., (2014) "A Software Defined Wireless Sensor Network" 2014 International Conference on Computing , Networking and Communications

[81] Hassan M.M., Alsanad A., "Resource Provisioning for Cloud-assisted Software Defined Wireless Sensor Networks" IEEE Sensor Journal 2016 Vol.16, Issue 20, pp.7401-7408.

[82] de Oliveira, B. T., Alves, R. C. A., and Margi, C. B. (2015) Software-defined wireless sensor networks and internet of things standardization synergism. In Standards for Communications and Networking (CSCN), 2015, pages 60–65.

[83] de Oliveira, B. T., Margi, C. B., and Gabriel, L. B. (2014) "TinySDN: Enabling multiple controllers for software-defined wireless sensor networks" In Communications (LATINCOM), 2014 IEEE Latin-America Conference on,pages 1–6.

[84] Namal S., Ahmad I., Saud S., Jokinen M., Gurtow A., (2016) "Implementation of OpenFlow based cognitive radio network architecture: SDN&R", Wireless Networks Springer, February 2016, vol.22, issue 2, pp.663-677.

[85] Moon S., LeAnh T., Kazmi A.S.M., Oo T.Z., Hong C-S., (2015)"SDN-based Optimal User Association and Resource Allocation in Heterogeneous Cognitive Networks", IEICE 2015

[86] Trevizan de Oliveira B., Cerqueira Alfonso R., Borges Margi C., (2015), "Software –Defined Wireless Sensor Networks and Internet of Things Standarization Synergism", IEEE Conf. on Standards for Communications and Networking 2015

[87] P. Berde et al., "ONOS: Towards an open, distributed SDN OS", in Proc. 3rd Workshop Hot Topics on Software Defined Networks. (HotSDN), 2014, pp. 1-6.

[88] Tootoonchian A., Ganjali Y.,(2010) "HyperFlow: A distributed control plane for OpenFlow", ' in Proc. Internet Netw. Manage. Conf. Res. EnterpriseNetw. (INM/WREN), 2010, p. 3.

[89] Yu M., Rexford J., Freedman M.J., Wang J.,(2011) "Scalable flow-based networking with DIFANE", ACM SIGCOMM Computer Communications Rev.,vol. 41, no. 4, pp. 351_362, Oct. 2011.

[90] A. R. Curtis, J. C. Mogul, J. Tourrilhes, P. Yalagandula, P. Sharma, and S. Banerjee, (2011)"DevoFlow: Scaling Fow management for high performance Networks",

ACM SIGCOMM Computer Communications Rev., vol. 41, no. 4, pp. 254_265, Aug. 2011.

[91] S. H. Yeganeh and Y. Ganjali, (2012) "Kandoo: A framework for efficient and scalable ofloading of control applications", Proc. 1st Workshop Hot Topics Softw. De_ned Netw. (HotSDN), 2012, pp. 19_24.

[92] K. Phemius, M. Bouet, and J. Leguay,(2014) "DISCO: Distributed multi-domain SDN controllers," in Proc. IEEE Netw. Oper. Manage. Symp. (NOMS), May 2014, pp. 1_4.

[93] A. Krishnamurthy, S. P. Chandrabose, and A. Gember-Jacobson, (2014) "Pratyaastha: An efficient elastic distributed SDN control plane", in Proc. 3rd Workshop Hot Topics Softw. Defined Netw. (HotSDN), 2014, pp. 133-138.

[94] A. Dixit, F. Hao, S. Mukherjee, T. V. Lakshman, and R. Kompella, (2013), "Towards an elastic distributed SDN controller", ACM SIGCOMM Comput. Commun. Rev., vol. 43, no. 4, pp. 7-12, Sep. 2013.

[95] Flauzac O. Gonzalez C., Nolot F., (2016) "Developing a distributed software defined networking testbed for IoT", 7th International Conference on Ambient Systems, Networks and Technologies, Elsevier, Computer Science vol.83, pp.680-684.

[96] Li X., Djukic P., Zhang H., (2014) "Zoning for hierarchical network optimization in software defined networks", in IEEE Network Operations and Management Symposium (NOMS), 2014, pp.1-8, May 2014

[97] OpenFlow Switch Specification, version 1.5.1, March 26 2015, Open Networking Foundation

[98] Mabrouk O., Minet P., Idoudi H., Saidane L., "Intra-Cluster Multichannel Scheduling Algorithm for Cognitive Radio Sensor Networks", (2015) International Wireless Communications and Mobile Computing Conference (IWCMC) August 2015.

[99] Saini D., Misra R., Yadav R.N., (2016) "Distributed Event Driven Cluster based Routing in Cognitive Radio Sensor Networks" IEEE Annual India Conference Dec. 2016.

[100] F. Restuccia, G. Anastasi, M. Conti, and S. K. Das, "Analysis and optimization of a protocol for mobile element discovery in sensor networks," IEEE Transactions on Mobile Computing, vol. 13, no. 9, pp. 1942–1954, 2014.

[101] J. S. Prashanth and S. V. Nandury, "Cluster-based rendezvous points selection for reducing tour length of mobile element in wsn," in Advance Computing Conference (IACC), 2015 IEEE International. IEEE, 2015, pp. 1230–1235.

[102] C. Tunca, S. Isik, M. Y. Donmez, and C. Ersoy, "Distributed mobile sink routing for wireless sensor networks: a survey," IEEE Communications Surveys & Tutorials, vol. 16, no. 2, pp. 877–897, 2014.

[103] M. Arquam, C. Gupta, and M. Amjad, "Delay constrained routing algorithm for wsn with mobile sink," in Computational Science and Engineering (CSE), 2014 IEEE 17th International Conference on. IEEE, 2014, pp. 1449–1454.

[104] Wang T., Li Y., Wang G., Cao J. Bhuiyan M.Z.A., Jia W., "Sustainable and Efficient and Data Collection from WSNs to Cloud", IEEE Transactions on Sustainable Computing, 31 March 2017, pp1-1.

[105] Wang, C.-W.; Wang, L.-C. Analysis of reactive spectrum handoff in cognitive radio networks. IEEE J. Sel. Areas Commun. 2012, 30, 2016–2028.

[106] M.Usman, M.S.Knan, H.Vu-Van, K.Insoo, "Energy Efficient Channel Handoff for Sensor Network-assisted Cognitive Radio Network", Sensor, vol. 15. Issue 8, pp. 18012-18039, August 2015

[107]Xiao, J.-J., Cui, S., Luo, Z.-Q., and Goldsmith, A.,(2006) "Power scheduling of universal decentralized estimation in sensor networks" IEEE Transactions on Signal Processing, vol. 54, pp. 413{422, Feb. 2006.

[108] NEOS Server: State-of-the-art Solvers for Numerical Optimization, https://neos-server.org/neos/, Winsconsin Institutes of Discovery at the University of Winsconsin Madison.

[109] Lee, D.; Yeo, W. Channel Availability Analysis of Spectrum Handoff in Cognitive Radio Networks. IEEE Commun. Lett. 2015, 19, 435–438.

[110] Sheikholeslami, F.; Nasiri-Kenari, M.; Ashtiani, F. Optimal Probabilistic Initial and Target Channel Selection for Spectrum Handoff in Cognitive Radio Networks. IEEE Trans. Wireless Commun. 2015, 14, 570–584.

[111] Song, Y.; Xie, J. ProSpect: A proactive spectrum handoff framework for cognitive radio ad hoc networks without common control channel. IEEE Trans. Mob. Comput. 2012, 11, 1127–1139.

[112] Mehedi Hassan M., Alsanad A., (2016) “Resource Provisioning for Cloud-Assisted Software Defined Sensor Network”, IEEE Sensors Journal, vol. 16, no. 20, pp. 7401-7408.

[113] Flauzac O. Gonzalez C., Nolot F., (2016) “Developing a distributed software defined networking testbed for IoT”, 7th International Conference on Ambient Systems, Networks and Technologies, Elsevier, Computer Science vol.83, pp.680-684.

[114] Gao S., Zeng Y., Luo H., Zhang H., (2014) “Scalable area-based hierarchical control plane for software defined information centric networking”, in 23rd International Conference on Computer Communication and Networks (ICCCN), 2014, pp.1,7, 4-7 Aug. 2014

[115] Kobo H.I., Abu-Mahfouz A., Hancke G., (2017) “A Survey on Software Defined Wireless Sensor Networks: Challenges and Design Requirements”, vol.5 pp.1872-1899.

[116] Farhady H., Lee H-Y.,Nakao A.,(2015) “Software-Defined Networking: A Survey”, Computer Networks, Elsevier, vol.81, 22 April 2015, pp.79-95

[117] Haque I.T., Abu-Ghazaleh N., (2016)“Wireless Software Defined Networking: A Survey and Taxonomy”, IEEE Communications Surveys and Tutorials, vol. PP, issue 99, 16 May 2016.

[118] Jagadeesan N.A., Krishnamachari B., (2015) “Software Defined Network Paradigms in Wireless Networks: A Survey”, Journal ACM Computing Surveys, Vol.47, Issue 2, article no.27, January 2015

[119] Ioanna Kakalou, Kostas E. Psannis, A Broadcast Protocol for Cognitive Radio Cloud with QoS and Collision Avoidance Provision (submitted at) IEEE Transanctions on Sustainable Computing

[120] J. Montalban, I.C. Angulo, Y. Wu, L.Zang, S-I Park, J-Y Joung Lee, H-M Kim, M. Velez, P. Angueira, “Performance Study of Layered Division Multiplexing Based on SDR Platform” IEEE Transanctions on Broadcasting 2015, Vol.61, Issue 3.

[121] L. Chen, K. Bian, X. Du, Multichannel Broadcast via Channel Hopping in Cognitive Radio Networks, IEEE Transactions on Vehicular Technology, VOL. 64, NO. 7, JULY 2015

[122] C. J. L. Arachchige, S. Venkatesan, R. Chandrasekaran, and N. Mittal,“Minimal time broadcasting in cognitive radio networks,” in Proc.ICDCN, 2011, pp. 364–375.

[123] L. Berlemann, C. Hoymann, G. Hiertz, and B. Walke, “Minimumlatency broadcast scheduling for cognitive radio networks,” in Proc. IEEESECON, 2013, pp. 389–397.

[124] M. H. Rehmani, A. C. Viana, H. Khalife, and S. Fdida, “Surf: A distributed channel selection strategy for data dissemination in multihop cognitive radio networks,” Computer Communications, vol. 36, no. 10, pp. 1172–1185, 2013.

[125] H.A. Bany Salameh, M.F. El-Attar, Cooperative OFDM based Virtual Clustering Scheme for Distributed Coordination in Cognitive Radio Networks, IEEE Transanctiosn on Vehicular Technology, vol.64, issue 8, pp.3624-3632, August 2015

[126] Y.Song, J.Xie, BRACER: A Distributed Broadcast Protocol in Multi-hop Cognitive Radio Ad Hoc Networks with Collision Avoidance, Transactions on Mobile Computing, vol.14, issue 3, 509-524 pp. March 2015

[127] L. Lazos, S. Liu, and M. Krunz, “Spectrum opportunity-based control channel assignment in cognitive radio networks,” in Proc. IEEE SECON, 2009, pp. 1–9.

[128]Al-Mathehaji Y, Boussakta S., Martin Johnston M., Fakhrey H., “CRBP-A Broadcast Protocol for Cognitive Radio Ad-Hoc Networks”, IEEE ICC 2015, London.

[129] Y.Song, J.Xie, “QB^2 IC: A QoS-Based Broadcast Protocol Under Blind Information for Multihop Cognitive Radio Ad-Hoc Networks”, IEEE Transactions on Vehicular Technology 2014, vol.63, no.3. March 2014.

[130] S.Ji, R.Beyah, Z.Cai, “ Broadcast Scheduling with Latency and Redundancy Analysis for Cognitive Radio Networks”, IEEE Transactions on Vehicular Technology 2015, vol.64, issue 7, pp.3090-3097.

[131 Y. R. Kondareddy and P. Agrawal, “Selective broadcasting in multi-hop cognitive radio networks,” in Sarnoff Symposium, 2008 IEEE, pp. 1–5, IEEE, 2008.

[132] M. Chraiti, H. Hakim, W. Ajib, and H. Boujemaa, “Spectrum sharing techniques for broadcast cognitive radio networks,” 2013.

[133] R.Meneguette, A.Boukerche, An Efficient Greeb-Aware Architecture for Virtual Machine Migration in Sustainable Vehicular Clouds, IEEE Transanctions on Sustainable Computing, (Early Access) 12 March 2019.

[134] I.Kakalou, K.Psannis, A Broadcast Protocol in Multi-Hop Cognitive Radio Ad-Hoc Networks with Guarentees, IEEE International Symposium on Broadband Multimedia Systems and Broadcasting (BMSB) 2017, 7-9 June 2017 Cagliari, Italy, pp.1-7.

[135] G. Ganesan and Y. Li. Cooperative spectrum sensing in cognitive radio networks. In Proc. of DySpan, pages 137–143, 2005.

[136] A. Ghasemi and E. Sousa. Collaborative spectrum sensing for opportunistic access in fading environments. In Proc. of DySPAN, pages 131–136, 2005.

[137] C. Han, J. Wang, Y. Yang, and S. Li. Addressing the control channel design problem: OFDM-based transform domain communication system in cognitive radio. Computer Networks, 2007.

[138] S. Mishra, A. Sahai, and R. Brodersen. Cooperative sensing among cognitive radios. In Proc. of ICC, 2006.

[139] K.S.Narendra, M.A.L. Thathachar, "Learning Automaton: An Introduction", Courier Corporation, 2013.

[140]M.E.Tanab, W.Hamouda, "Resource Allocation in Underlay Cognitive Radio Networks: A Survey", IEEE Communications Surveys and Tutorials 2017, vol. 19, issue 2, pp.1249-1276.

[141] Ioanna Kakalou and Kostas E, Psannis, Coordination without Collaboration in Imperfect Games: the Primary User Emulation Attack Example, IEEE Access Journal, January 2018.

[142] Dietmar Berwanger & Łukasz Kaiser (2010): Information Tracking in Games on Graphs. Journal of Logic, Language and Information 19(4), pp. 395–412.

[143] Dietmar Berwanger, Łukasz Kaiser & Bernd Puchala (2011): Perfect-Information Construction for Coordination in Games. In: Proceedings of the 31st Conference on Foundations of Software Technology and Theoretical Computer Science (FSTTCS'11), Leibniz International Proceedings in Informatics 13, Leibniz-

Zentrum fu¨r Informatik, Mumbai, India, pp. 387–398, doi:10.4230/LIPIcs.FSTTCS.2011.387.

[144] R Chen, JM Park, Ensuring trustworthy spectrum sensing in cognitive radio networks, in 1st IEEE Workshop on Networking Technologies for Software Defined Radio Networks, SDR '06, (Reston, 25 September 2006), pp. 110–119

[145] R Chen, JM Park, J Reed, Defense against primary user emulation attacks in cognitive radio networks. Selected Areas Commun., IEEE J. 26, 25–37 (2008)

[146] Z Chen, T Cooklev, C Chen, C Pomalaza-Raez, Modeling primary user emulation attacks and defenses in cognitive radio networks, in IEEE 28th International Performance Computing and Communications Conference (IPCCC), 2009, (Scottsdale, 14–16 December 2009), pp. 208–215

[147] Z Jin, S Anand, K Subbalakshmi, Detecting primary user emulation attacks in dynamic spectrum access networks, in IEEE International Conference on Communications, 2009. ICC '09, (Dresden, 14–18 June 2009), pp. 1–5

[148] Z Yuan, D Niyato, H Li, Z Han, Defense against primary user emulation attacks using belief propagation of location information in cognitive radio networks, in IEEE Wireless Communications and Networking Conference (WCNC), 2011, (Cancun, 28–31 March 2011), pp. 599–604

[149] L Huang, L Xie, H Yu, W Wang, Y Yao, Anti-PUE attack based on joint position verification in cognitive radio networks, in International Conference on Communications and Mobile Computing (CMC), 2010, Volume 2, (Shenzhen, 12–14 April 2010), pp. 169–173

[150] C Zhao, W Wang, L Huang, Y Yao, Anti-PUE attack base on the transmitter fingerprint identification in cognitive radio, in 5th International Conference on Wireless Communications, Networking and Mobile Computing, 2009. WiCom '09, (Beijing, 24–26 September 2009), pp. 1–5

[151] Mahmod Ammar, Nick Riley, Meftah Mehdawi, Anwar Fanan, & Mahsa Zolfaghari(2015): Physical Layer Security in Cognitive Radio Networks- Detection and Mitigation of Primary User Emulation Attacks, International Conference on Artificial Intelligence, Energy and Manufacturing Engineering (ICAEME'2015) Jan. 7-8, 2015 Dubai (UAE)

[152] ChungSheng, X. Song, M., Detection of PUE Attacks in Cognitive Radio Networks based on Signal Pattern Activity, IEEE Transactions on Mobile Computing, Vol.13, Issue 5, pp.1022-1034

[153] Yu R.,Yan Zhang Y., Liu Y., Gjessing S., Guizani M.,(2015) Securing Cognitive Radio Networks against Primary User Emulation Attacks, IEEE Network, vol.29, issue 4, July-August 2015

[154] M.Yan et al.(2011),"Game-Theoretic Approach against Selfish attacks in CRN" IEEE/ACIS 10th International Conf. Computer and Information Science (ICIS),May 16-18, pp.58-61.

[155] Zhu Han, Poor, H.V.(2009) "Coalition Games with Cooperative Transmission: A Cure for the Curse of boundary Nodes in Selfish Packet- Forwarding Wireless Networks" IEEE Transaction,Vol.57 Issue.1, 2009, pp.203-213.

[156] Yu-Wei Chan, Feng-Tsun Chein, Ronald Chang, Min-Kuan Chang, Yeh-Ching Chung(2013) "Spectrum sharing in multi-channel cooperative cognitive radio networks: a coalitional game approach "Springer, Issue 7, Vol. 19 ,2013, pp. 1553-1562.

[157] D. Hao and K. Sakurai,(2012) "A differential game approach to mitigating primary user emulation attacks in cognitive radio networks," in Proceedings of the IEEE 26th International Conference on Advanced Information Networking and Applications (AINA '12), pp. 495–502, March 2012.

[158] Nguyen-Thanh N., Philippe Ciblat P., Pham A.T., Nguyen V-T., (2015)Surveillance Strategies Against Primary User Emulation Attack in Cognitive Radio Networks, IEEE Transactions on Wireless Communications, vol. 14, no. 9, September 2015

[159] Nguyen-Thanh, N.; Ciblat, P.; Pham, A.T.; Nguyen, V.-T.(2014) Attack and surveillance strategies for selfish primary user emulator incognitive radio network, IEEE Global Conference on Signal and Information Processing (GlobalSIP-2014), pp. 1199-1203

[160] Bhattacharjee S., Marinescu D.C.,(2014) A Cloud Service for Trust Management in Cognitive Radio Networks, International Journal on Cloud Computing, vol 3, no.4 2014.

[161] Ioanna Kakalou, Theofanis Xifilidis, Kostas Psannis, Multiscale Decision Making Scheme for wideband spectrum sensing with sub-Nyquist sampling in Cognitive Radio Networks and fading channels (submitted at) IEEE Intelligents Systems.

[162] David L. Donoho, “Compressed Sensing”, IEEE Trans. on Information Theory, Apr. 2006, vol.52,no.4, pp. 1289-1306.

[163] Yuan Ma, Yue Gao, Ying-Chang Liang and Shuguang Cui, “Reliable and Efficient Sub-Nyquist Wideband spectrum Sensing in Cooperative Cognitive Radio Networks”, IEEE Journal of Selected Areas in Communications., Oct. 2016, vol.34, issue 10, pp.2750-2762.

[164] M. Bkassiny, S. K. Jayaweera, Robust, Non-Gaussian Wideband Spectrum Sensing in Cognitive Radios, IEEE Transactions on Wireless Communications, 2014, Vol. 13, Issue 11, pp. 6410 – 6421.

[165]X-L. Huang, , F. Hu, J. Wu, Member, H.-H. Chen, G. Wang, T. Jiang, Intelligent Cooperative Spectrum Sensing via Hierarchical Dirichlet Process in Cognitive Radio Networks, IEEE Journal on Selected Areas in Communications, 2015, Vol. 33, Issue 5, pp. 771 – 787.

[166] B.Li, S. Li, A. Nallanathan, Y. Nan, C. Zhao, Z. Zhou, Deep Sensing for Next-Generation Dynamic Spectrum Sharing: More Than Detecting the Occupancy State of Primary Spectrum, IEEE Transanctions on Communications, July 2015, vol. 63, no. 7, pp. 2442-2457.

[167] H. Li, X. Xing, J. Zhu, X. Cheng, K. Li, R. Bie, T. Jing, Utility-Based Cooperative Spectrum Sensing Scheduling in Cognitive Radio Networks, IEEE Transactions on Vehicular Technology, Vol. 66, Issue 1, pp. 645 – 655.

[168] F. Gao, J. Li, Tao Jiang, W. Chen, Sensing and Recognition When Primary User Has Multiple Transmit Power Levels, IEEE Transanctions on Signal Processing, May 15, 2015, vol. 63, no. 10, pp.2704-2717.

[169]Chang, H.S., et al., Multitime Scale Markov Decision Processes. IEEE Transactions on Automatic Control,2003 vol. 48, no.6, p.p 976-987.

[170] C.Wernz, A.Deshmukh, “Multi-Time Scale Decision Making for Strategic Agents Interactions”, Proceedings of Industrial Engineering Research Conference 2010, pp.1-6.

[171]Goldsmith A. “Wireless Communications”, Standford University, 2004

[172] Ioanna Kakalou, Ioannis Almalis, Kostas E. Psannis, An Optimal Filter with Kalman-like filtering of Particles for Non-Linear State Estimation (submitted at) IEEE Transactions on Ultrasonics, Ferroelectrics and Frequency Control.

[173] G. Welch, G. Bishop, Eds. An Introduction to the Kalman Filter, 2001.

[174] M.S. Arulampalam, S. Maskell, N. Gordon, T. Clapp. “A tutorial on particle filters for online nonlinear non Gaussian Bayesian tracking”,IEEE Trans. on Signal Processing, Vol. 50, nº 2, pp: 174-188, February 2002.

[175] N.J. Gordon, D.J Salmond, A.F.M. Smith. “Novel approach to nonlinear/non-Gaussian Bayesian state estimation”, IEE Proc. Part F, Vol. 140, n°2, pp: 107-113, April 1993.

[175a] A. Doucet, N. De Freitas, K. Murphy, S. Russell, “Rao-blackwellised particle filtering for dynamic bayesian networks,” in Proceedings of the Sixteenth conference on Uncertainty in artificial intelligence. Morgan Kaufmann Publishers Inc., 2000, pp. 176–183.

[176] F.Gustafsson, "Particle Filter Theory and Practice with Positioning

Applications", IEEE Aerospace and Electronic Systems Magazine, Vol.25, Issue.7, pp.53-82,2010

[177a] Namrata Vaswani, “Particle filtering for large-dimensional state spaces with multimodal observation likelihoods,” IEEE Transactions on Signal Processing, vol. 56, no. 10, pp. 4583– 4597, 2008.

[177] G.Chang, Marginal unscended kalman filter for cross-correlated process and observation noise at the same epoch, IET Radar, Sonar and Navigation, Vol.8, no. 1, January 2014.

[178] W. Liu, P. P. Pokharel, and J. C. Principe, “Correntropy: Properties, and applications in non-gaussian signal processing,” *IEEE Trans. Signal Process.*, vol. 55, no. 11, pp. 5286-5298, 2007.

[179] B. Chen, L. Xing, J. Liang, N. Zheng, and J. C. Principe, “Steady-State Mean-Square Error Analysis for Adaptive Filtering under the Maximum Correntropy Criterion,” *IEEE Signal Process. Lett.*, vol. 21, no. 7, pp. 880-884, 2014

[180] M. Raitoharju, R. Piché , H. Nurminen, A systematic approach for Kalman-type filtering with non-Gaussian noises, 2016 19th International Conference on Information Fusion (FUSION), 5-8 July, Heidelberg Germany, 2016

[181] K.Wang, Y.Li, C.Rizos, Practical Approaches to Kalman Filtering with Time-Correlated Measurement Errors, IEEE Transactions on Aerospace and Electronic Systems, April 2012, Vol. 48, no: 2, pp.1669-1681

[182]D. P.Mandic, J. Champers,. Recurrent neural networks for prediction: learning algorithms, architectures and stability. John Wiley & Sons, Inc., 2001.

[183] T. Li. A gap between simulation and practice for recursive filters: On the state transition noise. arXiv preprint arXiv:1308.1056, 2013.

[184] S.Saha, F.Gustafsson, Particle Filtering with dependent noise processes, IEEE Transactions on Signal Processing, Sept. 2012, Vol.60, no.9, pp.4497-4508.

[185] J.E.Potter, J.C.Deckert, A Conservative Bound on the Estimation Error Covariance Matrix in the Presence of Correlated Driving Noise and Correlated Measurement Noise, Journal of Mathematical Analysis and Applications, 1973, vol.43, pp.293-320.

[186] G.F.Barker, A.Berman, R.J.Plemmons, Positive Diagonal Solutions to Lyapunov Equations, MRC Technical Summary Report #1713, Mathematics Research Center, University of Wisconsin-Madison 1977

[187]Bialas S., Gora M., On the existence of common solution to Lyapunov equations, Bulletin of the Polish Academy of Sciences and Technical Sciences, vol.63, no.1, 2015

[188] R.A.Horn, C.R.Johnson, Matrix Analysis, Cambridge University Press 1991.

[189] Wu P.Y. Products of Positive Semidefinite Matrices, Linera Algebra and its Applications, Elsevier Science Publising, vol.111. pp.53-61 1988.

[190] P.Matisko, V.Havlena, Cramer Rao bounds for estimation of linear systems noise covariances, Proceedings of 18th International World Congress, The International Federation of Automatic Control, Milano-Italy 28 August-2 September 2011, pp.7791-7796.

[191] Šimandl M., Královec J. and Tichavský P. (2001). Filtering, predictive, and smoothing Cramér-Rao bounds for discrete time nonlinear dynamic systems. Automatica. Vol. 37, pp. 1703 – 1716.

[192] I.Kakalou, K.E.Psannis , Massive MIMO for Cognitive Radio Network and Cloud with Imperfect CSI and non- Reciprocal Channels (to be submitted)

[193] F. Boccardi, R. Heath, A. Lozano, T. L. Marzetta, and P. Popovski, "Five disruptive technology directions for 5G," IEEE Communications

Magazine, vol. 52, no. 2, pp. 74–80, February 2014.

[194] M. Petermann, M. Stefer, F. Ludwig, D. Wubben, M. Schneider, S. Paul, and K.-D. Kammeyer, "Multi-user pre-processing in multi-antenna OFDM TDD systems with non-reciprocal transceivers," IEEE Transactions on Communications, vol. 61, no. 9, pp. 3781–3793, September 2013.

[195] S. Durrani and M. E. Bialkowski, "Effect of mutual coupling on the interference rejection capabilities of linear and circular arrays in CDMA systems," IEEE Transactions on Antennas and Propagation, vol. 52, no. 4, pp. 1130–1134, April 2004.

[196] Y. Zou, O. Raeesi, R. Wichman, A. Tolli, and M. Valkama, "Analysis of channel non-reciprocity due to transceiver and antenna coupling mismatches in TDD precoded multi-user MIMO-OFDM downlink," in IEEE 80th Vehicular Technology Conference (VTC Fall), Sept 2014, pp.1–7.

[197] O. Raeesi, Y. Zou, A. Tolli, and M. Valkama, "Closed-form analysis of channel non-reciprocity due to transceiver and antenna coupling mismatches in multi-user massive MIMO network," in IEEE Global Communications Conference Workshops (GLOBECOM), Dec 2014, pp. 333–339.

[198] W. Zhang, H. Ren, C. Pan, M. Chen, R. de Lamare, B. Du, and J. Dai,“Large-scale antenna systems with UL/DL hardware mismatch: achievable rates analysis and calibration,” IEEE Transactions on Communications,vol. 63, no. 4, pp. 1216–1229, April 2015.

[199] Mohannad H. Al-Ali, Student Member, IEEE and K. C. Ho, Transmit Precoding in Underlay MIMO Cognitive Radio with Unavailable or Imperfect Knowledge of Primary Interference Channel, IEEE Transactions on Wireless Communications 2016

[200] Ali Cagatay Cirik, Member, IEEE, Miltiades C. Filippou, Member, IEEE, and Tharmalingam Ratnarajah, Transceiver Design in Full-Duplex MIMO Cognitive Radios under Channel Uncertainties, IEEE Transactions on Cognitive Communications and Networking

[201] Yongwei Huang∗ Qiang Li† Wing-Kin Ma† Shuzhong Zhang, Robust Secondary Multicast Transmit Beamforming for Cognitive Radio Networks under Imperfect Channel State, ICASSP 2011

[202] A.Massaudi, N.Selami, M.Siala, Joint Beamforming and Scheduling Scheme forUnderlay MIMO Cognitive Radio Networks with Imperfect Channel Knowledge

[203] Panayotis Mertikopoulos, Member, IEEE, and E. Veronica Belmega, Transmit without Regrets: Online Optimization in MIMO-OFDM Cognitive Radio Systems, IEEE Journal on Selected Areas in Communications, vol.32, no.11, November 2014.

[204] Jing Yang∗†, Trung Q. Duong‡, Maged Elkashlan§, Xianfu Lei¶, and Xiqi Gao, Multiuser Scheduling for Cognitive MIMO with Channel Estimation Errors and Feedback Delay, IEEE ICC 2015

[205] Yinglei Teng, Hang Weng Shuai, Yu Chaowei Wang, Mei Song, Optimal Beamforming Design for Minimal Energy Optimization in Cognitive MIMO System with Perfect/Imperfect Knowledge of PU’s Precoder,

[206] C.Li, S. Yan, N.Yang, On Channel Reciprocity to activate uplink channel training for downlink wireless transmission in tactile internet applications, 2018 IEEE

International Conference on Communications Workshops Proccedings, IEEE ICC Workshops 2018 Kansas City, United States, 24-28 May, 2018, pp.1-6.

[207] T. L. Marzetta, \Noncooperative cellular wireless with unlimited numbers of base station antennas," IEEE Transactions on Wireless Communications, vol. 9, no. 11, pp. 3590{3600, Nov. 2010.

[208] F. Rusek, D. Persson, B. K. Lau, E. G. Larsson, T. L. Marzetta, O. Edfors, and F. Tufvesson, \Scaling up MIMO: Opportunities and challenges with very large arrays," IEEE Signal Processing Magazine.

[Online]. Available: arxiv.org/abs/1201.3210.

[209] T. L. Marzetta, \Noncooperative cellular wireless with unlimited numbers of base station antennas," IEEE Transanctions Wireless Communications, vol. 9, no. 11, pp. 3590{3600, Nov. 2010.

[210] C. Li, S. Yan, and N. Yang, "On channel reciprocity to activate uplink channel training for downlink wireless transmission in Tactile Internet applications," in Proc. IEEE ICC 2018 Workshop on 5G & Beyond--Enabling Technologies and Applications focus on the Tactile Internet, May 2018, pp. 1-6.

[211] C. LHuang, G.C.Alexandropoulos, Deep Learning for UL/DL Channel Calibration in Generic Massive MIMO Systems, ICC 2019 - 2019 IEEE International Conference on Communications (ICC).

[212] F. Rusek, D. Persson, B. K. Lau, E. G. Larsson, T. L. Marzetta, O. Edfors, and F. Tufvesson, \Scaling up MIMO: Opportunities and challenges with very large arrays," IEEE Signal Processing Magazine.

[Online]. Available: arxiv.org/abs/1201.3210.

[213] Trung Kien Vu, Student Member, IEEE, Mehdi Bennis, Senior Member, IEEE,Sumudu Samarakoon, Student Member, IEEE, M´erouane Debbah, Fellow, IEEE, and Matti Latva-aho, Joint Load Balancing and Interference Mitigation in 5G Heterogeneous Networks, IEEE Transactions on Wireless Communications

[214] J. Hoydis, S. ten Brink, and M. Debbah, "Massive MIMO in the UL/DL of cellular networks: how many antennas do we need?" IEEE Journal on

Selected Areas in Communications, vol. 31, no. 2, pp. 160–171, February 2013.

[215] L. Lu, G. Y. Li, A. L. Swindlehurst, A. Ashikhmin, and R. Zhang, “An overview of massive MIMO: benefits and challenges,” IEEE Journal of

Selected Topics in Signal Processing, vol. 8, no. 5, pp. 742–758, Oct 2014.

[216] T. L. Marzetta, “Noncooperative cellular wireless with unlimited numbers of base station antennas,” IEEE Transactions on Wireless Communications,

vol. 9, no. 11, pp. 3590–3600, November 2010.

[217] H. Wei, D. Wang, and X. You, “Reciprocity of mutual coupling for TDD massive MIMO systems,” in Wireless Communications Signal Processing (WCSP), 2015 International Conference on, Oct 2015, pp. 1–5.

[218] F. Athley, G. Durisi, and U. Gustavsson, “Analysis of massive MIMO with hardware impairments and different channel models,” in 2015 9th European Conference on Antennas and Propagation (EuCAP), May 2015,pp. 1–5.

[219] H. Wei, D. Wang, J. Wang, and X. You, “Impact of RF mismatches on the performance of massive MIMO systems with ZF precoding,” Science China Information Sciences, vol. 59, no. 2, pp. 1–14, 2016. [Online]. Available: http://dx.doi.org/10.1007/s11432-015-5509-1.

[220] E. G. Larsson, O. Edfors, F. Tufvesson and T. L. Marzetta, “Massive MIMO for next generation wireless systems,” IEEE Commun. Mag., vol. 52, no. 2, pp. 186–195, Feb. 2014.

[221] F. Rusek, D. Persson, B. K. Lau, E. G. Larsson, T. L. Marzetta, O. Edfors and F. Tufvesson, “Scaling up MIMO: Opportunities and challenges with very large arrays,” IEEE Signal Process. Mag., vol. 30, no. 1, pp. 40–60, Jan. 2013.

[222] H. Holma and A. Toskala, *LTE for UMTS: Evolution to LTE-Advanced*, 2nd ed., West Sussex, John Wiley & Sons, 2011.

[223] Ioanna Kakalou, Kostas Psannis, Sotirios K. Goudos, Traianos V. Yioultsis, Nikolaos V. Kantartzis, Yutaκα Ishibasi, Radio Environment Maps for 5G Cognitive Radio Network, International Conference on Modern Circuits and Systems Technologies, Thessaloniki, Greece, 13-15 May 2019

[224] J. Van De Beek et al., ``How a layered REM architecture brings cognition to today's mobile networks," IEEE Wireless Communications., August. 2012. vol. 19, no. 4, pp. 17-24

[225] J. Pérez-Romero et al., ``On the use of radio environment maps for interference management in heterogeneous networks," IEEE Commun. Magazine, Aug. 2015., vol. 53, no. 8, pp. 184-191.

[226] May 2015. Guidance for National Implementation of a Regulatory Framework for TV WSD Using Geo-Location Databases. Electronic Communications Committee. Tech. Rep. 236. [Online]. Available:www.erodocdb.dk/Docs/doc98/of_cial/pdf/ECCREP236.PDF

[227] Y. Zhao, B. Le, and J.H. Reed, "Network Suppor - The Radio Enxvironment Map", Cognitive Radio Technology, Bruce Fette, Chapter 11, pp. 325-366, 2nd. Ed, Elsevier, 2006.

[228] M.Pesko, T.Javornik, A.Kosir, M.Stular, M.Mohorcic, Radio Enviroment Maps: The Survey of Construction Methods, KSII Transaction on Internet and Information Systsems December 2014, vol.8, no. 11, pp. 3789-3809.

[229] P.Gajewski, Propagation Models in Radio Environment Map Design, Baltic URSI Symposium 2018, 15-17 May 2018 Poznan, Poland.

[230] M. Pesko a.o.: "The Indirect Self-tunning Method for Constructing Radio Environment Maps Using Omnidirectional or Directional Transmitter Antenna", EURASIP Journal on Wireless Communications and Networking, March 2015, Springer

[231]K.Tsukamoto, M.Kitsenusuka, K.Kunihiro, Highly accurate radio environment mapping method based on transmitter localization and spatial intepolation in urban LoS/NLoS scenario, IEEE Topical Conference on Wireless Sensors and Sensors Networks 2018, 14-17 January 2018 Anaheim, CA, USA

[232]N.Ezzati, H.Taheri, Distributed Spectrum Sensing Using Radio Environemnt Maps in Cognitive Radio Networks, Wireless Personal Communications, Springer, 2018, vol.101, issue 4, pp. 2241-2254.

[233] K.Sato, T.Fujii, Kriging Based Interference Power Constraint: Intergrated Design of the Radio Environment Map and Transmission Power, IEEE

Transcanctions on Cognitive Communications and Networking March 2017, vol. 3, no. 1, pp. 13-25.

[234]P.Bednarek, D.Bicki, J.Lopatka, Radio Environment Map for Cognitive Radio Network Simulator, 49intl Journal of Electronics and Telecommunications, 2018, vol.64, no.1, pp.45-49.

[235]A.Kliks, P.Kryszkiewiicz, A.Umbert, J.Perez-Romero, F.Kazadevall, L.Kulacz, Application of Radio Environment Maps for Dynamic Broadband Access in TV Bands in Urban Areas, IEEE Access September 2017, vol. 5, pp. 19842-19863.

[236]A.Kliks, L.Goratti, T.Chen, REM: Revisiting a Cognitive Tool for Virtualized 5G Networks, 2016 23rd International Conference on Telecommunications (ICT), 16-18 May 2016, Thessaloniki, Greece.

The photos of the final page : Online at:

http://www.bu.edu/susilo/2019/10/28/human-aversion-to-algorithms-and-ways-to-overcome-it/

https://spacenews.com/orbital-atk-increases-government-satellite-work-to-make-up-for-commercial-shortfall/thaicom8/

https://www.mwrf.com/technologies/systems/article/21849809/the-race-to-5gand-6g

The following satellite photo taken on 23rd of June 2020 by IHSS NASA.

Algorithms for Cognitive Radio Network and Cognitive Radio Network Cloud

PhD Dissertation

6G

Ioanna Kakalou